



**MicroRNAs in Haematopoietic Stem Cell  
Transplantation Outcome**

**Sadaf Atarod**

Submitted in partial fulfilment of the requirements for the  
degree of Doctor of Philosophy

Haematological Sciences  
Institute of Cellular Medicine  
Newcastle University, UK

November 2014



## Abstract

Allogeneic haematopoietic stem cell transplantation (allo-HSCT) is a curative treatment for numerous haematological malignancies. Graft-versus-host disease (GVHD) is the major complication causing mortality and is classified into acute (aGVHD) and chronic. MicroRNAs play a significant role in inflammation and have reported potential as biomarkers of different diseases. This study has investigated the role of microRNAs in allo-HSCT outcomes and had two main aims; (1) identification of microRNAs specific to the aGVHD target organ, skin and (2) an investigation into the role of immune specific miRNAs (miR-146a and miR-155) in peripheral blood. Initially, pathway mining was performed on a list of 18 genes that were shown previously, to have deregulated expression levels with regards to GVHD. The pathway mining identified specific immunological pathways in relation to the genes and potential microRNA targets. Global microRNA profiling was performed on a discovery cohort that identified a signature microRNA list in skin biopsies obtained from patients at the time of cutaneous histopathological aGVHD onset (grades I-III) and healthy volunteers. Twelve microRNAs were selected for further validation and it was shown that miR-34a-5p, miR-34a-3p, miR-503-5p and let-7c-5p were elevated and significantly involved in allo-HSCT outcomes. There was an interaction between miR-34a-3p and miR-503-5p which was significantly diagnostic of aGVHD and let-7c-5p was significantly predictive of disease relapse. MiR-34a-5p protein targets; p53 and c-Myc were then evaluated in the same cohort. MiR-34a-5p expression levels and cells stained positively for p53 were significantly correlated in the epidermis. Preliminary optimization of miR-34a-5p knockdown study was successfully conducted which showed promising results in the reduction of T cell proliferation. The whole blood study showed that miR-146a-5p and its interaction with miR-155-5p was predictive of aGVHD incidence in pre-disease onset (Day+28) samples. Interestingly, the expression levels of miR-146a-5p and miR-155-5p negatively correlated with *SPI1 (PU.1)*. In conclusion, these investigations showed that (1) the microRNAs studied in this investigation may regulate the expression levels of the selected 18 genes, (2) microRNA expression levels in clinical skin biopsies obtained at the time of aGVHD onset could potentially be used as diagnostic biomarkers for aGVHD and as predictive biomarkers for overall survival as well as relapse and (3) miR-146a-5p and miR-155-5p expression levels in whole blood could be used as predictive biomarkers for aGVHD incidence.

## **Author's Declaration**

The material contained in this thesis is entirely the work of this author, unless otherwise stated and has not been submitted for a degree previous to this or any other University.

**Sadaf Atarod M.Sc.**

November 2014

# Dedication

*I dedicate this thesis to my parents, brother and grandmas (2011 & 2015)*

“Don’t grieve. Anything you lose comes round in another form.”

**-Rumi**

## Acknowledgements

The Ph.D. course is nothing but a 3 years of roller-coaster ride with you being the driver and experiencing moments of sheer joy, excitement, shock, disappointment and then a final adrenaline rush to have it all done with to being your next ride in life! Thus, I would like to take this opportunity and thank Anne Dickinson for giving me the chance to have a valuable research experience and to evolve into an independent researcher. I will forever be grateful to her, to Newcastle University, my *Alma Mater* and the Overseas Research Scholarship for funding and supporting me throughout this Ph.D. programme.

I am also very thankful to Jean Norden for taking me on board her 'molecular biology' team, her helpful nature, and quick feedbacks and for reading my entire thesis! Thank you, Xiao-nong Wang for being there to both share my moments of joy and despair- a supervisor whom I could always go to and have a good discussion about my life or Ph.D. I have learnt loads from you in terms of patience, teaching style and caring nature when it comes to students- thank you! Rachel Crossland, thank you for reading my result chapters and giving feedbacks.

Rachel Dickinson, thank you for reading my very first result chapter and for always being there to have interesting scientific discussions. Thank you for being as excited as myself when it came to public engagement activities. Kile Green, thank you very much for introducing me to 'R' and being ever so helpful to explain and provide me with the codes! Thank you for accepting our 'prICM' committee role. Graham Smith, thank you for reading my chapter based on the Ingenuity Pathway Analysis and the very helpful feedback on it. Kim Pearce, thank you very much for helping me with my statistics, teaching me how to perform all the complex survival tests and your valuable comments on the respective sections. I could not have done it without your help! From the start of my Ph.D. programme, I had always aimed to perform transfection experiments- thanks ever so much Lindsay Nicholson, for making this goal achievable! Clare and Dennis Lendrem, thank you both very much, for adding the '3D' dimension to my statistical analyses, for introducing me to a new world of advanced biostatistics and equipping me with the skills to perform them! Thank you both for introducing me to the 'JMP' software- you both are true intellectuals! A big thank you to Elizabeth Douglas, Cindy Carr and Jamie Watson for everything, in particular for ordering all the reagents, technical support and setting up the skin explant assays.

Thank you to the graduate school team- John Kirby, Richy Hetherington and Alison Tyson-Capper for their valuable encouragement, career advice and helping me with my career plans in many ways. Thank you Muzz Haniffa for supporting me with my very first fellowship application, for the scientific discussions and career advice- I will forever be grateful for what I learnt during the fellowship application.

Thanks to the undergraduate students; Shazmeen, Mahid and Hannah whom I supervised in the lab for their projects. All three thought were a good teaching experience. A special thanks to Mahid and Hannah for helping me generate some of the data that has been acknowledged in this thesis.

I will forever be also grateful to the 'tomorrow team' for their encouragement, providing nourishment especially 'chocolates' and taking care of me in the final stages of the Ph.D.- thank you, Rihab Gam, Monica Reis, Merry Gunawan, Marsela Qesari, Lindsay Nicholson and Urszula Cytlak! Thanks to Emily Mavin for her PBMCs and Katie Nurowski for her support and always making sure that I could have a meeting slot in Anne's diary. A big thank you to the 'Stem Cell Lab' for their help in finding me information on the patients. Thanks to David Ryan for never failing to ask me 'how was I doing'! Thanks to Matt and his group especially Naomi McGovern (thanks for the park runs) and Sarah Pagan. Shaheda Ahmed, thank you very much for being there for me especially at times when I was at the brink of a complete break-down! Shelagh Lowerson- thank you for the clinical information. A special thanks for setting up the 'Arty night'- it was always a pleasure to eat pizza, have artistic conversations and paint through the night! I have learnt loads from you and thanks for introducing me to the works of Charles Rennie Mackintosh! Sourima-thank you for being there throughout this journey which has been the beginning of a lifetime of friendship. Thanks for being my non-identical 'twin sister' and encouraging me to aim higher and higher!

A big thank you to my friends for their words of encouragement! Thank you Zara and Sonia for being my shoulder to cry on at any hour! Thanks to Soroush- for all the 'pizzas' that kept me alive during the write-up period! Thanks to my Moman and Baba for encouraging me to fly away from home to experience independent life and pursue a research career. I will always be indebted to both of you!

Last but not the least, thanks to all the patients and the healthy volunteers who donated skin and whole blood to this study- without their donations this research would not have been possible. In addition, thanks to the staff at the Freeman hospital.

## List of Abbreviations

aGVHD	Acute graft-versus-host disease
Alem	Alemtuzumab
Allo-HSCT	Allogeneic haematopoietic stem cell transplantation
AML	Acute myeloid leukaemia
ANOVA	Analysis of variance
ANP32A	Acidic leucine-rich nuclear phosphoprotein 32 family member A
APC	Antigen presenting cell
AUC	Area-under-curve
BAFF	B cell activating factor
BM	Bone marrow
Breg	Regulatory B cells
Bus	Busulfan
<i>C. elegans</i>	Caenorhabditis elegans
C1qTNF7	C1q and tumor necrosis factor related protein 7
CARD11	Caspase recruitment domain-containing protein 11
C-C (number)	Chemokine Receptor (number)
CD (number)	Cluster of differentiation
CD (number)-L	Cluster of differentiation (number)- ligand
cDNA	complementary DNA
CEACAM4	Carcinoembryonic antigen-related cell adhesion molecule 4
cGVHD	Chronic GVHD
C-index	Concordance index
CLL	Chronic lymphocytic leukaemia
CML	Chronic myelogenous leukaemia
CMF	Common myeloid progenitors
CMV	Cytomegalovirus
c-Myc	Myelocytomatosis oncogene
CR	Complete remission
CsA	Cyclosporine
CTL	Cytotoxic T lymphocyte
CTLA4	Cytotoxic T-lymphocyte antigen 4
CXCL (number)	Chemokine (C-X-C motif) ligand
Cyclo	Cyclophosphamide
DAGK- $\zeta$	Diacylglycerol kinase-zeta
DAMP	Danger associated molecular pattern
DC	Dendritic cell
DLI	Donor lymphocyte infusion
DMSO	Dimethyl sulphoxide
dNTP	Deoxyribonucleotide triphosphate
ds	double-stranded
DTT	Dichloro-diphenyl- trichloroethane
EBMT	European blood and marrow transplantation group

ECP	Extracorporeal photochemotherapy
EDTA	Ethylenediaminetetraacetic acid
ELISA	Enzyme-linked immunosorbent assay
FAM	6-carboxyfluorescein
FFPE	Formalin fixed-paraffin-embedded
Flu	Fludarabine
FOXP3	Fork head-winged helix transcription factor 3
FRET	Fluorescence resonance energy transfer
GAPDH	Glyceraldehyde 3-phosphate dehydrogenase
G-CSF	Granulocyte colony-stimulating factor
GLM	Generalised linear model
GMP	Granulocyte-monocyte progenitors
GVHD	Graft-versus-host disease
GVHR	Graft-versus-host reaction
GVL	Graft-versus-leukaemia
GVT	Graft-versus-tumour
HCLS1	Hematopoietic cell-specific Lyn substrate 1
HCV	Hepatitis C virus
HD	Hodgkin's disease
HGF	Hepatocyte growth factor
HLA	Human leukocyte antigen
HRP	Horseradish peroxidase
hsa-	homo sapiens
HSCT	Haematopoietic stem cell transplantation
HTRA1	HtrA serine peptidase 1
IFN (greek letter)	Interferon
IKB	Ingenuity knowledge base
IL (number)	Interleukin
INPP5D	Inositol polyphosphate-5-phosphatase
IPA	Ingenuity pathway analysis
IRAK1	Interleukin-1 receptor-associated kinase 1
IRAK2	Interleukin-1 receptor-associated kinase 2
IRF5	Interferon regulatory factor 5
I $\kappa$ B $\alpha$	Inhibitor of kappa B
JAK	Janus Kinase
KIR	Killer cell immunoglobulin-like receptor
LGALS7	Galectin-7
LGL	Large granular lymphocytes
LNA	Locked nucleic acid
Log	Logarithm
LPS	Lipopolysaccharides
LR	Likelihood ratio
LST1	Leukocyte-specific transcript 1
MDS	Myelodysplastic syndrome

Mel	Melphalan
MGB	Minor groove binder
MHC	Major histocompatibility complexes
miRISC	microRNAs RNA induced silencing complex
MiRNA/miR	MicroRNAs
MLR	Mixed lymphocyte reaction
MM	Multiple myeloma
MPS	Multiple proliferative syndrome
mRNA	Messenger ribonucleic acid
MSC	Mesenchymal stem cell
MSR1	Macrophage scavenger receptor 1
mTOR	Mammalian Target of Rapamycin
MUD	Matched unrelated donor
NFAT1	Nuclear factor of activated T cells-1
NFQ	Non-fluorescent quencher
NFκB	Nuclear Factor-κB
NHL	Non-Hodgkin's lymphoma
NIH	National institute of health
NK	Natural killer
NO	Nitric oxide
NRM	Non-relapse mortality
NTC	No template control
ORF	Open reading frame
OS	Overall survival
p53	Tumour protein p53
PAMP	Pathogen associated molecular pattern
PBMC	Peripheral blood mononuclear cell
PBS	Phosphate buffered saline
PBSC	Peripheral blood stem cell
PCR	Polymerase chain reaction
PIK3AP1	Phosphoinositide 3-kinase adapter protein 1
PMA	Phorbol myristate acetate
Pre-miRNA	Precursor microRNA
Pri-miRNA	Primary microRNA
PSTPIP1	Proline-serine-threonine phosphatase-interacting protein 1
PTGER2	Prostaglandin E2 receptor
PTPN7	Protein tyrosine phosphatase non-receptor type 7
qPCR	quantitative polymerase chain reaction
RA	Rheumatoid arthritis
RISC	RNA-Induced Silencing Complex
ROC	Receiver operator characteristic
RPMI	Roswell Park Memorial Institute
RQ	Relative quantity
Rs	Rho

RT	Reverse transcription
RT-qPCR	Reverse transcription- quantitative polymerase chain reaction
SD	Standard deviation
SEM	Standard error of the mean
SIB	Sibling
siRNA	Small interfering ribonucleic acid
Sirt1	Sirtuin 1
SLE	Systemic lupus erythematosus
SNP	Single nucleotide polymorphism
SOCS1	Suppressor of cytokine signaling 1
SPI1	Transcription factor PU.1
STAT1-a	Signal transducers and activators of transcription 1- alpha
TAB2	TGF-beta activated kinase 1/MAP3K7 binding protein 2
TAP1	Transporter associated with Antigen Processing 1
TBI	Total body irradiation
TCR	T cell receptor
TGFβ	Transforming growth factor beta
TGM2	Tissue transglutaminase
Th-	T helper
TLDA	Taqman low density array
TLR (number)	Toll-like receptor
Tm	Melting temperature
TNF	Tumour necrosis factor
TRAF6	TNF receptor associated factor 6
Treg	Regulatory T cell
TREM2	Triggering receptor expressed on myeloid cells 2
Tx	Transplant
UBD	Ubiquitin D
UCB	Umbilical cord blood
Unt	Untreated
UTR	Untranslated region

## List of Figures

- Figure 1.1** Conditioning regimen damages the host tissues
- Figure 1.2** Donor T cells are primed activated by APCs
- Figure 1.3** Cytotoxic T cells and NK cells cause end organ damage in the host
- Figure 1.4** Chronic GVHD pathophysiology
- Figure 1.5** Classification of aGVHD as per the NIH consensus criteria
- Figure 1.6** The Major Histocompatibility Complex
- Figure 1.7** Three signals activate T cells
- Figure 1.8** Prophylaxis, treatment and factors influencing the outcome of HSCT
- Figure 1.9** Graft-versus-host reaction in allo-HSCT patient
- Figure 1.10** The three categories of risk factors associated with allo-HSCT
- Figure 1.11** Dicer independent non-canonical pathway
- Figure 1.12** MicroRNA biogenesis
- Figure 1.13** Therapeutic applications of miRNAs.
- Figure 2.1** Total RNA was extracted from clinical skin biopsies using the *mirVana* miRNA isolation kit.
- Figure 2.2** Total RNA was extracted from whole blood using the PAXgene Blood miRNA kit.
- Figure 2.3** Total RNA was extracted from PBMCs using the *mirVana* PARIS kit.
- Figure 2.4** Ideal qPCR amplification curve.
- Figure 2.5** Taqman reverse transcription step.
- Figure 2.6** Real-time PCR steps when using Taqman chemistry
- Figure 2.7** MiRCURY LNA™ Universal RT microRNA PCR System.
- Figure 2.8** MiRCURY LNA™ RT-qPCR step.
- Figure 2.9** Melting curve analysis.
- Figure 2.10** Representative electropherograms of the total RNA analyzed using the Nano assay.
- Figure 2.11** Raw C<sub>q</sub> values detected in all the nine samples.
- Figure 2.12** Raw C<sub>q</sub> values shown for the positive and negative controls.
- Figure 2.13** Expression of reference controls in clinical skin biopsies.
- Figure 2.14** Representative standard curve for IRF5 and STAT1-a using the assay standard.
- Figure 2.15** Immunohistochemical staining of skin biopsies from the *in vitro* skin explant assay.
- Figure 2.16** The legend shows the main symbols and lines used in the generation of networks and canonical pathways
- Figure 3.1** Network 1 shows the interaction of the 18 genes with the NFκB pathway suggesting their role in inflammation.
- Figure 3.2** Network 2 shows the interaction of the 18 genes with the tumour suppressor TP53.

- Figure 3.3** Network 3, 4 and 5 are graphical representations of the molecular relationship between a focus gene and other identified molecule in the Ingenuity Knowledge Base.
- Figure 3.4** Canonical pathways relevant to GVHD.
- Figure 3.5** Interferon- $\gamma$  indirectly acts on six of the focus genes.
- Figure 3.6** IFN- $\gamma$  inducible genes may be expressed at the effector phase of aGVHD
- Figure 4.1** Pathogenesis of cutaneous aGVHD.
- Figure 4.2** Diagram is showing the time of clinical skin biopsy collection from patient's post- allo-HSCT.
- Figure 4.3** Chapter 4 study design.
- Figure 4.4** Correlation of aGVHD grades in clinical skin biopsies from allo-HSCT patients.
- Figure 4.5** Dendrogram shows two distinct clusters, one consisting of the post allo-HSCT skin biopsies and the other normal controls.
- Figure 4.6** Heat map showed three distinct miRNA expression levels.
- Figure 4.7** Venn diagram showed the differentially expressed miRNAs between normal controls vs Grade I and Grades II-III.
- Figure 4.8** MicroRNAs were differentially expressed across skin biopsies with skin histopathological grades I, II-III and normal controls.
- Figure 4.9** Five miRNAs from the validation list were predicted to target the 18 gene list.
- Figure 4.10** Bland-Altman plots for the two RT-qPCR based methods.
- Figure 4.11** Diagram showing the time of clinical skin biopsy collection from patient post- allo-HSCT.
- Figure 4.12** Let-7c-5p, miR-503-5p and miR-365a-3p validated in skin biopsies.
- Figure 4.13** MiR-34a-5p expression was significantly up-regulated post allo-HSCT in skin biopsies and its expression positively correlated with miR-34a-3p expression.
- Figure 4.14** Skin histopathological aGVHD grade correlated positively with the number of necrotic cells.
- Figure 4.15** Statistically significant negative correlations existed between miRNA expression levels and the number of inflammatory cells infiltrating the skin biopsies.
- Figure 4.16** ROC and Kaplan-Meier survival analysis for miR-503-5p and miR-34a-3p expression.
- Figure 4.17** MiR-503-5p expression is associated with aGVHD severity.
- Figure 4.18** Rotational 3D scatterplots demonstrating miR-503-5p and miR-34a-3p conditional interaction.
- Figure 5.1** Chromosomal location of miR-34 family
- Figure 5.2** MiR-34a interactions with p53 and cMyc
- Figure 5.3** Chapter 5 study hypothesis.
- Figure 5.4** Skin sections positively stained for c-Myc protein.
- Figure 5.5** Skin sections positively stained for p53 protein.

- Figure 5.6** p53 expressions in the epidermis positively correlated with miR-34-5p expression.
- Figure 5.7** PBMCs were viable post- transfection.
- Figure 5.8** Optimisation of the electroporation using different voltages.
- Figure 5.9** Optimisation of the transfection using different concentrations of the inhibitor.
- Figure 5.10** MiR-34a-5p was significantly inhibited in primary PBMCs
- Figure 5.11** MiR-34a-5p knockdown may result in lower T cell proliferation.
- Figure 5.12** MiR-34a expressions in the skin explant model.
- Figure 5.13** MiR-34a expression is not influenced by cyclosporine A.
- Figure 6.1** MiR-146a negatively regulates TRAF6 and IRAK via the TLR4 signalling pathway and NFκB activation
- Figure 6.2** MiR-146a is required to prevent Th1-mediated immune response
- Figure 6.3** MiR-155 is involved in myeloid cell development
- Figure 6.4** ROC curve and Kaplan-Meier survival analysis for miR-146a-5p.
- Figure 6.5** Estimated cumulative incidence curves for NRM and relapse.
- Figure 6.6** MiR-155-5p and miR-146a-5p expression directly correlated with SPI1 mRNA levels.
- Figure 6.7** MiRNA expression levels in the whole blood of normal volunteers and transplant patients.
- Figure 6.8** PBMCs stimulated with IFN-γ for 48 hrs showed significantly reduced miR-146a-5p expression.
- Figure 6.9** Cyclosporine A had no impact on the expression of miR-146a-5p and miR-155-5p.
- Figure 6.10** MiR-146a-5p and miR-155-5p mechanism of action during early stages of inflammation
- Appendix 1**
- Figure 1** Validation of miRNAs in clinical skin biopsies using histopathological grades.
- Appendix 2**
- Figure 1** MiRNA targets for miR-146a and miR-155.

## List of Tables

<b>Table 1.1</b>	Clinical aGVHD staging system for each organ
<b>Table 1.2</b>	Overall clinical aGVHD grading system for each organ
<b>Table 1.3</b>	Acute and chronic GVHD categories based on the NIH consensus
<b>Table 1.4</b>	The EBMT risk score points for all the five different clinical risk factors
<b>Table 1.5</b>	List of cell-specific miRNAs in whole blood of healthy individuals
<b>Table 1.6</b>	Potential biomarkers of GVHD
<b>Table 2.1</b>	Taqman miRNA cDNA synthesis master mix.
<b>Table 2.2</b>	Taqman miRNA RT-qPCR master mix.
<b>Table 2.3</b>	MiRCURY LNA™ Universal cDNA synthesis mater mix.
<b>Table 2.4</b>	MiRCURY LNA™ RT-qPCR master mix.
<b>Table 2.5</b>	Reverse transcription master mix for gene expression assays.
<b>Table 2.6</b>	Quantitative PCR master mix for standard gene expression assays.
<b>Table 2.7</b>	Taqman gene expression prime-probes for qPCR.
<b>Table 2.8</b>	Catalogue numbers and detection ranges for the specific ELISA kits used in this project.
<b>Table 2.9</b>	Summary of transfection reagents
<b>Table 2.10</b>	Quickscore intensity and proportion criteria
<b>Table 3.1</b>	Annotation results of the 18 focus genes.
<b>Table 3.2</b>	Involvements of the 18 focus genes in top diseases and disorders.
<b>Table 3.3</b>	Function of focus genes in molecular and cellular processes.
<b>Table 3.4</b>	Physiological System Development and Function.
<b>Table 3.5</b>	Functional annotation of focus genes.
<b>Table 3.6</b>	Canonical Pathways.
<b>Table 3.7</b>	Summary of predictive miRNAs that may target the 18 gene list.
<b>Table 4.1</b>	Histological criteria used for grading cutaneous aGVHD
<b>Table 4.2</b>	Patient characteristics (n=5) for the global miRNA profiling analysis using skin biopsies taken from allo-HSCT patients.  Fourteen miRNAs were identified as differentially expressed between skin biopsies from allo-HSCT patients with overall clinical aGVHD grades II-IV compared to normal controls.
<b>Table 4.3</b>	Twelve microRNAs were differentially expressed between skin biopsies from allo-HSCT patients with skin histopathological aGVHD grades I-III and normal controls.
<b>Table 4.4</b>	MicroRNAs differentially expressed between skin biopsies from allo-HSCT patients with grades I, grades II-III and normal controls.
<b>Table 4.5</b>	Normalized mean miRNA expression values across skin biopsies with skin histopathological Grades I, II-III and normal controls.
<b>Table 4.6</b>	Patient characteristics for the validation of the miRNA signature list.
<b>Table 4.7</b>	Eight miRNA exhibited a significant trend in expression levels.
<b>Table 4.8</b>	Patient characteristics for the overall survival analysis

<b>Table 4.10</b>	ROC curve analysis of miRNA expression with overall survival.
<b>Table 4.11</b>	Univariate Kaplan-Meier analysis of miRNA expression with overall survival.
<b>Table 4.12</b>	Case processing summaries for all the 11 validated miRNAs showing the number of events and censored cases per group.
<b>Table 4.13</b>	Univariate Kaplan-Meier analysis of clinical risk factors with survival.
<b>Table 4.14</b>	Univariate Cox regression analysis of clinical risk factors and miRNAs with survival.
<b>Table 4.15</b>	MiR-503-5p and miR-34a-3p were significant in predicting overall survival
<b>Table 4.16</b>	Patient characteristics for patients with no relapse and relapse.
<b>Table 4.17</b>	Univariate Cox regression analysis of miRNAs with relapse.
<b>Table 4.18</b>	Quasi-complete separation for let-7c-5p expression.
<b>Table 6.1</b>	Summary of mir-146a functions and relevant, validated targets
<b>Table 6.2</b>	Summary of mir-155 functions and relevant, validated targets
<b>Table 6.3</b>	Frequency of patient characteristics in patients with and without incidence of aGVHD grades I-III.
<b>Table 6.4</b>	Test of homogeneity of variances for all the continuous covariates used in the generalized linear model
<b>Table 6.5</b>	Test of multicollinearity.
<b>Table 6.6</b>	Confusion matrix based on the observed aGVHD and predicted aGVHD grades.
<b>Table 6.7</b>	Frequency of patient characteristics in patients with aGVHD grades 0-I and II-III.
<b>Table 6.8</b>	Frequency of patient characteristics for those who did not relapse and those that relapsed.
<b>Table 6.9</b>	ROC curve analysis of miRNA expression with overall survival
<b>Table 6.10</b>	Case processing summaries for all the 11 validated miRNAs showing the number of events and censored cases per group.
<b>Table 6.11</b>	Frequency of patient characteristics which were alive and those who were deceased.
<b>Table 6.12</b>	Gray's test summary for relapse and non-relapse mortality
<b>Appendix I</b>	
<b>Table 1</b>	Patient characteristic for the validation of the miRNA signature list (n=16) using the overall clinical aGVHD grades.
<b>Appendix II</b>	
<b>Table 1</b>	Spearman correlation showed significant positive correlation between all the mRNA targets in whole blood collected from allo-HSCT patients (n=51- 54) on Day+28.
<b>Table 2</b>	Spearman Correlation statistics between miR-146a-5p expression and its validated targets at pre-transplant.

<b>Table 3</b>	Spearman Correlation statistics between miR-146a-5p expression and its validated targets at Day+28 and three months in the no aGVHD cohort (Grade 0).
<b>Table 4</b>	Spearman Correlation statistics between miR-146a-5p expression and its validated targets at Day+28 and three months in the aGVHD cohort (Grades I-III).
<b>Table 5</b>	Spearman Correlation statistics between miR-146a-5p expression and STAT1- $\alpha$ and IRF5 protein targets at pre-transplantation.
<b>Table 6</b>	Spearman Correlation statistics between miR-146a-5p expression and STAT1- $\alpha$ and IRF5 protein targets at Day+28 and three months in the no aGVHD cohort (Grade 0).
<b>Table 7</b>	Spearman Correlation statistics between miR-146a-5p expression and STAT1- $\alpha$ and IRF5 protein targets in the aGVHD cohort (Grades I-III).

## List of publications resulting from this work

**Chapter 1:** The literature review on miRNAs involved in transplantations and GVHD contributed to a review article.

- **Atarod, S.** and Dickinson, A.M. (2013). MicroRNAs: the missing link in the biology of graft-versus-host disease? *Frontiers in Immunology* 4.

**Chapter 6:** Quantification of miR-146a-5p and miR-155-5p expression in whole blood of healthy volunteers contributed to a methods article.

- **Atarod, S.,** Smith, H., Dickinson, A.M., Wang, X.N. (2014). MicroRNA levels quantified in whole blood varies from PBMCs. *F1000 Research*.

## List of conference presentations resulting from this work

### International oral presentations

- **Atarod, S.,** Cope, W., Norden, J., Wang, X.N., Collin, M., Dickinson, A.M. (April 2013). MiR-146a-5p and its targets in graft-versus-host disease. In: 39th European Group for Bone and Marrow Transplantation. London, United Kingdom
- **Atarod, S.,** Norden, J., Dickinson, A.M. Potential biomarkers for GVHD. (March 2012). In: GVH-GVL Meeting, Regensburg, Germany.

### National and international poster presentations

- **Atarod, S.,** Cope, W., Norden, J., Collin, M., Dickinson, A.M. (January 2013). Role of miR-146a expression in graft-versus-host disease. In: Biogenesis and Turnover of Small RNAs Conference. Edinburgh, Scotland.
- **Atarod, S.,** Cope, W., Norden, J., Collin, M., Dickinson, A.M. (September 2012). Role of miR-146a expression in GVHD. *Immunology*. In: European Congress of Immunology. Glasgow, Scotland: Wiley-Blackwell Publishing Ltd. (published)
- **Atarod, S.,** Cope, W., Norden, J., Collin, M., Dickinson, A.M. (April 2012). MiR-146a expression in graft-versus-host disease. *Bone Marrow Transplantation*. In: 38th European Group for Bone and Marrow Transplantation. Geneva, Switzerland: Nature Publishing Group. (published)

# Table of Contents

<b>ABSTRACT</b>	<b>III</b>
<b>AUTHOR'S DECLARATION</b>	<b>IV</b>
<b>DEDICATION</b>	<b>V</b>
<b>ACKNOWLEDGEMENTS</b>	<b>VI</b>
<b>LIST OF ABBREVIATIONS</b>	<b>VIII</b>
<b>LIST OF FIGURES</b>	<b>XII</b>
<b>LIST OF TABLES</b>	<b>XV</b>
<b>LIST OF PUBLICATIONS RESULTING FROM THIS WORK</b>	<b>XVIII</b>
<b>LIST OF CONFERENCE PRESENTATIONS RESULTING FROM THIS WORK</b>	<b>XVIII</b>
<b>TABLE OF CONTENTS</b>	<b>XIX</b>
<b>CHAPTER 1. INTRODUCTION AND STUDY AIMS</b>	<b>1</b>
<b>1.1 HAEMATOPOIETIC STEM CELL TRANSPLANTATION</b>	<b>2</b>
<b>1.2 GRAFT-VERSUS-HOST DISEASE</b>	<b>3</b>
1.2.1 PATHOPHYSIOLOGY OF AGVHD	4
1.2.2 PATHOPHYSIOLOGY OF CGVHD	8
1.2.3 HISTOPATHOLOGY AND GRADING OF GVHD	9
1.2.3.1 Grading of aGVHD	10
1.2.3.2 Classification of cGVHD	13
<b>1.3 IMPORTANT CELLS, CYTOKINES AND CHEMOKINES INVOLVED IN THE PATHOGENESIS OF GVHD</b>	<b>13</b>
1.3.1 HUMAN LEUKOCYTE ANTIGENS	13
1.3.2 HUMAN KILLER CELL IMMUNOGLOBULIN-LIKE RECEPTORS	14
1.3.3 DONOR T-CELL ACTIVATION	15
1.3.4 CHEMOKINES AND CYTOKINES	16
1.3.5 CELLULAR COMPONENTS	17
1.3.6 INFLAMMATORY EFFECTORS	18
<b>1.4 GRAFT-VERSUS-HOST DISEASE PROPHYLAXIS AND TREATMENT</b>	<b>19</b>
<b>1.5 OTHER ALLO-HSCT OUTCOMES</b>	<b>21</b>
1.5.1 GRAFT-VERSUS-LEUKEMIA/ GRAFT-VERSUS-TUMOR EFFECT	21

1.5.2	OVERALL SURVIVAL, RELAPSE AND NON-RELAPSE MORTALITY	23
<b>1.6</b>	<b>MICRORNAs</b>	<b>26</b>
1.6.1	MICRORNA NOMENCLATURE	28
<b>1.7</b>	<b>MICRORNA BIOGENESIS</b>	<b>28</b>
1.7.1	MICRORNA TRANSCRIPTION	28
1.7.2	MICRORNA MATURATION	29
1.7.3	ASSEMBLY OF MICRORNA IN RNA-INDUCED SILENCING COMPLEX	31
1.7.4	MESSENGER RNA CLEAVAGE	32
1.7.5	TARGET RECOGNITION	34
<b>1.8</b>	<b>MICRORNAs AS BIOMARKERS OF DISEASES</b>	<b>34</b>
1.8.1	MICRORNAs IN SKIN	35
1.8.2	MICRORNAs IN IMMUNE CELLS	36
1.8.3	MICRORNAs IN GVHD	37
1.8.4	MICRORNAs IN UMBILICAL CORD BLOOD	41
1.8.5	MICRORNAs IN GRAFT REJECTION	42
<b>1.9</b>	<b>MICRORNAs IN THERAPEUTICS</b>	<b>42</b>
1.9.1	THE CURRENT OUTLOOK FOR THIS INVESTIGATION	44
<b>1.10</b>	<b>HYPOTHESES AND AIMS</b>	<b>45</b>
<b>CHAPTER 2. MATERIALS AND METHODS</b>		<b>47</b>
<b>2.1</b>	<b>PATIENTS AND HEALTHY VOLUNTEER COHORT</b>	<b>48</b>
2.1.1	ETHICS AND CONSENT	48
2.1.2	CLINICAL INFORMATION	48
<b>2.2</b>	<b>TISSUE CULTURE METHODS</b>	<b>48</b>
2.2.1	GENERAL CELL CULTURE MEDIA	48
2.2.2	ISOLATION OF PBMCs	49
2.2.3	CRYOPRESERVATION OF PBMCs	49
2.2.4	PREPARATION OF SERUM	49
2.2.5	THAWING OF CRYOPRESERVED PBMCs	50
<b>2.3</b>	<b>TOTAL RNA EXTRACTION FROM DIFFERENT TISSUES</b>	<b>50</b>
2.3.1	CLINICAL SKIN BIOPSIES AND IN VITRO SKIN EXPLANT MODEL	50
2.3.2	WHOLE BLOOD	51
2.3.3	PERIPHERAL BLOOD MONONUCLEAR CELLS	54
<b>2.4</b>	<b>REAL-TIME PCR BASIC CONCEPTS</b>	<b>56</b>
2.4.1	REAL-TIME PCR AMPLIFICATION CURVE	56
2.4.2	TAQMAN CHEMISTRY	57
2.4.3	LNA™- SYBR 1 DYE CHEMISTRY	60
2.4.4	TAQMAN GENE EXPRESSION ASSAYS	62
<b>2.5</b>	<b>REAL-TIME PCR DATA ANALYSIS</b>	<b>64</b>
2.5.1	AMPLIFICATION CURVE ANALYSIS	64
2.5.2	MELTING CURVE ANALYSIS	65
<b>2.6</b>	<b>GLOBAL MIRNA PROFILING AND INDIVIDUAL MIRNA ASSAYS</b>	<b>66</b>
2.6.1	PRELIMINARY QUALITY CONTROLS OF TOTAL RNAs	67
2.6.1.1	Total RNA was of high quality	67

2.6.1.2	Absence of PCR inhibitors	68
2.6.2	NORMALISATION OF INDIVIDUAL MIRNA ASSAYS	70
<b>2.7</b>	<b>ENZYME LINKED-IMMUNOSORBENT ASSAYS</b>	<b>70</b>
2.7.1	GENERAL ELISA PROTOCOL USED FOR THE DETECTION OF THE FOUR MIRNA TARGETS	71
2.7.2	STANDARD CURVE ANALYSIS	71
<b>2.8</b>	<b>HUMAN <i>IN VITRO</i> SKIN EXPLANT MODEL FOR GVHR</b>	<b>72</b>
2.8.1	EXPERIMENTAL SET-UP OF THE IN VITRO SKIN EXPLANT ASSAY	72
2.8.2	HISTOPATHOLOGY	73
<b>2.9</b>	<b>TRANSFECTION EXPERIMENTS</b>	<b>74</b>
2.9.1	TRANSFECTION BASICS	74
2.9.2	TRANSFECTION NEGATIVE CONTROLS AND INHIBITORS	74
2.9.3	CYTOSPIN	75
2.9.4	MICRORNA INHIBITION EXPERIMENTS	75
<b>2.10</b>	<b>T CELL PROLIFERATION ASSAY</b>	<b>76</b>
<b>2.11</b>	<b>MIXED LYMPHOCYTE REACTION ASSAY</b>	<b>76</b>
2.11.1	MIXED LYMPHOCYTE REACTION STIMULATED WITH CYCLOSPORINE A	77
2.11.2	PBMCs STIMULATED WITH IFN- $\gamma$	77
<b>2.12</b>	<b>SEMI-QUANTITATION OF C-MYC AND P53 PROTEINS</b>	<b>77</b>
2.12.1	IMMUNOHISTOCHEMICAL STAINING	77
2.12.2	SKIN HISTOPATHOLOGICAL SCORING	78
<b>2.13</b>	<b>CELL IMAGING</b>	<b>78</b>
<b>2.14</b>	<b>STATISTICAL ANALYSIS</b>	<b>79</b>
2.14.1	GENERAL STATISTICS USED IN THE INVESTIGATIONS	79
2.14.2	RECEIVER OPERATING CHARACTERISTIC CURVES	79
2.14.3	HOMOGENEITY OF VARIANCE	81
2.14.4	MODEL BUILDING	81
<b>2.15</b>	<b>INGENUITY PATHWAY ANALYSIS</b>	<b>82</b>
2.15.1	DATA SOURCE	82
2.15.2	ANALYSES CRITERIA	83
2.15.3	ANNOTATION OF FOCUS GENES	83
2.15.4	FUNCTIONAL ANALYSES OF DATA SETS AND NETWORKS	83
2.15.5	CANONICAL PATHWAY ANALYSES	83

**CHAPTER 3. PATHWAY MINING OF CANDIDATE GENES ASSOCIATED WITH GRAFT-VERSUS-HOST DISEASE** ----- **85**

<b>3.1</b>	<b>INTRODUCTION</b>	<b>86</b>
3.1.1	SPECIFIC STUDY AIMS	87
<b>3.2</b>	<b>RESULTS</b>	<b>88</b>
3.2.1	ANNOTATION OF THE FOCUS GENES	89
3.2.2	NETWORK ANALYSIS OF THE FOCUS GENES	89
3.2.3	FUNCTIONAL ANALYSES OF THE FOCUS GENES	94
3.2.4	CANONICAL PATHWAY ANALYSES	99
3.2.5	MORE THAN 1000 MICRORNAs TARGET THE 18 GENES	101
<b>3.3</b>	<b>DISCUSSION</b>	<b>103</b>

**CHAPTER 4. MICRORNA EXPRESSION IN CLINICAL SKIN BIOPSIES OF ALLOGENEIC STEM CELL TRANSPLANTATION PATIENTS -----109**

**4.1 INTRODUCTION ----- 110**

4.1.1 CUTANEOUS AGVHD-----110

4.1.2 MICRORNAS IDENTIFIED AS BIOMARKERS OF AGVHD -----112

4.1.3 SPECIFIC STUDY AIMS -----114

**4.2 RESULTS ----- 115**

4.2.1 GLOBAL MICRORNA EXPRESSION PROFILE OF CUTANEOUS BIOPSIES -----115

4.2.1.1 Study cohort -----115

4.2.1.2 Data analyses-----118

4.2.1.3 Grading system for determination of miRNA signature list -----120

4.2.1.4 Overall clinical aGVHD grade does not correlate with histopathological grade-----121

4.2.1.5 Distinct microRNA expression clusters exist between post allo-HSCT and normal skin biopsies-----122

4.2.2 COMPARISONS USING OVERALL CLINICAL AGVHD GRADES -----125

4.2.2.1 MicroRNA signature list identified using overall clinical aGVHD grades -----125

4.2.3 COMPARISONS USING SKIN HISTOPATHOLOGICAL AGVHD GRADES -----127

4.2.3.1 MicroRNA signature list was determined using the skin histopathological aGVHD grades-----127

4.2.3.2 Five of the miRNAs selected for further validation were predicted to target the 18 genes-----131

4.2.3.3 Twelve microRNAs were selected for further validation -----133

4.2.4 REAL-TIME PCR BASED MICRORNA ARRAYS AND INDIVIDUAL RT-QPCR ASSAYS AGREED WITH EACH OTHER-----134

4.2.5 VALIDATION OF THE SIGNATURE MICRORNA LIST -----136

4.2.5.1 Study cohort -----136

4.2.5.2 Data analyses-----139

4.2.5.3 Five miRNAs were significantly differentially expressed between pre- and post allo-HSCT skin biopsies independent of aGVHD grading system-----139

4.2.5.4 Let-7c-5p, miR-503-5p and miR-365a-3p were differentially expressed in the skin biopsies post allo-HSCT-----140

4.2.5.5 MiR-34a-5p was over-expressed post allo-HSCT and its expression positively correlated with miR-34a-3p expression in the skin biopsies -----142

4.2.5.6 MiR-34a-5p showed the most significant trend with regards to aGVHD severity -----144

4.2.6 COMPARISONS BETWEEN MICRORNA EXPRESSION LEVELS, THE NUMBER OF NECROTIC CELLS AND INFLAMMATORY CELL INFILTRATES -----144

4.2.6.1 The number of necrotic cells positively correlated with skin histopathological aGVHD grade-----145

4.2.6.2 Three microRNA expression levels negatively correlated with the number of inflammatory cell infiltrates-----146

4.2.7 ASSOCIATION BETWEEN MICRORNA EXPRESSIONS WITH OVERALL SURVIVAL-----147

4.2.7.1 Study cohort -----147

4.2.7.2 Data analyses-----148

4.2.7.3	Lower miR-503-5p and miR-34a-3p expressions are associated with improved overall survival-----	150
4.2.7.4	Association of clinical risk factors with overall survival -----	155
4.2.8	ASSOCIATION OF MICRORNA EXPRESSION WITH RELAPSE -----	158
4.2.8.1	Study cohort -----	158
4.2.8.2	Data analyses -----	158
4.2.8.3	Let-7c-5p expression may have a protective role against relapse -----	160
4.2.9	MODEL FOR MICRORNA EXPRESSION LEVELS-----	162
4.2.9.1	Significant interaction between miR-503-5p and miR-34a-3p-----	162
<b>4.3</b>	<b>DISCUSSION -----</b>	<b>165</b>

## **CHAPTER 5. THE FUNCTIONAL ROLE OF MIR-34A IN ALLOGENEIC HAEMATOPOIETIC STEMS**

### **CELL TRANSPLANTATION ----- 174**

<b>5.1</b>	<b>INTRODUCTION-----</b>	<b>175</b>
5.1.1	STUDY HYPOTHESIS -----	178
5.1.2	SPECIFIC STUDY AIMS -----	180
<b>5.2</b>	<b>RESULTS -----</b>	<b>181</b>
5.2.1	STUDY COHORT -----	181
5.2.2	DATA ANALYSES-----	181
5.2.3	IMMUNOHISTOCHEMICAL ANALYSES OF C-MYC AND P53 PROTEINS-----	182
5.2.3.1	c-Myc and p53 positive-cells were present in cutaneous biopsies of allo-HSCT patients--	182
5.2.3.2	P53 positively correlated with miR-34a-5p expression-----	185
5.2.4	SILENCING THE EXPRESSION OF MIR-34A IN PRIMARY PERIPHERAL BLOOD MONONUCLEAR CELLS-----	187
5.2.4.1	PBMCs were viable post-transfection -----	187
5.2.4.2	PBMCs had the optimal transfection when electroporated at 350Vs -----	188
5.2.4.3	PBMCs had the highest transfection when 500 nM of miRNA inhibitor was used -----	190
5.2.4.4	Preliminary miR-34a knockdown results-----	191
5.2.4.5	Preliminary miR-34a-5p functional impact on T cell proliferation-----	192
5.2.4.6	MiR-34a expression was not differential in the in vitro skin explant model with regards to GVHR severity -----	194
5.2.4.7	Stimulation with Cyclosporine A had no direct impact on miR-34a expression levels -----	195
<b>5.3</b>	<b>DISCUSSION -----</b>	<b>197</b>

## **CHAPTER 6. EXPRESSION OF MIRNAS WITH SPECIFIC IMMUNE FUNCTIONS IN THE WHOLE**

### **BLOOD OF ALLO-HSCT PATIENTS ----- 201**

<b>6.1</b>	<b>INTRODUCTION-----</b>	<b>202</b>
6.1.1	IMMUNE SPECIFIC MIRNAS: MIR-146A AND MIR-155-----	202
6.1.1.1	MiR-146a function and known mechanism of action-----	203
6.1.1.2	MiR-155 functions and known mechanism of action -----	206
6.1.2	SPECIFIC STUDY AIMS -----	209
<b>6.2</b>	<b>RESULTS -----</b>	<b>210</b>
6.2.1	STUDY COHORT -----	210
6.2.2	DATA ANALYSES-----	212

6.2.3	ASSOCIATIONS WITH AGVHD INCIDENCE AND SEVERITY -----	213
6.2.3.1	Acute GVHD incidence was significantly predictable using miRNA expression levels -----	213
6.2.3.2	Variance was equal and multicollinearity absent across all groups-----	215
6.2.3.3	The interaction between miR-146a-5p and miR-155-5p was significant in predicting aGVHD incidence at day+28 post allo-HSCT-----	216
6.2.3.4	Acute GVHD severity was not predictable when using miRNA expression levels -----	217
6.2.4	ASSOCIATIONS WITH RELAPSE, OS AND NRM -----	219
6.2.4.1	MiR-146a-5p and miR-155-5p expression in whole blood was not associated with relapse-----	219
6.2.4.2	Low miR-146a-5p expression was associated with better overall survival-----	221
6.2.4.3	HLA class I mismatches was associated with risk of death -----	223
6.2.4.4	Clinical risk factors were associated with relapse and non-relapse mortality-----	225
6.2.5	CORRELATION ASSESSMENT BETWEEN THE MIRNAS AND THEIR TARGETS -----	227
6.2.5.1	Positive correlation was present among miR-146a targets at the mRNA level both at pre and post allo-HSCT time-points -----	227
6.2.5.2	IRF5 mRNA expression positively correlated with its protein levels measured in whole blood at Day+28 in aGVHD patients-----	228
6.2.5.3	In the whole blood of aGVHD patients at Day+28, MiR-155-5p and miR-146a expression correlated with the transcription factor, SPI1 -----	229
6.2.6	MICRORNA EXPRESSION LEVELS BETWEEN NORMAL VOLUNTEERS AND TRANSPLANT PATIENTS -----	230
6.2.7	IN VITRO STIMULATION STUDIES ASSESSING THE IMPACT OF MIRNA EXPRESSION LEVELS -----	231
6.2.7.1	MiR-146a-5p expression declines upon stimulation with IFN- $\gamma$ -----	231
6.2.7.2	Stimulation with Cyclosporine A had no direct impact on miRNA expression levels -----	233
<b>6.3</b>	<b>DISCUSSION -----</b>	<b>235</b>
 <b>CHAPTER 7. CONCLUDING REMARKS AND FUTURE WORK -----</b>		<b>242</b>
 <b>7.1 INTRODUCTION -----</b>		<b>243</b>
7.1.1	EIGHTEEN GENES WERE ASSOCIATED WITH IMMUNE-RELATED, INFLAMMATORY, HEMATOLOGICAL AND CUTANEOUS CONDITIONS -----	244
7.1.2	SCREENING EXPERIMENT IN SKIN BIOPSIES: MiR-503-5P, MiR-34A AND LET-7C-5P WERE ASSOCIATED WITH ALLO-HSCT OUTCOMES -----	245
7.1.3	MIR-34A-5P POSITIVELY CORRELATED WITH P53-POSITIVE CELLS IN THE EPIDERMIS -----	245
7.1.4	WHOLE BLOOD INVESTIGATION OF IMMUNE-SPECIFIC MIRNAS: MiR-146A-5P AND MiR-155-5P WERE ASSOCIATED IN THE PREDICTION OF AGVHD INCIDENCE-----	246
 <b>APPENDIX I -----</b>		<b>249</b>
 <b>APPENDIX II -----</b>		<b>252</b>
 <b>ETHICS APPROVAL FOR WHOLE BLOOD STUDY -----</b>		<b>258</b>
 <b>ETHICS APPROVAL FOR THE SKIN STUDY: PRE- AND POST ALLO-HSCT BIOPSIES -----</b>		<b>261</b>

**ETHICS APPROVAL FOR THE SKIN STUDY: HEALTHY VOLUNTEERS SKIN BIOPSIES----- 264**

**BILIOGRAPHY ----- 266**



# Chapter 1. Introduction and Study Aims

“Facts are the air of scientists. Without them, you can never fly.”

**-Linus Pauling**

**Sections of this chapter have been published in a review article.**

Atarod, S. and Dickinson, A.M. (2013). MicroRNAs: the missing link in the biology of graft-versus-host disease? *Frontiers in Immunology* 4.

## 1.1 Haematopoietic Stem Cell Transplantation

As a consequence of the nuclear power development and the Cold War, individuals were affected by high doses of radiation. This led to haematopoietic stem cell transplantation (HSCT) being used for the treatment of patients exposed to these radiations (Welniak *et al.*, 2007). Investigations by Lorenz *et al.* (Lorenz *et al.*, 1952) showed that the intravenous injection of bone marrow in mice exposed to lethal doses of radiation was the cure. As a result, complete depletion of bone marrow cells using high doses of radiation and intravenous administration of bone marrow from genetically identical or non-identical mice was used to treat experimental tumors (Welniak *et al.*, 2007). However, it was Thomas and colleagues (Thomas *et al.*, 1957) who carried out the first human allogeneic haematopoietic stem cell transplantation (allo-HSCT) more than 50 years ago, on six patients. The patients were subjected to radiation and had undergone chemotherapy as part of the treatment regimen (Thomas *et al.*, 1957). Tragically, all the patients developed severe graft-versus-host disease (GVHD) and failed to survive (Appelbaum, 2007). The first successful non-identical sibling allo-HSCT was performed in 1968 (Fredhutch.org, 2014). Since then, allo-HSCT has become the treatment of choice to cure numerous haematological neoplasia and diseases. At present more than 25,000 allo-HSCTs are carried out globally, with a transplant mortality rate (time to death without disease relapse) of 25% (7-9% for matched sibling and 22% for matched unrelated donor) (Pasquini MC, 2011).

Patients undergo allo-HSCT when either their bone marrow or immune system is impaired. Allo-HSCT is a treatment of choice under specific conditions for haematological malignancies such as acute myeloid leukemia, non-hodgkins and hodgkins lymphoma . Therefore, only patients who are non-responsive to chemotherapy or earlier treatments (refractory) and those who have had disease relapse undergo allo-HSCTs. There are still serious complications associated with transplantation such as disease relapse, GVHD, graft rejection and infections as a consequence of long-term immune-suppression (Welniak *et al.*, 2007). The extent of the complications vary depending on the disease type, stage of diagnosis, age of the

transplant patient, overall health of the patient and the relationship of donor to patient (Passweg *et al.*, 2004; Gratwohl, 2012).

Until the 1990s, bone marrow (BM) was the only source of donor haematopoietic stem cells (HSCs) and it was only in 1995 that peripheral blood (PB) products were reported as a source of HSCs (Schmitz *et al.*, 1995). Since the last two decades, umbilical cord blood (UCB) has been recognized as a rich source of HSCs and this was initially used for paediatric allo-HSCT, due to the limited volume of the product (Wagner *et al.*, 1995). It was in 2004 that UCB from unrelated donors were first successfully transplanted in adults.

## **1.2 Graft-Versus-Host Disease**

Graft-Versus-Host Disease is still the major risk factor of any allo-HSCT, irrespective of the improvements made in treatment methods, Human Leukocyte Antigen typing (HLA) (Section 1.3.1), patient support and earlier diagnosis of the haematological disorder. The complexity of GVHD is further expanded with the manifestation of the disease in two classes; acute and chronic phase. However, Graft-Versus-Host Reaction (GVHR) is present in all allo-HSCTs regardless of the risk factors. The overall incidence of GVHD is approximately 50% in allo-HSCT patients (Pavletic and Fowler, 2012). Acute GVHD (aGVHD) has been classically described as onset within the first 100 days of transplantation (Shlomchik, 2007) [incidence of moderate to severe aGVHD grade II-IV being 39% in sibling donors and 59% in Matched Unrelated Donor (MUD)] (Jagasia *et al.*, 2012) where damage is seen in the skin, liver and gastrointestinal tract. Chronic GVHD (cGVHD) classically occurs after 100 days post-transplant (Shlomchik, 2007) in 40% of HLA identical sibling transplants, 50% of HLA non-identical sibling transplants and 70% of MUD transplants (Apperley and Masszi, 2012). Acute and cGVHD vary in pathophysiology, etiology and response to treatment regimens (Welniak *et al.*, 2007). Acute GVHD is commonly characterized by a T-helper 1 (Th1)-type cellular response (Mohty *et al.*, 2005), while cGVHD may resemble autoimmune disorders as the balance between B-cells is disturbed which results in elevated levels of B-cell Activating Factor (BAFF) (Graze and Gale, 1979; Sarantopoulos *et al.*, 2009). However, aGVHD and cGVHD have been observed to overlap, making an accurate diagnosis between them

difficult. This simultaneous presentation of acute and cGVHD after day 100 has been termed as 'overlap syndrome' (Filipovich *et al.*, 2005). The incidence of overlap syndrome appears to be increasingly common due to improved treatment methods (calcineurin inhibitors and reduced intensity conditioning regimens) (Welniak *et al.*, 2007). Moreover, involvement of populations of regulatory T cells (Treg), regulatory Antigen Presenting Cells (APCs), regulatory B cells (Breg) (Shimabukuro-Vornhagen *et al.*, 2009) and Mesenchymal Stem Cells (MSCs) have further extended the pathophysiological complexity of aGVHD.

### **1.2.1 Pathophysiology of aGVHD**

According to the classical model of aGVHD, there are three quite distinct phases in the development of the disease. The first two phases are the afferent phase while the third phase is the efferent phase of GVHD (Antin and Ferrara, 1992; Krenger *et al.*, 1997).

**Phase 1: Effects of Conditioning Regimen:** The primary phase of aGVHD begins when the patient is undergoing conditioning therapy prior to transplantation (Figure 1.1). There are various conditioning treatments involved, including; irradiation and chemotherapy, all of which cause damage to the host tissues depending on the toxic level of the treatment (Jaksch and Mattsson, 2005). As a consequence, the host tissues signal the presence of injury to the immune system via the generation of cytokines, chemokines and adhesion molecules (Ferrara, 1993). The host epithelium is damaged due to conditioning regimens resulting in the cytokine storm ( TNF- $\alpha$  and IL-1) via the endothelium (Xun *et al.*, 1994). The signals generated cause the host APCs such as Dendritic Cells (DC) to be stimulated (Matzinger, 2002). Endotoxins such as Lipopolysaccharides (LPS) are also translocated across the damaged intestinal mucosa, resulting in a further activation of the host's innate immune system and cytokine storm (Teshima and Ferrara, 2002). There are 11 Toll-like receptors (TLRs 1-11) that recognize different pathogens as part of the innate immune system (Takeda and Akira, 2005). LPS is recognized by TLR4 (Pålsson-McDermott and O'Neill, 2004) (See Section 6.1.1.1)

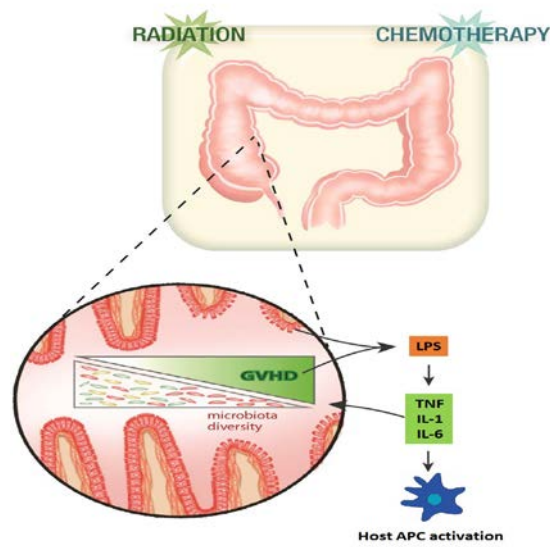


**Figure 1.1 Conditioning regimen damages the host tissues** (adopted from (Markey *et al.*, 2014)). In Phase 1, the gut homeostasis of the allo-HSCT patient is distorted due to either radiation and/or chemotherapy. Danger and/Pathogen Associated Molecular Patterns (DAMPs/PAMPs) and LPS are released in the blood. Following this, the recipient cells secrete proinflammatory cytokines such as TNF, IL-1 and IL-6. The cytokines activate the host APCs both in the gut and lymphatics.

**Phase 2:** Activation of Donor T cells: As a result of the cytokine storm naïve donor CD4+ T cells are recruited, activated and expanded leading to interaction with host APCs (Figure 1.2). At this stage, DCs initiate GVHD and prime naïve T cells (Matzinger, 2002). The level of T cell response depends on the disparity between the donor and recipient major (MHC) and minor histocompatibility complexes. CD8+ T cells are activated by the variations in MHC class I and CD4+ T cells by MHC class II (Sprent *et al.*, 1988). The recipient haematopoietic APCs activate the donor CD8+ T cells while, in the gut, the non-haematopoietic APCs can activate the donor CD4+ T cells for the induction of aGVHD (Koyama *et al.*, 2012).

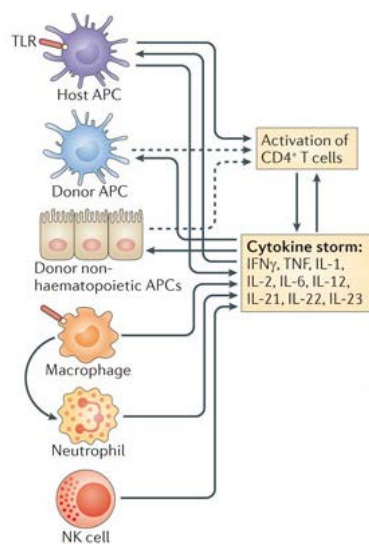


**Figure 1.2 Donor T cells are activated by APCs** (adopted from (Blazar *et al.*, 2012)). The Phase 2 of aGVHD pathophysiology involves the priming and activation of T cells in the graft which results in the release of several cytokines such as IFN- $\gamma$ , TNF, IL-1, IL-2, IL-6, IL-12, IL-21, IL-22 and IL-23. This cytokine storm initiates the differentiation of T-cells along various lineages. Natural Killer (NK) cells and neutrophils also secrete cytokines that further damages host tissues.

**Phase 3:** The efferent phase: In this phase, the donor T cells are involved in specific as well as non-specific mechanisms to cause further injury to the host tissues. Secretion of inflammatory cytokines such as TNF-  $\alpha$ , IL-1 and macrophage- derived nitric oxide (NO) as well as the involvement of cytotoxic T lymphocytes (CTLs) with Fas- and perforin- mediated mechanisms, NK cells and large granular lymphocytes (LGLs) leads to development of a complex cascade in the efferent phase (Reddy and Ferrara, 2003). The interaction of innate Large Granular Lymphocytes (LGL) and allo-reactive T-cells (CD8+) results in organ damage.

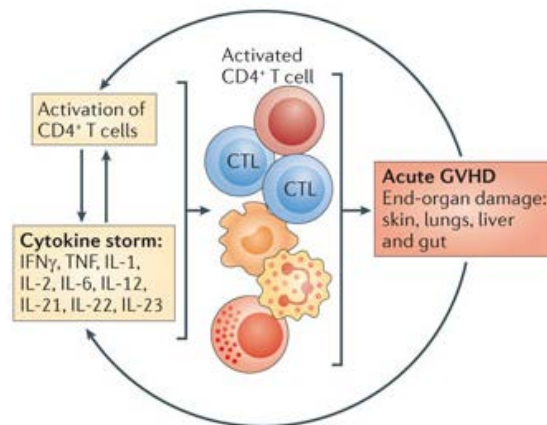


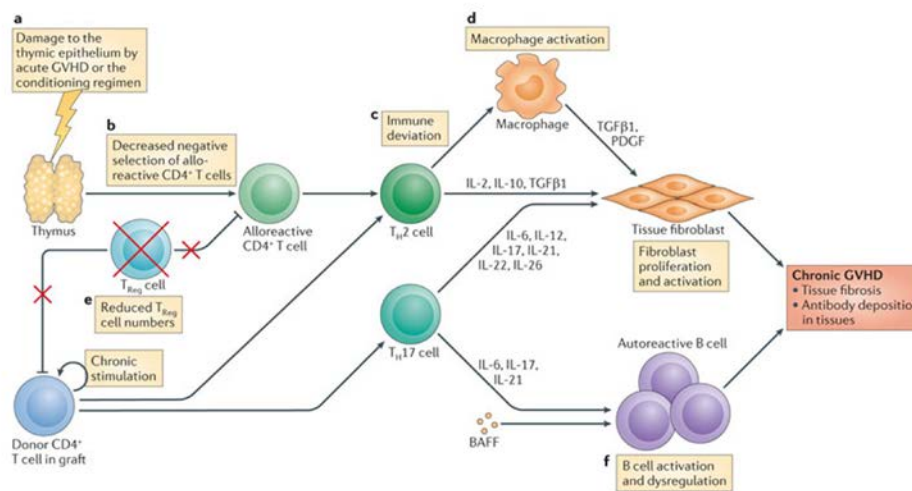
**Figure 1.3** Cytotoxic T cells and NK cells cause end organ damage in the host (adopted from (Blazar *et al.*, 2012)). In Phase 3, as a result of the cytokine storm and continuous activation of T cells damage is caused to several host organs such as the skin, lungs, liver and gut.

### **1.2.2 Pathophysiology of cGVHD**

More than 50% of allo-HSCT patients suffer from cGVHD (NIH consensus disease classification), with the long-term survivors of the transplant experiencing major complications and a high rate of mortality (Socie and Ritz, 2014). Chronic GVHD can manifest simultaneously from aGVHD, develop after treatment of aGVHD or develops as *de novo* disease (Shimabukuro-Vornhagen *et al.*, 2009). As mentioned earlier, classically, cGVHD develops after 100 days and up to three years post allo-HSCT.

There are several risk factors that are attributed to the development of cGVHD including; disparity in HLA typing, source of stem cells, exhibition of aGVHD, age and patient/ donor gender (Carlens *et al.*, 1998). The use of Peripheral Blood Stem Cells (PBSCs) has been accounted for an increased risk of cGVHD (Mohty *et al.*, 2002).

Chronic GVHD can manifest in several organs of which the main ones are, the liver, gut, skin, lungs and mucous membranes. It may also involve serous membranes and exocrine glands, which leads to the disease resembling collagen vascular diseases (Deeg and Storb, 1986). Chronic GVHD is more complex with no distinguishable phases as in aGVHD, therefore, making accurate diagnosis more difficult. The main players in cGVHD are the donor T and B cells (Socie and Ritz, 2014). Studies have shown that low Treg level was associated with higher cGVHD incidence (Zorn *et al.*, 2005). Activation of tissue fibroblasts by Transforming Growth Factor beta (TGF $\beta$ ) caused fibrosis that is the chief hallmark of cGVHD (Socie and Ritz, 2014). The main stages and key factors involved in cGVHD are depicted in Figure 1.4.



Nature Reviews | Immunology

**Figure 1.4 Chronic GVHD pathophysiology** (Blazer, Murphy, et al., 2012). (a) Damage to thymic epithelium either due to a prior aGVHD incidence or damage caused during the conditioning regimen (b) Lower allo-reactive CD4<sup>+</sup> T cells (c) Deactivation of immune cells T helper 2 cells and T helper 17 cells (d) Activation of macrophages results in the secretion of TGFβ that enhances fibrosis in host tissues (e) Reduction in regulatory T cells (f) Activation of B cells which leads to higher levels of BAFF (B cell activating Factor) in cGVHD patients.

### 1.2.3 Histopathology and grading of GVHD

The main histologic feature of GVHD is the observance of apoptotic cells in the epithelial layer of skin, intestine and biliary duct as well as basal and suprabasal layer of the epidermis. Skin biopsies are mainly used to diagnose GVHD while gut biopsies are taken to analyze the gastrointestinal symptoms of transplant patients. Liver biopsies can provide further information on whether the patient is suffering from a viral infection, experiencing drug toxicity or hepatic GVHD (Devergie, 2008). However, liver biopsies are rarely taken while skin and gut biopsies are more frequently taken from patients.

### **1.2.3.1 Grading of aGVHD**

Classically, patients were diagnosed with aGVHD if they developed histopathological and clinical symptoms within 100 days post allo-HSCT. Acute GVHD has been graded since 1974 according to the guidelines set by Glucksberg and the aGVHD consensus in 1994 (Glucksberg H, 1974; Przepiorka *et al.*, 1995). In the Glucksberg classification system, the skin, liver and gut are staged from 0 to IV (Table 1.1). The sum of the stages is then used to calculate an overall clinical grade for the GVHD patient (Table 1.2). Nearly 25% of patients manifesting grade III GVHD survive while only 5% of those with grade IV GVHD survive (Cahn *et al.*, 2005). However, the National Institute of Health (NIH) consensus criteria is commonly used now and it classifies aGVHD taking into consideration the time of disease onset as well as symptoms (Filipovich *et al.*, 2005). The NIH criteria categorizes aGVHD into two distinct groups, (1) **classic aGVHD** that manifests within 100 days post allo-HSCT and present the clinical features associated with aGVHD and (2) **persistent, recurrent, late onset aGVHD** which develops after 100 days post allo-HSCT and presents with aGVHD symptoms (Table 1.3). In both groups, cGVHD is absent in patients at the time of aGVHD diagnosis. If cGVHD is present, the disease is classed as overlap syndrome. Acute GVHD presents with various intensities that are classified into mild, moderate and severe based on the severity of histopathological and clinical symptoms presented in the patients at the time of diagnosis (Filipovich *et al.*, 2005).

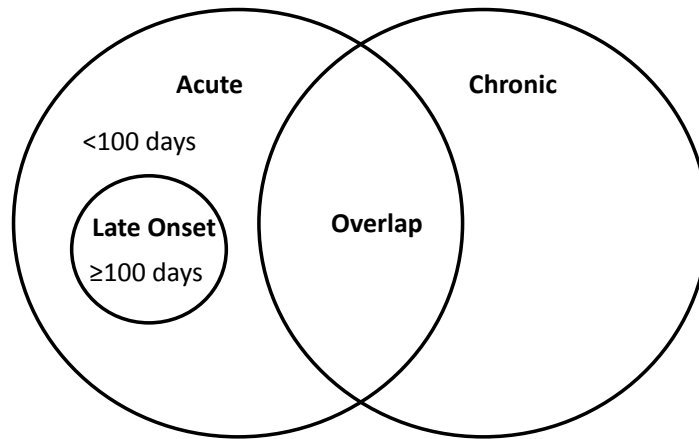


**Figure 1.5 Classification of aGVHD as per the NIH consensus criteria** (adopted from (Pasquini, 2008)). The Venn diagram shows classic aGVHD and persistent, recurrent or late aGVHD onset as two groups within aGVHD. It also shows the overlap syndrome which is the presentation of both aGVHD and cGVHD features at the time of disease diagnosis.

Grading System: Stage for each organ			
Stage	Skin (Maculo-papular rash %)	Liver (Bilirubin mg/dL)	Gut (Diarrhoea mL/d)
0	No rash	<2	None
1	<25% of body surface	2 to <3	>500- 1000
2	25-50% of body surface	3 to <6	>1000 - 1500
3	Generalised erythroderma	6 to <15	>1500
4	Generalised erythroderma with bullae formation & desquamation	≥ 15	Severe abdominal pain with or without lieus involvement

**Table 1.1 Clinical aGVHD staging system for each organ** (adopted from (Przepiorka *et al.*, 1995)).

Glucksberg: Overall Grading System		
Grade	Severity	Degree of organ involvement
0	None	None
I	Mild	Skin: 1-2
II	Moderate	Skin:3
		Gut and/or liver:1
		Mild decrease in clinical performance
III	Severe	Skin: 2-3
		Gut and/or Liver: 2-3
		Marked decrease in clinical performance
IV	Life threatening	Skin: 2-4
		Gut and/or Liver: 2-4
		Extreme decrease in clinical performance

**Table 1.2 Overall clinical aGVHD grading system for each organ** (adopted from (Przepiorka *et al.*, 1995; Pavan and Reddy, 2013)).

GVHD Classification	Category	Time of symptoms after HSCT or DLI	aGVHD features	cGVHD features
Acute	Classic	≤100 days	Yes	No
	Persistent, recurrent or late onset	>100 days	Yes	No
Chronic	Classic	No time limit	No	Yes
	Overlap syndrome	No time limit	Yes	Yes

**Table 1.3 Acute and chronic GVHD categories based on the NIH consensus** (Filipovich *et al.*, 2005).

### **1.2.3.2 Classification of cGVHD**

Classically, cGVHD was categorized as per the Seattle study (Shulman *et al.*, 1980) into limited and extensive. This system only considered the number of organs or sites involved in the disease and not severity (Socie, 2009). Nowadays, cGVHD is classified based on the presentation of diagnostic features as per the NIH consensus (Filipovich *et al.*, 2005) as well as a distinctive difference from aGVHD. At least one symptom is required in order to class the disease as cGVHD. This classification has a scoring system where both the organ and/or the site of cGVHD involvement are scored (0-3). The primary organs that manifest cGVHD features are; skin, nails, scalp and body hair, mouth, eyes, genitalia, liver, gastrointestinal tract, lungs, joints and fascia (Pavan and Reddy, 2013). Disease severity is classified into mild, moderate and severe which is the summation of organ and site scores (Filipovich *et al.*, 2005).

## **1.3 Important Cells, Cytokines and Chemokines Involved in the Pathogenesis of GVHD**

### **1.3.1 Human leukocyte antigens**

Human Leukocyte Antigens (HLAs) are polymorphic and are expressed by the Major Histocompatibility Complex (MHC) (Figure 1.6). There are three classes of HLA proteins of which HLA class I; A, B and C are present in all nucleated cells, class II: DR, DQ and DP are expressed on haematopoietic cells (York IA, 1996; Boss, 1997) and class III: encode the components of the complement system (Beck and Trowsdale, 2000). HLA class II proteins can also be stimulated by other types of cells as a consequence of inflammation or damage to the cells. Siblings have a 25% possibility of being a match at all the MHC loci while parents and other family members can differ from zero to three loci at HLA-A, HLA-B and HLA-DR on the second haplotype. It is the mis-matching of the HLA proteins between the donor and the recipient that result in the manifestation of aGVHD in bone marrow transplantations (Lee *et al.*, 2007). However, minor histocompatibility antigens are also present and are encoded outside of the MHC locus. The minor histocompatibility antigens are polymorphic peptides that arise

due to either SNPs or gene deletions. They are immunogenic and bind to the HLA class I or class II receptors and are thereby presented to the T-cells (Dzierzak-Mietla *et al.*, 2012). It is the disparity between the donor and recipient's minor histocompatibility antigens that further increases the incidence of GVHD in matched unrelated transplantations in comparison to identical donor grafts (Welniak *et al.*, 2007). However, approximately, 40% of recipients who have undergone HLA-identical or matched sibling transplants may still develop GVHD (Ferrara *et al.*, 2009).

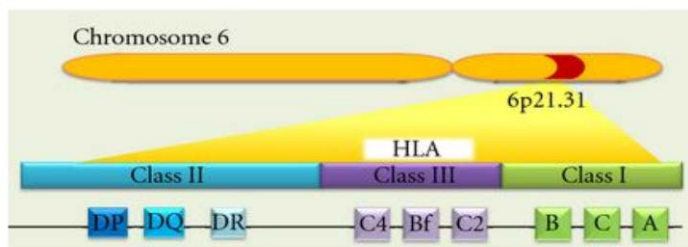


**Figure 1.6 The Major Histocompatibility Complex** (adopted from (Ayala *et al.*, 2012)). The MHC complex is present on the p arm of Chromosome 6. It encodes for the three classes of HLA; class I, II and III. HLA class I are present on all nucleated cells while HLA class II are present only on monocytes and macrophages as well as on B, activated T, dendritic, endothelium and epithelial cells. HLA class III encodes the genes of the complement system.

### 1.3.2 Human killer cell immunoglobulin-like receptors

Human Killer Cell Immunoglobulin-like Receptors (KIR) have also been recently associated with the risk of GVHD. KIRs are inherited independent of HLA and are expressed on natural killer cells (NK) (Welniak *et al.*, 2007) as well as on a subset of activated T cells, mainly the CD8+ cells (Mingari *et al.*, 1996; Mingari *et al.*, 1998). KIRs recognize HLA-A, HLA-B, and HLA-C alleles and function both as an inhibitor and an activator (Barao and Murphy, 2003). Activation of NK cells is regulated by the balance of signals (inhibitory and activator) generated from KIRs and other NK cell receptors. It is this activation that affects GVHD (Ruggeri *et al.*, 2002). In some instances, KIR/KIR ligand incompatibilities have been demonstrated to affect graft rejection, GVHD and Graft-Versus-Leukemia effect (GVL) (Ruggeri *et al.*, 2002)

### 1.3.3 Donor T-cell activation

There are several signals that can co-stimulate T cells (Figure 1.7). Engagement of T cell receptors with specific antigens presented by MHC molecules (autologous MHC for bacterial or virus induced T cell response; allogeneic & autologous MHC for allo-antigen stimulated T cell response - GVHD pertains to the allo-antigen stimulated T cell response). The second critical signal is from the engagement of CD28 expressed on T cells with CD80 and CD86 expressed on APCs. Both first and second signal must exist to induce T cell activation. In the absence of the second signal, the presence of the first signal induces T cell anergy rather than T cell activation. The third signal involves the engagement of certain cytokines with corresponding receptors expressed on T cells and/or APCs - an important example is IL-2 and CD25 engagement. The third signal mainly contributes to the polarisation (magnitude) of a T cell response (Yu *et al.*, 1998; Snanoudj *et al.*, 2007).

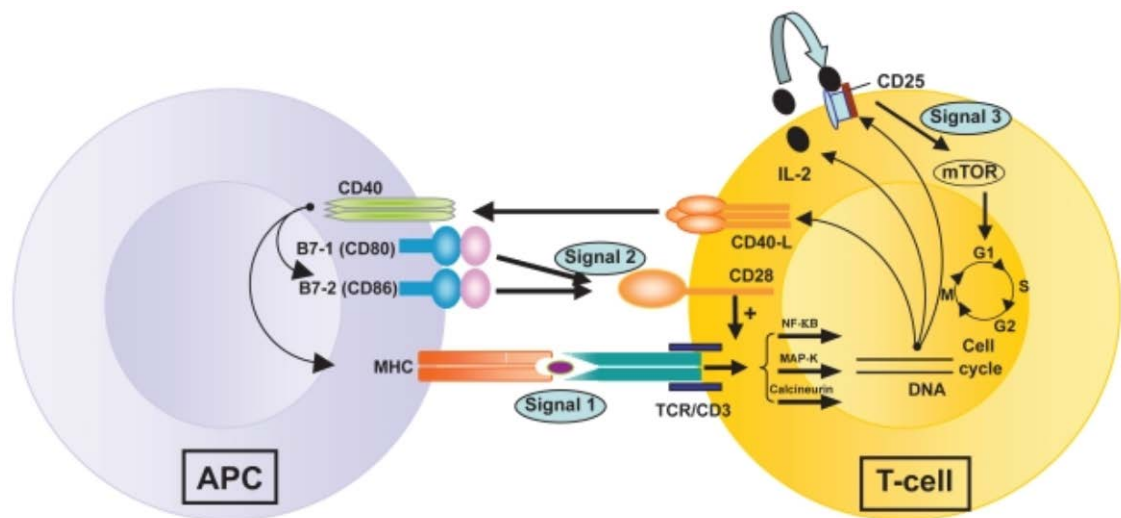


**Figure 1.7 Three signals activate T cells** (adopted from (Snanoudj *et al.*, 2007)). (1) Signal 1 involves the Donor APCs presentation of antigens to T Cell Receptors (TCR) and (2) Signal 2 involves the linkage between donor APCs and the CD28 on T cells. This results in the activation of the Nuclear Factor- $\kappa$ B (NF $\kappa$ B), the mitogen-activated protein (MAP) kinase and the calcium-calcineurin pathway. CD40-L also binds to the CD40 present on APCs that results in antibody secretion and induction of the MHCs and (3) Signal 3 involves the binding of IL-2 to CD25 which activates the mTOR and results in T cell proliferation.

### **1.3.4 Chemokines and cytokines**

Monocytes, macrophages, resident cells, epithelial, endothelial or fibroblastic cells are stimulated by pro-inflammatory cytokines such as IL-1, TNF- $\alpha$  or IFN- $\gamma$  and stimuli such as LPS (Jaksch and Mattsson, 2005). This stimulation results in the expression of inflammatory chemokines in these infiltrated cells. Effector T cells, monocytes and granulocytes are recruited by these inflammatory chemokines. Thus, chemokines as well as their receptors have been shown to be involved in the manifestation of GVHD. Chemokine Receptors; (CCR-number) CCR1, CCR2, CCR3 and CCR5 have all been shown to be associated with aGVHD (Jaksch *et al.*, 2005).

**Interleukins:** IL-2 is the initial cytokine that is involved in aGVHD. This has been established due to its pivotal role as a T cell growth factor and also because inhibition of IL-2 by the prophylactic drug, cyclosporine (CsA) is an effective treatment for aGVHD (Goker H, 2001). Moreover, it has also been shown in both animal and clinical studies that aGVHD can be prevented by administration of monoclonal antibodies against IL-2 after stem-cell transplantation (SCT) (Ferrara *et al.*, 1986). Cytokines such as IL-15 have also been investigated in humans showing that IL-15 could also induce aGVHD by activating T cells and NK cells (Kumaki S, 1998; Xian Chang Li, 2001). IL-1 has been shown in murine investigations to elevate GVHD and increase the risk of transplant related mortality (Atkinson *et al.*, 1991). The main cellular targets of IL-18 are macrophages, NK cells, T cells and B cells. Both Th 1- and Th 2-mediated reactions are influenced by the production of IL-18 (Jaksch and Mattsson, 2005). The effect of IL-18 production or clinical administration on aGVHD varies depending on the type of T cells involved. Min *et al.*, have demonstrated this in a GVHD model study, wherein administration of IL-18 decreased the survival of CD8<sup>+</sup>- mediated GVHD but increased survival in CD4<sup>+</sup>-mediated GVHD (Min *et al.*, 2004).

**IFN- $\gamma$ :** In murine models it has been shown that mice with aGVHD have higher levels of Ifn- $\gamma$  compared to the no-GVHD group (Hill *et al.*, 1997). IFN- $\gamma$  and IL-2 both play a role in T cell proliferation, stimulation of CTL and NK-cell responses, recruitment of mononuclear phagocytes to generate IL-1 and TNF- $\alpha$  (Jaksch and Mattsson, 2005). Moreover, both TNF- $\alpha$  and IFN- $\gamma$  directly cause tissue injury in GVHD (Dickinson AM,

1991). IFN- $\gamma$  suppresses the immune system via stimulation of nitric oxide (NO) and expression of Fas-ligand (Klimpel *et al.*, 1990; Wall DA, 1994). IFN-  $\gamma$  can both reduce and increase GVHD similar to IL-2, depending on the conditions (Heremans H, 1987). Acute GVHD is augmented by IFN- $\gamma$  which leads to the maturation of DC, stimulation of macrophages to generate cytokines and NOs (Jaksch and Mattsson, 2005). However, donor T cell response to host antigens can be reduced through enhancing the expression of Fas receptors on donor T cells, which leads to activated cell death. As a consequence of this the degree of aGVHD is reduced (Yang YG, 1998).

**Granulocyte- Colony Stimulating Factor:** There is contradictory evidence regarding the function of granulocyte colony-stimulating factor (G-CSF) in GVHD. In a murine model of HSCT, pretreatment of donor PBSCs decreased early transplant mortality in aGVHD mice (Pan *et al.*, 1995). The study assumed that as a result of G-CSF treatment, the donor T cells were polarized to Th2 (Pan *et al.*, 1999). However, administration of G-CSF to patients after HSCT actually enhanced the risk of aGVHD and transplant related mortality in patients (Ringdén O, 2004).

### **1.3.5 Cellular components**

**Natural Killer cells:** These cells exhibit effector as well as suppressive effects on aGVHD. Rapidly reconstituted NK cells can be major producers of IFN- $\gamma$ , TNF- $\alpha$  and NO upon induction and as a result associated with tissue injury in GVHD (Ferrara *et al.*, 1989; Filep *et al.*, 1996). On the other hand, in both murine and human models it has been demonstrated that NK cells can inhibit GVHD and enhance GVL effect either by producing TGF- $\beta$  or stimulating its production in other cells (Asai *et al.*, 1998; Ruggeri *et al.*, 2001; Ruggeri *et al.*, 2002).

**Regulatory T cells:** Regulatory T (Tregs) cells comprise only 5-10% of the whole CD4+ T cell population in humans and play a role in GVHD inhibition. However, the results on their mechanism of action are still controversial. Tregs suppress the activation of CD4+ and CD8+ T cells upon directly affecting the target T cells or APCs. Reduction of CD25+ T cells has been shown to increase the development of GVHD in murine models of SCT as reviewed by (Jaksch and Mattsson, 2005) . In mismatched HSCT, it has been demonstrated that Tregs when administered along with conventional T cells can aid in

more rapid immune reconstitution and prevent manifestation of GVHD without a decline in the GVL effect. The patients in the study did not receive any post-transplant immune-suppressive treatment (Di Ianni *et al.*, 2011).

**Regulatory B cells:** Recipient B cells have been shown to inhibit the manifestation of aGVHD by reducing the expansion of CD4+ T cells and repressing Th1 differentiation. The majority of the host B cells are destroyed by the irradiation regimen but those producing IL-10 have been shown to be resistant and thus become APC in the host. Furthermore, regulatory B cells can generate other immunomodulatory cytokines such as TGF $\beta$  that can also inhibit T-cell responses (Mauri and Ehrenstein, 2008).

In a murine study, donor B cells inhibited aGVHD in a MHC-II and Treg-dependent manner. However, the role of B lymphocytes in GVHD has proven to be controversial and interventions by microRNA (miRNA) and proteomic studies are required to further elucidate the main role and mechanism of action of these specialized cells in GVHD (Segalen *et al.*, 2010).

### **1.3.6 Inflammatory effectors**

**Donor T-cell derived TNF-alpha:** Cytotoxic T Lymphocytes are involved via the classical pathways of perforin/granzyme and Fas/FasL (Jaksch and Mattsson, 2005). The function of TNF- $\alpha$  in the pathogenesis of GVHD has been well established and it has been shown to be caused by monocytes and macrophages of donors or the host (Ferrara *et al.*, 1999). Donor-derived TNF has been shown to increase the incidence of GVHD (Cooke *et al.*, 1998; Couriel *et al.*, 2004).

**Macrophage-secreted TNF-alpha:** TNF- $\alpha$  is responsible for numerous inflammatory effects in the immune system such as activating DC, increasing alloantigen presentation and stimulation of inflammatory chemokines and recruitment of neutrophils, T cells and monocytes into the target organs (Jaksch and Mattsson, 2005). It also directly results in tissue damage through necrosis and apoptosis (Wall DA, 1994). It has been shown that serum levels of TNF- $\alpha$  increase in GVHD patients after allo-HSCT (Holler *et al.*, 1990).

**Nitric oxide:** Nitric Oxide (NO) plays an essential function in host defense as well as the antimicrobial and tumouricidal role of macrophages (Jaksch and Mattsson, 2005). In acute GVHD, macrophages are activated as a consequence of increased secretion of IFN- $\gamma$  and accumulation of LPS. This leads to the secretion of inflammatory compounds such as TNF- $\alpha$ , NO and IL-1. High levels of IFN- $\gamma$  have been shown to decrease the levels of LPS needed to induce macrophages to secrete inflammatory products (Gifford GE, 1987; Ding *et al.*, 1988). However, macrophages are primed as a consequence and very low levels of LPS stimulate the macrophages to produce NO and TNF- $\alpha$  (Nestel FP, 1992). NO inhibits immune activation and also inactivates non-heme iron-containing enzymes that are responsible for expansion of epithelial stem cells in the intestine and skin as reviewed by (Jaksch and Mattsson, 2005).

## 1.4 Graft-versus-Host Disease Prophylaxis and Treatment

Both prophylaxis and treatment regimens of GVHD have severe toxic effects on not only the immune system, but the entire biological system of the patient. Thus, extensive care and monitoring of the patient is required to ensure earlier diagnosis and detection of infections as well as to reduce side-effects. Since allo-HSCT patients are immuno-compromised, anti-fungal drugs are administered prophylactically to all patients as a preventive measure against fungal infections (Ferrara *et al.*, 2009). Figure 1.8 illustrates the various time-points for conditioning and prophylaxis in allo-HSCT patients.

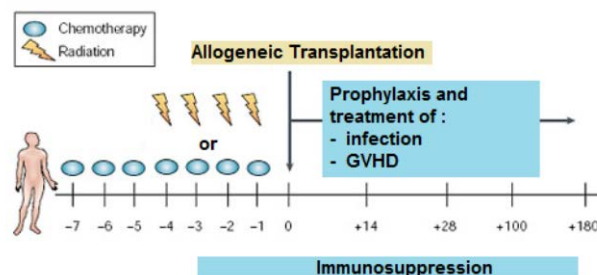


**Figure 1.8** Prophylaxis, treatment and factors influencing the outcome of HSCT, adopted from (Barker and Wagner, 2003a). Chemotherapy and/ radiation start pre-transplant (day -7) as shown in the therapeutic timeline. At day 0, the patients receive HSC and immunosuppressive drugs are administered to patients undergoing allo-HSCT (Barker and Wagner, 2003b).

In some of the present transplant protocols when the patient is predicted of high GVHD risk, T-cell depleted grafts are used for the transplantation procedure. Transplant protocols vary, based on whether the donor is a sibling or MUD. There are also various medications administered to the patients. Calcineurin inhibitors (Cyclosporine A and Tacrolimus) block the production of interleukin (IL)-2 and proliferation of T cells. Cytokine response inhibitors (Rapamycin) expand regulatory T cells. Lympholytic agents such as corticosteroids are administered alone or in combination with the other drugs. *In vivo* T cells depletion is achieved with either anti-thymocyte globulin or humanized antibody against CD25 (CAMPATH-1H) for the control of GVHD as well as graft failure or rejection (reviewed by Welniak *et al.* (Welniak *et al.*, 2007)). Globally, there is a difference between the transplantation protocols in one centre to another which adds to the heterogeneity of disease population studied at the various sites. Therefore, this factor must be considered when analyzing investigations at individual sites and necessitates multi-centre studies to validate findings from one site at another centre.

Steroids are still the current treatment of choice for aGVHD and are included as part of first-line therapy. Topical steroids are administered for the treatment of mild GVHD (Grade I- skin) while systemic steroids are used for more severe GVHD (Ferrara *et al.*, 2009). Studies have shown that the use of steroids for GVHD treatment results in 50% remission in less than half of the patients (MacMillan *et al.*, 2002). However, at the same time steroid refractoriness can be a problem in some patients.

As a primary treatment in some centres, methyl-prednisolone is administered to patients who manifest aGVHD. It has been shown that 25-40% of those with severe aGVHD (II-IV) respond positively to this treatment. In cases where the patient does not respond to the primary treatment regimen, a secondary treatment is administered. For those exhibiting GVHD of the skin phototherapy may be used and in severe visceral GVHD, monoclonal and polyclonal (Atgam and Thymoglobuline) antibodies are administered (Devergie, 2008).

Monoclonal antibodies directly target specific antigens, while the polyclonal antibodies (e.g. Atgam and Thymoglobulin) suppress T lymphocytes and result in their lysis.

Commonly administered monoclonal antibodies are Inolonomab, Basiliximab, Daclizumab, Denileukin Diftox (target IL-2 receptor), Infliximab and Etanercept (target TNF $\alpha$  antibody), CAMPATH-1H/ Alemtuzumab (targets CD25), ABX/CBL (targets CD-147 antibody) and Visilizumab (targets CD3) (Devergie, 2008). Although a major predictor of cGVHD is the manifestation of aGVHD, control and remission of aGVHD has not been shown to be effective in decreasing the risk of cGVHD (Fraser and Scott Baker, 2007).

At present, cyclosporine or tacrolimus are administered for the treatment of cGVHD in combination with prednisolone (Sullivan *et al.*, 1988). Immuno-suppressants used in the treatment of cGVHD are extremely toxic and lead to lower survival of these patients as they tend to suffer more from infections due to the suppression of their immune system.

Presently, no effective secondary treatment is used for patients who have failed the primary treatment regimen (Devergie, 2008). However, extracorporeal photochemotherapy (ECP) has been successful in the treatment of cutaneous and drug-resistant cGVHD as reviewed by (Horwitz and Sullivan, 2006). In addition, recent studies using rituximab which is an anti-CD20 monoclonal antibody have shown promising results (Cutler *et al.*, 2006).

## **1.5 Other allo-HSCT outcomes**

### ***1.5.1 Graft-versus-leukemia/ Graft-versus-tumor effect***

Graft-Versus-Tumor (GVT) effect was recognized as early as 1961 (Reshchikov *et al.*, 1961). Donor T cells not only attack the patient's normal hematopoietic cells but also react against leukemia/ tumor cells resulting in GVL or GVT effect (Weiden *et al.*, 1979). The recognition of restricted minor HLA present on haematopoietic cells by donor T cells may initiate the GVL effect (Figure 1.9). On the other hand, when the donor T cells recognize mismatches in the HLA of recipient epithelial and haematopoietic tissues GVHD is induced (Bleakley and Riddell, 2004). The GVL effect has been clearly demonstrated in studies of relapsed transplant patients with Chronic Myelogenous Leukemia (CML) where in infusion of donor lymphocytes resulted in

remission of the disease in SCT patient (Kolb *et al.*, 1995). As a result of the advantageous effects of GVL, in instances of high relapse risk, donor lymphocyte infusions (DLI) and mobilized donor cells are used as part of an adoptive immunotherapy (Kolb, 2008). Indeed, every patient undergoing the transplant procedure has some degree of GVH reaction otherwise the underlying disease for which the patient had been transplanted for would not be eliminated. Therefore, in the clinic, it is important to maintain the balance between GVH and GVL as this can ensure no disease relapse and patient recovery from cancer.

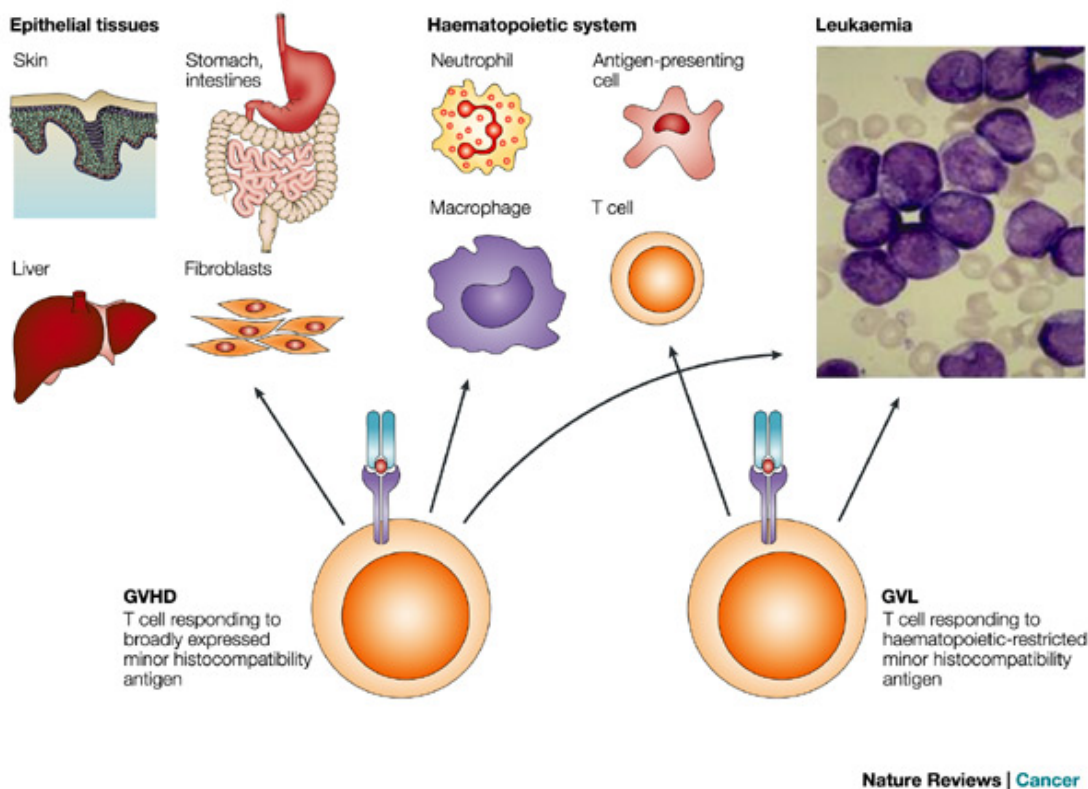


**Figure 1.9 Graft-versus-host reaction in allo-HSCT patient** (adopted from (Bleakley and Riddell, 2004)). GVHR is present in every allo-HSCT patient. However, what may determine the severity and extent of the reaction is the recognition of mismatches by donor T cells in the recipient epithelial and haematopoietic stem cells. When donor T cells react to haematopoietic- restricted minor HLA, GVL effect is induced while when the same cells react to the broadly presented minor HLA, GVHD is initiated. The balance between GVH and GVL effect is crucial in the treatment of allo-HSCT patients.

### 1.5.2 Overall survival, relapse and non-relapse mortality

The ultimate goal of allo-HSCT is to cure patients of the underlying disease. Thus, several outcomes are assessed in addition to GVHD such as disease relapse, overall survival (OS) and non-relapse mortality (NRM). There are three main types of clinical risk factors: pre-transplant, peri-transplant and post-transplant factors (Figure 1.10). Pre-transplant factors are assessed and used to calculate risk scores for patients to predict transplantation outcome and in turn, alter specific allo-HSCT criteria to improve outcome. Peri-transplant factors encompass the transplantation procedure which includes patient-care, the conditioning regimen, GVHD prophylaxis and also the source of stem cells (Bone Marrow/Peripheral Blood Stem Cells) (Gratwohl, 2012). In contrast, post-transplant risks are far more complicated as they are relatively unpredictable at the time of allo-HSCT such as GVHD or risk of relapse (Gratwohl, 2012). Infections are also a major post allo-HSCT complication as the patient's immune system is compromised to receive the donor cells.

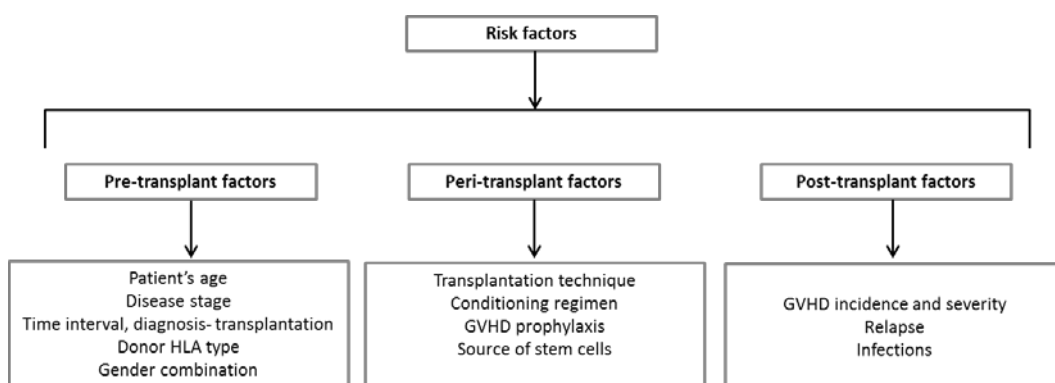


**Figure 1.10** The three categories of risk factors associated with allo-HSCT. There are pre-, peri- and post-transplant risk factors that may determine allo-HSCT outcome. Pre-transplant factors are used to calculate the EBMT risk score and decide upon the type of transplant protocols and procedures performed for the patients. Peri-transplant risk factors also stem from the pre-transplant factors but it is the post-transplant factors that are difficult to determine.

The EBMT risk score was developed to assist clinicians in predicting post allo-HSCT outcomes: relapse, OS and NRM (Gratwohl *et al.*, 1998; Gratwohl, 2012). The risk score is comprised of five main clinical factors: patient age, disease stage, and time from diagnosis to transplant, donor type and the gender combination of donor to recipient

(Thomas *et al.*, 1975; Goulmy *et al.*, 1976; Armitage, 1994; Sierra *et al.*, 1997; Kroger *et al.*, 2009; Gupta *et al.*, 2010). The EBMT risk score is commendatory especially as it is independent of the underlying disease (Gratwohl *et al.*, 2009; Gratwohl *et al.*, 2010). The risk score is simple and is a summation of the different points on a scale that ranges 0-7, with 0 being the ideal and 7 being the worst score (Table 1.4). As an example of EBMT risk score generation, a male patient of 25 years (score 1), having late stage disease (score 2), having 17 months from diagnosis to transplant (score 1), having an HLA-identical sibling donor (score 0) and having a male donor (score 0) would have an EBMT risk score of  $1+2+1+0+0=4$ .

Clinical Risk factor	Score points
<u>1. Patient age at time of Transplant (years)</u>	
<20	0
20–40	1
>40	2
<u>2. Disease stage<sup>a</sup></u>	
Early	0
Intermediate	1
Late	2
<u>3. Time interval from diagnosis to transplant (months)<sup>b</sup></u>	
<12	0
>12	1
<u>4. Donor type</u>	
HLA-identical sibling donor	0
Unrelated donor	1
<u>5. Donor recipient sex combination</u>	
All other	0
Female donor, male recipient	1

**Table 1.4** The EBMT risk score points for all the five different clinical risk factors (adopted from (Gratwohl, 2012)). <sup>a</sup> does not apply for aplastic anemia: score 0. <sup>b</sup> does not apply for patients transplanted in first complete remission: score 0.

The effects of the five pre-transplant clinical risk factors have been established in the literature. The intensity and extent of post allo-HSCT complications are directly proportional to the age at which the patients undergo the transplantation procedure. Therefore, in the EBMT risk score, age is divided into three ranges covering the young (below 20 years), the intermediate group (20-40 years) and the higher risk group (40 and above years). Due to an aging population and advancements in the clinical science

of transplantation (RIC regimens), more elderly patients undergo allo-HSCTs. Similarly, there are three different stages of disease as per the EBMT scoring guideline (early, intermediate and late). The staging in this case is disease specific. Aplastic anemia is not categorized into stages; all the other hematological malignancies are classed into stages. Since the EBMT score was first developed for patients diagnosed with CML, the time interval from diagnosis to transplantation was very critical and a main risk factor. However, for other diseases (Acute Myeloid Leukemia, Myelodysplastic Syndrome and Non-Hodgkin's Lymphoma) the time interval can only be considered when information on the time from diagnosis to first remission and then to transplantation is present. Generally, a short time interval of less than a year is considered to lead to better allo-HSCT outcome. Recently, more patients undergo allo-HSCT with MUDs which is mainly due to the advancements in HLA typing and also the increasing number of donors available in transplantation banks. Some studies have shown that a younger MUD donor can improve allo-HSCT outcome in comparison to an identical SIB donor (Schlenk *et al.*, 2010). Yet, the degree of HLA matching is an important indicator of allo-HSCT and its outcome. It is well established that sex incompatibility is a major risk factor in particular for male patients who have female donors as they tend to have shorter OS even though lower incidence of relapse. The sex incompatibility arises due to fact that male-specific chromosome Y has H-Y (male specific histocompatibility) (Simpson *et al.*, 1997) antigens that stimulate female T and B cells and thus lead to allogeneic reactions with fatal complications such as allo-HSCT failure and/or severe GVHD (Goulmy *et al.*, 1976).

The concordance index (c-index) quantifies the concordance between the risk score and actual survival time (Harrell *et al.*, 1984). The c-index ranges from 0.5 to 1; 0.5 signifies no diagnostic ability; 1 indicates perfect diagnostic ability. The c-index for the EBMT risk score has been calculated as being just 0.621 (n=56,505) (Gratwohl *et al.*, 2009). In recent years, researchers have focused on trying to improve risk score as regards predictive value. These efforts have included addition of other factors such as the patient-donor CMV status and genomic factors for instance the presence or absence of specific SNPS in genes (Dickinson *et al.*, 2010; Ljungman *et al.*, 2010).

## 1.6 MicroRNAs

MicroRNAs (miRNAs) are 19-22 nucleotide RNAs that are produced in every animal and plant cell. These short, single stranded RNAs have crucial regulatory roles by targeting messenger RNAs (mRNAs). MicroRNAs target nearly 30% of mRNAs and are thus classed as one of the major and most abundant group of translational regulators (Lewis *et al.*, 2003). They not only suppress translation of mRNA but can activate it depending on their role. In 1991, Wightman *et al.* (Wightman *et al.*, 1993) demonstrated that *lin-4* was repressed via the product of the gene itself, however at that time, miRNAs had not yet been discovered and so the repression was not attributed to their involvement. MicroRNAs were first officially discovered in 1993 by Rosalind Lee and Rhonda Feinbaum in the nematode, *C. elegans* (Lee *et al.*, 1993). Their study demonstrated that *lin-4*, which is associated with the control of temporal larval development in *C. elegans*, is not transcribed into mRNA but results in the generation of two single-stranded small RNAs. One RNA strand is 19-22 nucleotides, while the other strand is 61 nucleotides. Ambros and Ruvkun were able to demonstrate that *lin-4* miRNA was complimentary to several sites in the 3'UTR (untranslated region) of *lin-14*. Their study showed that miRNAs bind to the 3'UTR of the mRNA and hypothesized that the repression of *lin-14* was due to *lin-4* miRNA activity (as reviewed by (Bartel, 2004a)). The main function of *lin-4* was found to be the transition of the nematode from the first larval stage to the second stage, of its developmental cycle. The groups established the importance of the complimentary sites in the regulatory function of miRNAs and that the level of *lin-14* mRNA did not significantly change, even though the level of LIN-14 protein decreased (as reviewed by Bartel *et al.* (Bartel, 2004a)).

Recognition of the important roles of miRNAs through the discovery of *lin-4* spurred on research in this area of molecular biology. Hence, the list of functions attributed to miRNAs has expanded over the past several years which encompasses; control of apoptosis, cell proliferation, metabolism of lipids in flies (Brennecke *et al.*, 2003; Xu *et al.*, 2003), mammalian transition of haematopoietic lineage differentiation (Chen *et al.*, 2004; Gangaraju and Lin, 2009), development of haematopoietic disorders such as

leukemia (Zhao *et al.*, 2010), and as prognostic biomarkers of diseases such as diabetes (Zampetaki *et al.*, 2010) and rheumatic diseases (Alevizos and Illei, 2010).

MicroRNAs have been shown to exhibit unique expression patterns depending on which cell or organ they are expressed in (Bartel, 2004a). For instance, miR-1 is a heart-specific miRNA (Lee and Ambros, 2001; Lagos-Quintana *et al.*, 2002) while miR-122 is mainly expressed in the liver (Lagos-Quintana *et al.*, 2002). Moreover, certain miRNAs have a high copy number per cell, for instance, miR-2 and miR-58 are each present at more than 50,000 molecules per adult worm cell (Lim *et al.*, 2003). On the other hand, there are certain miRNAs such as miR-124 that have a very low copy number per cell (Lim *et al.*, 2003). As a result of the variable and distinct expression pattern of miRNAs, determining an expression profile of miRNAs in a particular disease can lead to the identification of biomarkers that could aid disease diagnosis and prognosis.

Since cloning of miRNAs in low count cells and those expressed under specific conditions can be missed; the use of computational approaches has proven to be more effective at identifying these small miRNAs (Bartel, 2004a). Hence, several strategies have been implemented to more accurately determine this variable class of miRNAs by performing homology searches to identify orthologs and paralogs of the already known miRNA genes, proximity searches for looking at other stem-loops that could be representative of genes in a cluster and also by looking at the conserved regions that are in the intronic segment of the genome and could possibly form stem loops. MiRscan and MiRseeker were the first bioinformatics search engines that were able to identify genes associated with the expression of miRNAs (as reviewed by Bartel *et al.* (Bartel, 2004a)). Due to associated functions of miRNAs in numerous conditions there has been an upsurge of databases that assist in miRNA target prediction, analysis of expression data, pathway involvement and interpretation of their roles in diseases, such as DIANA LAB (Alexiou *et al.*, 2010), mimiRNA (Ritchie *et al.*, 2009), FERROLAB (Lagana *et al.*, 2009), HOCTAR (Gennarino *et al.*, 2008), in addition to the initial and accessible databases such as PicTar (Lall *et al.*, 2006), miRanda (Betel *et al.*, 2008) and TargetScan (Lewis *et al.*, 2005). Studies have shown that around 50% of all the genes are regulated by microRNAs, thereby further increasing the importance of understanding their involvement in disease (Bentwich, 2005). According to the

miRbase version 20, there are nearly 2000 miRNAs in humans (Kozomara and Griffiths-Jones, 2014). In humans the miRNA genes are present on every chromosome except on the Y chromosome (Sun *et al.*, 2009).

### **1.6.1 MicroRNA nomenclature**

MicroRNAs are named starting with a three letter identifier which signifies the organism (example- hsa in *homo sapiens*), followed by 'miR' prefix, a specific number and then a single letter (example -a, -b ) (Ambros *et al.*, 2003). The number is assigned in a sequence depending on the time of miRNA discovery. It must be noted that identical miRNAs are assigned the same number independent of the organism in which they are present in. The last letters in the miRNA name which are after the unique number shows the relationship of one miRNA with another (example: hsa-miR-146a is related to hsa-miR-146b) (Griffiths-Jones *et al.*, 2006). Mature miRNAs are noted as 'miR' whilst the precursors as 'mir.' MiRNAs have two strands, and it was initially assumed that only the -5p strand was functional while the -3p strand was degraded. Now it is known that -3p strand that was previously denoted as miR\* can also function (Yang *et al.*, 2011). Due to the various complications in using miR\*, the new nomenclature has adopted -5p and -3p instead of miR and miR\*, respectively (Griffiths-Jones *et al.*, 2006). The miRNA genes are called the same way but are written in italics, capitalized or hyphenated (Ambros *et al.*, 2003).

## **1.7 MicroRNA Biogenesis**

### **1.7.1 MicroRNA transcription**

The majority of miRNA genes are derived from the earlier non-annotated parts of the genome, while substantial small groups are derived from the non-coding regions of pre-mRNAs (Lagos-Quintana *et al.*, 2001; Lau *et al.*, 2001; Lee and Ambros, 2001). MiRNAs may also be transcribed as a cluster in the genome rather than as individual regulatory molecules. The expression pattern of these clustered miRNAs suggests that the transcription is from a primary transcript (Lagos-Quintana *et al.*, 2001; Lau *et al.*, 2001; Lee and Ambros, 2001). It was assumed that miRNAs in a cluster are related to

one another (Lagos-Quintana *et al.*, 2001; Lau *et al.*, 2001) with a similar expression pattern, however, with studies have shown that not only they may vary in expression pattern but are also not related to one another and may have unique functions. A few examples of miRNA clusters include the Hox and miR-17 to miR-92 clusters in humans. The Hox cluster has been shown to play a role in animal development (Lagos-Quintana *et al.*, 2003) while miR-17-92 clusters commonly act as an oncogene (Mendell, 2008).

It has also been shown that all cloned miRNAs are evolutionary conserved among humans and mouse (Lagos-Quintana *et al.*, 2003). There are two sets of miRNAs, those that are present in the non-coding region of the genome and those that are present in the conserved regions. The intronic miRNAs are assumed to share regulatory elements and primary transcripts with the pre-mRNA host gene while the other miRNAs are thought to have been transcribed from their own promoters. The primary miRNA transcripts are referred to as pri-miRNAs (Lee *et al.*, 2002) and are transcribed in the nucleus. Pri-miRNAs are longer than the 19-22 nucleotides stem looped structures known as miRNA because their transcription is from a single primary transcript (Lagos-Quintana *et al.*, 2001; Lau *et al.*, 2001).

MicroRNA transcription, particularly from the non-coding regions of the genes, are performed by polymerase II rather than polymerase III (pol III). This is because pri-miRNAs are longer than 1 Kb in length with internal uridine residues. These residues result in premature halting of the pol III transcription. . (Bartel, 2004a).

### **1.7.2 MicroRNA maturation**

There are various factors that are involved in the biogenesis of miRNAs these include; RNase-III family proteins, double-stranded (ds) binding proteins and the export receptor. The RNase-III family comprises of Drosha and Dicer, which are endonucleolytic enzymes (Kim, 2005). The ds-binding protein comprises of the DiGeorge Syndrome Critical Region 8 (DGCR8) which is a well-conserved motif with numerous functions. It is partly involved in the processing of miRNA by Drosha and Dicer (Kim, 2005). The human export receptor (Exportin-5) consists of a nuclear transport domain and is commonly present in the Ran-dependent nuclear transport factors (Nakielny and Dreyfuss, 1999).

Initially the pri-miRNA in the nucleus is cleaved by Drosha RNase III (Lee *et al.*, 2003) and this results in the release of an approximately 60-70 nucleotide stem-loop structure referred to as precursor miRNA (pre-miRNA) (Lee *et al.*, 2002; Zeng *et al.*, 2003). Drosha is part of the microprocessor protein complex which also includes DGCR8 (Gangaraju and Lin, 2009). P53 has also been shown to function as a modulator in the processing of miRNA, due to its involvement in assembling of the Drosha complex (Suzuki *et al.*, 2009). As a result of the staggered cut by Drosha RNase III, there is a 5' phosphate and a 3' overhang (~2nt) (Basyuk *et al.*, 2003; Lee *et al.*, 2003). At this point, the pre-miRNA is translocated from the nucleus to the cytoplasm through Exportin-5 by Ran-GTP (Yi *et al.*, 2003; Lund *et al.*, 2004).

Dicer, the second enzyme involved in the maturation of the miRNA, is secreted in the cytoplasm (Lee *et al.*, 2003) and has an affinity for the 5' phosphate and the 3' overhang of the pre-miRNA (Bartel, 2004a). The terminal base pairs of the pre-miRNA are cleaved by Dicer through a double-stranded cut at about two helical turns from the base of the pre-miRNA. At present it is hypothesized that Drosha makes a cleavage at a specific sequence of the RNA while Dicer randomly cuts any double-stranded RNA (Zamore *et al.*, 2000; Bernstein *et al.*, 2001; Elbashir *et al.*, 2001; Zhang *et al.*, 2002).

In addition, it has been recently shown that miRNAs can be processed by other non-canonical pathways (Gangaraju and Lin, 2009) which involve Dicer or are independent of it (Yang *et al.*, 2012). To date two other Dicer dependent pathways have been described. The initial part of the first pathway employs a spliceosome and then a debranching enzyme to produce the short-hairpin structure for processing by Dicer (Gangaraju and Lin, 2009). The second pathway uses unknown nucleases to produce the hair-pin structure which is later processed by Dicer. MicroRNAs derived via the first pathway are termed as mitrons (Okamura *et al.*, 2007) while those from the second pathway are referred to as endogenous short hairpin (sh)-derived miRNAs (Babiarz *et al.*, 2008). In the Dicer independent pathway, the pre-miRNA is cleaved by Argonaute 2 (Ago2) which results in the generation of mature miRNA (Figure 1.11).

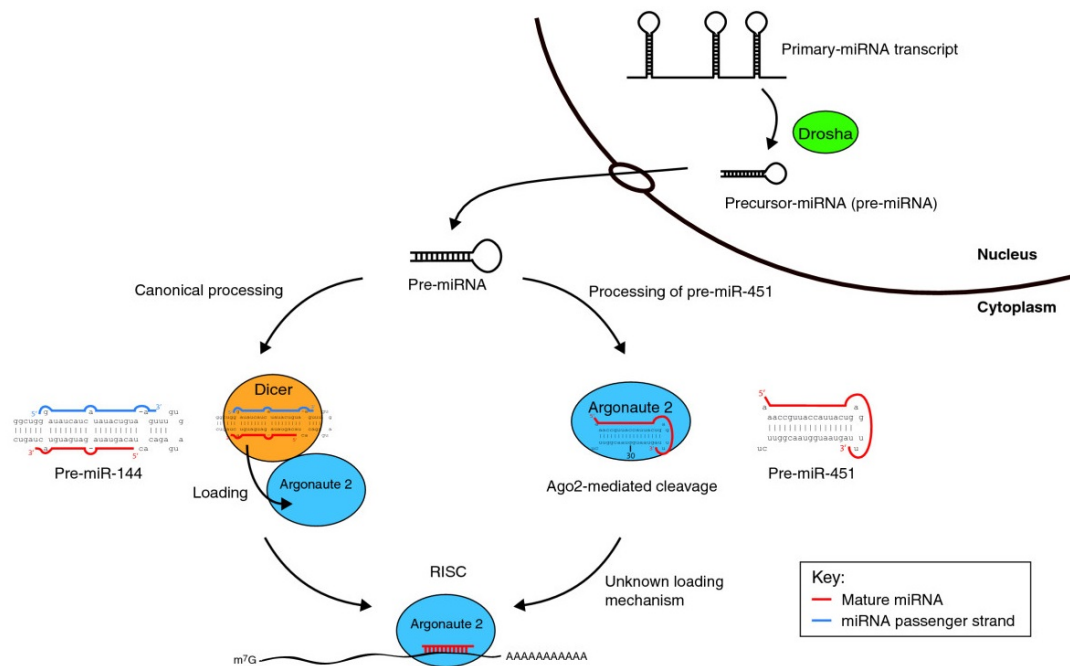


**Figure 1.11 Dicer independent non-canonical pathway** (adopted from (Dueck and Meister, 2010)). Maturation of miR-451 that is an erythropoiesis specific miRNA via Ago2 mediated pathway. Pre-miRNA once exported into the cytoplasm can either be processed via the canonical pathway or Ago2-mediated pathway. Pre-miR-144 is cleaved by Dicer while pre-miR-451 is processed into the mature miR-451 by Ago-2.

### 1.7.3 Assembly of microRNA in RNA-induced silencing complex

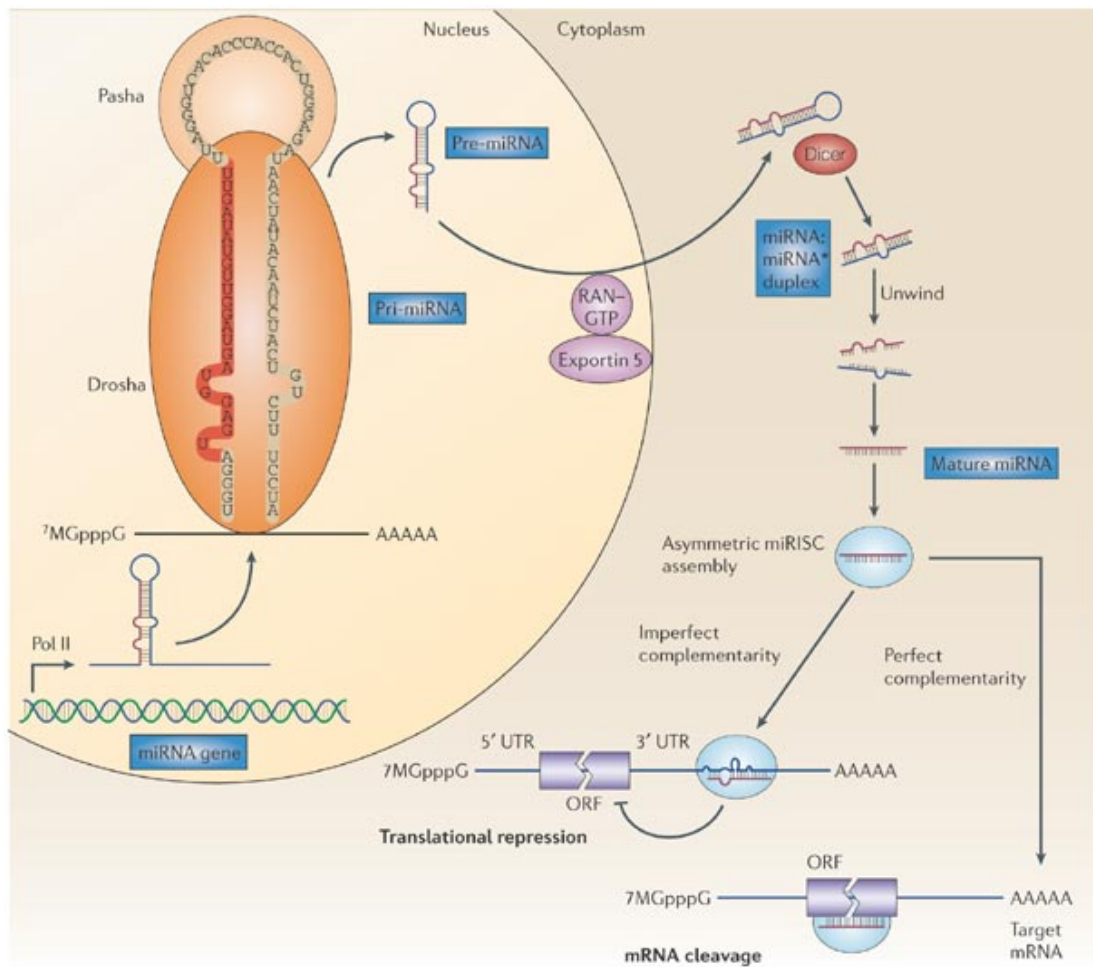
The ribonucleoprotein complex consists of a member of the Argonaute protein family and is called the RNA Induced Silencing Complex (RISC). Argonaute proteins act as the catalytic part of the RISC complexes and are located in certain parts of the cytoplasm referred to as the P-bodies (Filipowicz *et al.*, 2008). The P-body is the region where the majority of mRNA degradation and miRNA activity occurs in the cytoplasm (Filipowicz *et al.*, 2008; Williams, 2008). The duplex (miRNA-5p: miRNA-3p) comprises both strands of miRNA of which only the guide strand (miRNA-5p) will be incorporated into the RISC (Sonkoly and Pivarcsi, 2009). As mentioned earlier, it has been shown that miRNA-3p is not always degraded. Studies have revealed that both the guide miRNA-5p and miRNA-3p are active and their roles depend on the particular condition under which they are expressed and processed (Ro *et al.*, 2007; Okamura *et al.*, 2008). The incorporation of the single-stranded miRNA onto the RISC is the first step in achieving target repression. Strand selection is based on the relative internal stability of the two

ends of the duplex and it is usually the strand with the less stable -5p end that is selected (Khvorova *et al.*, 2003; Schwarz *et al.*, 2003). The RISC can identify target mRNA based on extensive complementarity in the exons or UTR of the specific miRNA and the target mRNA. The majority of miRNAs are tightly associated with RISC complexes, and only less than 3% are present on their own. It is due to this fact that miRNAs are stable in cells with an extremely long half-life of days to several months (Liu *et al.*, 2004; Martinez and Tuschl, 2004; Tang *et al.*, 2008).

#### **1.7.4 Messenger RNA cleavage**

MicroRNAs down-regulate gene expression via RISC by either mRNA cleavage or translational repression (Bartel, 2004a). The mechanism of regulation is dependent on the target mRNA. Messenger RNA cleavage is achieved when the incorporated miRNA in the RISC has extensive complementarity with the target mRNA and in cases of lesser complementarity, translational repression is performed (Figure 1.12). Upon cleavage, the miRNA remains incorporated in the RISC to perform additional cleavages.

Olsen and Ambros (Olsen and Ambros, 1999) explained translational repression through two hypotheses with respect to *lin-4* miRNA. In the first hypothesis, translational repression might occur at a later stage after initiation of translation such that the number of ribosome's are not changed directly but decline gradually to a halt. In the second hypothesis, suppression is achieved as a consequence of product degradation, whilst the rate of translation remains unaltered.



Copyright © 2005 Nature Publishing Group  
Nature Reviews | Cancer

**Figure 1.12 MicroRNA biogenesis** (Esquela-Kerscher and Slack, 2006). Pri-miRNA is transcribed from the miRNA gene and processed by Drosha in the nucleus. This pre-miRNA is then exported into the cytoplasm by Exportin 5 and cleaved into mature miRNA by Dicer. Mature miRNA is loaded onto RISC/miRISC and delivered to the mRNA where it represses translation and/or results in mRNA cleavage. Pol II: Polymerase II; Pri-miRNA: Primary MicroRNA; Pre-miRNA: Precursor MicroRNA; miRISC: MicroRNA Induced Silencing Complex; ORF: Open Reading Frame; UTR: Untranslated Region; mRNA: Messenger RNA.

### **1.7.5 Target recognition**

The complementarity of the -5p end of the miRNA to the mRNA is crucial for the regulation of gene expression (Bartel, 2004a). Wightman (Wightman *et al.*, 1993) was first to observe this complementarity between the -5p end of *lin-4* miRNA and the *lin-14* UTR. Lai (2002) showed that residues 2-8 of several miRNAs have nearly perfect complementarity to the 3'UTR region of the target mRNA. These residues are now referred to as the miRNA seed and are located in the -5p end of the miRNA (Sonkoly and Pivarcsi, 2009). In a later study by Stark *et al.* (Stark *et al.*, 2003), it was demonstrated that the imperfect complementarity of the mRNA residues with the seed sequence are conserved in orthologous messages of other species. Also, the seed sequences are conserved among homologous miRNAs. Furthermore, miRNA target recognition via seed sequence is more productive than to any other region of the miRNA. In plants, there should be total complementarity between the miRNA and the mRNA sequence while in animals partial complementarity at only the seed sequence is required for translational inhibition.

## **1.8 MicroRNAs as Biomarkers of Diseases**

Recent biomarker literature has focused on the numerous characteristics of miRNAs as potential and specific biomarkers of various diseases, including rheumatoid arthritis (Alevizos and Illei, 2010) and cancer (Lawrie *et al.*, 2007). Studies have shown that around 50% of all genes are regulated by miRNAs, thereby further emphasizing the importance of understanding their involvement in disease (Bentwich, 2005). Hence, miRNAs are classed as one of the primary and most abundant group of translational regulators (Lewis *et al.*, 2003). Since most of the miRNAs in cells and tissues have been identified, it is now possible to perform expression studies in GVHD samples in order to develop a miRNA signature for the disease.

As mentioned earlier, miRNAs are not only abundant but are also highly stable due to their resistance to nucleases (Lau *et al.*, 2001). This fact enables expression studies using formalin fixed-paraffin-embedded (FFPE) samples (Hasemeier *et al.*, 2008) and salivary samples possible (Park *et al.*, 2009). The fixation process involved in making

FFPEs does not degrade miRNAs as they are very short and highly stable as mentioned above, therefore, they are ideal sources for profiling experiments (Culpin *et al.*, 2013). Since most research institutions possess archives of patient samples, a substantial number of relevant patient materials (serum, plasma, FFPE, urine) are available for biomarker discovery investigations. Also, studies have shown that there is a correlation between serum and biopsy miRNA profiles in a number of cancer studies as reviewed by Alevizos and Illei (2010). Mitchell *et al.* (2008) have demonstrated that circulating miRNAs in plasma and serum are stable and that their measurements correlate with each other. This finding strengthens the hypothesis that tumor-derived miRNAs are translocated into the blood and hence, measurement of plasma or serum derived miRNAs may serve as cancer biomarkers (Mitchell *et al.*, 2008). The availability of potential circulatory diagnostic miRNAs (Alevizos and Illei, 2010) could reduce the need for invasive methods such as skin biopsies for the diagnosis of GVHD in allo-HSCT patients and aid in disease monitoring. Moreover, miRNAs are expressed under certain conditions that can be representative of the physiological and pathological state of the disease such as rheumatic diseases (Alevizos and Illei, 2010). Since, miRNA expression patterns may be disease specific, distinguishing between normal, inflamed and damaged organs are possible (Babak *et al.*, 2004). MicroRNA patterns already established in systemic lupus erythematosus and other systemic autoimmune diseases can be useful in understanding the pathogenesis of cGVHD (Shen *et al.*, 2012).

Although a single prognostic marker may be clinically useful, a series of validated markers which can provide, in addition to clinical factors, information regarding survival, disease progression and patient's response to treatment would be advantageous. Thus, identification of a signature miRNA profile for GVHD could serve both as a prognostic biomarker of the disease as well as aid in further understanding the complexity of the disease biology. Specific biomarkers can also assist in the development of new therapies and more effective drugs for the treatment of GVHD.

### **1.8.1 MicroRNAs in skin**

Since the skin is one of the first target organs of GVHD, the role of skin-specific miRNAs in GVHD skin biopsies is an exciting area of investigation. A number of highly expressed

miRNAs in the epidermis and hair follicle have already been discovered to be essential for the normal development of the skin (for example: miR-199 family, miR-205, miR-27b, miR-203, miR-125b, miR-16, miR-126, miR-143, miR-21) (Yi et al., 2006; Banerjee et al., 2011). Skin specific miRNAs such as miR-203 are related to skin morphogenesis (Yi et al., 2008; Sand et al., 2009). Indeed, expression studies have shown the effect of miRNAs in malignant skin conditions such as melanoma, Kaposi's sarcoma (McClure and Sullivan, 2008) and autoimmune diseases such as psoriasis (Sonkoly et al., 2007). For instance in psoriasis, miR-146a, miR-203 and miR-21 are up-regulated while miR-125b is down-regulated (Sonkoly et al., 2008). Up-regulation of TNF- $\alpha$  is observed when miR-125b is expressed at low levels (Sand et al., 2009) and similarly, expression of miR-21 is shown to be elevated by pro-inflammatory cytokines such as IL-6 (Loffler et al., 2007). MiR-21 has also been shown to function as an oncogene in various cancer tissues (Liu et al., 2012; Yang et al., 2012b). Although miR-21 has been shown to be associated with Tregs (see below) there is lack of evidence to suggest that the impact of miR-21 in skin tissue is primarily via Tregs and no other cell type.

### **1.8.2 *MicroRNAs in immune cells***

Thymus-derived natural Treg cells and the peripherally stimulated Tregs are well characterized T lymphocytes and their function in GVHD has been highlighted through various studies (Di Ianni *et al.*, 2011). Natural Tregs and peripherally induced Tregs are distinguished via the expression of the fork head-winged helix transcription factor (FOXP3) and the  $\alpha$ -chain of the IL-2 receptor (CD25) (Rouas et al., 2009). A study performed *ex vivo* in humans by Rouas et al. (2009) has identified five main miRNAs (miR-21, miR-31, miR-125a, miR-181c and miR-374) particular to non-activated natural Tregs (Rouas et al., 2009). Natural Tregs affect both the innate and adaptive immune system (Sakaguchi, 2004). Moreover, the same group demonstrated the direct negative regulation of miR-31 through targeting of *FOXP3* mRNA and positive indirect regulation of *FOXP3* by miR-21 (Rouas et al., 2009).

Furthermore, Allantaz et al. (Allantaz et al., 2012) have shown the existence of cell-specific miRNAs in the whole blood of healthy individuals (Table 1.5). Initially, the authors examined miRNA expression in nine different types of immune cells

comprising of; neutrophils, eosinophils, B, NK, CD4+ T and CD8+ T-cells, myeloid DCs, plasmacytoid DCs and monocytes (Allantaz et al., 2012). Four miRNAs were characterized as cell specific (miR-378, miR-31, miR-143 and miR-935) while nine miRNAs were common in two to three other cell types (miR-362-5p, miR-532-5p, miR-500\*, miR-663, miR-125a-5p, miR-150, miR-223 and miR-652) (Allantaz et al., 2012). The group also investigated mRNA expression of the miRNA targets in the same samples to validate whether the cell-specific miRNAs regulated their predicted mRNA targets, as identified via miRNA target prediction databases. MiRs -143, -125, -500, -150, -652 and -223 were all found to regulate their mRNA target transcripts (Allantaz et al., 2012). These investigations reiterate the critical regulatory roles of miRNAs in immune cells and provide a valuable starting point for miRNA studies in GVHD.

MicroRNAs	Cell type
miR-378	Monocytes
miR-31	T cells
miR-935	Eosinophils
miR-143	Neutrophils
miR-362-5p	Monocytes, pDCs
miR-532-5p	
miR-500*	
miR-663	B cells, NK cells
miR-125a-5p	T cells, Neutrophils
miR-150	B cells, T cells, NK cells
miR-223	Monocytes, Eosinophils, Neutrophils
miR-652	

**Table 1.5 List of cell-specific miRNAs in whole blood of healthy individuals** (adopted from (Allantaz et al., 2012)).

### **1.8.3 MicroRNAs in GVHD**

In a recent murine study, it has been shown that miR-146a is under-expressed in aGVHD and correlates with its severity (Stickel *et al.*, 2014). Additionally, the established miR-146a target, Traf6 was over-expressed in aGVHD, thereby inducing NFκB activity. The authors also showed that in humans, the SNP rs2910164 in grafts caused a reduction in miR-146a levels that escalated severe aGVHD (Grades III-IV) in allo-HSCT patients (Stickel *et al.*, 2014). The rs2910164 SNP (G/C) is located in the stem

region of pre-miR-146a. It causes a C: U miss-pair rather than a G: U pair. It is a functional SNP and therefore effects the processing of pre-miR-146a into miR-146a, the mature strand (Iwai and Naraba, 2005). A panel comprising of four miRNAs (miR-423, miR-199-3p, miR-93-3p and miR-377) has been shown to be over-expressed 16 days pre-clinical diagnosis, in the plasma of aGVHD patients when compared to the non-GVHD patient cohort (Xiao et al., 2013). All the up-regulated miRNAs have been suggested to have critical functions in the regulation of inflammation, cell proliferation, apoptosis and autophagy (Xiao *et al.*, 2013). The authors hypothesized that plasma identified miRNAs may have significant functions in the 'donor T-cells attacking process' and play a potential role in injury-mediated responses in aGVHD target organs. In addition, miR-100 (Leonhardt et al., 2013), miR-34a (Wang et al., 2013) and miR-155 (Ranganathan et al., 2012) have also been implicated in GVHD. MiR-100 was shown to be up-regulated in the gut of mice without GVHD, thereby preventing neovascularization in the tissue and demonstrating a possible protective role of miR-100 in GVHD (Leonhardt et al., 2013). Likewise, miR-34a expression was studied in the gut of pre- and post-transplanted Fanconi anaemia patients with aGVHD (Wang et al., 2013). MiR-34a was shown to be up-regulated in the gut of the transplanted Fanconi anaemia patients with grades II-IV aGVHD in comparison to patients with grades 0-I aGVHD and pre-transplant biopsies (Wang et al., 2013). DNA repair mechanisms are disrupted in Fanconi anaemia patients and this result in the activation of p53 pathways, ultimately leading to apoptosis (Freie et al., 2003). Thus, the investigators assessed the number of apoptotic cells in relation to the levels of miR-34a and *TP53* (Wang et al., 2013). The authors found that miR-34a levels in the gut correlated with the number of apoptotic cells and not *TP53* levels (Wang et al., 2013). Therefore, the authors hypothesized that it was the elevation of miR-34a in the epithelial gut cells which was responsible for the damage observed in the gut tissues rather than *TP53* expression (Wang et al., 2013). Similarly, the regulatory role of miR-155, which is required for the normal function of B and T lymphocytes in humans, has been demonstrated in an aGVHD study (Ranganathan et al., 2012). This investigation showed an up-regulation of miR-155 in the gut of aGVHD patients, while expression was absent in the gut of normal volunteers (Ranganathan et al., 2012). A clinical trial to further establish the significance of miR-155 in aGVHD is ongoing at present

(ClinicalTrials.gov identifier: NCT01521039). Thus, miRNAs evidently not only play a role in the manifestation of GVHD but could potentially be used as prognostic and diagnostic biomarkers of disease because of their highly specialized roles. Moreover, Schulte et al. (2013) have demonstrated that miRNAs have specialized functions and a hierarchy in controlling inflammation. In their research, miR-155 is significantly involved in the regulation of inflammation only when the statutory limit of miR-146a has been exceeded (Schulte et al., 2013). Their study highlights the combinatorial effect of miRNAs in regulating inflammation and also shows that investigating several miRNAs important in a disease-type can provide a more informative outlook on the pathophysiology of the disease.

The review by Paczesny lists the array of potential prognostic and diagnostic biomarkers that have been identified for the detection of GVHD in allo-HSCT patients (Paczesny, 2012) (Table 1.6). However, despite the tremendous advances in our knowledge of GVHD there are no precise clinical disease markers available in the clinic that can aid in early detection of GVHD and monitor its severity. At present, there is extensive knowledge on the cellular mechanism of GVHD but less is known about the molecular biology of the disease. The molecular studies carried out so far have focused on identifying Single Nucleotide Polymorphisms (SNPs) (Dickinson and Holler, 2008) and specific genes involved in the development of GVHD (Baron *et al.*, 2007) However, there have been fewer studies focusing on the molecular regulation of GVHD.

<b>Biomarkers of aGVHD</b>
Interleukin-2 receptor $\alpha$ chain, CD25 (IL-2R $\alpha$ )
Interleukin-6 (IL-6)
Interleukin-8 (IL-8)
Interleukin-10 (IL-10)
Interleukin-12 (IL-12)
Interleukin-18 (IL-18)
Chemokine (C-C motif) ligand 8 (CCL8)
Chemokine (C-X-C motif) ligand 10 (CXCL10)
Tumor necrosis factor $\alpha$ (TNF $\alpha$ )
Tumor necrosis factor receptor-1 (TNFR-1)
Hepatocyte growth factor (HGF)
Cytokeratin-18 fragments (KRT18)
Elafin (PI3)
Regenerating islet-derived 3 $\alpha$ (REG3 $\alpha$ )
<b>Biomarker of cGVHD</b>
B cell-activating factor (BAFF)

**Table 1.6** Potential prognostic and diagnostic biomarkers of GVHD (adopted from (Levine et al., 2012; Paczesny, 2012))

#### **1.8.4 MicroRNAs in umbilical cord blood**

Weitzel et al. (Weitzel *et al.*, 2009) have described miR-184 as a regulator of nuclear factor of activated T cells-1 (NFAT1) protein expression in umbilical cord blood (UCB) CD4<sup>+</sup> T cells. Expression of miR-184 inhibits NFAT1, which results in a reduced inflammatory response. The lower expression of NFAT1 in UCB CD4<sup>+</sup> T cells in comparison to adult blood is one of the main differences between UCB-derived CD4<sup>+</sup> T cells and those obtained from adult blood. This study has shown that over-expression of miR-184 in UCB CD4<sup>+</sup> T cells may be a reason for the decreased incidence of GVHD in UCB grafts compared to adult HSCT (Weitzel et al., 2009). In addition, Charrier et al. (2012) have also shown that UCBs express significantly higher levels of miR-146a and miR-155 compared to adult blood. Previous studies have shown that miR-146a (Sonkoly et al., 2007; Sonkoly et al., 2008) and miR-155 (Ranganathan et al., 2012; Zhong et al., 2012) are associated with immune regulation. Thus, the authors hypothesize that the lower incidence of GVHD which occurs when UCB is used instead of adult blood is due to the up-regulated expression of immune-regulatory miRNAs (miR-146a and miR-155), resulting in the down-regulation of target proteins (toll-like receptor 9, myeloid differentiation primary response 88, interleukin-1 receptor-associated kinase 1, interferon regulatory factor 7) in the toll-like receptor 9 signaling pathway (Charrier et al., 2012). This post-transcriptional regulation leads to a decrease in the interferon- $\alpha$  mediated response, which dampens down the inflammatory reaction in UCBs as opposed to adult blood (Charrier et al., 2012). In addition, it has also been shown that miR-155 is over-expressed in UCB derived CD14<sup>+</sup> cells and not in the adult peripheral blood CD14<sup>+</sup> cells when stimulated with either IFN- $\gamma$  or LPS (Takahashi et al., 2012). This may be reflective of the biological response in GVHD or infection. However, in the same study miR-146a was under-expressed in UCB derived CD14<sup>+</sup> cells after stimulation with IFN- $\gamma$ . The controversy regarding miR-146a expression may be reflective of study populations investigated. Indeed, Charrier et al. (2012) have looked at whole UCB and adult blood rather than an isolated CD14<sup>+</sup> subset as used by Takahashi et al (2012). Merkerova et al. (2010) compared UCB and bone marrow miRNA signatures in cell lineages CD34<sup>+</sup> cells, T cells, monocytes and

granulocytes and found distinct miRNA expression patterns indicating differences in regulation of the cells within bone marrow and UCB.

### **1.8.5 MicroRNAs in graft rejection**

Investigations in renal allograft rejection have shown the existence of 17 specific miRNAs involved in the acute rejection process (let-7c, miR-10a, miR-10b, miR-125a, miR-200a, miR-30a-3p, miR-30b, miR-30c, miR-30e-3p, miR-32, miR-142-5p, miR-142-3p, miR-223, miR-155, miR-146b, miR-146a and miR-342) (Anglicheau et al., 2009). This study also highlights the application of miRNAs as prognostic biomarkers for disease and in particular for transplantation. The significance of miRNAs in graft failure has also been determined in liver, lung and bowel solid organ transplantations as reviewed by Sarma et al. (2012). Furthermore as in HSCT some residual host T cells or natural killer cells can reject incoming grafts (Martin, 2000), and high levels of CD34<sup>+</sup> cells can improve engraftment (Weaver et al., 1995). A study in the role of miRNAs in these situations would aid in the understanding of haematopoiesis, engraftment and rejection settings.

## **1.9 MicroRNAs in therapeutics**

Recently, the potential of miRNAs in the development of new therapies has been investigated. There are two models via which miRNAs may be used for the treatment of diseases. Firstly, miRNA antagonists can be used to dampen up-regulated endogenous miRNA expression in diseased tissues. For instance, miR-122, which is a liver-specific miRNA, has a crucial role in the replication of hepatitis C virus (HCV) and is up-regulated in HCV positive patients (Haussecker and Kay, 2010; Lanford et al., 2010; Iorio et al., 2012). Miravirsen (anti-miR-122) which consists of modified locked nucleic acids (LNA) is now in a phase II clinical trial (ClinicalTrials.gov Identifier: NCT01727934). Miravirsen efficacy, activity and safety have been shown in a multi centre Phase I (ClinicalTrials.gov Identifiers: NCT00688012, NCT00979927) and Phase IIa (ClinicalTrials.gov Identifier: NCT01200420) clinical trial. Miravirsen sequesters miR-122 and inhibits it from binding to the HCV genome thereby preventing its RNA multiplication (Janssen et al., 2013). Thus, miravirsen is a potential new therapy for the

treatment of HCV-positive patients. Secondly, miRNA mimics (synthesized miRNA-like strands), such as miR-34a (Wiggins et al., 2010) and let-7 (Trang et al., 2010), can be used to restore the function of miRNAs which are lost in the diseased cells (Bader et al., 2010). Unlike gene therapy that can be difficult to achieve because of the need to introduce large plasmids into the target tissue, miRNA mimics can be delivered using silencing RNA technology (Figure 1.13). The fact that miRNA mimics is small and representative of the endogenous miRNA sequences means that mRNA target specificity is increased and thus off- target effects (targeting many mRNAs) are less problematic. MicroRNA mimics target the same mRNAs as the endogenous miRNA population which is lost due to the disease (Bader et al., 2010). With the array of technologies that are constantly being developed and made available in the miRNA field, normalization of deregulated miRNAs may, therefore, be feasible in particular disease settings.

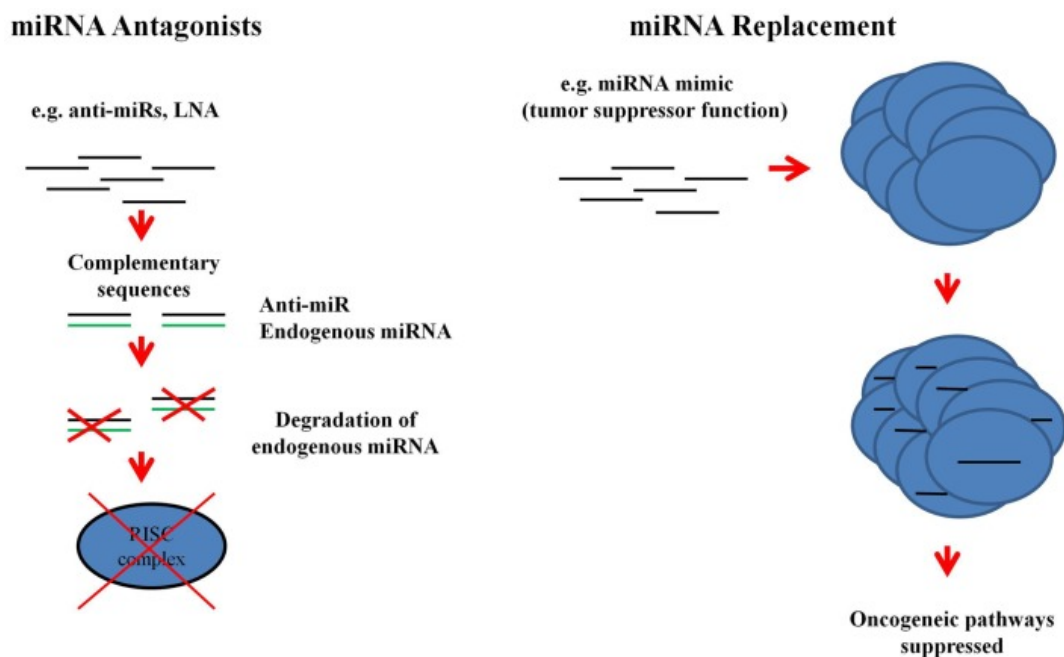


**Figure 1.13 Therapeutic applications of miRNAs.** MiRNA antagonists, which are modified oligonucleotides with complementary sequences to the endogenous miRNAs, can be used to degrade over-expressed miRNAs. Loss of function of the endogenous miRNA prevents it being processed by RISC. MiRNA mimics are also oligonucleotides, but they replace the lost function due to the disease state of the cell (Bader *et al.*, 2010).

### ***1.9.1 The current outlook for this investigation***

Although miRNA studies in the field of GVHD are in their infancy, recent investigations have demonstrated the tremendous potential for these small regulatory molecules as diagnostic, prognostic and therapeutic markers. Clinical applications exploiting our knowledge of miRNA function may play a crucial role in the future of GVHD management and treatment. An early diagnosis of GVHD can prevent patient's suffering from severe GVHD (grades III-IV) as appropriate clinical interventions such as immunosuppressive drugs and steroids can be administered or their doses modulated accordingly. It will also increase the patient's quality of life and decrease mortality due to GVHD severity.

Thus, the overall aims of this investigation was to identify a signature list of miRNAs for aGVHD disease diagnosis using clinical skin biopsies and also to understand the role of immune related miRNAs in whole blood for investigating the potential of these miRNAs in monitoring GVHD and its response to therapy.

## 1.10 Hypotheses and Aims

### General hypotheses and overall aim

Biomarkers that can be used in the transplantation clinic are absent. MicroRNAs have established roles in inflammatory and immune-related diseases. They are highly specific, sensitive, and reliable and can be quantified from various tissues and peripheral blood. The overall aim was to better understand the regulatory molecular mechanism involved in the pathophysiology of aGVHD which may aid patient stratification for improved therapies and also result in the identification of robust diagnostic and predictive biomarkers for use in the clinic.

**Chapter 3.** Pathway mining is a useful tool in identifying genes, proteins and miRNAs that may be directly or indirectly related to a set of disease specific genes. Previous experiments in our group had shown that there was an association between a list of 18 genes and allo-HSCT outcome (i.e GVHD).

### Specific aims

- (1) Determination of specific pathways that the 18 genes associate with during allo-HSCT and GVHD.
- (2) Identification of miRNAs that may target the 18 genes and therefore control their expression levels.

**Chapter 4.** MicroRNAs are deregulated in the skin as a result of allo-HSCT and aGVHD.

### Specific aims

- (1) Identification and validation of a signature list of miRNAs in cutaneous aGVHD biopsies that could have diagnostic biomarker application for aGVHD and also predict OS and disease relapse.
- (2) Assessment of whether the miRNAs identified in the signature list targeted the 18 genes.
- (3) Identification of downstream miRNA targets for the identified miRNA signature list.

**Chapter 5.** MicroRNAs impact their downstream targets at the protein translation stage.

**Specific aims**

- (1) To test the correlation between the miRNA targets and the most significant miRNA from the identified signature list in Chapter 4.
- (2) To establish the preliminary optimization methods required to conduct future miRNA-based functional experiments.

**Chapter 6.** MiR-146a-5p and miR-155-5p have immune-specific functions in several inflammatory and autoimmune conditions. Their expression has been detected in the peripheral blood of both allo-HSCT patients and healthy volunteers.

**Specific aims**

- (1) Evaluate whether miR-146a-5p and miR-155-5p are differentially expressed prior to aGVHD disease onset.
- (2) Assess whether the expression levels of both miR146a-5p and miR-155-5p could be used to predict aGVHD onset and severity as well as OS, relapse and NRM.
- (4) To assess the correlation between miR-146a-5p and miR-155-5p with their established targets (IRAK1, TRAF6, STAT1- $\alpha$ , IRF5 and the transcription factor *SPI1*) both at the mRNA and protein level.

## Chapter 2. Materials and Methods

“You never change things by fighting the existing reality.  
To change something, build a new model that makes the existing model obsolete.”  
- **R. Buckminster Fuller**

This Chapter includes all the reagents, experimental methods and statistical analyses used for all the investigations mentioned throughout this thesis.

## **2.1 Patients and Healthy Volunteer Cohort**

### **2.1.1 Ethics and consent**

The patients and healthy volunteers consented for both the skin and whole blood collection and molecular testing. Consent was taken prospectively by trained personnel. The project was approved by the Newcastle and North Tyneside I Research Ethics Committee (Whole Blood study: STEMDiagnosics: 07/H0906/131, Allo-HSCT skin study: 05/Q0905/200 and Healthy Volunteers skin: 2002/204). For further information on the approvals see Ethics Approval Section (page 258). All the investigations were conducted in accordance with the Helsinki Declaration.

### **2.1.2 Clinical information**

The overall clinical aGVHD grade was diagnosed by clinicians in accordance with the NIH consensus. All the clinical data were collected from the ProMISE database (Project Manager Internet Server) as used by the European Society for Blood and Marrow Transplantation. Overall clinical aGVHD grades and cutaneous histopathological grades were assessed using standard criteria (Glucksberg H, 1974; Lerner *et al.*, 1974).

## **2.2 Tissue Culture Methods**

All tissue culture work was performed in a Class II safety cabinet under aseptic conditions. Incubation of cultures was at 37°C in a humidified incubator (Flow Laboratories IR 1500 incubator) with 5 % carbon dioxide and 95% air.

### **2.2.1 General cell culture media**

Peripheral blood mononuclear cells were cultured in Roswell Park Memorial Institute (RPMI) 1640 medium (PAA) supplemented with 2 mM L-glutamine (Life Technologies), 10% Heat Inactivated Fetal Calf Serum (Life Technologies), 100 IU/ml penicillin and 100 µg/ml streptomycin (Sigma).

### **2.2.2 Isolation of PBMCs**

PBMCs were isolated from peripheral blood or leukocyte reduction system cones using the density centrifugation method. Peripheral blood was collected from patients and healthy volunteers in Universal Container (Sterilin) that had 500 IU sodium-heparin as the anti-coagulant. Peripheral blood was then diluted (1:1) with Earle's Balanced Salt Solution (EBSS, Gibco) and then carefully layered onto Lymphoprep™ (Axis Sheilds). Samples were centrifuged (Fischer) at 800 g for 15 minutes at room temperature. Supernatant was discarded and PBMCs were collected from the interphase layer using sterile Pasteur pipette. PBMCs were washed in EBSS twice by centrifugation at 500 g, room temperature for 5 minutes. Washed cells were resuspended in RPMI 1640 supplemented medium. Cells were counted on an Improved Neubauer Haemocytometer (Weber Scientific International Ltd) and percentage viability was determined by the Trypan Blue (Sigma) exclusion test.

Acknowledgement: Dr Emily Mavin provided some of the healthy volunteer PBMCs.

### **2.2.3 Cryopreservation of PBMCs**

Cryopreservation of cells was performed by using freezing solution containing 70% RPMI 1640 medium, 20% HI FCS and 10% dimethyl sulphoxide (DMSO) (DMSO, Kocklight Ltd). Cell pellets were resuspended in cold freezing solution and aliquoted into cryovials ( $3 \times 10^6$  -  $10 \times 10^6$  cells/ vial) (Nunclon). To regulate the freezing process the cryovials were wrapped in bubble plastic and stored at -80 °C for approximately 24 hours and then transferred for long term storage to -140 °C freezers.

### **2.2.4 Preparation of serum**

Peripheral blood was collected into 7 ml vacutainer tubes coated with potassium Ethylenediaminetetraacetic acid (EDTA) (Becton Dickinson). The blood clot was allowed to retract for 4-7 hours at 4 °C and then centrifuged at 500g, room temperature for 5 minutes. Serum was collected from the supernatant and dispensed into sterile Eppendorf tubes (250 µl). All sera were stored immediately on collection at -80 °C freezer.

### **2.2.5 Thawing of cryopreserved PBMCs**

Cryopreserved PBMCs were retrieved from the -140 °C freezer and quickly transferred to 37 °C water bath. Thawed cells were transferred into 10 ml warmed RPMI 1640 supplemented medium using sterile Pasteur pipette. Cells were washed twice by centrifuging at 500 g, room temperature for 5 minutes. The pellet was resuspended in RPMI 1640 supplemented medium or Phosphate Buffered Saline (PBS), counted and Trypan Blue exclusion test performed for viability.

## **2.3 Total RNA Extraction from Different Tissues**

### **2.3.1 Clinical skin biopsies and in vitro skin explant model**

Total RNA was extracted from clinical skin biopsies (1- 4mm) and skin from the *in vitro* skin explant model using the *mirVana* miRNA Isolation kit (Life Technologies, USA) (Figure 2.1). Initially, the skin biopsies were homogenised on a sterile petri-dish, in 60 µl of Lysis Buffer using sterile scalpel. The lysate was transferred into an Eppendorf and made up to 300 µl with the Lysis Buffer. To enhance homogenisation, the Homogenate Additive (30 µl) was added to each sample and incubated on ice for 10 minutes. The organic extraction was performed by adding phenol:chloroform (300 µl) to the samples, vortexing for 60 seconds and centrifugation at 10, 000 g for 5 minutes. The upper phase was carefully transferred to a fresh Eppendorf and 100% Ethanol (375 µl) added. The mix was then loaded onto a Filter Cartridge and centrifuged at 10,000 g for 15 seconds. The flow through was discarded and the Wash Buffer 1 (700 µl) added onto the filter and centrifuged at 10,000 g for 15 seconds. The flow through was again discarded and total RNA was washed twice with Wash Buffer 2/3 (500 µl) and centrifuged at 10, 000 g for 1 minute. The Filter Cartridge was dried by centrifugation at 14,000 g for 1 minute to remove all the chemicals. Then the Filter was transferred to a new Eppendorf and pre-heated nuclease-free water (100 µl) at 95°C was used to elute the total RNA by centrifugation at 14,000 g for 20-30 seconds.

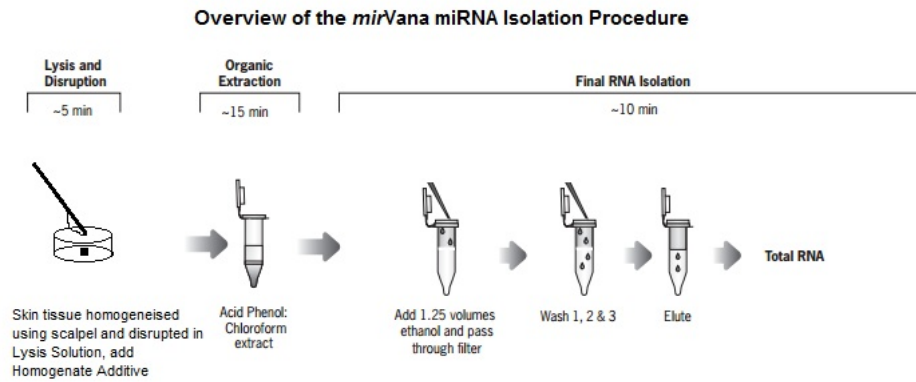


**Figure 2.1** Total RNA was extracted from clinical skin biopsies using the *mirVana* miRNA isolation kit (adopted from Life Technologies). There are three steps main steps performed in the extraction of total RNA from clinical skin biopsies; (1) Lysis and cell disruption, (2) organic extraction and (3) total RNA isolation and elution.

### 2.3.2 Whole blood

Peripheral blood (2.5 ml) was collected in PAXgene Blood RNA Tubes containing a reagent that results in immediate cell lyses and RNA stabilization (Figure 2.2). Two tubes were collected from each allo-HSCT patient at the following time-points, 7 days pre-transplant and post-transplant at: 28 days and 3 months. For healthy volunteers only 2.5 ml of peripheral blood was collected. Total RNA was extracted using PAXgene Blood miRNA kit (Qiagen/BD Company) which is phenol/chloroform free and a silica membrane based protocol. PAXgene Blood RNA Tubes were stored at -20°C until extraction and incubated overnight at room temperature to increase total RNA yield. To collect pellet PAXgene Blood RNA Tubes were centrifuged at 3,500 g for 10 minutes (Fisher Scientific) (Figure 2.2). The pellet was washed in 4 mls of RNase-Free water and spun as above. The cell pellets were re-suspended in 350 µl buffer BM1. Then 300 µl of the binding buffer BM2 was added and 40 µl proteinase K and incubated for 10 min at 55°C on a shaker- incubator set at 400- 1400 rpm to degrade any proteins. Lysate clumps have active RNases that can degrade RNA and decrease its integrity thus to de-clump, lysates were shredded further using needle-syringe (1 ml), transferred into the PAXgene Shredder spin Column and centrifuged for 3 min at 14,000 rpm. Gently, the entire supernatant was transferred from the flow-through to a fresh Eppendorf and

Isopropanol (Fisher Scientific) added (700  $\mu$ l) to increase the binding of total RNA to silica membrane. This mix was loaded onto the Spin Column that contained the silica membrane and centrifuged at 14,000 rpm for 1 minute. After every spin the processing tube was discarded and a new one used for the next step. The wash buffer (BM3) was then added (350  $\mu$ l) to the Spin column and centrifuged for 1 min at 14,000 rpm. DNase 1 mix was made by adding 10  $\mu$ l of the stock DNase 1 (1500 Kunitz) to 70  $\mu$ l DNA digestion buffer (RDD) per sample. Gentle mixing was performed as DNase 1 is sensitive to denaturation. DNase 1 mix was loaded to every Spin Column and incubated at room temperature for 15 minutes. This treatment ensured that all DNA was digested in order to obtain purified RNA. The reaction was stopped by adding BM3 (350  $\mu$ l) to the Spin Column and centrifuged for 1 minute at 14, 000 rpm. Wash Buffer 2 (BM4) (500  $\mu$ l) was loaded onto the Spin Column and centrifuged for 15 seconds at 14,000 rpm. This step was carried twice to completely remove any of the chemicals from the RNA. The Spin Column was then spun empty for 1 minute at 14,000 rpm to dry the silica membrane. The Spin Column was transferred to a fresh Eppendorf (1.5 ml) and the total RNA was eluted using elution buffer BR5 (80  $\mu$ l). The Spin Column was centrifuged for 1 minute at 14,000 rpm. The Spin Column was discarded and total RNA concentration and purity of the total RNA was determined using the spectrophotometer, Nanodrop 1000 (Thermoscientific). Total RNA was stored at -20 °C until further use.

### The Manual PAXgene Blood miRNA Procedure

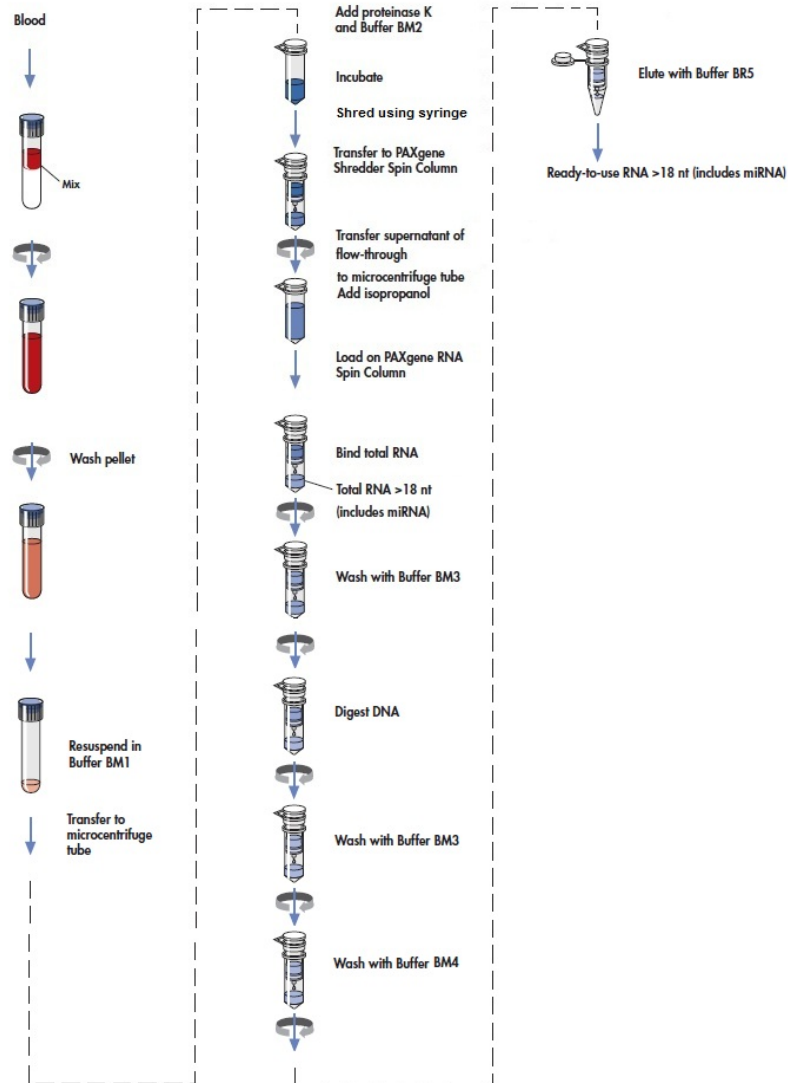


**Figure 2.2 Total RNA was extracted from whole blood using the PAXgene Blood miRNA kit (adopted from Qiagen).** Firstly, the cells were pelleted and then resuspended using BM1. Proteins were degraded by incubating samples at 55 °C with buffer BM2 and proteinase K, respectively. Samples were then homogenized using 1 ml syringe and then loaded onto the Shredder column for additional homogenisation. Supernatant was collected into a new Eppendorf; Isopropanol was added onto the Spin Column and then centrifuged. BM3 was added in the wash step and centrifuged again. DNase 1 treatment was performed for 15 minutes. Two wash steps were performed, one with BM3 and twice with BM4, respectively. Purified total RNA was then eluted using buffer BR5 and the concentration was determined using the Nanodrop.

### **2.3.3 Peripheral blood mononuclear cells**

The *mirVana* PARIS kit allowed the extraction of total RNA, DNA as well as protein from the same sample. Therefore, it was used for experiments where both total RNA and protein isolation from the same sample was required. All the steps are depicted in Figure 2.3.

Working solutions were prepared as follows; 2-mercaptoethanol (375  $\mu$ L) (Life Technologies) was added to 2X Denaturing Solution, 100% ethanol (21 mL) was added to Wash Solution 1 and (40 mL) to Wash Solution 2/3.

Three main steps were performed in this method; (1) sample disruption, (2) lysate separation for RNA and protein isolation, (3) organic extraction. Initially, cells were pelleted via centrifugation at 2, 500 rpm for 5 minutes. The pellet was washed with 1 mL PBS, re-pelleted as above and then stored on ice. Cells were lysed by addition of ice-cold Cell Disruption Buffer (100-625  $\mu$ L depending on cell count, example: 300  $\mu$ L for more than  $10^6$  cells) and vortexing for 10-15 seconds. Lysate was stored on ice and split into two, one-half for total RNA extraction and the other for protein isolation.

The lysate that was used for the **protein extraction** was incubated on ice for 5-10 min and then passed through a syringe needle (1 ml) several times on ice for further homogenisation. Extracted protein was then stored at  $-20$  °C until further use.

The lysate for **RNA isolation** was mixed with an equal volume of 2X Denaturing Solution (up to 625  $\mu$ l) at room temperature. If the sample volume was less than 100  $\mu$ l, Cell Disruption Buffer was added to bring the volume to 100  $\mu$ l before the addition of 2X Denaturing Solution as mentioned above. Mixtures were incubated on ice for 5 min. A volume of Acid-Phenol: Chloroform that was equal to the total volume of the sample lysate plus 2X Denaturing Solution was added to the mixture and vortexed for 30-60 seconds. The mixture was centrifuged for 5 min at 10,000 x g to separate it into aqueous and organic phase. The upper aqueous phase was removed carefully, without disturbing the lower phase or the interphase, and transferred it to a fresh tube. The volume recovered was noted for the later steps. Then 100% ethanol (1.25 the volume recovered) was added to the aqueous phase and loaded onto a Filter Cartridge that

contained glass-fibres to immobilize the total RNA and centrifuged for 30 seconds. The flow-through was discarded. Total RNA was washed by addition of Wash Solution 1 (700  $\mu$ L) and centrifuged at 14, 000 rpm for 15 seconds. Wash Solution 2/3 (500  $\mu$ L) was then added and centrifuged as above. This step was repeated again. Residual fluids were removed and the Filter Cartridge dried by centrifugation at 14,000 rpm for 1 minute. Total RNA was eluted using nuclease-free water (100  $\mu$ L) preheated at 95°C and centrifugation at 14,000 rpm for 30 seconds. The concentration and purity of total RNA was determined using the Nanodrop.

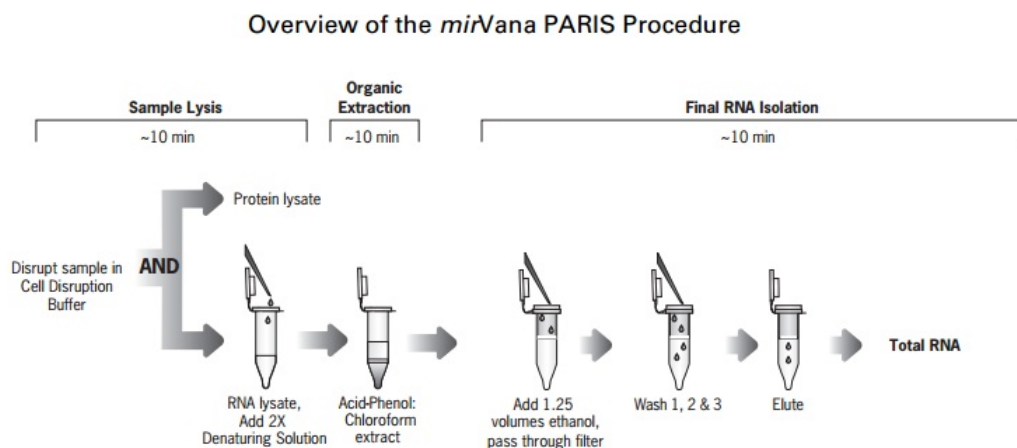


**Figure 2.3** Total RNA was extracted from PBMCs using the *mirVana* PARIS kit (adopted from Life Technologies). Cells were washed, pelleted and homogenised using Cell Disruption Buffer. Lysate was split into two; (1) protein and (2) total RNA isolation. The RNA lysate was mixed with 2X Denaturing solution and then acid-Phenol: Chloroform extraction performed. The upper phase was collected and ethanol was added and the solution passed through filter cartridge. Total RNA was then washed with Wash Buffer 1 and Wash Buffer 2/3. Elution was performed by addition of nuclease-free water preheated at 95 °C.

## 2.4 Real-Time PCR Basic Concepts

### 2.4.1 Real-time PCR amplification curve

In brief, amplification of cDNA in real-time is a two-step process. In the first step, cDNA is synthesized by reverse transcription (RT) and in the second step this cDNA is quantified using real-time PCR machine.

The qPCR amplification curve has three phases: the baseline or background phase, exponential phase and plateau phase. Baseline was set between 3-15 cycles of the RT-qPCR, this eliminated any background fluorescence. At baseline fluorescence is present but not sufficient to be detected by the lasers as a positive signal. Threshold was set (either automatically or manually depending on the experimental investigation) at the exponential phase of the RT-qPCR and this determined the cycle threshold ( $C_t$ ) or cycle quantification ( $C_q$ ). The aim of setting threshold was to calculate the relative quantity (RQ) of input cDNA (template) present at the start of the PCR reaction. The amplification or reaction curve shown in figure 2.4 is representative of RT-qPCR data.  $\Delta Rn$  (delta Reaction) values were plotted on the y-axis and cycle numbers on the x-axis.  $\Delta Rn$  is the ratio of fluorescence of FAM dye by fluorescence of ROX dye. ROX was the passive reference (accounts for pipetting variations) dye and was present in the Taqman master mixes. The Exiqon LNA-based master reagents did not have ROX. Pilot investigation (data not shown) showed that there was no significant pipetting error and therefore it was considered not necessary to add ROX to the LNA master mixes. Thus, ROX detection was disabled when LNA based primers were used for the qPCR reaction.

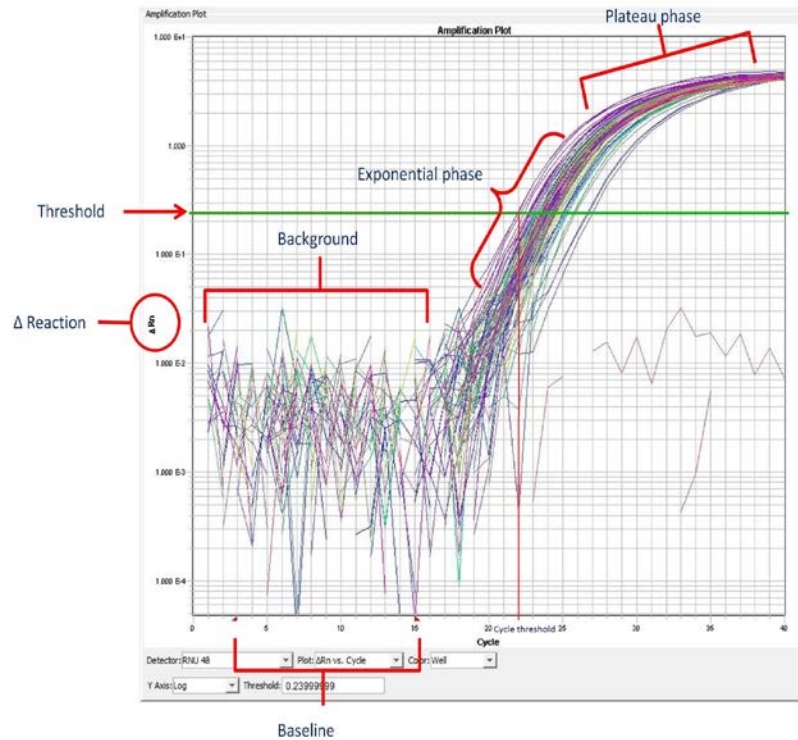


**Figure 2.4 Ideal qPCR amplification curve.** The three different phases of the RT-qPCR are marked on the curve as; background, exponential and plateau phase.

For all of the total RNA extractions, concentration of total RNA was determined using the NanoDrop 1000 (Thermo Scientific). For all the qPCRs, each sample was run in triplicate on 7900HT Fast Real-Time PCR (Life Technologies), using the standard thermal cycling conditions on the machine.

Two different cDNA synthesis and real-time PCR chemistries were used; (1) **Taqman** labelled hydrolysis probes (Life Technologies, USA) and (2) **Locked-Nucleic Acids- SYBR 1** dye detection (Exiqon, Denmark).

### **2.4.2 Taqman chemistry**

The Taqman chemistry for quantification of miRNAs was a two-step process. In the first step, miRNA specific cDNAs were synthesized. This process involved the addition of miRNA specific stem-loop primers that bound to the -3p end of the template. The

enzyme reverse transcriptase extended the primer by the addition of nucleotides for the cDNA strand to be synthesized (Figure 2.5).

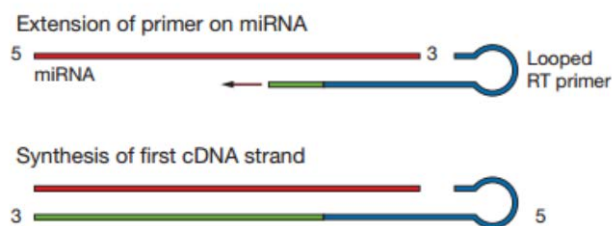


**Figure 2.5 Taqman reverse transcription step (adopted from Life Technologies).** In brief, the specific reverse transcription stem-looped primer was bound to the miRNA template and this resulted in the first strand synthesis of cDNA.

For the Taqman miRNA specific cDNA synthesis, 1- 10 ng of total RNA was reverse transcribed in a 15  $\mu$ l reaction using Taqman specific RT primers and the Taqman miRNA Reverse Transcription Kit (Life Technologies). In brief, the master mix consisted of the miRNA specific primers, nuclease free water, buffer, reverse transcriptase (Rtase), RNase inhibitor, dNTPs and diluted RNA (Table 2.1). All the steps were performed on ice. The following settings were set on the thermal cycler (Applied Biosystems, 2720 Thermal Cycler) for cDNA synthesis; 16°C for 30 minutes, 42°C for 30 minutes and 85°C for 5 minutes to denature the enzyme. The cDNA assay was then stored at -4°C till use.

Taqman cDNA Master Mix	1X ( $\mu$ l)
Nuclease-free H <sub>2</sub> O	4.16
Buffer	1.5
Rtase	1
Inhibitor	0.19
dNTPs	0.15
Primer	3
Template total RNA (Diluted)	5
Total volume	15

**Table 2.1 Taqman miRNA cDNA synthesis master mix.**

Taqman chemistry consisted of a set of primers, both forward and reverse and a Taqman probe (Figure 2.6). All the primers used were off-the-shelf and these were designed to bind on either side of the template and extend, accordingly. Taqman

hydrolysis probes were based on fluorescence resonance energy transfer (FRET). The probes consisted of a quencher dye (3' end) at one end and a reporter fluorescent dye (5' end) at the other end. The non-fluorescent quencher (NFQ) dye decreased the fluorescence emission of the reporter dye when the probe was unbound to the template sequence. The NFQ had a minor groove binder (MGB) moiety bound to it (MGB-NFQ). This allowed shorter probes to be made with greater stability, in particular for miRNA based investigations. In the presence of the template, the hydrolysis probe was bound downstream from one of the primer sites. As the primer extended the template, Taq DNA polymerase degraded the reporter dye. The Reporter dye was then released as a result and the fluorescence was detected by the laser system in the real-time PCR machine. The fluorescence was directly proportional to the initial amount of template in the reaction. In all the experiments the dyes bound to the primer sequence were 6-carboxyfluorescein (FAM) and the quencher moiety was MGB-NFQ.

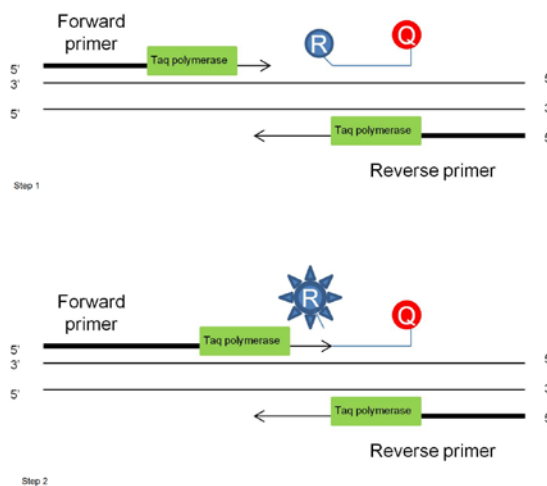


**Figure 2.6 Real-time PCR steps when using Taqman chemistry (adopted from Life Technologies).** 'R' denotes reporter fluorescent dye and 'Q' denotes quencher dye. Step 1 shows the polymerisation of the template strand by Taqman polymerase. Step 2 shows the degradation of the reporter fluorescent dye from the quencher by the Taqman polymerase.

The miRNA specific cDNAs were used for the RT-qPCR step using the miRNA specific Taqman probes. In brief, the master mix comprised of the specific cDNA, nuclease-free water, Taqman primer-probe sets and TaqMan® Universal Master Mix. Every sample was run in triplicate, 10 µl/well. The triplicate volumes included 20% excess for volume loss from pipetting (Table 2.2).

<b>Real-time PCR Master Mix</b>	<b>Volume (µl) per triplicate</b>
Taqman Primer-Probe	1.8
Taqman Universal Master Mix	18
Nuclease Free- Water	13.8
cDNA	2.5
Total Volume	36.1

**Table 2.2** Taqman miRNA RT-qPCR master mix.

### **2.4.3 LNA™- SYBR 1 dye chemistry**

Locked nucleic acids (LNA) are RNA analogs with high affinity. For efficient Watson-Crick binding the ribose ring is “locked” in the most stable conformation thereby leading to rapid hybridisation to the cDNA. Thus, LNA™ oligonucleotides have greater thermal stability during cDNA synthesis and are shorter than other DNA or RNA oligonucleotides used conventionally. The melting temperature of LNA based primers are normalised to increase robustness regardless of varied GC content. The LNA primers are therefore specific and sensitive in particular for the detection of miRNAs.

Universal cDNAs were synthesized using the LNA primers. Initially, poly-A tails were added to the mature miRNA template. The primers had a poly-T tail, a 3’ degenerate anchor and a 5’ universal tag. The poly-T tail was bound to the poly-A tail while the 3’ degenerate anchor guided the cDNA synthesis (Step 1, Figure 2.7).

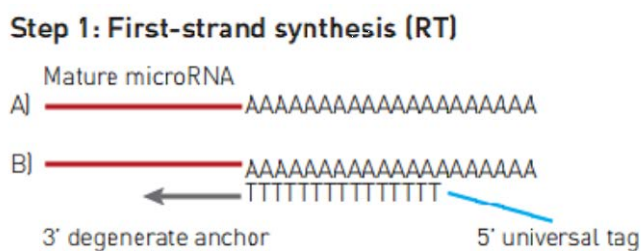


**Figure 2.7 MiRCURY LNA™ Universal RT microRNA PCR System (adopted from Exiqon).** Step 1 (A) involves the cDNA synthesis where polyA tail is incorporated to the miRNA sequence. Step 1 (B) poly-T primer with a 3' degenerate anchor and a 5' universal tag were used to synthesise the universal cDNA.

All the reagents and reaction steps for the reverse-transcription step were performed at 4°C (on ice). Lyophilised forward and reverse primers were re-suspend by adding nuclease-free water (220 µl). The primers were vortexed, spun down and incubated on ice for 20-30 minutes before use. First strand cDNA was synthesized by diluting total RNA samples (5 ng/µl) using nuclease-free water. The universal cDNA master mix (Product No: 203301) comprised of; 5X reaction buffer, nuclease-free water, enzyme and the diluted total RNA (Table 2.3). The thermal cycler (Applied Biosystems, 2720 Thermal Cycler) reactions set up were as follows; 42°C for 60 minutes, 95°C for 5 minutes and then samples stored at -4°C till use.

LNA cDNA Master Mix	1X (µl)
5X Reaction buffer	4
Nuclease-free H <sub>2</sub> O	10
Enzyme mix	2
Template total RNA (5 ng/µl)	4
Total volume	20

**Table 2.3 MiRCURY LNA™ Universal cDNA synthesis mater mix.**

In the real-time PCR reaction step, miRNA specific forward and reverse primers were used to amplify the miRNA of interest (Step 2, Figure 2.8). SYBR1 Green dye was used for the detection of amplified miRNA products. Since, SYBR1 dye could be non-specific and bind to primer-dimers in addition to the amplified miRNA, melting curve analysis was performed which is explained in more detail in the next section.

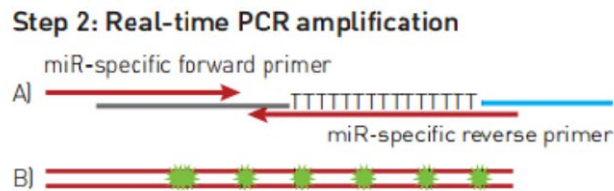


**Figure 2.8 MiRCURY LNA™ RT-qPCR step (adopted from Exiqon).** In Step 2 which is the real-time PCR reaction, (A) the universal cDNA is used as the template to amplify specific miRNAs. LNA specific forward and reverse primers are used in this process. (B) The SYBR 1 Green dye is used to detect the specific miRNAs.

Complementary DNA that was synthesized in the first step was diluted 80x by adding nuclease-free water (1580  $\mu$ l H<sub>2</sub>O per 20  $\mu$ l RT). The real-time PCR master mix comprised of the following reagents; ExiLent SYBR® Green (Product No: 203402) master mix, specific PCR mix and the diluted cDNA (Table 2.4). The MicroAmp® Optical 96-well reaction plates without barcodes (Life Technologies) were used for all the qPCR steps. The primer names were as per mirbase version 19.0.

Real-time PCR Master Mix	Volume ( $\mu$ l) per triplicate
SYBR Green master mix	15
Specific PCR primer mix	3
Diluted cDNA template	12
Total volume	30

**Table 2.4 MiRCURY LNA™ RT-qPCR master mix.**

#### **2.4.4 Taqman gene expression assays**

The reverse transcription step for gene expression assays comprised of universal random hexamers. The cDNA mix was first made using; random hexamers (Thermo Scientific), dichloro-diphenyl- trichloroethane (DTT) (Invitrogen), first strand buffer (Invitrogen) and dNTPs mix (Roche Diagnostics) (Table 2.5, B). In brief, total RNA was denatured at 65 °C for 5 minutes and was reverse transcribed using equal volume of master mix (ratio1:1). The cDNA PCR master mix consisted of the cDNA mix, reverse transcriptase, MMLV RT (Invitrogen) and Rnase inhibitor, RNasin (Promega). The

reaction mix was incubated using a thermal cycler (ABI 2720) at 37 °C for 2 hrs and 10 min at 65 °C to denature the enzymes. The cDNA was used to run qPCR for using specific Taqman off-the-shelf hydrolysis probes.

<b>A. dNTP Mix</b>	<b>Volume (μl) 3X</b>
dATP	50
dCTP	50
dGTP	50
dTTP	50
Nuclease-free H <sub>2</sub> O	300
Total volume	500
<b>B. cDNA Mix</b>	<b>Volume (μl) 10X</b>
Buffer	332.5
dNTP mix	166.25
Random hexamers	210
DTT	166.25
Total volume	875
<b>C. cDNA PCR Master Mix</b>	<b>Volume (μl) 10X</b>
cDNA mix	100
MMLV RT	7
Rnasin	3.5
Total volume	110.5

**Table 2.5 Reverse transcription master mix for gene expression assays.**

The RT-qPCR mix comprised of; total RNA (10-100 ng), nuclease-free water, 2X Taqman Gene Expression Master Mix and target specific primer-probes (Life Technologies) (Table 2.6). The MicroAmp® Optical 96-well reaction plates without barcodes were used for all the qPCR steps. The qPCR was performed on 7900HT Fast- Real Time PCR system (Life Technologies). For all the gene expression studies, Human glyceraldehyde 3-phosphate dehydrogenase (*GAPDH*: 4352934E, Life Technologies) was used as the reference gene. A summary list of all the assays used in the various investigations is mentioned in table 2.7.

qPCR Master Mix	Volume ( $\mu$ l) per triplicate
Taqman gene expression master mix	22.5
Specific primer-probe	2.25
Nuclease free water	19.75
cDNA	2.4
Total volume	46.9

**Table 2.6 Quantitative PCR master mix for standard gene expression assays.**

Manufacturer	PCR Chemistries	Taqman primer-probes	Assay IDs
Exiqon	Locked Nucleic Acids	hsa-miR-103a-3p	204063
		SNORD48	203903
		hsa-miR-21-3p	204302
		hsa-let-7c	204767
		hsa-miR-34a-3p	204318
		hsa-miR-34a-5p	204486
		hsa-miR-142-3p	204291
		hsa-miR-23b-3p	204790
		hsa-miR-365a-3p	204622
hsa-miR-503-5p	204334		
Life Technologies	Taqman	hsa-miR-103a-3p	439
		SNORD48	1006
		hsa-miR-24-3p	402
		hsa-miR-493	2364
		hsa-miR-200b	2251
		hsa-miR-2110	121216_mat
		hsa-miR-146a-5p	468
		hsa-miR-155-5p	479
		TRAF6	Hs00371512_g1
		IRAK1	Hs01018347_m1
		STAT1- $\alpha$	Hs01014003_m1
		IRF5	Hs00158114_m1
		SPI1	Hs02786711_m1
GAPDH	4352934E		

**Table 2.7 Taqman gene expression prime-probes for qPCR.** For the gene expression assays, GAPDH was used as the reference control. For the individual miRNA assays, miR-103a-3p and SNORD48 were used as the reference controls.

## 2.5 Real-time PCR Data Analysis

### 2.5.1 Amplification curve analysis

Efficiency of the hydrolysis probes or LNA primers determined the progress of the amplification curve. Efficiency of off-the-shelf assays (Taqman and LNA) was

considered to be 90-100%. Hence, efficiency (E) was set at 2 ( $RQ = 1/E^{C_q}$ , when  $E=2$ , then  $RQ = 2^{-C_q}$ ). In relative quantification the  $C_q$  value for gene/miRNA of interest was normalized to the  $C_q$  of reference gene/ miRNA ( $\Delta C_q = C_q \text{ gene of interest} - C_q \text{ reference gene}$ ). This resulted in the first derivative of  $C_q$  which was  $\Delta C_q$ . The second derivative ( $\Delta\Delta C_q = \Delta C_q \text{ (diseased sample)} - \Delta C_q \text{ (reference sample)}$ ) was determined if there was a reference sample present such as normal controls. The RQ was calculated using the formulae,  $RQ = 2^{-\Delta\Delta C_q}$  or  $RQ = 2^{-\Delta C_q}$ . Since  $\Delta C_q$ ,  $\Delta\Delta C_q$  and RQ values were all linear values and qPCR data is non-linear (exponential) the values were transformed (Log transformation =  $\log_2 RQ$ ) using logarithms. In addition, biological data is usually not normally distributed and thus suffers from heterogeneity of variance (McDonald, 2009). In order to be able to use parametric statistical tests on qPCR data the RQ values must be transformed logarithmically to create a normal distribution of these values. Otherwise, the result could be misleading. Log transformation also helps when there are outliers present in the data. The higher values are concentrated together while the smaller values are spread (Rieu and Powers, 2009). Statistical analysis and plotting of qPCR data were all performed on the Log transformed data.

### ***2.5.2 Melting curve analysis***

When LNA-SYBR Green dye was used for the detection of miRNAs in the qPCR reaction, melting or dissociation curve analysis was performed to identify any primer-dimer formation and/or non-specific amplifications. Melting temperature ( $T_m$ ) is based on the length of the product sequence and its GC content. Therefore, it is an ideal indicator for non-specific product amplification such as primer-dimers. A ramp step was therefore included after the real-time PCR reaction was completed. In this step the temperature was increased gradually (from annealing (62°C) to denaturation temperature (95°C) and the SYBR1 Green dye was detected as the products dissociated. The  $T_m$  was the maximum point of the peak where almost 50% of the products had dissociated (Figure 2.9). Any peak before the actual peak of the dissociation curve could be indicative of primer-dimers.

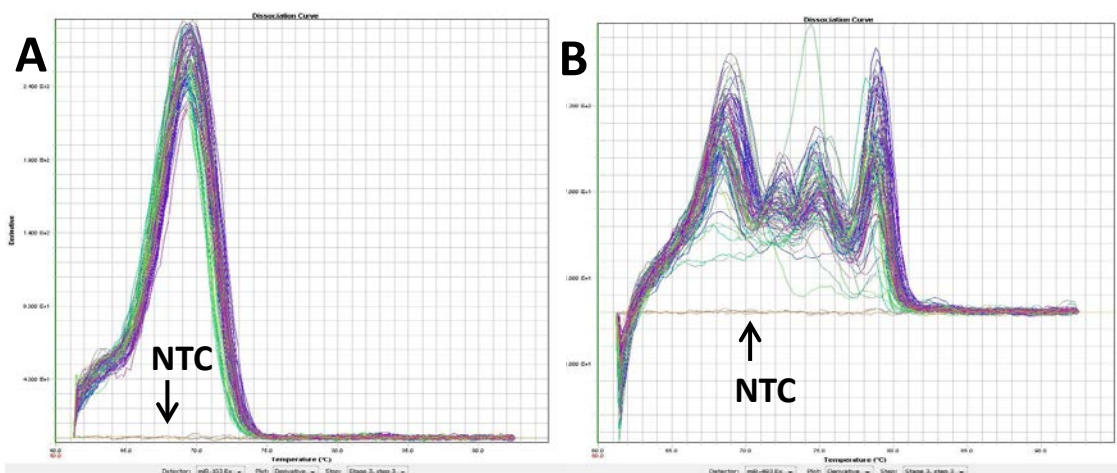


**Figure 2.9 Melting curve analysis.** (A) Absence of non-specific amplification as the  $T_m$  of all the products overlaps and is very similar. (B) The  $T_m$  of the products vary and there is non-specific primer binding. The reactions for both A and B are contaminant-free as the no-template control (NTC) is not amplified.

## 2.6 Global miRNA Profiling and Individual MiRNA Assays

Global miRNA profiling of skin biopsies (Chapter 4) was performed using the Exiqon miRNA qPCR services. Total RNA was sent to the Exiqon services and three quality control checks were performed for each sample to assess RNA integrity, purity and detect PCR inhibitors (if present). The nine (total RNA) samples passed quality control checks for use in the global profiling experiment.

Briefly, 40 ng of total RNA was reverse transcribed to cDNA as per the miRCURY LNA™ Universal RT miRNA PCR protocol. Each cDNA was diluted 100X and then run on both Human panel I (372 miRNAs) and Human panel II (367 miRNAs) consisting of a total of 739 miRNAs and three inter-plate calibrators, six reference controls and one control set (RNA spike-in). No pre-amplification of total RNA was performed for this global miRNA profiling experiment. The workflow consisted of five main steps from the experimental setup to quality controls and up to analysis. (1) Universal RT miRNA PCR (as described in Section 2.4.2) - All the miRNAs were polyadenylated and reverse transcribed into cDNA. The cDNAs and the SYBR Green master mix were then transferred to the two qPCR panels (Human I and II). The panels had 739 preloaded primers. The pipetting was automated (robot) to reduce errors. This was followed by the qPCR step which was run on a Roche Light cycler 480. (2) Data was collected and

analysed for non-specific amplifications and primer-dimer formations (melting curves). Reactions with efficiencies lower than 1.6 were eliminated from further analysis. (3) Negative control evaluation- Reactions with  $C_q$  values that were within 5 values of the NTC were also eliminated from further analysis.(4) All data were then normalized. (5) Preliminary data analysis was performed.

## 2.6.1 Preliminary quality controls of total RNAs

### 2.6.1.1 Total RNA was of high quality

The RNA integrity number (RIN) was obtained for each of the nine samples prior to performing the profiling experiment. The RIN number was calculated by performing an electrophoretic measurement using the bioanalyzer (Agilent 2100). Results showed that the quality of total RNA extracted was of high (greater than or equal to 7) for all the samples. There were single peaks at the 18 and 28S ribosomal RNA (Figure 2.10).

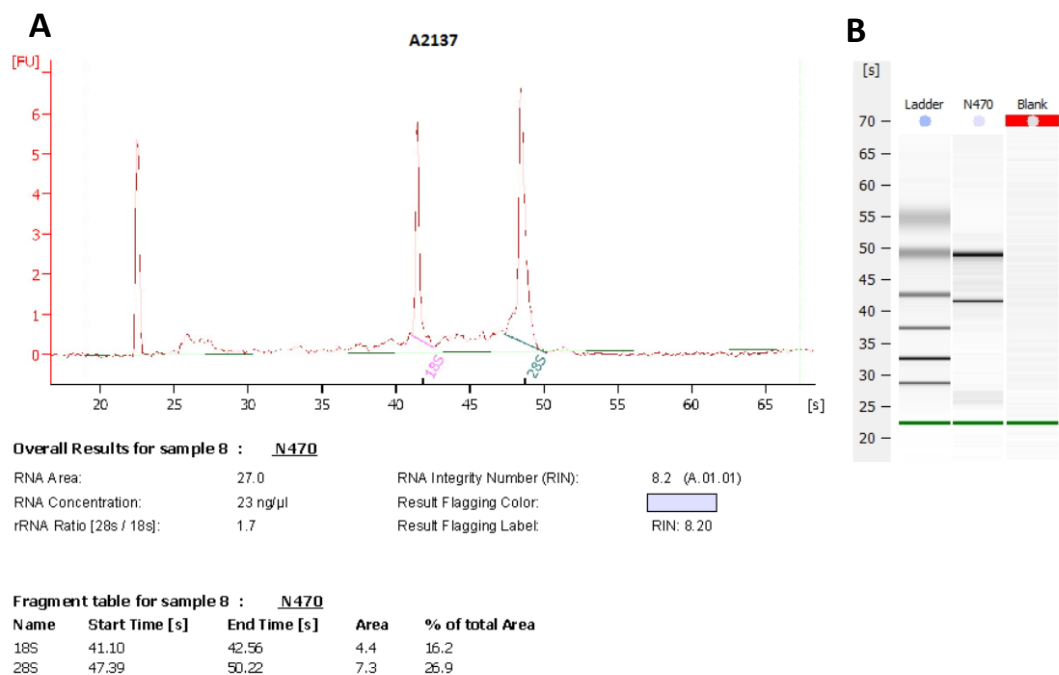


**Figure 2.10 Representative electropherograms of the total RNA analyzed using the Nano assay.** (A) The electropherogram of an allo-HSCT skin biopsy and (B) is the gel image of the same sample. MicroRNAs were detectable at approximately 25-27s which is equivalent to 22-25 nucleotides. The gel image did not show any sign of total RNA degradation. Flu: fluorescence that is shown on the y-axis.

### 2.6.1.2 Absence of PCR inhibitors

To ensure that the samples were of the same quality and were extracted reproducibly, the number of miRNAs detected as well as the mean  $C_q$  values for all the nine samples were initially investigated. RNA spike-in (Sp6) control was also included in the quality control analysis to detect any PCR inhibitors. The miRNAs were detectable in all the nine samples and there was no RT-qPCR inhibitors present (Figure 2.11).

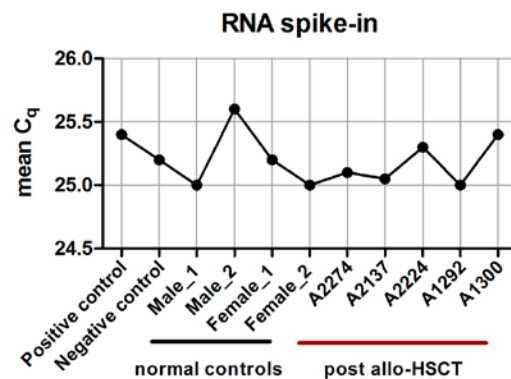


**Figure 2.11 Raw  $C_q$  values detected in all the nine samples.** The steady state shown with minor sample variations was indicative of no-PCR inhibitors.

To further assess the quality of the total RNAs prior to the profiling experiment, the NTCs were analysed. For the profiling experiment it was necessary that the miRNAs detected had five  $C_q$  values lower than that of the NTCs. A panel of synthetic miRNAs were included as positive controls in this analysis (Figure 2.12). For assays that were non-detectable on the negative control, the  $C_q$  was set to 37.

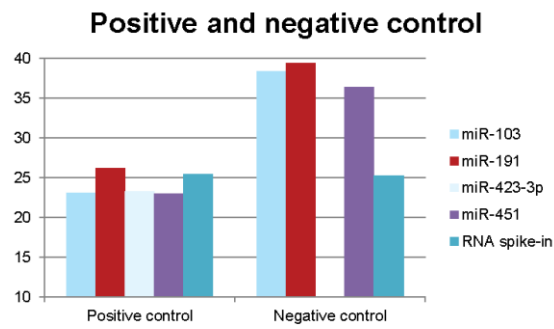


**Figure 2.12 Raw C<sub>q</sub> values shown for the positive and negative controls.** The mean C<sub>q</sub> values for all of the nine samples showed that miR-103, miR-191, and miR-423-3p were expressed at a steady level in majority of the samples. These microRNAs were recommended as the reference controls for the further validation studies. The y-axis shows the raw C<sub>q</sub> values.

**Acknowledgement:**

The two male normal volunteers were recruited via Alcyomics Limited.

## 2.6.2 Normalisation of individual miRNA assays

The best reference controls for normalization of individual miRNA assays was determined by using Normfinder and the results of the Exiqon quality controls. Mir-103a-3p and SNORD48 were selected and quantified in 20 skin biopsies. Both were stably expressed across all the clinical skin biopsies (Figure 2.13). To reduce variation, geometric means were calculated and therefore used in the validation study.

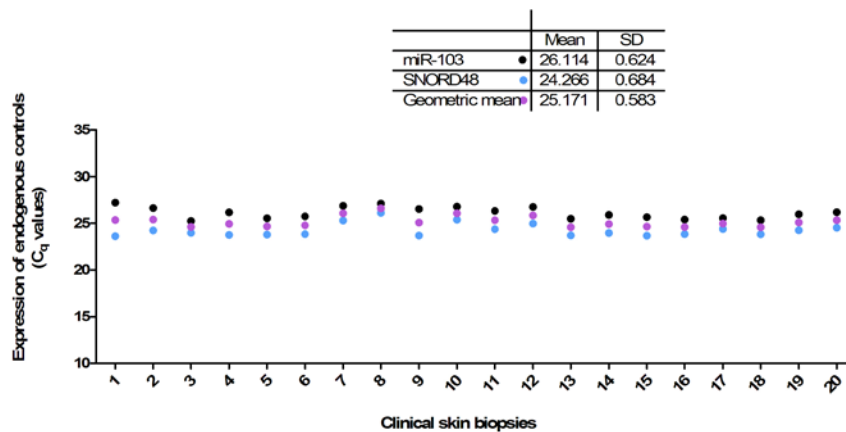


**Figure 2.13 Expression of reference controls in clinical skin biopsies.** Quantitative RT-PCR was used to measure the expression of miR-103a-3p and SNORD48 in 20 clinical biopsies. Geometric mean was calculated and used as the reference control. Cq: Cycle Quantification; SD: Standard Deviation.

## 2.7 Enzyme Linked-Immunosorbent Assays

A sandwich Enzyme Linked-Immunosorbent Assay (ELISA) technique was used for the detection of protein targets (TRAF6, STAT1- $\alpha$ , IRAK1 and IRF5). The specific antibody was pre-coated on the ELISA plates and standards were provided in the kit. Specific protein and standards were bound by the antibody. The primary antibody was conjugated with biotin and the secondary antibody was avidin-conjugated Horseradish Peroxidase (HRP). All the reagents were incubated for 30 minutes at room temperature before performing the experimental steps. All the steps were performed as per the manufacturer's guidelines (CUSABIO, China).

### **2.7.1 General ELISA protocol used for the detection of the four miRNA targets**

**Dilutions:** Biotin-antibody required a 100-fold dilution- 10 µl of Biotin-antibody + 990 µl of Biotin-antibody Diluent. HRP-avidin required a 100-fold dilution- 10 µl of HRP-avidin + 990 µl of HRP-avidin Diluent. Wash Buffer Concentrate required a 25-fold dilution- 20 ml of Wash Buffer Concentrate + distilled water to prepare 500 ml of Wash Buffer (1 x).

**The assay procedure was as follows:** Standards and samples (100µl/well) were added to each well and covered with an adhesive strip. Incubation was for 2 hours at 37°C. Standards and samples were removed from each well using an auto-washer system. The plate was not washed in this step. Biotin- antibody (1x) (100µl) was added to each well and the plate was covered with a new adhesive strip. Incubation was for 1 hour at 37°C. The plate was aspirated and washed three times using an auto-washer. HRP-avidin (1x) (100 µl) was added to each well, covered with a new adhesive strip and incubated for 1 hour at 37°C. The plate was aspirated and washed five times using an auto-washer. TMB Substrate (90 µl) was added to each well and the plate was protected from light and incubated for 15-30 minutes at 37°C. Stop Solution (50µl) was added to each well and the plate was gently tapped to ensure thorough mixing. Microplate reader was used to detect the colour change that corresponded to protein concentration. The plate was read at 450 nm within 5 minutes.

### **2.7.2 Standard curve analysis**

A representative standard curve for IRF5 and STAT1- $\alpha$  is shown in figure 2.14. The standard was diluted in serial steps in the assay buffer provided in the kit. Each point on the graph represents the mean of the duplicates. The standards were within the linear area of the line of best fit.

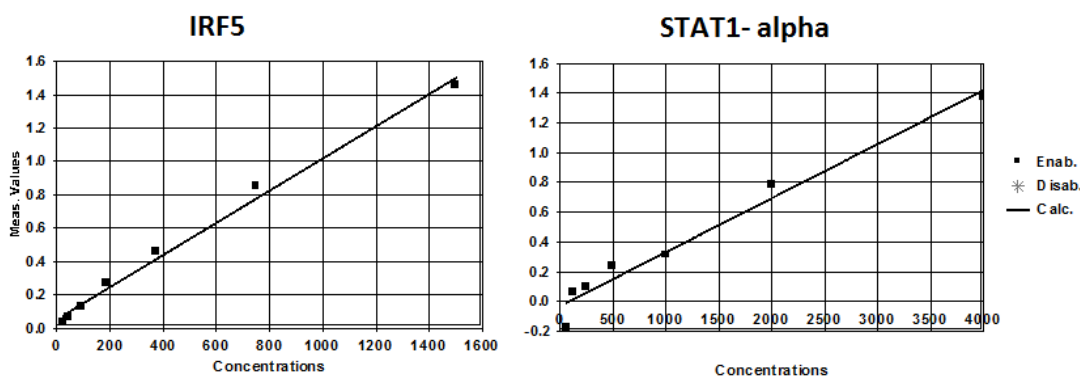


**Figure 2.14** Representative standard curve for IRF5 and STAT1- $\alpha$  using the assay standard.

Protein	Catalogue Number	Detection Range (pg/ml)
TRAF6	CSB-E14078h	39-2500
IRAK1	CSB-E09933h	312-20000
STAT1- $\alpha$	CSB-E11755h	62.5-4000
IRF5	CSB-EL011820HU	23.5-1500

**Table 2.8** Catalogue numbers and detection ranges for the specific ELISA kits used in this project.

## 2.8 Human *in vitro* Skin Explant Model for GVHR

The *in vitro* skin explants were set up as previously reported by Dickinson *et al.* (Dickinson *et al.*, 1998).

### 2.8.1 Experimental set-up of the *in vitro* skin explant assay

Skin biopsies were obtained from allo-HSCT patients, washed with EBSS and then dissected using aseptic techniques in a petri-dish. The epidermis and dermis were left intact and only the fatty tissue was removed from the skin section.

Irradiated PBMCs ( $1 \times 10^6$  /ml) from HSCT patients (stimulators) were cultured with PBMCs ( $1 \times 10^6$  /ml) from HLA matched or mismatched donors (responders) in a mixed lymphocyte reaction for 7 days at 37°C with 5% CO<sub>2</sub> and 95% air. The MLR primed responder cells were then co-cultured with skin sections that were autologous to the

stimulator in a 96 U-bottomed well plate. In addition, parallel control skins were cultured in medium alone. Standard complete medium was used which contained 20% heat inactivated patient autologous serum for MLR with skin co-cultures (Wang *et al.*, 2006). Skin explants were harvested on days 1, 2 and 3. The duplicate skin sections cultured in MLR primed responder cells or medium alone were collected for total RNA extraction, in *RNAlater* buffer® and the other fixed in 10% buffered formalin for histological staining with hematoxylin and eosin.

### Acknowledgement

The skin explants were set up by Elizabeth Douglas and Cindy Carr.

### 2.8.2 Histopathology

Skin tissue fixations and stainings with hematoxylin and eosin were all performed by the pathology staff at the Royal Victoria Infirmary. Two independent assessors, who were blinded to the origin of the samples, graded the sections according to the histological criteria (Lerner *et al.*, 1974). Skin histopathological Grade I in medium alone culture was considered as the negative control only. The grading criteria used and the histological changes that are evident at each grade are shown in figure 2.15.

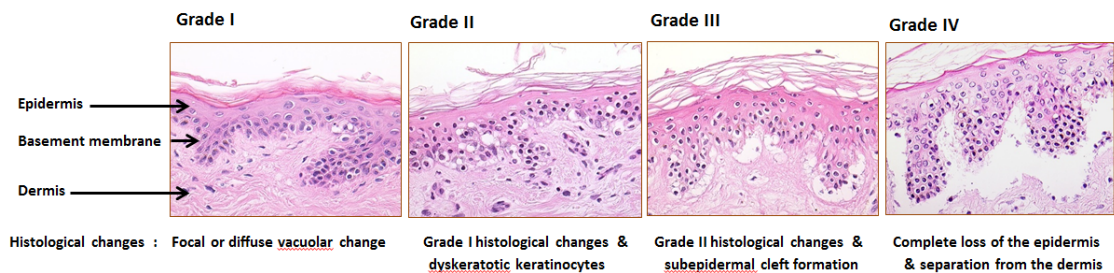


**Figure 2.15 Immunohistochemical staining of skin biopsies from the *in vitro* skin explant assay.** (A) Grade I (B) Grade II (C) Grade 3 (D) Grade 4. Lerner’s histological criterion was used for the grading assessment (Lerner *et al.*, 1974)

### Acknowledgements:

The pictures were courtesy of Dr Xiao-nong Wang

Prof Anne Dickinson and Dr Xiao-nong Wang graded the sections.

## 2.9 Transfection experiments

### 2.9.1 Transfection basics

Delivery of nucleic acids into eukaryotic cells is termed as transfection. There are numerous delivery methods either using chemical based reagents or electric current. The most commonly used methods are as follows; (1) Lipofection: polymer based transfection using positively charged lipid based reagents, (2) Transduction: packaging of nucleic acids in a viral vector, (3) Electroporation: disrupting the cell membrane for the nucleic acids to enter the cells performed using electric current, (4) utilizing chemically modified small interfering RNAs (siRNAs). There are two main controls for transfection experiments; (1) mock (2) negative control. A mock control is to control for the impact of reagents or the method of transfection on the cells.

### 2.9.2 Transfection negative controls and inhibitors

The negative control for the transfection experiments introduced a non-targeting sequence into a cell to control for any non-specific/off-target effects. *C. elegans* based negative controls were used in the transfection investigations in this project. The *C. elegans* sequences are non-homologous to human sequences. The miRIDIAN microRNA transfection reagents were resuspended in RNase-free water (stock concentration= 20  $\mu$ M). Aliquots were stored at -20 °C to limit freeze-thawing.

miRIDIAN microRNA Hairpin Inhibitor			
	Transfection Control with Dy547	Transfection Inhibitor	Transfection Inhibitor
ID	cel-miR-67	hsa-miR-34a-5p	hsa-miR-34a-3p
Accession No	MIMAT0000039	MIMAT0000255	MIMAT0004557
Sequence	UCACAACCUCCUAGAAAGAGUAGA	UGGCAGUGUCUUAGCUGGUUGU	CAAUCAGCAAGUAUACUGCCCU
Molecular weight	18379.0 g/ml	18,053.4 g/mol	18,121.9 g/mol
Catalog Item	IP-004500-01-05	IH-300551-08-0005	IH301145-02-0005

**Table 2.9** Summary of transfection reagents (Dharmacon, GE Lifesciences).

### **2.9.3 Cytospin**

Cytospin is a standard cytology method that is used for concentrating cells onto a slide for counting cells, their visualization and acquiring of images. For all the transfection experiments using the miRNA hairpin inhibitor,  $10^3$ - $20^3$  cells were harvested for the cytopsin procedure so that the transfection efficiency could be determined. The procedure was as follows; filters were pre-wet by centrifugation (Cytospin™ cytocentrifuge, ThermoScientific) with 200  $\mu$ l of PBS at 500 rpm for 5 minutes. Next, 300  $\mu$ l of the cells were spun at 700 rpm for 10 minutes. The filters were removed from the slides very carefully and were allowed to air-dry for 30 minutes. DAPI-mounting solution was added for visualization of dead cells. All the slides were stored at 4°C till imaging. Coated slides (Shandon Inc) were only used for the cytopsin procedure as it allowed the fixation of the slides directly upon spinning.

### **2.9.4 MicroRNA inhibition experiments**

Cells (PBMCs/cell lines) were counted and re-suspended at  $1 \times 10^7$  cells/ml in complete medium (RPMI medium and 10% FCs) but without any antibiotics. Cell lines such as Pre- B697 (leukemia cell line) were used as the positive transfection control as they had been successfully transfected with siRNAs, previously. The protocol was optimized and ten million cells were transfected with the negative control and the miRNA specific inhibitor at a final concentration of 500 nM (12.5  $\mu$ l per transfection). The transfection reagents (see table 2.9) were added to the cells (500  $\mu$ l) in a 4 mm cuvette prior to electroporation at 350 V, single pulse for 10 ms, using the EPI 2500 gene pulser (Fischer, Heidelberg, Germany). The cells were incubated for 15 minutes at room temperature for the closure of the pores that were opened upon electroporation. The cells were then diluted (10x) with complete medium supplemented with antibiotics (penicillin/streptomycin). Cells were seeded in multiple wells in either a 96 or a 24 well plate and incubated at 37°C with 5% CO<sub>2</sub> and 95% air. Cells were harvested at 24, 48, 72, 96 and 144 hrs for viability test and examined by fluorescence microscopy for determination of transfection efficiency. Transfection efficiency was calculated by counting the number of positive cells over the total number of cells present in a field

of view. Cells were allowed to recover for 24 hrs prior to setting up a mixed lymphocyte reaction using the transfected cells as responder cells. Levels of knockdown were calculated relative to the negative control and assessed by RT-qPCR using the LNA chemistry.

## **2.10 T cell proliferation assay**

T cell proliferation was measured using the <sup>3</sup>H-thymidine assay in which dividing cells incorporate the radioactive compound. Mis-matched MLRs were cultured in 96-well round bottomed plates (200ul/well). Control wells included the auto-MLRs. Triplicate wells were set up for each test condition. The MLR was incubated for five days under standard tissue culture conditions (37°C, humidified incubator with 5% CO<sub>2</sub> and 95% air) and were co-cultured with the <sup>3</sup>H-thymidine (10 µl/well=0.037 MBq/well) for the last 18 hours. The cells were then harvested onto a filter mat using the INOTECH cell harvester (CH-5610 Wohlen). <sup>3</sup>H-thymidine incorporation was measured by scintillation counting with a Direct Beta Counter (MATRIX 9600, Packard Instrument).

### **Acknowledgement:**

The <sup>3</sup>H-thymidine T cell proliferation assays were setup by Dr Lindsay Nicholson.

## **2.11 Mixed Lymphocyte Reaction Assay**

Peripheral blood mononuclear cells were obtained from healthy volunteers and mis-matched MLRs set-up. The principle of mis-matched MLR is that PBMCs from incompatible volunteers will stimulate each other and therefore proliferate. In contrast to auto-MLRs where the individuals own PBMCs are used as stimulator, the cells will not proliferate and therefore there is no allogeneic immune response. In one way, MLRs the PBMCs from one volunteer were inactivated using irradiation (20 Gy) and co-cultured with an incompatible volunteer PBMCs that were the responder cells.

Mis-matched MLR assays were set-up using equal concentrations of irradiated (stimulator or effector) PBMCs collected from one healthy volunteer with non-irradiated PBMCs from a second normal volunteer (responder). Auto-MLR assays were

set up with PBMCs from normal volunteers against themselves. Depending on the experiment, the concentrations of cells were adjusted accordingly.

### **2.11.1 Mixed lymphocyte reaction stimulated with cyclosporine A**

In Chapter 5 and Chapter 6, standard allogeneic (mismatched) MLRs were stimulated with different doses of cyclosporine A to test the impact of the drug and indirectly the T cell inhibition on miR-34a, miR-146a-5p and miR-155-5p expression levels, respectively. The assays were set-up in 24 well plates. Auto-MLRs were set up as the allogeneic response control. The MLRs were co-cultured without cyclosporine A (0 ng/ml) and with 50, 100, 200 and 300 ng/ml of cyclosporine A for 96 hours before the cells were harvested and total RNA extracted using the *mirVana* PARIS kit.

#### **Acknowledgement:**

Alcyomics Limited provided the cyclosporine A (Abcam: ab120114) aliquots.

### **2.11.2 PBMCs stimulated with IFN- $\gamma$**

In Chapter 6, PBMCs were co-cultured with two different doses of recombinant human IFN- $\gamma$  (50 and 100 ng/ml) in 24 well plates. The doses were determined from the existing literature on the amount of IFN- $\gamma$  (R & D Systems) sufficient to host a response (Takahashi *et al.*, 2012). The cells were harvested after 24 and 48 hours, respectively. The *mirVana* PARIS kit was used to extract total RNA from the cells. Taqman based RT and qPCRs were then performed, and the relative levels of both miR-146a-5p and miR-155-5p were determined.

## **2.12 Semi-quantitation of c-Myc and p53 proteins**

### **2.12.1 Immunohistochemical staining**

The pre (n=5) and post (n=17) allo-HSCT skin biopsies were cut and stained for c-Myc (Abcam, Epitomics at 1:10 dilution) and p53 (Pre-diluted from Ventana) proteins using

FFPE immunohistochemistry method. The pathology department performed both procedures (Royal Victoria Infirmary, Newcastle upon Tyne).

### 2.12.2 Skin histopathological scoring

The well-established quick score semi-quantitative method (Detre *et al.*, 1995) was used to score the c-Myc and p53 positive cells. The quick score was calculated considering both the intensity and proportion of the cells stained positive. The complete section was used for scoring as well scoring the epidermis and dermis separately. Two independent researchers, who were both blinded to the origin of the sections, scored the samples. The mean quick score was used to perform all the statistical calculations. The proportion of cells was defined as per the criteria mentioned in table 2.10. Quickscore formula = (Intensity<sub>0</sub>xProportion) + (Intensity<sub>1</sub>xProportion) + (Intensity<sub>2</sub>xPrportion) + (Intensity<sub>3</sub>xProportion)

Intensity	Proportion
	1= 0-4%
	2= 5-20%
0= no staining	3=21-40%
1= light staining	4= 41-60%
2= moderate staining	5=61-80%
3= strong staining	6=81-100%

**Table 2.10 Quickscore intensity and proportion criteria.**

#### Acknowledgement:

Dr Rachel Crossland also scored for p53 and c-Myc positive cells.

### 2.13 Cell imaging

The images of the immunohistochemistry sections were obtained using bright field microscopy (Zeiss Axiolmager). The images of the transfections were acquired using fluorescent microscopy (Zeiss Axiolmager).

## **2.14 Statistical Analysis**

### ***2.14.1 General statistics used in the investigations***

In general, statistical analyses were performed using either SPSS version 21 (IBM) and/or GraphPad Prism version 5 (GraphPad Software). The Mann-Whitney U tests were used to determine the statistical significance when there were two groups only and  $p \leq 0.05$  was considered as significant. Kruskal-Wallis, which is a non-parametric analysis of variance, was performed when there were three or more groups in the comparison. Only for the global profiling experiments parametric ANOVA was used as it was essential to select the miRNAs based on their significance. Dunn's or Bonferroni post-test were used to safeguard against false positive when performing multiple comparisons. Bland-Altman plots were generated for method comparisons that showed the agreement between two methods by calculating the difference (bias) between them (Bland and Altman, 2012). Spearman correlation was performed to test for strength of association between two groups.

### ***2.14.2 Receiver operating characteristic curves***

Receiver Operating Characteristic (ROC) curve is used in clinical research to determine the threshold or cut-off value of a particular biomarker or test. The cut-off value segregates the normal population from the diseased population. Normal groups are usually considered as negative and assigned the binary digit '0' while the diseased group is positive and assigned the binary digit '1'. In clinical research, not all the samples identified by the test as belonging in the diseased group will have the disease. True positive or sensitivity is the ratio of the positives identified by a test to the total number of individuals that have the disease. Similarly, the analysis also identifies some normal or negatives to having the disease. Likewise, true negative rate or specificity is the ratio of the number of normal that were determined by the test to have the disease over the total number of individuals that were normal.

In the ROC curve, sensitivity is plotted on the y-axis and 1-specificity on the x-axis. The area under the ROC curve is a measure of clinical test accuracy. An area under the curve= 1 demonstrated that the test is 100% accurate as sensitivity and specificity are both= 1. In such a scenario, there are no false positives or false negatives present. In contrast, an inaccurate test will have an area that is below 0.5. This test will be unable to distinguish the normal from the diseased population. The area under the curve (A) of 0.5 signifies that the miRNA is of no diagnostic ability; an area under the curve of 1 signifies that the miRNA has perfect diagnostic ability. The p-value accompanying the area under the curve tests the null hypothesis that the area under the curve is 0.5.

The optimal operating point on the ROC curve occurs where the slope of the ROC is equal to:

$$\left( \frac{AC_{fp} P(D-)}{AC_{fn} P(D+)} \right)$$

Where P(D+) is the prior/pre-test probability of disease (i.e. prevalence of disease in the population)

$AC_{fp}$  = average cost associated with false positive diagnosis.

$AC_{fn}$  = average cost associated with false negative diagnosis.

The 'cost' can be a financial cost *or* a health cost.

In many cases, we do not have accurate estimates of the additional health or financial costs and we take

$$\left( \frac{AC_{fp}}{AC_{fn}} \right) = 1$$

Hence the cut-off point is taken to be where the slope on the ROC curve equals

$$\frac{P(D-)}{P(D+)}$$

Pre-test probability is the probability that the patients have the disease and for all the investigation it was set to 0.6 as approximately 60% of the patients had aGVHD or were deceased at the point of analysis. The cost ratio was set to default one. The cut-off values and the area under the curves (AUC) were all calculated using statistical software SigmaPlot 12.5.

### **2.14.3 Homogeneity of variance**

Variance is a measure of the spread of continuous data from the mean. Levene's test assumes that the difference between groups is equal and was performed to assess the homogeneity of variance in the different cohorts for model fitting. A difference of greater than 0.05 was indicative of equal variance.

### **2.14.4 Model building**

There are several known clinical risk factors that may influence the outcome (aGVHD, relapse, non-relapse mortality) of allo-HSCT such as patient's age at the time of transplant, donor-patient relationship, patient and donor gender, graft source (BM/PBSC) and the underlying disease. However, when building models, all the clinical risk factors cannot be included as it can result in the variance of the predictions. Therefore, variables that show the least association with outcome are eliminated and not included in the model building method. In relevant Chapters, frequency tables are presented which show the number and percentage of patients per specific group. Univariate Fisher's exact test was conducted to determine the difference in proportions when time was not included in the analysis. For OS and relapse where time was a factor, univariate Kaplan-Meier and Cox regression analysis were performed to test for proportions. Continuous variables such as patient's age, Cyclosporine A dose and time to onset of aGVHD are all presented as median and range. Survival analysis was performed using the Kaplan-Meier log-rank test and multivariate Cox regression analysis.

Graft-versus-host disease outcome is measured on an ordered categorical scale ranging from 0-IV (0: without aGVHD, I: mild aGVHD, II: moderate aGVHD and III: severe aGVHD). Thus, the outcome cannot be assumed to have a normal distribution. Additionally, basic statistical approaches only identify the main effects or difference between variables and not the most complex interactions involved with regards to a particular outcome. In such instances, advanced statistical model building methods are considered such as the generalised linear models (GLMs) that can result in more

precise analysis of the data (Brown and Prescott, 1999). GLMs allow both the main and interaction effects to be investigated in the covariates with regards to the outcome. Main effect is statistically defined as an effect of an independent variable on the outcome (Hinton, 2014) while an interaction is a measure of two or more independent variables on the dependent outcome (Hinton, 2014). In this scenario, the main effect was the effect of the individual miRNA expressions or significant clinical risk factors on aGVHD outcome and the interaction was a measure of the effect of one independent miRNA expression level as it differed at every condition in comparison to the other independent miRNA expression levels (Hinton, 2014).

There are various classifications of GLMs using different link functions and based on ANOVA or regression depending on whether the outcome variable is a scale, count, ordinal, binary or a mixture as this indicates the distribution of the outcome variable. Thus, in order to predict aGVHD outcome from a list of covariates, GLMs were built using the binary and/or ordinal logistic regressions. The equation for the binary or ordinal regression models that was used for determining aGVHD grade (outcome) is as follows;

aGVHD grade (cumulative logit function) =  $\beta_0 + \beta_1 (\text{miRNA expression}_1) + \beta_2 (\text{miRNA expression}_2) + \beta_3 (\text{miRNA expression}_1 \times \text{miRNA expression}_2)$ .  $\beta_0$  = intercept coefficient and  $\beta_{1-3}$  = the coefficient of each miRNA expression. SPSS version 21.0 was used to run the GLMs.

## **2.15 Ingenuity Pathway Analysis**

### **2.15.1 Data source**

Total RNA extracted from normal skin biopsies (n=12), pre-transplant (n=12) and aGVHD onset skin biopsies (n=17) with a range of different histopathological and clinical grades (0-III) were used to synthesize universal cDNA and then amplified using custom made Taqman Low Density Arrays (TLDA) (Life Technologies) to screen for candidate GVHD genes (Norden et al., (unpublished) and patent (Publication Number: WO2012080359 A3) (Dickinson *et al.*, 2012)). Skin biopsies from normal individuals

were used as control. The initial three custom-made TLDA were used to test for 282 genes. Genes with  $\leq 25$  fold change in expression (n=38) were further assessed in the validation cohort. The final list contained 18 genes that were incorporated into the pathway mining analysis using Ingenuity Pathway Analysis (IPA) software (*ANP32A*, *C1qTNF7*, *CARD11*, *CEACAM4*, *CXCL9*, *HCLS1*, *HTRA1*, *LGALS7*, *LST1*, *MSR1*, *PIK3AP1*, *PSTPIP1*, *PTGER2*, *PTPN7*, *TAP1*, *TGM2*, *TREM2* and *UBD*). These genes were considered as focus genes throughout the analyses.

### **2.15.2 Analyses criteria**

The IPA software provides several types of analyses that can be used for pathway mining. Since gene lists were used for this pathway mining analysis, the core analysis was performed. Genes were individually searched and identified from the Ingenuity Knowledge Base. The report also included endogenous chemicals. The filter for species was set for humans only, and the confidence options present in IPA was set for highly predicted and/or experimentally observed data only. The Benjamini-Hochberg method which derives the corrected p-value was used to determine the significance of the biological functions and/or diseases in relation to the focus genes (n=18).

### **2.15.3 Annotation of focus genes**

The data set comprising the 18 focus genes was used to derive Entrez gene names and their locations and types from the Ingenuity Knowledge Base.

### **2.15.4 Functional analyses of data sets and networks**

Functional analysis was divided into three main categories; Diseases and Disorders, Molecular and Cellular Functions and Physiological System Development and Function. Each category included an annotation of the top five significant functions and the focus genes involved, respectively.

### **2.15.5 Canonical pathway analyses**

The significance of the relationship between the data set and the canonical pathway was measured in ratios and p-values. IPA calculates the ratio by dividing the number of genes into a given pathway that meet the particular selected or automatic cut-off and the total number of genes in that canonical pathway. The right-tailed Fisher's exact test was used to calculate the p-value, which determined the probability that the relationship between the focus genes and the canonical pathway was explained by chance alone.

A comprehensive list of the molecular and relationships used in the generation of networks and canonical pathways are presented in figure 2.16.

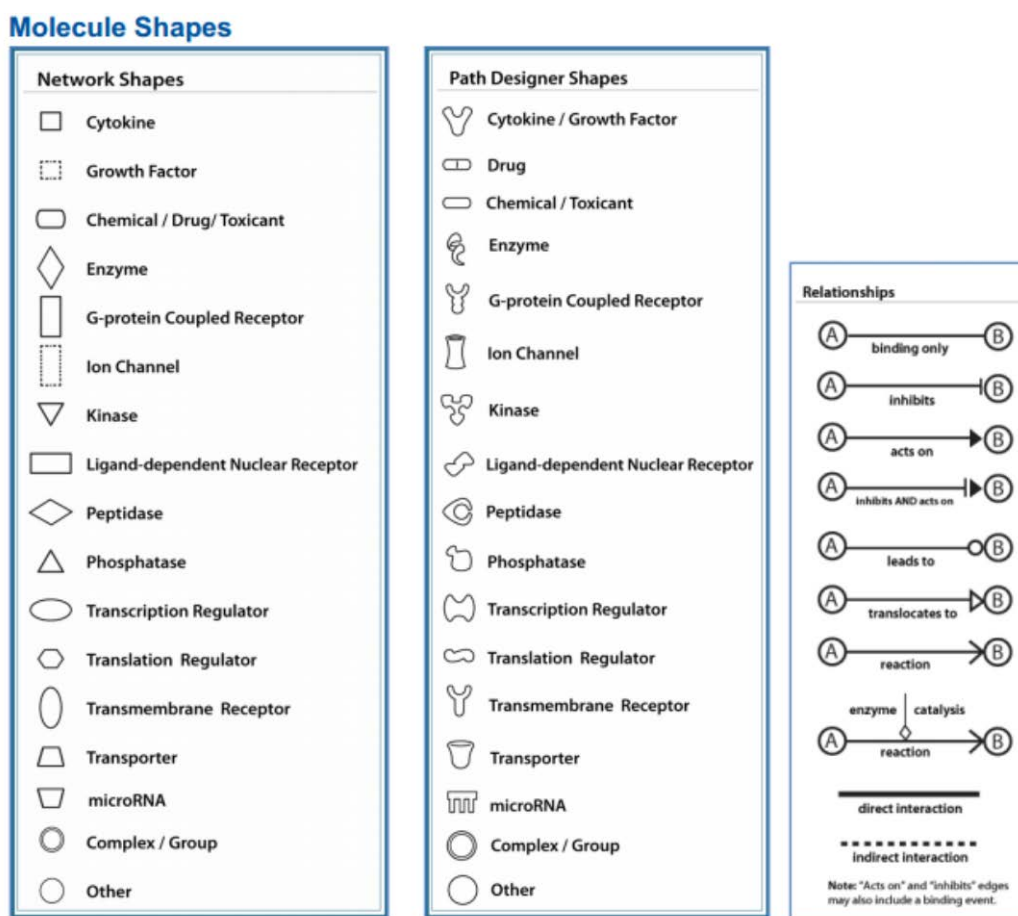


**Figure 2.16** The legend shows the main symbols and lines used in the generation of networks and canonical pathways (adopted from [www.ingenuity.com/](http://www.ingenuity.com/)).

## **Chapter 3. Pathway Mining of Candidate Genes Associated with Graft-Versus-Host Disease**

“When you make the finding yourself - even if you're the last person on Earth to see  
the light - you'll never forget it.”

**-Carl Sagan**

### 3.1 Introduction

Experiments to identify gene expression signatures associated with a specific disease state are now routinely performed. Such profiling experiments utilize microarray, barcoding (Nanostring) or RT-qPCR technologies. These high-throughput technologies generate a wealth of data that need to be analysed both quantitatively (i.e. expression levels) and functionally (i.e. biological functions, pathways). Thus, pathway-mining can be employed to decipher the potential biological roles and downstream impacts of the genomic and proteomic data generated through these experiments (Huang da *et al.*, 2009). Pathway analysis also depicts the overall picture of all the genes experimentally investigated in relation to one another, as well as in relation to other relevant molecules.

Furthermore, the gene signatures identified using each of the different techniques may not overlap, due to several reasons such as technical and technology based variations, small sample size, and sample heterogeneity especially when using samples from transplant and/or cancer patients. To reduce the challenges of analysing results from several gene expression arrays a meta-analysis based method is employed. This approach permits the combination of gene expression results from several studies in order to identify a signature pattern. There are numerous meta-analysis methods available and used in the literature (Rhodes *et al.*, 2004; Shen *et al.*, 2004; Choi *et al.*, 2007). One method uses the statistical p-value derived from various investigations for a particular gene to discriminate diseased from healthy tissues (Rhodes *et al.*, 2004). Others have used Bayesian methods whereby probabilities are determined to distinguish cancer cell from that of normal (Shen *et al.*, 2004; Wang *et al.*, 2004).

Analysing array results based on their biological associations in established, as well as predicted pathways is the new upcoming meta-analysis method. Pathway-based approaches can use both the p-values obtained from gene expression arrays or selectively utilize the signature list to identify specific pathways. Currently, there are several bioinformatics resources available for pathway-mining and pathway-based

meta-analysis such as DAVID (the database for annotation, visualization and integrated discovery) (Huang da *et al.*, 2007), GoMiner (Zeeberg *et al.*, 2005), GoToolBox (Martin *et al.*, 2004) and more recently, Ingenuity Pathway Analysis (IPA) software (QIAGEN Redwood City, USA) (Systems, 2012). The pathways generated can lead to the identification of new therapeutic targets. Indeed, Arasappan *et al.*, (2011) have shown that meta-signatures can clearly distinguish patients with systemic lupus erythematosus (SLE) from that of the controls. The investigation utilized gene expression results from five independent microarray experiments performed on PBMCs derived from SLE and normal controls (Arasappan *et al.*, 2011) and was analysed using IPA.

### **3.1.1 Specific study aims**

In this present study Ingenuity Pathway software was used to perform pathway mining to enrich for common biological functions among the signature gene list, the associated pathway and any other biological molecules involved in the process. The signature list comprised of genes that had been shown to be differentially expressed with regards to aGVHD incidence. The signature gene list was identified by Norden *et al.*, (unpublished) and a patent has been filed (Publication Number: WO2012080359 A3) (Dickinson *et al.*, 2012).

Therefore, the aims of this investigation were as follows;

1. To utilize the existing GVHD signature gene list to identify relevant pathways and networks involved in this disease process
2. To identify potential genes/proteins and miRNAs that may target the signature GVHD list and, therefore, represent new potential therapeutic targets.

## 3.2 Results

Norden et al., (unpublished) conducted TLDA on skin biopsies collected at query onset (GVHD assessed as per clinical disease symptoms prior to histopathological analysis report) aGVHD time-points, to screen for candidate genes associated with aGVHD. Eighteen genes that were significantly differentially expressed between normal controls and aGVHD skin biopsies of various grades (0-IV) were further validated using RT-qPCR. The final dataset comprised of the 18 genes and was uploaded into the Ingenuity Pathway Analysis software.

The core analysis was performed identifying both direct and indirect relationships. Direct relationships (interactions) were defined as one molecule or transcription factor directly binding and impacting the expression level of a gene. Indirect relationships were defined as those interactions where no direct binding was reported yet it was mediated via other molecules and influenced the expression level of the gene. Molecules from the dataset that were associated with haematological, dermatological or immunological functions or diseases were considered for the analysis. The Benjamini-Hochberg method was the preferred method, as prior information on the significance of the associations was absent. Also, this unsupervised approach reduced the introduction of bias in the study, as it allowed the software to generate networks based on the inbuilt algorithms and curated literature. Molecules from the data set that met the filter criteria and that were associated with a canonical pathway in Ingenuity Knowledge Base were considered for analysis. The significance of the association between the dataset and the canonical pathway was measured by ratios and p-values.

### 3.2.1 Annotation of the focus genes

The dataset was mapped to the Ingenuity Knowledge Base. The Entrez gene name, location and type were determined for each of the 18 focus genes. A summary of the annotations is presented in Table 3.1.

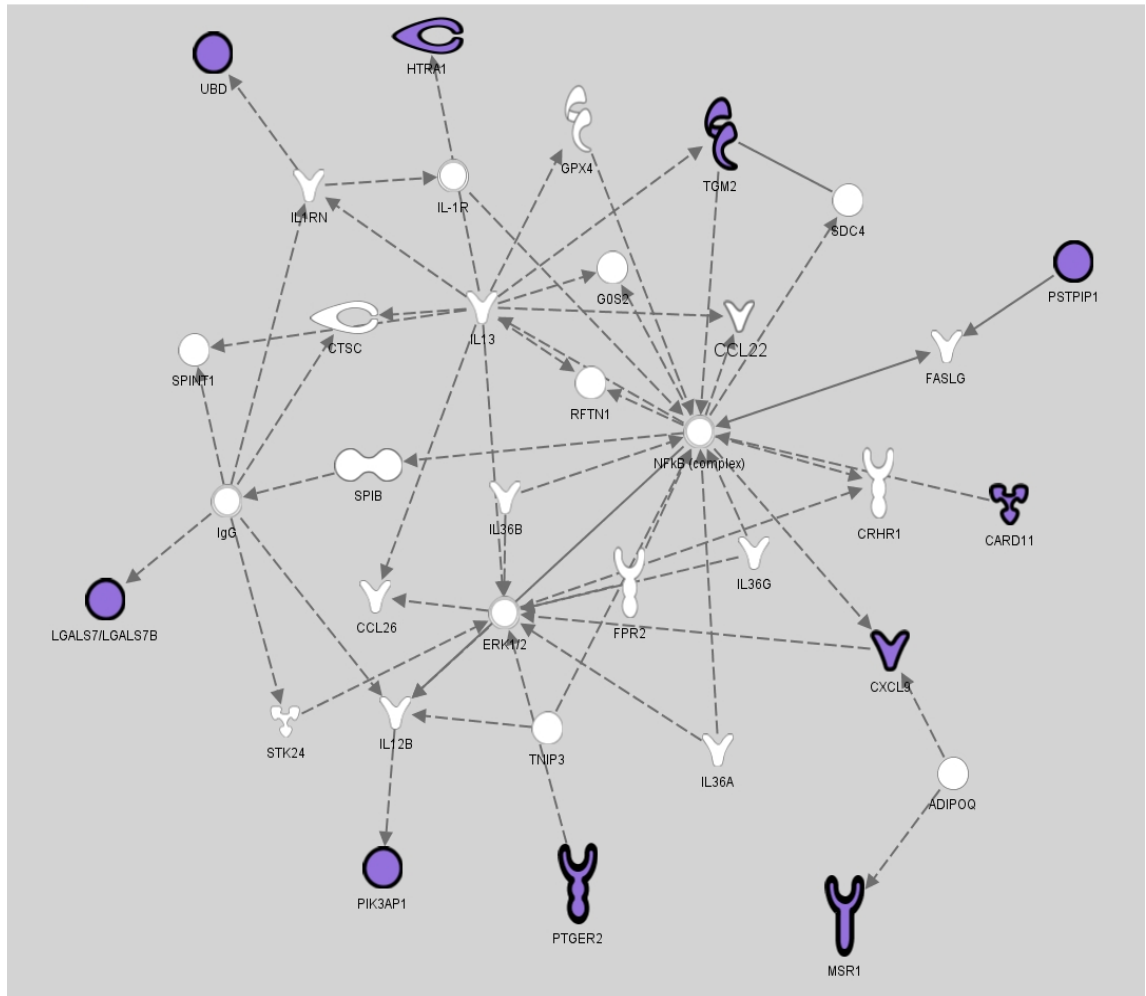
Symbol	Entrez Gene Name	Location	Type(s)
<b>ANP32A</b>	acidic (leucine-rich) nuclear phosphoprotein 32 family, member A	Nucleus	other
<b>C1QTNF7</b>	C1q and tumor necrosis factor related protein 7	Extracellular Space	other
<b>CARD11</b>	caspase recruitment domain family, member 11	Cytoplasm	kinase
<b>CEACAM4</b>	carcinoembryonic antigen-related cell adhesion molecule 4	Plasma Membrane	other
<b>CXCL9</b>	chemokine (C-X-C motif) ligand 9	Extracellular Space	cytokine
<b>HCLS1</b>	hematopoietic cell-specific Lyn substrate 1	Nucleus	transcription regulator
<b>HTRA1</b>	HtrA serine peptidase 1	Extracellular Space	peptidase
<b>LGALS7/ LGALS7B</b>	lectin, galactoside-binding, soluble, 7	Extracellular Space	other
<b>LST1</b>	leukocyte specific transcript 1	Plasma Membrane	other
<b>MSR1</b>	macrophage scavenger receptor 1	Plasma Membrane	transmembrane receptor
<b>PIK3AP1</b>	phosphoinositide-3-kinase adaptor protein 1	Cytoplasm	other
<b>PSTPIP1</b>	proline-serine-threonine phosphatase interacting protein 1	Cytoplasm	other
<b>PTGER2</b>	prostaglandin E receptor 2 (subtype EP2)	Plasma Membrane	G-protein coupled receptor
<b>PTPN7</b>	protein tyrosine phosphatase, non-receptor type 7	Cytoplasm	phosphatase
<b>TAP1</b>	transporter 1, ATP-binding cassette, sub-family B	Cytoplasm	transporter
<b>TGM2</b>	transglutaminase 2	Cytoplasm	enzyme
<b>TREM2</b>	triggering receptor expressed on myeloid cells 2	Plasma Membrane	transmembrane receptor
<b>UBD</b>	ubiquitin D	Nucleus	other

**Table 3.1. Annotation results of the 18 focus genes.** The location and type of proteins are mentioned in the table.

### 3.2.2 Network analysis of the focus genes

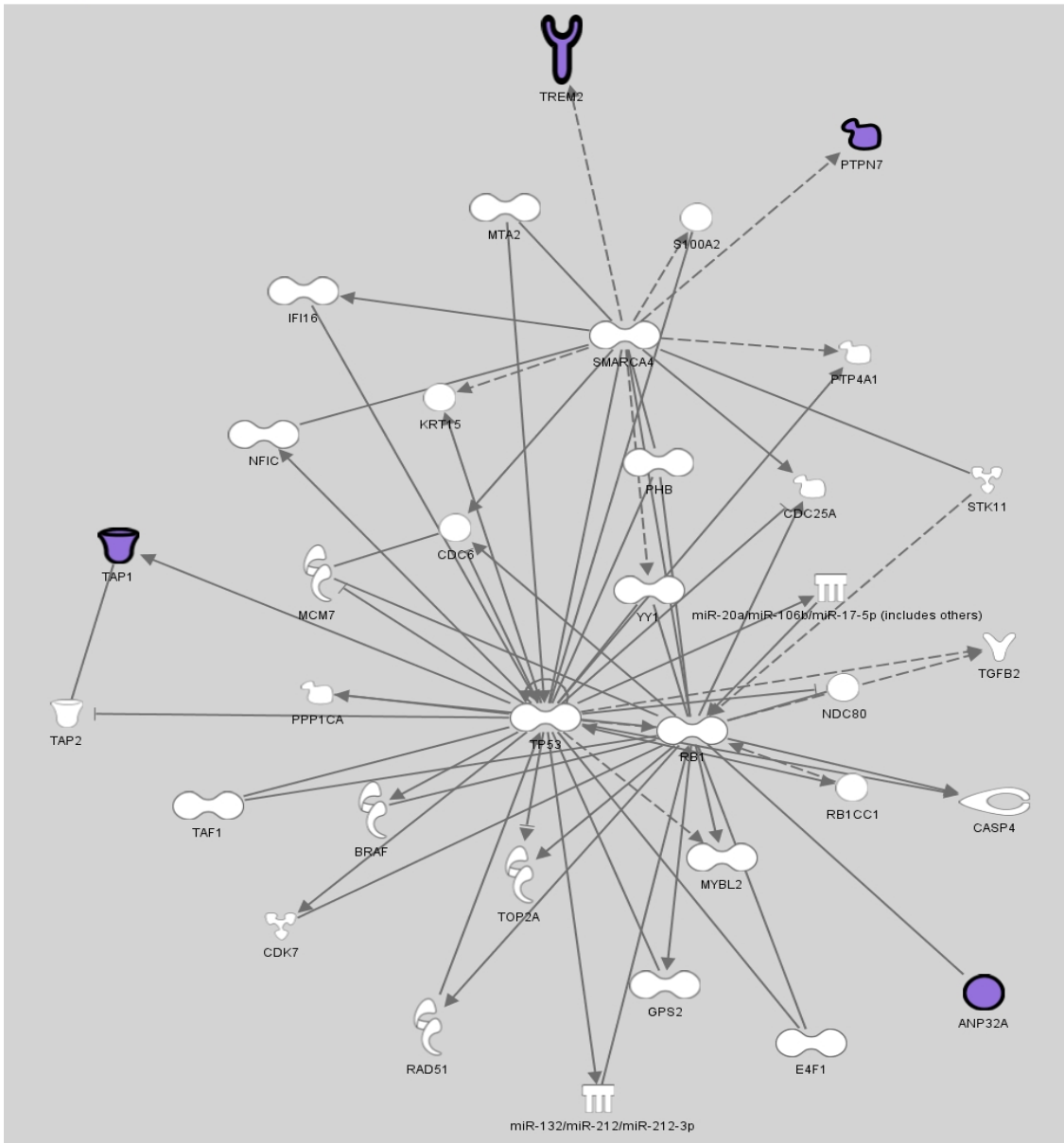
The focus genes (18 signature genes) were used to deduce molecular networks based on algorithms that take into account the connection of the genes according to information available in Ingenuity Knowledge Base (curated database). Network analysis predicted five networks in which the focus genes could have potential involvement. Direct and indirect interactions were determined *de novo* using the network analysis, and these were based upon the input genes. All direct interactions indicated that the two genes were directly in contact i.e. direct binding of a molecule or transcription factor and the gene. On the other hand, indirect interactions showed the impact of one molecule on another as a result of a signalling cascade.

Ten of the 18 focus genes were involved in Network 1 (Figure 3.1). NFkB complex was indirectly associated with all the focus genes in Network 1 (*UBD*, *HTRA1*, *LGALS7/LGALS7B*, *PIK3AP1*, *PTGER2*, *MSR1*, *CXCL9*, *CARD11* and *PSTIP1*). Four of the focus genes (*ANP32A*, *TAP1*, *TREM2* and *PTPN7*) were present in Network 2 (Figure 3.2). Networks 3, 4 and five each had only one of the focus genes involved (Figure 3.3 (a), (b) and (c)). In Network 3, *C1qTNF7* and *NR3C1* (nuclear receptor subfamily 3, group C, member 1) were shown to interact, and both genes are known to play roles in cancer, cellular assembly and organization. *NR3C1* is known as the glucocorticoid receptor. *CEBPA* (CCAAT/enhancer binding protein (C/EBP), alpha) is a transcription regulator located in the nucleus and directly acts on *LST1*. *CEBPA* and *LST1* are involved in cell cycle, cellular growth and proliferation as well as connective tissue development and function. Network 5 showed the involvement of *LYN* (v-yes-1 Yamaguchi sarcoma viral related oncogene homolog) and *SYK* (spleen tyrosine kinase), *F2* (coagulation factor II) and *HCLS1*. *LYN* and *SYK* both belong to the kinase family and are located in the cytoplasm. *HCLS1* is a transcription regular located in the nucleus. *F2* is a peptidase found in the extracellular space. All the four genes play a role in energy production, molecular transport and nucleic acid metabolism. Interestingly, *CEACAM4* was the only gene that was not involved in any network. All the interactions mentioned in the Networks are in humans and indirect unless otherwise stated.



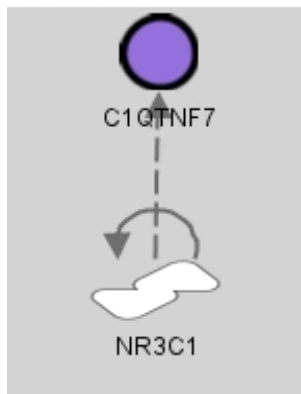
© 2000-2011 Ingenuity Systems, Inc. All rights reserved.

**Figure 3.1** Network 1 shows the most significant interactions of the 18 genes with the NFκB pathway suggesting their role in inflammation. The network illustrates the relationship of ten focus genes (purple) with other genes (white) and the NFκB complex. As part of this network, the ten focus genes play a role in inflammatory responses, cell-to-cell signalling and inflammatory diseases. Solid lines represent direct interactions while dashed lines; indirect interactions. For a comprehensive list of symbols see Chapter 2, Section 2.15.5.



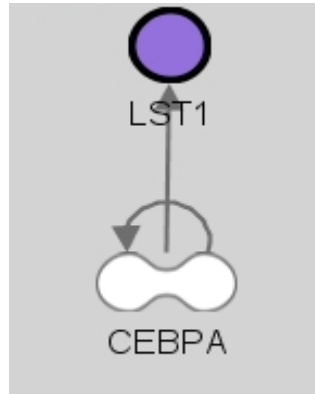
© 2000-2011 Ingenuity Systems, Inc. All rights reserved.

**Figure 3.2 Network 2 shows the most significant interactions of the 18 genes with the tumour suppressor TP53.** This network illustrates the involvement of four of the focus genes in relation to other genes and miRNAs that function in cell cycle, DNA replication, recombination, and repair as well as cellular growth and proliferation. Solid lines represent direct interactions while dashed lines; indirect interactions. For a comprehensive list of symbols see Chapter 2, Section 2.15.5.



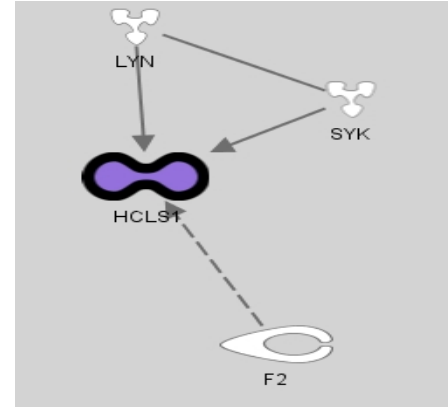
© 2000-2011 Ingenuity ...

**Network 3 (a)**



© 2000-2011 Ingenuity ...

**Network 4 (b)**



© 2000-2011 Ingenuity Systems, Inc

**Network 5 (c)**

**Figure 3.3** Network 3, 4 and 5 are graphical representations of the molecular relationship between a focus gene and other identified molecule in the Ingenuity Knowledge Base. (a) Network 3. This network shows that C1qTNF7 expression is indirectly affected by the activation of NR3C1. (b) Network 4. CEBPA directly interacts with LST1. (c) Network 5. HCLS1 is indirectly affected by F2 while directly acted on by LYN and SYK. The three limited networks identified using the Ingenuity Knowledge Base are the most comprehensive for each of the genes; C1qTNF7, LST1 and HCLS1 (accessed date: December 2011). Solid lines represent direct interactions while dashed lines; indirect interactions. For a comprehensive list of symbols see Chapter 2, Section 2.15.5.

### **3.2.3 Functional analyses of the focus genes**

Functional analyses were divided into three main categories; Diseases and Disorders (Table 3.2), Molecular and Cellular Functions (Table 3.3) and Physiological System Development and Function (Table 3.4). Each category included annotation of the top five significant features and the focus genes involved, respectively. The top five diseases and disorders were; infectious disease, cancer, connective tissue & genetic disorders and inflammatory diseases. Likewise, the top molecular and cellular processes were; cellular growth and proliferation, cell morphology, cell to cell signalling and interaction, cellular development and biochemical processes.

Performing functional analyses on the focus data set revealed the involvement of the genes in 301 processes. Eight genes were identified to affect arthritis disease (*CXCL9*, *HCLS1*, *HTRA1*, *LST1*, *PIK3AP1*, *PSTPIP1*, *PTGER2* and *TAP1*) and nine genes to affect autoimmune disease (*CARD11*, *CXCL9*, *HCLS1*, *HTRA1*, *LST1*, *PIK3AP1*, *PTGER2*, *TAP1* and *TGM2*). A summary of the focus genes involved with relevance to GVHD processes is presented in Table 3.5.

<b>Category</b>	<b>Functions</b>	<b>Genes</b>
<b>Infectious Disease</b>	1. infection by bacteria	<i>CXCL9,MSR1,UBD</i>
	2. leprosy	<i>MSR1,UBD</i>
<b>Cancer</b>	1. formation of mammary tumor	<i>MSR1</i>
	2. B-cell non-Hodgkin's disease	<i>CARD11,LGALS7/LGALS7B</i>
	3. hydatidiform mole	<i>PTGER2</i>
	4. metastatic colorectal cancer	<i>HCLS1,HTRA1</i>
	5. diffuse large B-cell lymphoma	<i>CARD11</i>
<b>Connective Tissue Disorders</b>	1. arthritis	<i>CXCL9,HCLS1,HTRA1,LST1PIK3AP1,PSTPIP1,TAP1</i>
	2. rheumatoid arthritis	<i>CXCL9,HCLS1,HTRA1,LST1,PIK3AP1,TAP1</i>
	3. ankylosing spondylitis	<i>CXCL9</i>
<b>Genetic Disorder</b>	1. asthma, nasal polyps, and aspirin intolerance	<i>PTGER2</i>
	2. polycystic lipomembraneous osteodysplasia	<i>TREM2</i>
	3. exudative age-related macular degeneration	<i>HTRA1</i>
	4. chronic small and large plaque psoriasis	<i>CXCL9</i>
	5. exfoliation syndrome	<i>TGM2</i>
	6. maturity-onset diabetes of the young	<i>TGM2</i>
	7. ankylosing spondylitis	<i>CXCL9</i>
	8. tuberculoid leprosy	<i>UBD</i>
	9. progressive supranuclear palsy	<i>TGM2</i>
	10. osteoporosis	<i>PTGER2</i>
<b>Inflammatory Disease</b>	1. familial recurrent arthritis	<i>PSTPIP1</i>
	2. asthma, nasal polyps, and aspirin intolerance	<i>PTGER2</i>
	3. inflammatory disorder	<i>C1QTNF7,CXCL9,HCLS1,HTRA1,LST1,PIK3AP1,PSTPIP1,PTGER2,TAP1</i>
	4. rheumatoid arthritis	<i>CXCL9,HCLS1,HTRA1,LST1, PIK3AP1,TAP1</i>
	5. dermatomyositis	<i>CXCL9</i>

**Table 3.2 Involvements of the 18 focus genes in top diseases and disorders.**

Category	Functions Annotation	Genes
Cellular Growth and Proliferation	1. proliferation of peripheral blood leukocytes	<i>CARD11,LST1</i>
	2. growth of neuroblastoma cells	<i>LGALS7/LGALS7B</i>
	3. proliferation and co-stimulation of peripheral T lymphocyte	<i>CARD11</i>
	4. proliferation of mesangial cells	<i>CXCL9</i>
	5. proliferation of skin cancer cell lines	<i>PTGER2</i>
	6. colony formation of colon cancer cell lines	<i>LGALS7/LGALS7B</i>
	7. proliferation of fibroblast cell lines	<i>TGM2</i>
Cell Morphology	1. branching of actin filaments	<i>HCLS1</i>
	2. multinucleation of colon cancer cell lines	<i>UBD</i>
	3. polarization of hematopoietic progenitor cells	<i>CXCL9</i>
	4. morphology and cell spreading of embryonic cell lines	<i>MSR1</i>
	5. morphology and cell spreading of kidney cell lines	<i>MSR1</i>
	6. morphology and cell spreading of epithelial cell lines	<i>MSR1</i>
	7. reorganization of actin cytoskeleton	<i>CXCL9</i>
	8. autophagy of brain cancer cell lines	<i>PTGER2</i>
Cell-To-Cell Signalling & Interaction	1. attachment of keratinocyte cancer cell lines	<i>PTGER2</i>
	2. activation of smooth muscle cell lines	<i>TGM2</i>
	3. activation of smooth muscle cells	<i>TGM2</i>
	4. activation of embryonic cell lines	<i>TGM2</i>
	5. activation of epithelial cell lines	<i>TGM2</i>
	6. phagocytosis of monocyte-derived macrophages	<i>TGM2</i>
	7. activation of kidney cell lines	<i>TGM2</i>
	8. adhesion of hematopoietic progenitor cells	<i>CXCL9</i>
	9. adhesion of leukocyte cell lines	<i>TGM2</i>
	10. binding of melanoma cell lines	<i>CXCL9</i>
	11. co-stimulation of T lymphocytes	<i>CARD11</i>
	12. phagocytosis of leukemia cell lines	<i>TGM2</i>
	13. adhesion of blood cells	<i>CXCL9,TGM2</i>
	14. binding and adhesion of embryonic cell lines	<i>MSR1</i>
	15. binding and adhesion of epithelial cell lines	<i>MSR1</i>
	16. binding and adhesion of kidney cell lines	<i>MSR1</i>
Cellular Development	1. branching of actin filaments	<i>HCLS1</i>
	2. growth of neuroblastoma cells	<i>LGALS7/LGALS7B</i>
	3. differentiation of myeloid dendritic cells	<i>UBD</i>
	4. differentiation of neuroblastoma cell lines	<i>TGM2</i>
Small Molecule Biochemistry	1. conjugation, modification and trans-amidation of histamine	<i>TGM2</i>
	2. deposition, transport and efflux of cholesterol	<i>MSR1</i>
	3. synthesis of leukotriene B4	<i>PTGER2</i>
	4. fatty acid metabolism	<i>MSR1,PTGER2</i>

**Table 3.3 Function of focus genes in molecular and cellular processes.**

Category	Functions Annotation	Genes
<b>Haematological System Development and Function</b>	1. proliferation of peripheral blood leukocytes	<i>CARD11,LST1</i>
	2. polarization of hematopoietic progenitor cells	<i>CXCL9</i>
	3. cell movement of T lymphocytes	<i>CXCL9,TGM2</i>
	4. aggregation, adhesion and chemotaxis of hematopoietic progenitor cells	<i>CXCL9</i>
	5. differentiation of myeloid dendritic cells	<i>UBD</i>
	6. phagocytosis of monocyte-derived macrophages	<i>TGM2</i>
	7. adhesion of leukocyte cell lines	<i>TGM2</i>
	8. co-stimulation and proliferation of T lymphocytes	<i>CARD11</i>
	9. chemotaxis of eosinophils	<i>CXCL9</i>
<b>Tissue Development</b>	1. attachment of keratinocyte cancer cell lines	<i>PTGER2</i>
	2. aggregation and adhesion of hematopoietic progenitor cells	<i>CXCL9</i>
	3. development of dendrites	<i>LST1</i>
	4. adhesion of leukocyte cell lines	<i>TGM2</i>
	5. adhesion of embryonic, epithelial and kidney cell lines	<i>MSR1</i>
	6. proliferation of fibroblast cell lines	<i>TGM2</i>
<b>Tumor Morphology</b>	1. formation of mammary tumor	<i>MSR1</i>
<b>Hair and Skin Development and Function</b>	1. re-epithelialization of wound	<i>LGALS7/LGALS7B</i>
	2. activation of epithelial cell lines	<i>TGM2</i>
	3. cell spreading, morphology, binding and adhesion of epithelial cell lines	<i>MSR1</i>

**Table 3.4 Physiological System Development and Function.**

<b>Function Annotation</b>	<b>Genes</b>
increases activation of leukocytes	<i>CARD11, CXCL9, TREM2</i>
increases apoptosis of tumor cell lines	<i>HCLS1, LGALS7/LGALS7B, MSR1, TGM2</i>
affects arthritis	<i>CXCL9, HCLS1, HTRA1, LST1, PIK3AP1, PSTPIP1, PTGER2, TAP1</i>
affects autoimmune disease	<i>CARD11, CXCL9, HCLS1, HTRA1, LST1, PIK3AP1, PTGER2, TAP1, TGM2</i>
increases cell death of tumor cells	<i>CXCL9, HCLS1, LGALS7/LGALS7B, MSR1, TGM2</i>
affects dermatological disorder	<i>ANP32A, CARD11, CXCL9, MSR1, UBD</i>
affects differentiation of cells	<i>CARD11, LGALS7/LGALS7B, PTGER2, TGM2, UBD</i>
affects digestive system disorder	<i>C1QTNF7, CARD11, CXCL9, HTRA1, LST1, TAP1, TGM2, UBD</i>
affects hematological disorder	<i>CARD11, CXCL9, HCLS1, LGALS7/LGALS7B, MSR1, PTGER2, TGM2</i>
affects immune response	<i>CARD11, MSR1, PIK3AP1, PTGER2, TGM2, TREM2</i>
affects inflammatory disorder	<i>C1QTNF7, CARD11, CXCL9, HCLS1, HTRA1, LST1, PIK3AP1, PSTPIP1, PTGER2, TAP1, TGM2</i>
affects leukocyte migration	<i>CXCL9, MSR1, TGM2, TREM2</i>
affects metastasis	<i>HCLS1, HTRA1, PTGER2</i>
affects migration of cells	<i>CXCL9, MSR1, PTGER2, TGM2, TREM2</i>
affects non-Hodgkin's disease	<i>CARD11, CXCL9, LGALS7/LGALS7B</i>
affects proliferation of cells	<i>CARD11, LGALS7/LGALS7B, MSR1, PIK3AP1, PTGER2, TGM2</i>
affects quantity of leukocytes	<i>CARD11, PIK3AP1, PTGER2, TAP1</i>
affects response of cells	<i>CARD11, CXCL9, MSR1, TGM2, TREM2</i>
affects rheumatoid arthritis	<i>CXCL9, HCLS1, HTRA1, LST1, PIK3AP1, TAP1</i>
affects skeletal and muscular disorder	<i>CXCL9, HCLS1, HTRA1, LST1, PIK3AP1, PSTPIP1, PTGER2, TAP1, TGM2</i>

**Table 3.5 Functional annotation of focus genes.** Functional analysis of the 18 focus genes identified the diseases and processes in which the genes may have an impact on.

### 3.2.4 Canonical pathway analyses

Canonical pathway analyses identified the metabolic and signalling pathways that were most significant to the focus genes. The top five canonical pathways were T cell receptor, NFκB and interferon signalling, and DC maturation (Table 3.6 and Figure 3.4). Six of the focus genes were either directly or indirectly associated with IFN-γ (*TAP1*, *CXCL9*, *LST1*, *LILRA5*, *IL1R2* and *UBD*) (Figure 3.5).

Canonical Pathway	Gene	Networks
T Cell Receptor Signalling & NFκB Signalling	<i>CARD11</i>	1
T Cell Receptor Signalling	<i>PTPN7</i>	2
Interferon Signalling	<i>TAP1</i>	2
Dendritic Cell Maturation	<i>TREM2</i>	2

**Table 3.6 Canonical Pathways.** The relevant canonical pathways were selected and the involvement of the 18 focus genes in these pathways determined. The networks in which the focus genes are involved in are indicated in the table. The Networks are numbered as mentioned in Section 3.3.2.

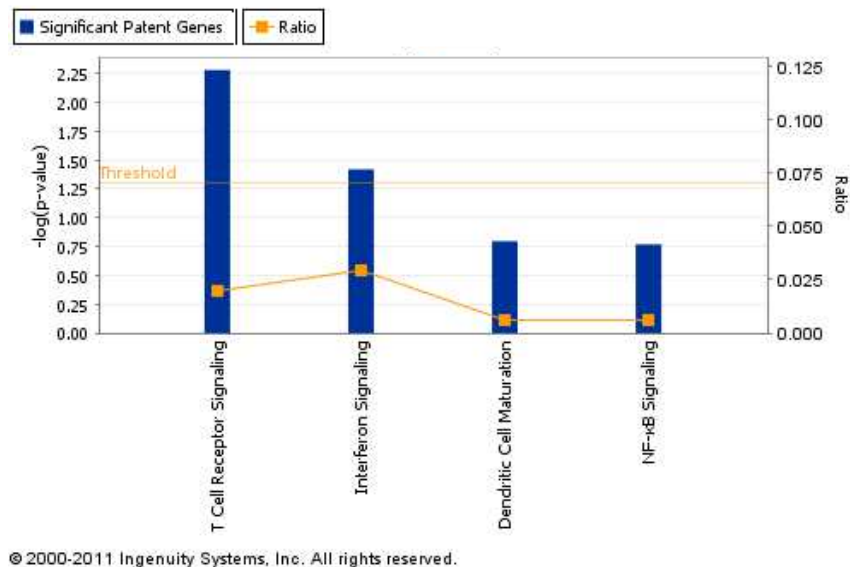
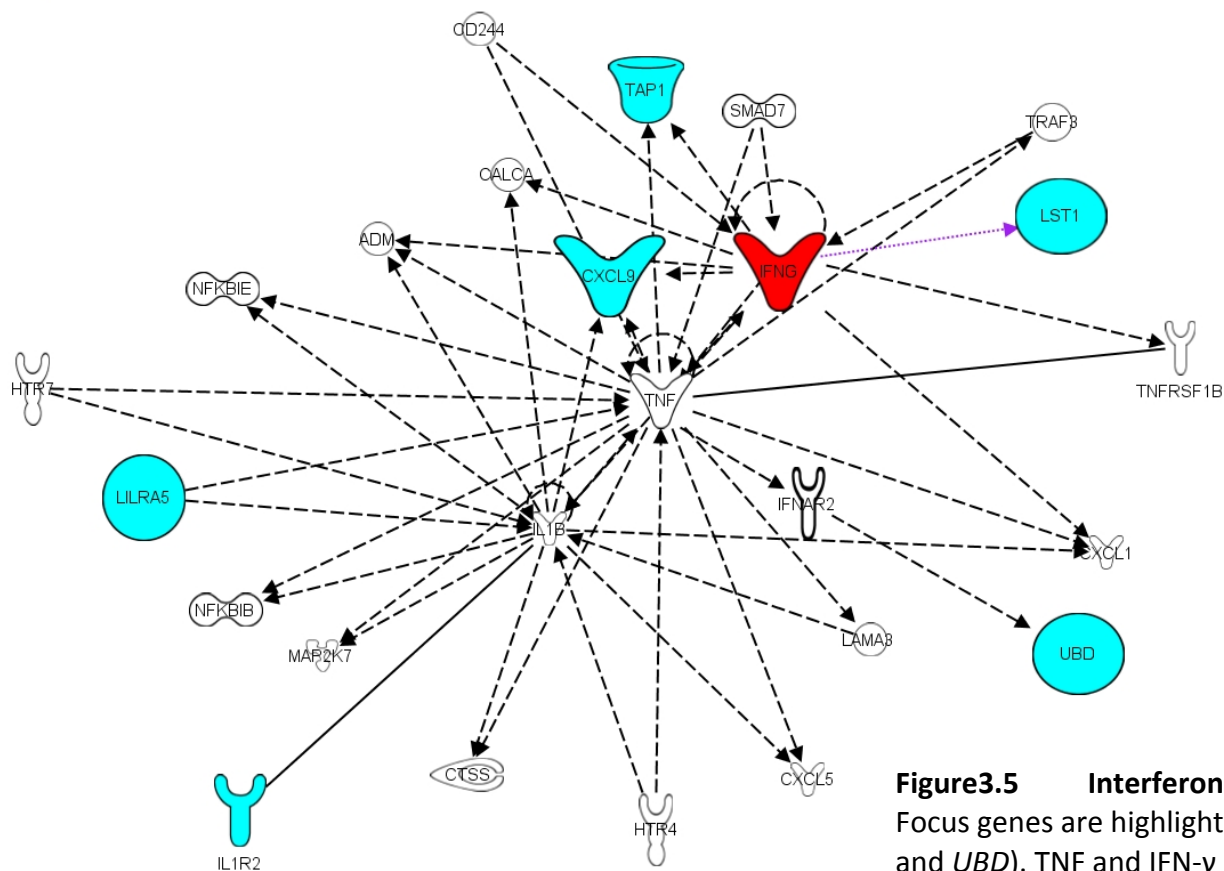


**Figure 3.4 Canonical pathways relevant to GVHD.** T Cell Receptor and Interferon Signalling were the main pathways associated with GVHD with the maximum number of the focus genes present in these pathways. The four selected canonical pathways are displayed along the x-axis. The height of the bars represents the number of genes associated with that specific canonical pathway. IPA calculated the ratios by dividing the number of genes in a pathway that met the automatic cut-off and the total number of genes in that canonical pathway. Then the software used the right-tailed Fisher's exact test to calculate the p-values.



Key	Symbol	Category
--- Relationship	White Y-shape	Transporter
..... Relationship	White Y-shape	Cytokine/Growth Factor
— Relationship	White Y-shape	Unknown
	White Y-shape	Peptidase
	White Y-shape	G-protein Coupled Receptor
	White Y-shape	Transcription Regulator
	White Y-shape	Kinase
	White Y-shape	Transmembrane Receptor

**Figure3.5 Interferon- $\gamma$  indirectly acts on six of the focus genes.** Focus genes are highlighted in blue (*TAP1*, *CXCL9*, *LST1*, *LILRA5*, *IL1R2* and *UBD*). TNF and IFN- $\gamma$  directly interact as well as with the focus genes in this pathway. *LST1* was also found to be influenced by IFN- $\gamma$  and was therefore added to the pathway. This finding is depicted with the dashed purple line from IFN- $\gamma$  to *LST1*. For a comprehensive list of symbols see Chapter 2, Section 2.15.5.

### **3.2.5 More than 1000 microRNAs target the 18 genes**

MicroRNA prediction for the 18 genes was performed using the miRWalk database (Dweep *et al.*, 2011). MicroRNAs that were identified by at least three databases (miRanda, miRDB, miRWalk, RNA22 and Targetscan) were considered as predicted targets. In total 1500 miRNAs were predicted to target the 18 genes. Table 3.7 shows a summary of the predicted miRNAs that may each regulate the 18 genes. MiR-34a was the most interesting miRNA as its role in aGVHD has been recently reported in the literature (Wang *et al.*, 2013). However, the study had focused on gastrointestinal biopsies and not skin biopsies.

Gene	miRNA	miRanda	miRDB	miRWalk	RNA22	Targetscan	SUM
PTPN7, TAP1	hsa-let-7g	1	0	1	0	1	3
CXCL9, SLCO1B1, TGM2	hsa-miR-1	1	0	1	0	1	3
MSR1, TAP1	hsa-miR-101	1	0	1	0	1	3
HTRA1, MSR1, PIK3AP1, PTPN7	hsa-miR-105	1	0	1	0	1	3
MSR1, C1qTNF7, CXCL9	hsa-miR-106	1	1	1	1	1	5
CARD11, PIK3AP1	hsa-miR-107	1	0	1	0	1	3
C1qTNF7, CARD11, PIK3AP1, TAP1	hsa-miR-10a	1	0	1	0	1	3
C1qTNF7, CARD11, PIK3AP1, TAP1	hsa-miR-10b	1	0	1	0	1	3
C1qTNF7, CEACAM4	hsa-miR-1182	1	0	1	0	1	3
PIK3AP1, PTGER2, TAP1, TAP1	hsa-miR-1184	1	0	1	0	1	3
C1qTNF7, PTPN7, TGM2	hsa-miR-1197	1	0	1	0	1	3
PTPN7, TAP1, TGM2	hsa-miR-122	1	0	1	0	1	3
PTPN7, TGM2	hsa-miR-1233	1	0	1	0	1	3
ANP32A, C1qTNF7, CXCL9, MSR1, PTPN7, TAP1	hsa-miR-1236	1	0	1	0	1	3
C1qTNF7, MSR1, PIK3AP1, PTGER2	hsa-miR-1237	1	1	1	0	1	4
C1qTNF7, CXCL9	hsa-miR-124	1	0	1	0	1	3
CXCL9, TAP1	hsa-miR-1251	1	0	1	0	1	3
C1qTNF7, CXCL9, HCLS1, TGM2	hsa-miR-1252	1	1	1	0	1	4
CXCL9, PTPN7, TAP1	hsa-miR-1253	1	0	1	0	1	3
CARD11, TAP1	hsa-miR-1254	1	0	1	0	1	3
C1qTNF7, CEACAM4, HCLS1, TAP1, TGM2	hsa-miR-125a-3p	1	0	1	0	1	3
TAP1, TGM2	hsa-miR-125b	1	0	1	0	1	3
C1qTNF7, HCLS1, PTGER2, TGM2	hsa-miR-128	1	0	1	0	1	3
ANP32A, CXCL9, MSR1, PIK3AP1	hsa-miR-132	1	1	1	0	1	4
PTPN7, TAP1, TGM2	hsa-miR-134	1	0	1	0	1	3
CXCL9, TGM2	hsa-miR-135a	1	0	1	0	1	3
CXCL9, PTPN7, TGM2	hsa-miR-143	1	0	1	0	1	3
C1qTNF7, CARD11, MSR1	hsa-miR-181a	1	0	1	0	1	3
C1qTNF7, CARD11, MSR1, PIK3AP1	hsa-miR-181b	1	0	1	0	1	3
C1qTNF7, MSR1	hsa-miR-200a	1	0	1	0	1	3
ANP32A, CXCL9, MSR1, PIK3AP1	hsa-miR-212	1	1	1	0	1	4
PIK3AP1, TGM2	hsa-miR-34b	1	0	1	0	1	3
PTGER2, TGM2	hsa-miR-34c-3p	1	0	1	0	1	3
MSR1, PIK3AP1, PSTPIP1, PTGER2	hsa-miR-659	1	0	1	0	1	3
CARD11, PIK3AP1, PTPN7, TAP1, TGM2	hsa-miR-661	1	0	1	0	1	3
C1qTNF7, MSR1, PIK3AP1, TAP1	hsa-miR-664	1	1	1	0	1	4
TAP1, TGM2, PTPN7	hsa-miR-665	1	0	1	0	1	3
CXCL9, HCLS1, PTPN7, TAP1	hsa-miR-671-5p	1	0	1	0	1	3
C1qTNF7, CXCL9, PIK3AP1, TAP1	hsa-miR-7	1	0	1	0	1	3
CXCL9, PTPN7, TAP1, TGM2	hsa-miR-708	1	0	1	0	1	3
C1qTNF7, HTRA1, PIK3AP1, PTPN7	hsa-miR-890	1	1	1	0	1	4
C1qTNF7, CXCL9, MSR1, PIK3AP1, TAP1	hsa-miR-9	1	0	1	0	1	3
CXCL9, MSR1, PIK3AP1	hsa-miR-944	1	1	1	0	1	4
PIK3AP1, TAP1	hsa-miR-96	1	0	1	0	1	3
PIK3AP1, PTPN7, TGM2	hsa-let-7d/c	1	0	1	0	1	3
CXCL9, PTGER2,	hsa-miR-142-3p	1	0	1	0	1	3
SLCO1B1, CXCL9, PIK3AP1, TGM2	hsa-miR-142-5p	1	0	1	0	1	3
C1qTNF7, CXCL9, MSR1, PTGER2	hsa-miR-200b	1	0	1	0	1	3
MSR1	hsa-miR-21	1	0	1	1	1	4
TGM2	hsa-miR-23b	1	0	1	0	1	3
CEACAM4, CXCL9, PTPN7, TGM2	hsa-miR-24	1	0	1	0	1	3
ANP32A, C1qTNF7, HTRA1, TGM2	hsa-miR-34a	1	0	1	0	1	3
MSR1, PIK3AP1	hsa-miR-493	1	0	1	0	1	3
MSR1, TGM2	hsa-miR-503	1	0	1	0	1	3

**Table 3.7 Summary of predictive miRNAs that may target the 18 genes.** The most interesting miRNA (miR-34a) is highlighted in yellow due to its recent reported association with gastrointestinal aGVHD (Wang *et al.*, 2013).

### 3.3 Discussion

The candidate gene list was derived from an investigation by Norden et al (unpublished) using Taqman Low Density Arrays. Total RNA extracted from clinical aGVHD skin biopsies (grades 0-IV) and normal controls were used in this profiling experiment. The highly differentially expressed genes were selected, validated by RT-qPCR and the signature gene list (n=18) used for this pathway-mining study. Ingenuity Pathway Analysis was used to determine the pathways and networks in which the significant 18 focus genes were involved, either through direct or indirect association. This investigation also aimed to identify additional molecules that may be associated with the existing 18 focus genes or pathways. These new molecules could potentially be studied further as new leads in understanding the pathobiology of GVHD. The 18 focus genes were analysed using the core IPA analysis, which permits the study of the dataset in a biological context (processes, diseases and disorders). *In silico* pathway analysis approaches, such as IPA, allow researchers to predict the biological mechanisms underlying their genomic experiments.

The pathway analysis demonstrated that the 18 genes were involved in five networks. **Network 1** analysis showed that IL13 protein could indirectly act on *HTRA1* mRNA expression, as a result of which *HTRA1* mRNA expression is reduced in human monocytes (Scotton *et al.*, 2005). On the other hand, IL-13 increases the expression of *TGM2* mRNA (Scotton *et al.*, 2005). IFN- $\gamma$  increases *UBD* mRNA expression while IL1RA protein indirectly decreases *UBD* mRNA expression (Hurgin *et al.*, 2007). In keratinocytes, *LGALS7* mRNA is reduced by human IgG complexes which exhibit pemphigus vulgaris (Nguyen *et al.*, 2004). In cytotoxic T-lymphocyte cultures, IL12B enhances the expression of *PIK3AP1* mRNA (Chowdhury *et al.*). ERK1/2 proteins are regulated by PTGER2 (Donnini *et al.*, 2007). It has been demonstrated in human derived macrophages that ADIPOQ protein reduces the expression of *MSR1* mRNA (Ouchi *et al.*, 2001). When macrophages are LPS treated, ADIPOQ decreases CXCL9 expression (Okamoto *et al.*, 2008). PSTPIP protein enhances the localization of FASLG to the intracellular space (Baum *et al.*, 2005). In Jurkat cells, CARD11 increases NF $\kappa$ B complexes (Ishiguro *et al.*, 2006). Interestingly, both *HTRA1* and *LGAL7* have been

shown to be significantly reduced (Norden et al, unpublished) in aGVHD skin which overlaps with the finding of IPA in Network 1.

**Network 2** involved four focus genes; *TAP1*, *PTPN7*, *ANP32A* and *TREM2*. Investigations have shown that p53 directly acts on *TAP1* and is essential for its mRNA expression (Daoud *et al.*, 2003) while SMARCA4 protein is indirectly involved in *PTPN7* and *TREM2* expression (Hendricks *et al.*, 2004). There is direct relationship between *TAP1* and p53; whereby binding of p53 to it, enhances *TAP1* expression levels. SMARCA4 is a transcription factor with a role as a tumour suppressor. Studies have shown that both *ANP32A* and SMARCA4 expression is regulated by miR-21 which is responsible for tumour growth (Schramedei *et al.*, 2011). No change in the expression of *ANP32A* was observed in the experimental validation (Norden et al, unpublished), but higher levels were found in an aGVHD rat skin explant model (Novota *et al.*, 2011). This may indicate that *Anp32a* expression is regulated via a different mechanism in humans and rats and there might be a differential level of miR-21 and/*Smarca4* expression in the rat skin explant model. In the validation cohort, *TAP1* expression was up-regulated in aGVHD human skin as well as the rat skin explant model (Norden et al, unpublished). Thus, it might be biologically reasonable to investigate p53 mRNA and protein expression in the same skin biopsies and correlate the expression with *TAP1* levels. P53 is an established regulator of apoptosis (Fridman and Lowe, 2003) and understanding its interaction with *TAP1* may explain the increased levels of apoptosis seen in cutaneous aGVHD.

According to **Network 3**, NR3C1 protein indirectly impacts *C1qTNF7* mRNA expression (Lu *et al.*, 2007). NR3C1 is the glucocorticoid receptor gene and plays a role in inflammatory responses and cellular proliferation (Ray and Prefontaine, 1994). According to the findings of IPA, in Network 3, NR3C1 indirectly interacts with *C1qTNF7* which is a gene with very limited associated literature available on it. In allo-HSCT glucocorticoids are administered as first line GVHD therapy. In the validation study, low levels of *C1qTNF7* mRNA expression were observed in both aGVHD skin (Norden et al, unpublished) and the rat skin explant model. Thus, the interaction found in Network 3 might provide additional insight in how *C1qTNF7* is regulated and functions in aGVHD.

**Network 4** showed that CEBPA protein directly enhances *LST1* mRNA expression (Tavor *et al.*, 2003). CEBPA is a gene that is associated with familial AML (Smith *et al.*, 2004). CEBPA has been shown to be significantly up-regulated in the PBMC of aGVHD patients. In the rat skin explant model *Lst1* was up-regulated, while in human cutaneous aGVHD its levels were down-regulated (Norden et al, unpublished). CEBPA has tissue specific expression with high levels being present in peripheral blood (Antonson and Xanthopoulos, 1995). There is 92% similarity between the rat and human CEBPA protein sequence (Antonson and Xanthopoulos, 1995). The IPA network finding thus shows that it would be insightful to also investigate CEBPA levels in the same skin biopsies and to test for interactions as well as correlations.

**Network 5** showed the involvement of HCLS1. F2 protein indirectly acts on HCLS1 and increases its mRNA expression while SYK and LYN protein directly act on HCLS1 to enhance its expression (Brunati *et al.*, 2005). Experimentally, HCLS1 levels were unaltered in aGVHD human skin while they were up-regulated in the rat skin explant model (Norden et al, unpublished). In fact, HCLS1 has a binding site in its promoter for CEBPA, which was identified in Network 5 to interact with LST1 (van Rossum *et al.*, 2005). It is therefore possible that CEBPA, HCLS1 and LST1 interact in GVHR. A preliminary aGVHD investigation in peripheral blood has shown that LST1 and CEBPA are over-expressed prior to aGVHD onset that may indicate the initiation of an inflammatory response (Buzzeo *et al.*, 2008). However, the results of the investigation must be cautiously interpreted as their cohort comprised of AML patients who had undergone allo-HSCT procedure. As mentioned earlier, CEBPA may be mutated and also is present in familial AML (Smith *et al.*, 2004).

Moreover, six of the focus genes were either directly or indirectly associated with IFN- $\gamma$  (TAP1, CXCL9, LST1, LILRA5, IL1R2 and UBD) and this has also been demonstrated experimentally by Norden et al (unpublished). The genes also interacted with TNF- $\alpha$  which has established roles in aGVHD onset in particular during Phase 1 when target organs namely the skin and gut are damaged due to the conditioning regimen. TNF- $\alpha$  is released during the effector stage (Phase 3) and leads to organ damage in aGVHD. This may suggest that the IFN- $\gamma$  inducible genes in this study are secreted after donor T cell

activation when both IFN- $\gamma$  and TNF- $\alpha$  are present exacerbating organ damage during the effector phase (Figure 3.6).

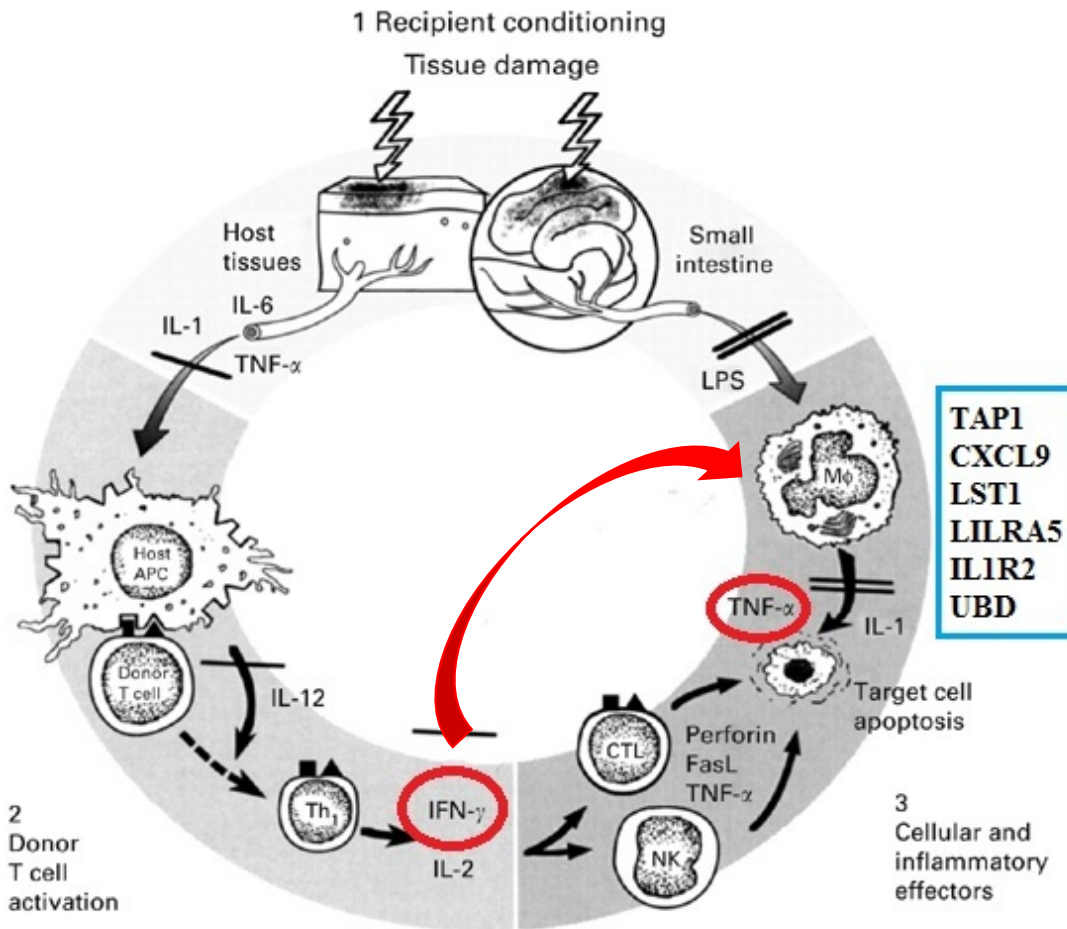


**Figure 3.6** IFN- $\gamma$  inducible genes may be expressed at the effector phase of aGVHD (adopted from (Hill and Ferrara, 2000)). *TAP1*, *CXCL9*, *LST1*, *LILRA5* and *UBD* have been shown both via pathway mining analysis and experimentally (Norden et al, unpublished) to be induced by IFN- $\gamma$ . IPA analysis has also shown that the genes interact both directly and indirectly with TNF- $\alpha$ . This may suggest their involvement in the effector phase of cutaneous aGVHD.

T cell receptor, NFκB and IFN signalling as well as dendritic cell maturation were identified as one of the four canonical pathways using IPA. Each pathway involved one of the focus genes. CARD11, PTPN7, TAP1 and TREM2 were part of each pathway. The same genes were also part of two of the networks identified in this analysis, primarily Network 2 and 1. All the pathways have been shown to be involved in GVHD pathogenesis. The common findings between the network and canonical pathway analysis may suggest that the above mentioned genes could be more likely involved in aGVHD.

Interestingly, more than 1000 miRNAs were predicted to target the 18 genes. This is in support of the well-known fact that a single miRNA can target more than 200 genes and 50% of the genes are controlled by these short nucleotides (Bartel, 2009). Surprisingly, miR-34a that has reported associations with gastrointestinal aGVHD (Wang *et al.*, 2013) was also identified to target four of the 18 genes (*ANP32A*, *C1qTNF7*, *HTRA1*, and *TGM2*).

Overall, all the 18 genes were identified to be involved in immune-related and/or autoimmune diseases and disorders. It is well known that GVHD is an immune-mediated reaction. The 18 focus genes were identified using skin biopsies and IPA identified the role of some of these genes in tissue, hair and skin development which may suggest the tissue-specificity of the genes. A caveat of pathway analysis is that pathways generated are based on statistical probability rather than the actual biological involvement of the genes. Thus, the additional genes identified in a pathway and the interactions depicted in the networks are only suggestive of potential roles and need to be verified experimentally to validate them.

Moreover, the genes in this study were evaluated in total RNA from the whole skin biopsy, which contains a heterogeneous population of cell types (keratinocytes, epithelial cells, fibroblasts, T cells etc.). Thus, the deregulation observed experimentally could have been as a result of the contribution of all the various cell types, yet the pathway analysis was able to identify skin specific functions. The focus

genes were also highly involved in haematological system development and function, which again reflects the contribution of all the different cell types in the skin.

A limitation of using IPA or other *in silico* pathway analysis software is that the analysis is based on literature that has been curated in the database, rather than the whole field. This limitation can be overcome by a thorough search of the literature and careful examination of the pathways and networks created using IPA. In this investigation, LST1 was not identified to be impacted by IFN- $\gamma$ . However, Norden *et al* (unpublished), identified literature on LST1 and the impact of IFN- $\gamma$  on this gene. Therefore, LST1 was included in the canonical pathway (Figure 3.4) showing the indirect influence of IFN- $\gamma$  on this focus gene.

Similarly, a limitation of this investigation was that the genes for pathway analysis were pre-selected and thus, the fold change results were not analysed using the software. This method of analysis might have introduced bias and therefore eliminated genes that may have had additional potential roles to play in related pathways and networks.

In conclusion, the present pathway analysis using IPA corroborates the role of the 18 focus genes in inflammation and autoimmune disorders as well as roles in T- and dendritic cells. There is an extensive literature on the function of both T and DCs in the pathobiology of GVHD. More importantly, the findings of the miRNA prediction search provided additional clues for the selection of the most significant miRNAs in the next skin study (Chapter 4) that was based on the identification of a signature list of miRNAs associated with aGVHD incidence and other allo-HSCT outcomes.

## **Chapter 4. MicroRNA Expression in Clinical Skin Biopsies of Allogeneic Stem Cell Transplantation Patients**

“Do not go where the path may lead, go instead where there is no path and leave a trail.”

**-Ralph Waldo Emerson**

## 4.1 Introduction

Skin is the largest organ of the human body and the most frequently affected aGVHD target organ. In brief, the skin is divided into three primary layers: the epidermis (outer-most), the dermis (centre) and the hypodermis (inner-most). The epidermis is mainly made up of proliferative keratinocytes while the dermis is composed of fibroblasts. The basement membrane separates the epidermis from the dermis. The hypodermis comprises of adipose cells. Melanocytes and APCs are also present in the epidermis (Mancini *et al.*, 2014). The immune compartment of the skin constitutes; DCs, macrophages and T cells. It has been established that the number of T cells and DCs in the skin are more than present in the circulation, which highlights their function in immunosurveillance (Clark *et al.*, 2006).

### 4.1.1 Cutaneous aGVHD

The overall clinical aGVHD is still classified into four grades (I-IV) as per the 1994 NIH consensus conference (Przepiorka *et al.*, 1995). Skin is staged based on how severely it is affected by the disease as well as the presence of any blistering or epidermolysis (Przepiorka *et al.*, 1995). The staging of skin is based on Glucksberg criteria (Glucksberg H, 1974). Conversely, the skin histopathological grading system used even today was established in 1974, by Lerner *et al.*, (Lerner *et al.*, 1974). Skin aGVHD is histopathologically graded based on the degree of vacuolization observed in the 'basal layer of the epidermis and skin appendages such as the hair (Ziemer, 2013). Lymphocytic inflammatory cell infiltrates are also considered as well as the percentage of apoptotic cells comprising of keratinocytes and lymphocytes. Apoptotic lymphocytes are referred to as satellite necrotic cells (Ziemer, 2013). Table 4.1 shows the histological changes that are considered for grading cutaneous aGVHD in patients.

Cutaneous aGVHD grading	Histological changes
Grade I	Focal or diffuse vacuolar change
Grade II	Grade I histological changes + dyskeratotic keratinocytes
Grade III	Grade II histological changes + subepidermal cleft formation
Grade IV	Complete loss of the epidermis and separation from the dermis

**Table 4.1 Histological criteria used for grading cutaneous aGVHD**

Cutaneous aGVHD manifests as a result of a sequence of events that is divided into three phases (Figure 4.1). Phase I of cutaneous aGVHD involves the activation of resting Langerhans cells (LCs) that are myeloid DCs present in the epidermis. Depletion of host LCs in murine models has been shown to prevent cutaneous aGVHD, and also they have been found to persist in the tissue post-engraftment (Merad *et al.*, 2004). This activation is due to the release of cytokines as a consequence of damage to host tissues during chemotherapy regimen and/irradiation therapy. Apoptosis of keratinocytes also leads to the release of danger signals in the skin. HLA class I and II molecules are also overexpressed during this period. Phase II of cutaneous aGVHD occurs post allo-HSCT when the activated donor T cells recognize the antigens presented by activated host DCs. In this phase, premature keratinocytes undergo apoptosis due to the ‘cytokine storm’, this exacerbates histological skin damage.

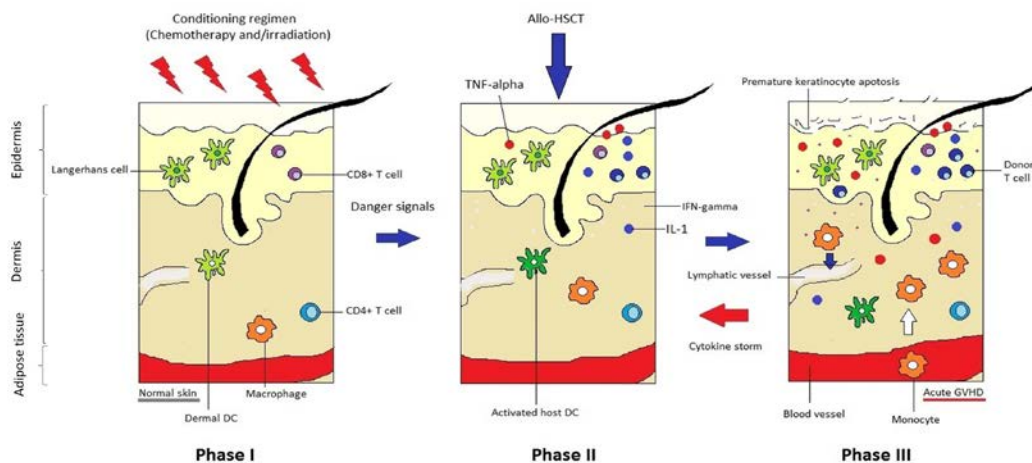


**Figure 4.1 Pathogenesis of cutaneous aGVHD.** The three phases that are involved in cutaneous aGVHD are depicted where in; phase I, danger signals are released due to the damage caused to the host skin tissue, phase II, post allo-HSCT, cytokines are released and host DCs are activated which coincides with phase III and further monocyte-macrophage differentiation. In this phase, premature keratinocytes undergo apoptosis; donor T cells mediated cytokine storm results in further damage to the host tissue. Skin homeostasis and morphology are disturbed, and histological changes are clearly evident (Hofmeister *et al.*, 2004).

As mentioned in Chapter 1, aGVHD is commonly treated with corticosteroids. Initial first-line therapy for mild cutaneous aGVHD is topical steroids. Calcineurin inhibitors such as Cyclosporine A are also administered as part of GVHD prophylaxis. In addition to the above medications, moderate-severe cutaneous aGVHD can also be treated with phototherapy or ECP (Ziemer, 2013).

#### 4.1.2 MicroRNAs identified as biomarkers of aGVHD

Currently, biomarkers that can be used in the clinic to stratify patients to improve response to treatments, diagnose or predict aGVHD or patient survival outcome are absent. Recently, the role of several miRNAs have been investigated in aGVHD as these very short regulatory molecules have been shown to have significant functions in numerous autoimmune diseases [rheumatoid arthritis (Leah, 2011), psoriasis (Sonkoly

*et al.*, 2007), and systemic lupus erythematosus (Wang *et al.*, 2012)] as well as cancers [lymphoma (Lawrie *et al.*, 2007), oral (Park *et al.*, 2009) and colorectal (Bandres *et al.*, 2006)]. MiR-146a has been shown to be down-regulated in severe aGVHD murine models, and its target Traf6 was elevated, leading to the activation of NFκB pathway (Stickel *et al.*, 2014). The crucial role of miR-155, which has established functions in immune system control, has been highlighted in the development of aGVHD (Ranganathan *et al.*, 2012). Elevated levels of miR-155 were expressed in the gut of severe aGVHD patients compared to normal controls (Ranganathan *et al.*, 2012). Likewise, the function of miR-34a (Wang *et al.*, 2013) and miR-100 have also been reported with regards to aGVHD. MiR-34a was expressed at higher levels in the gut of patients with aGVHD grades II-IV compared to pre-transplant biopsies and patients with aGVHD grades 0-I (Wang *et al.*, 2013). The authors hypothesized that gut damage was a consequence of up-regulated miR-34a, which resulted in apoptosis of epithelial gut cells (Wang *et al.*, 2013). Similarly, miR-100 expression was increased in the gut of mice without aGVHD, therefore suggesting a protective function (Leonhardt *et al.*, 2013). More recently, a predictive signature list of miRNAs for aGVHD have been detected in the plasma of allo-HSCT patients (Xiao *et al.*, 2013). The authors showed that miRNAs (miR-423, -199a-3p, -93\*, and -377) in the plasma could discriminate patients who would develop aGVHD from those who would not (non-aGVHD group). The miRNAs were also associated with reduced OS as well as aGVHD severity (Xiao *et al.*, 2013). No functional experiments were performed in their study thus the role of their signature miRNA in GVHD is yet to be determined.

### **4.1.3 Specific study aims**

Therefore, experiments in this Chapter aimed to identify the key miRNAs that may be involved in the onset and development of aGVHD as well as be used to predict patient survival and/disease-free state outcomes. As mentioned previously, skin is one of the major target organs affected by aGVHD. Firstly, the global profiling of miRNAs was performed in skin biopsies taken at the time of aGVHD onset from allo-HSCT patients. In this investigation, we used skin biopsies from patients who underwent plastic surgery (two females) and healthy volunteers (two males) as normal controls. Female controls were used when all the cases in the initial discovery cohort were males to see if there was any sex-dependent miRNA expression patterns. Moreover, the initial discovery cohort did comprise of two additional cases that were female but had to be excluded from the study due to their clinical profiles (post-DLI aGVHD and late aGVHD onset). Secondly, a validation cohort comprising of both clinical allo-HSCT (n=17) biopsies and normal controls (n=6) was also used to identify any false-positives either due to technical reasons or as a result of cohort heterogeneity and small sample size in the discovery set. The validation set identified miRNAs that retained their significantly different expression levels across the groups. The main aims of this study were as follows;

1. To identify a list of miRNAs that may have significant potential in diagnosing aGVHD severity.
2. To validate the significance of the signature list of miRNAs in clinical skin biopsies, with the overall goal of using the identified miRNAs as diagnostic markers.
3. To predict OS, relapse and NRM using miRNA expression levels in the skin
4. To develop a model showing the interaction between the validated miRNAs with regards to allo-HSCT outcome (GVHD, OS, relapse)

## **4.2 Results**

### ***4.2.1 Global MicroRNA Expression Profile of Cutaneous Biopsies***

#### ***4.2.1.1 Study cohort***

Global miRNA expression profiling was performed on clinical skin biopsies obtained from allo-HSCT patients (n=5) with various overall clinical and skin histopathological aGVHD grades. The overall clinical aGVHD grade was determined in the clinic, taking into account the sum of stages for the three different target organs (skin, gut and liver) as mentioned in Chapter 1, Section 1.1.5. Clinical aGVHD was evaluated based on the NIH consensus. Skin histopathological aGVHD grade was determined by two independent histopathologists who were blinded to the origin of the samples and used Glucksberg criteria (Glucksberg H, 1974). Skin biopsies were collected upon routine examination in the clinic at the time of aGVHD onset (Figure 4.2). Skin biopsies were also obtained from healthy (n=2 males) and plastic surgery volunteers (n=2 females) and used as normal controls. Thus, profiling was performed on a total of nine biopsies. The exclusion criteria included any patient who had been biopsied post-DLI/ had cyclosporine withdrawal/ had received steroids and/or had developed late aGVHD. The patients with classic aGVHD (allo-HSCT to onset  $\leq 100$  days) were only included in the comprehensive profiling analysis.

The characteristics of the five patients used in this investigation are provided in Table 4.2. The group comprised of five male patients with heterogeneous underlying diseases and median age 61 (range: 19-66) who had undergone allo-HSCT (2010-2012). This heterogeneity was regarded as representative of the allo-HSCT clinic. All the patients had received PBSC as the graft. Four patients had reduced conditioning regimens (Fludarabine and Melphalan) while one had myeloablative treatment (total body irradiation and cyclophosphamide). All five patients were in complete remission at the time of transplantation. Median aGVHD onset was 33 days (range: 18-79) post allo-HSCT. All had MUDs except for the youngest patient (19 years old) in this cohort who had a sibling donor and had undergone myeloablative conditioning. Four patients

developed cGVHD 100 days after transplantation, and one patient had died before assessment. None of the patients in this group relapsed.

### Skin Biopsies Collection

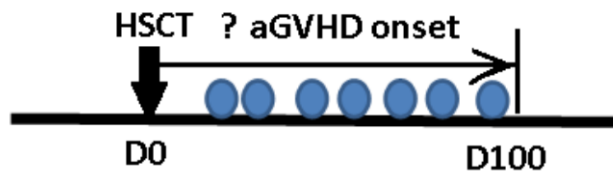


**Figure 4.2** Diagram is showing the time of clinical skin biopsy collection from patient's post- allo-HSCT. Clinical biopsies were collected from patients at the time of query aGVHD onset. Patients with classic aGVHD onset were only included in this investigation. Therefore, the period for biopsy collection was any day post allo-HSCT up to 100 days. D0 was the day that the patients received grafts.

<b>Patient Characteristics</b>	<b>A1292</b>	<b>A2224</b>	<b>A2274</b>	<b>A1300</b>	<b>A2137</b>
Diagnosis	NHL	MDS	ALL	CLL	AML
Patient Age	63	58	19	61	66
Transplant Type	MUD	MUD	SIB	MUD	MUD
Source	PBSC	PBSC	PBSC	PBSC	PBSC
Protocol	Flu Mel	Flu Mel	TBI Cy	Flu Mel	Flu Mel
Campath	60	90	30	60	60
Reduced Intensity Conditioning	Yes	Yes	No	Yes	Yes
Status at Transplant	CR1	CR1	CR1	CR	CR2
CMV Patient	-	+	+	+	-
CMV Donor	-	-	+	+	+
Patient Sex	M	M	M	M	M
Donor Sex	M	F	F	M	M
Skin Histopathological aGVHD grade	2	3	2	1	1
No. of Days from Tx (aGVHD Onset)	23	18	79	76	33
Overall Clinical aGVHD Grade	2	4	2	0	2
Chronic GVHD	N/A	YES	YES	YES	YES
Relapse	No	No	No	No	No

**Table 4.2 Patient characteristics (n=5) for the global miRNA profiling analysis using skin biopsies taken from allo-HSCT patients.** Exiqon miRCURY LNA™ Universal Reverse Transcription miRNA Human Panel I and II were used for the global profiling analysis. Abbreviations:- AML: Acute Myeloid Leukemia, MDS: Myelodysplastic Syndrome, CLL: Chronic Lymphocytic Leukemia, NHL: Non-Hodgkins Lymphoma, ALL: Acute Lymphocytic Leukemia, SIB: Sibling transplant, MUD: Matched Unrelated Donor, PBSC: Peripheral Blood Stem Cells, Flu: Fludarabine, Mel: Melphalan, Alem: Alemtuzumab, CR1: Complete Remission 1, CR2: Complete Remission 2, CR: Complete Remission, CMV: Cytomegalovirus, M: Male, F: Female, +: Positive, -: Negative, CMV: N/A: Not applicable as patient deceased before assessment.

#### **4.2.1.2 Data analyses**

Data were initially analysed based on the overall clinical aGVHD grades, as results from gene expression studies by Norden et al. (unpublished) had shown a significant correlation between these grades and gene expression. Thus, the initial signature list of miRNAs was selected based on the profiling results using the overall clinical aGVHD grades. Since the overall clinical aGVHD grade is the summation of the different stages of the target organs, as mentioned in Chapter 1, Section 1.2.3.1, the data was also analysed based on the skin histopathological aGVHD grade. All validation results presented have been analysed using both grades. Figure 4.3 shows the study design for this Chapter.

Unsupervised hierarchical clustering analysis was performed using RStudio™ Version 0.98.501 (RStudio, Inc., U.S.A). An unsupervised approach allows data to be analysed without prior assumptions, therefore reducing bias. The global profiling results were analysed using one-way ANOVA with Bonferroni multiple-comparison correction on SPSS version 21 (IBM, SPSS Inc, USA). The differential expression of miRNAs in skin biopsies between all groups (normal controls, pre-transplant, grades 0-I and grades II-III/IV) for the validation of the signature miRNA list was determined using Kruskal-Wallis one-way analysis of variance with Dunn's post-hoc test on GraphPad Prism 5 (GraphPad Software, Inc, USA). Significance was set at  $p > 0.05$ . Jonckheere–Terpstra test (SPSS version 21) was also performed for the miRNAs in the signature list to test for trends in the expression levels for aGVHD severity. Generalised Linear models (Ordinal logistic regression) were run to find the main effects and interactions between miRNAs in the signature list SPSS version 21 (IBM, SPSS Inc, USA). Rotational 3D scatterplots were generated using JMP®, Version 11 (SAS Institute Inc., Cary, NC, 1989-2007).

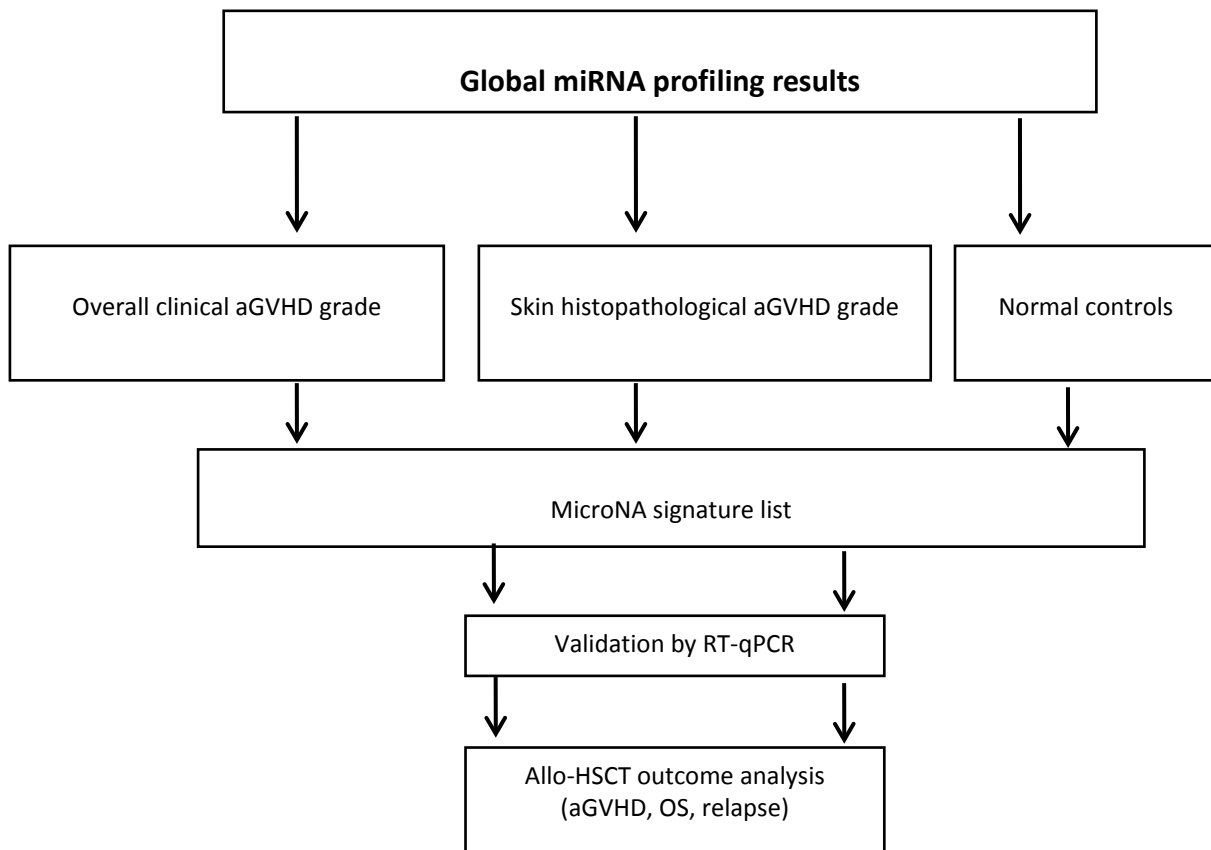


**Figure 4.3 Chapter 4 study design.** Global miRNA profiling was performed initially and then miRNA expressions were analysed based on the overall clinical and the skin histopathological aGVHD grades. A miRNA signature list was then derived based on the significant differences between the diseased skin biopsies and controls which included biopsies from normal individuals and plastic surgery patients. The signature list was validated by RT-qPCR and results were again analysed based on the two grading systems mentioned above for the aGVHD outcome study. MicroRNA expression results from the signature list were also used for relationship (interaction) analysis and survival outcome predictions.

#### **4.2.1.3 Grading system for determination of miRNA signature list**

Global miRNA profiling was performed, using the Exiqon miRCURY LNA qPCR human panels I and II. The aim was to identify a potential set of miRNAs significantly associated with aGVHD onset and severity. The expressions of 739 miRNAs present on human panels I and II were studied in total RNA extracted from skin biopsies of patients with various aGVHD grades (n=5) and also in normal skin biopsies (n=4) that were used as controls. Of the 739 miRNAs assessed, 186 were detectable in all the samples in this cohort. For statistical calculations, 245 miRNAs with expressions in at least three skin biopsies per group were included ( $C_q < 35$ ). The mean of the 186 detected miRNAs ( $C_q < 31$ ) was used to normalize individual assay expression. As mentioned earlier, multiple analyses were performed on the global profiling data to select the signature list for further validation by RT-qPCR. Two analyses were performed to determine the differentially expressed miRNAs; (1) using overall clinical aGVHD grades and (2) using skin histopathological grades. Interestingly, miR-34a-5p and miR-142-3p were identified as differentially expressed using either approach.

#### 4.2.1.4 Overall clinical aGVHD grade does not correlate with histopathological grade

The overall clinical aGVHD and histopathological grade of the skin were also used to determine the correlation between the two grading systems (Figure 4.4, A). Results corroborated with the literature, and no significant correlation was observed ( $r_s=0.50$ ,  $p=0.083$ ). Similarly, correlation between grading of the same skin biopsy by two independent histopathologists was evaluated (Figure 4.4., B). Results showed a significant positive correlation between the two histopathologists ( $r_s=0.77$ ,  $p=0.000$ ). Therefore, the consensus skin histopathological grade was used for further investigations.

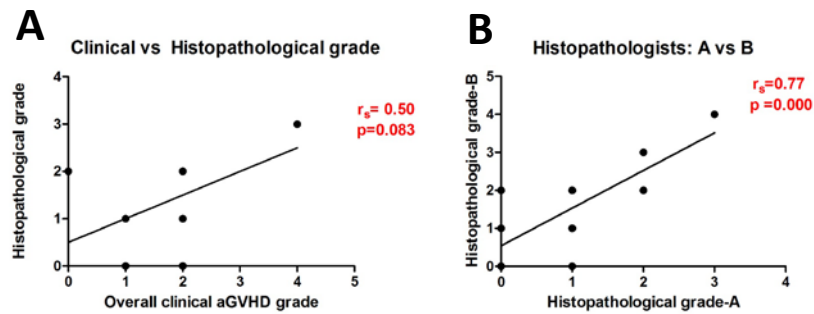


**Figure 4.4 Correlation of aGVHD grades in clinical skin biopsies from allo-HSCT patients.** (A) No significant correlation between the overall clinical aGVHD grade of the patient and the histopathological grade of the skin biopsy (B) Significant correlation between the grading of the same skin biopsy by two independent histopathologists ( $p=0.000$ ). The p-values ( $p$ ) were calculated by Spearman correlation. Simple linear regression is shown by the line of best fit.  $r_s$ : Spearman's rho.

#### **4.2.1.5 *Distinct microRNA expression clusters exist between post allo-HSCT and normal skin biopsies***

MicroRNAs (rows) and skin biopsies (columns) with similar expression values were grouped by performing the hierarchical clustering. As mentioned earlier, an unsupervised approach was employed to perform the hierarchical clustering, as it is assumption-free and aids in identifying under-expressed miRNAs. The top 50 miRNAs that were expressed in all the skin biopsies (n=9), including the normal controls with the highest standard deviation were selected for the analysis. MicroRNA expression in skin biopsies collected from post allo-HSCT patients (n=5) and normal controls (n=4) was used to plot the dendrogram (Figure 4.5) and heat-map (Figure 4.6). The dendrogram shows a clear segregation of the skin biopsies into two distinct clusters; the normal in one branch and the allo-HSCT group in the other. Interestingly, miRNA expression profiles within the normal cluster were highly dissimilar, as shown by the height of the branches. This is unlike the miRNA expression profile in the post allo-HSCT cluster which was highly similar. The heat-map shows three distinct expression regions. Highly up-regulated miRNAs cluster in the first-top section and the down-regulated miRNAs in the lower section of the heat map. MiR-720 was expressed consistently high in all the nine skin biopsies. MiR-34a-5p expression was distinctly different between normal and allo-HSCT group. MiR-451-5p is expressed highly in erythrocytes and its levels were highly variable in all the skin biopsies.

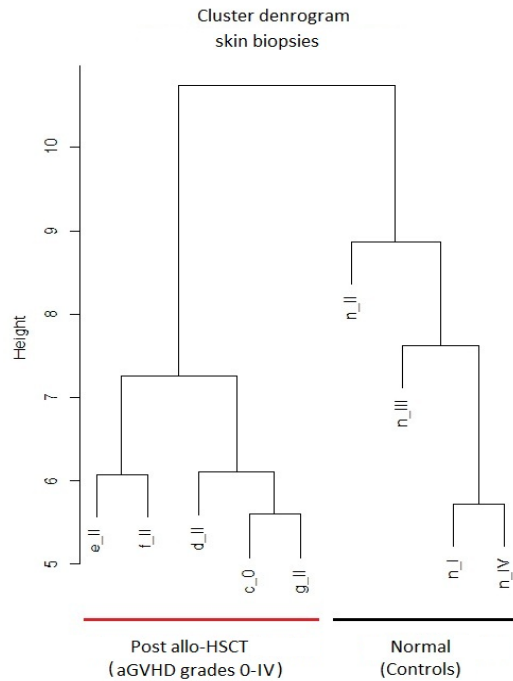


**Figure 4.5** Dendrogram shows two distinct clusters, one consisting of the post allo-HSCT skin biopsies and the other normal controls. The post allo-HSCT patients had a distinct expression profile separating them from that of normal skin biopsies. The height on the y-axis shows the distance that represents dissimilarity between the observations. The x-axis shows the nodes that represent the individual patients/healthy volunteers. RStudio™ was used to plot the dendrogram.

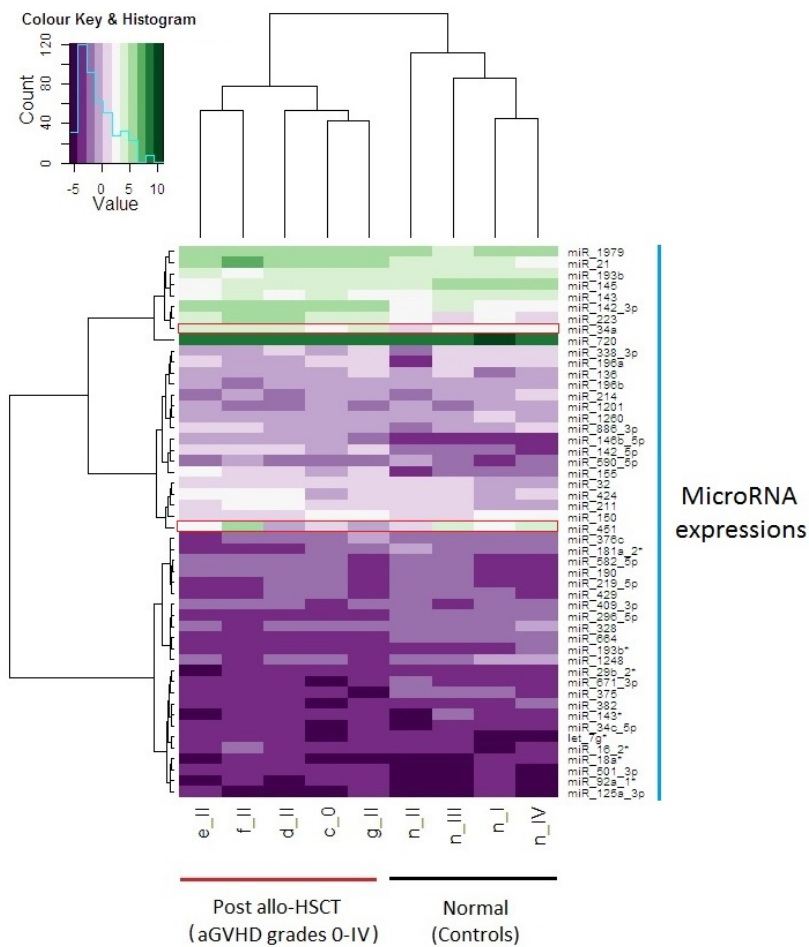


**Figure 4.6 Heat map showed three distinct miRNA expression levels.** Unsupervised hierarchical clustering was performed using the expression levels from all the 186 detectable miRNAs in the total investigation cohort (n=9). The top 50 miRNAs that were expressed in all 9 samples. The dendrogram on the left shows that there are three distinct miRNA clusters based on the expression values in each row. The horizontal scale of the dendrogram shows the distance that represents dissimilarity between the clusters. There is dissimilarity between two of the miRNA clusters [overexpressed (green) to intermediate (light purple) and under-expressed (dark purple)]. The dendrogram on the top shows the clustering of the samples as in Figure 4.5. Normalized  $\log_2$  values were used for this analysis. The average linkage method was used for the unsupervised hierarchical clustering of the normalized expression results. The histogram represents under-expressed (dark purple) to over-expressed (green) miRNAs in all samples. Fold change range is from -5 to 10. Each row is representative of one miRNA and each column represents one sample.

## **4.2.2 Comparisons Using Overall Clinical aGVHD Grades**

### **4.2.2.1 MicroRNA signature list identified using overall clinical aGVHD grades**

Clinical skin biopsies were categorised based on their overall clinical aGVHD grades. There was only one patient without aGVHD (grade 0), three with aGVHD grades II and one with aGVHD grade IV. Thus, the miRNA expression levels in four of the patients (grades II-IV) and normal controls (n=4) were used to perform one-way ANOVA to identify a signature list of miRNAs for further validation by RT-qPCR. Fourteen miRNAs were identified as differentially expressed between normal and aGVHD grades II-IV (Table 4.3). Out of these 14 miRNAs, the expression of only four miRNAs (miR-142-3p, miR-142-5p, miR-155-5p and miR-34a-5p) met the Bonferroni correction p-value ( $p \leq 0.0002$ ). The four miRNAs were over-expressed in the allo-HSCT skin biopsies in comparison to the expression in normal skin biopsies. This corrected p-value was calculated in order to rule out false positives.

MicroRNAs	p-value	aGVHD grades II-IV (Mean expression)	Normal (Mean expression)
hsa-miR-142-3p	<u><b>0.00002</b></u>	5.60	2.95
hsa-miR-142-5p	<u><b>0.00005</b></u>	0.57	-2.41
hsa-miR-155-5p	<u><b>0.00013</b></u>	1.66	-2.19
hsa-miR-34a-5p	<u><b>0.00016</b></u>	3.67	1.97
hsa-miR-21-3p	0.0003	-1.10	-4.29
hsa-miR-21-5p	0.00043	6.20	3.69
hsa-miR-181c-5p	0.00052	-4.91	-3.67
hsa-miR-503-5p	0.00056	-1.19	-5.49
hsa-let-7c-5p	0.00061	1.49	2.41
hsa-miR-223-5p	0.00073	4.92	2.03
hsa-miR-23b-3p	0.00082	4.69	5.32
hsa-miR-146b-5p	0.00094	-0.73	-3.11
hsa-miR-125b-5p	0.00146	4.92	6.13
hsa-miR-365a-3p	0.00166	2.03	2.83

**Table 4.3** Fourteen miRNAs were identified as differentially expressed between skin biopsies from allo-HSCT patients with overall clinical aGVHD grades II-IV compared to normal controls. MiR-142-3p, miR-142-5p, miR-155-5p and miR-34a-5p were the only miRNAs that met the Bonferroni corrected p-value. All the four miRNAs were over-expressed in the allo-HSCT skin biopsies in comparison to the expression in normal biopsies. One way-ANOVA was performed to determine the significant difference. Bonferroni corrected p-value was calculated ( $p \leq 0.0002$ ). Mean expression value per group was calculated using the miRNA expression levels of all the samples in that group. MicroRNA p-values that met the Bonferroni correction value are underlined, in bold.

### 4.2.3 Comparisons Using Skin Histopathological aGVHD Grades

#### 4.2.3.1 MicroRNA signature list was determined using the skin histopathological aGVHD grades

The skin biopsies were also categorized on the basis of cutaneous histopathological grades. The initial one-way ANOVA with two groups (Grades I-III vs Normal) showed that only miR-142-3p and its other strand, miR-142-5p, met the Bonferroni corrected p-value ( $p \leq 0.0002$ ) (Table 4.4). Both miRNAs were over-expressed in the allo-HSCT skin biopsies.

MicroRNAs	p-value	aGVHD grades II-IV (Mean expression)	Normal (Mean expression)
hsa-miR-142-3p	<b><u>0.00005</u></b>	5.48	2.95
hsa-miR-142-5p	<b><u>0.00020</u></b>	0.47	-2.41
hsa-miR-34a-5p	0.00073	3.49	1.98
hsa-miR-21-3p	0.00114	-1.27	-4.29
hsa-miR-223-5p	0.00141	4.874	2.0325
hsa-miR-21-5p	0.00189	6.08	3.70
hsa-miR-146b-5p	0.00250	-0.77	-3.11
hsa-miR-328-5p	0.00411	-2.36	-1.37
hsa-miR-155-5p	0.00418	1.238	-2.1875
hsa-miR-664-5p	0.00484	-3.19	-2.37
hsa-miR-503-5p	0.00513	-1.74	-5.49
hsa-let-7c-5p	0.00659	1.59	2.41

**Table 4.4 Twelve microRNAs were differentially expressed between skin biopsies from allo-HSCT patients with skin histopathological aGVHD grades I-III and normal controls.** MiR-142-3p and its other strand, miR-142-5p were the only miRNAs that met the Bonferroni correct p-value. Both miRNAs were over-expressed in the allo-HSCT skin biopsies in comparison to the normal skin. One way-ANOVA was performed to determine the significant difference. Bonferroni multiple testing corrected p-value was calculated ( $p \leq 0.0002$ ). Mean expression value per group was calculated using the miRNA expression levels of all the samples in that group. MicroRNA p-values that met the Bonferroni correction value are underlined, in bold

Skin histopathological grading allowed the segregation of the five skin biopsies into two groups (Grade I (n=2) and Grades II-III (n=3)). Therefore, multiple comparisons were possible (Grade I vs Grade II-III vs Normal). None of the miRNAs met the Bonferroni post-hoc adjusted p-value ( $p \leq 0.0002$ ) in any of the comparison groups (Table 4.5). Since, the miRNAs and the samples were independent it was justifiable to

not use the Bonferroni post-hoc and set significance value at  $p \leq 0.05$ . Ten miRNAs were observed as significantly differentially expressed between normal and aGVHD Grade I skin biopsies (miR-142-3p/-5p, miR-21-3p/-5p, miR-223-5p, miR-146b-5p, miR-34a-5p, miR-125b-5p, miR-155-5p and let-7c-5p). Likewise, nine miRNAs were also significantly differentially expressed between Normal and aGVHD Grades II-III (miR-142-3p/-5p, miR-34a-5p, miR-21-3p/-5p, miR-223-5p, miR-328-5p, miR-146b-5p and miR-664-5p). However, none of the miRNAs were differentially expressed between aGVHD grade I and Grades II-III. Venn diagrams were generated to identify the common as well as the unique miRNAs between the three groups (Figure 4.7). Six miRNAs (MiR-181c-5p, miR-23b-3p, miR-328-5p, miR-365a-3p, miR-503-5p and miR-664-5p) were unique to the comparison between normal and aGVHD Grades II-III while none were only unique to the normal and aGVHD Grades I.

Normal vs Grade I		Normal vs Grades II-III		Grade I vs Grades II-III	
MicroRNA	p-value	MicroRNA	p-value	MicroRNA	p-value
miR-142-3p	0.0004	miR-142-3p	0.0001	miR-34a-5p	0.151
miR-142-5p	0.001	miR-142-5p	0.0003	miR-503-5p	0.213
miR-21-3p	0.008	miR-34a-5p	0.001	miR-664-5p	0.3072
miR-223-5p	0.009	miR-21-3p	0.002	miR-23b-3p	0.389
miR-21-5p	0.0092	miR-223-5p	0.0021	miR-142-3p	0.41
miR-146b-5p	0.0093	miR-21-5p	0.0031	miR-328-5p	0.4566
miR-34a-5p	0.017	miR-328-5p	0.0046	miR-365-3p	0.82
miR-125b-5p	0.0236	miR-146b-5p	0.0048	let-7c-5p	1
miR-155-5p	0.03	miR-664-5p	0.0051	miR-21-3p	1
let-7c-5p	0.053	miR-155-5p	0.0056	miR-155-5p	1
miR-328-5p	0.0619	miR-503-5p	0.006	miR-21-5p	1
miR-181c-5p	0.0726	let-7c-5p	0.008	miR-142-5p	1
miR-503-5p	0.083	miR-125b-5p	0.0124	miR-181c-5p	1
miR-664-5p	0.1049	miR-23b-3p	0.019	miR-146b-5p	1
miR-23b-3p	0.38	miR-181c-5p	0.031	miR-223-5p	1
miR-365-3p	0.428	miR-365-3p	0.046	miR-125b-5p	1

**Table 4.5** MicroRNAs differentially expressed between skin biopsies from allo-HSCT patients with grades I, grades II-III and normal controls. Histopathological grades were used for the grouping of one way-ANOVA.

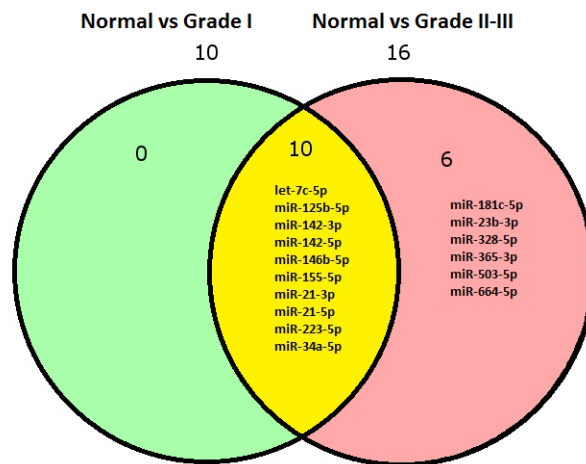


**Figure 4.7** Venn diagram showed the differentially expressed miRNAs between normal controls vs Grade I and Grades II-III. Six miRNAs were unique to the comparison between normal and aGVHD Grades II-III. None of the miRNAs were unique to the normal vs aGVHD grade I only. The skin biopsies were all categorised based on the skin histopathological aGVHD grade. Ten miRNAs (let-7c-5p, miR-125b-5p, miR-142-3p, miR-142-5p, miR-146b-5p, miR-155-5p, miR-21-3p, miR-21-5p, miR-223-5p and miR-34a-5p) were common between normal versus Grades I-III. The Venn diagram was generated using the miRNAs that had  $p \leq 0.05$  from the comparison in table 4.5. The available online software was used to generate the Venn diagrams (<http://www.bioinformatics.lu/venn.php>).

Eight miRNAs (MiR-503-5p, miR-21-3p, miR-34a-5p, let-7c-5p, miR-142-3p, miR-365a-3p, miR-23b-3p and miR-24-3p) were selected for further validation by RT-qPCR, based on their differential expression levels between normal and aGVHD groups when either the overall clinical aGVHD or skin histopathological grades were used for categorisation and analysis. Normalized mean miRNA expression levels across all the three groups when skin histopathological grades were used are presented in Table 4.6. From the calculated fold-changes it was noted that miR-34a-5p, miR-503-5p, miR-21-3p and miR-142-3p expression were up-regulated in all the skin biopsies post allo-HSCT, independent of the aGVHD grade when compared to the normal controls. Similarly, Let-7c-5p fold-change was lower in the post allo-HSCT skin biopsies in comparison to the normal controls. Interestingly, miR-503-5p expression was more highly expressed in the aGVHD grades II-III when compared to grade I (Figure 4.8). The

expression levels of miR-24-3p and miR-365a-3p were approximately constant in all the nine skin biopsies, regardless of aGVHD or normal status.

MicroRNAs	Mean expression (LOG <sub>2</sub> RQ)		
	Grade I	Grades II-III	Normal
miR-34a-5p	3.08	3.76	1.97
miR-503-5p	-2.9	-0.97	-5.49
let-7c-5p	1.72	1.5	2.41
miR-142-3p	5.2	5.67	2.94
miR-365a-3p	2.38	2.04	2.83
miR-23b-3p	5	4.67	5.31
miR-24-3p	6.58	6.35	6.76
miR-21-3p	-1.6	-1.05	-4.29

**Table 4.6 Normalized mean miRNA expression values across skin biopsies with skin histopathological Grades I, II-III and normal controls.** MicroRNA expression levels were all log<sub>2</sub> transformed. Mean expression per group (Grade I, Grade II-III and Normal) was calculated using the log<sub>2</sub> values of all the samples in that group.

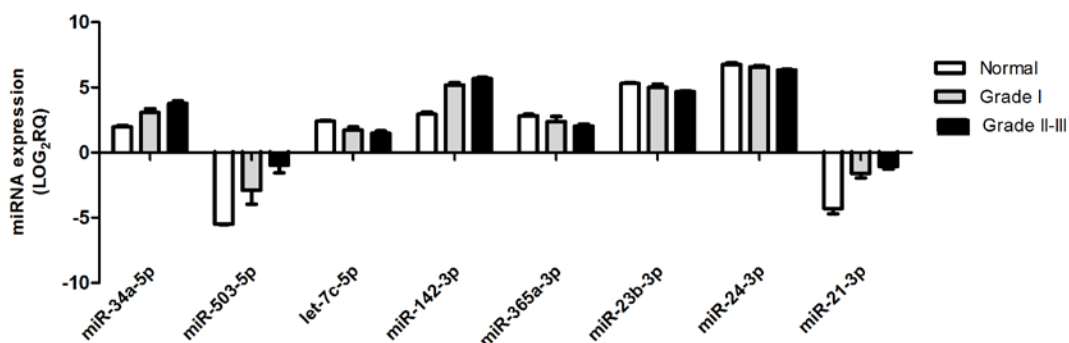


**Figure 4.8 MicroRNAs were differentially expressed across skin biopsies with skin histopathological grades I, II-III and normal controls.** MicroRNA expression results were all log<sub>2</sub> transformed. Each bar represents mean with SEM.

#### **4.2.3.2 Five of the miRNAs selected for further validation were predicted to target the 18 genes**

As mentioned in Chapter 1, there are numerous miRNA online databases that aid the prediction of miRNAs target genes and *vice versa*. The online database miRwalk (Dweep *et al.*, 2011) can retrieve both validated and predicted miRNA and gene targets from multiple databases (miRanda, miRDB, miRWalk, RNA22 and Targetscan). Since each of the databases are created based on their unique algorithms and seed sequence matching (between the miRNA and its targets), retrieval from multiple databases can increase the prediction accuracy. Thus, miRwalk was used to predict miRNAs that could target the 18 genes analysed in Chapter 3 (*ANP32A, C1qTNF7, CARD11, CEACAM4, CXCL9, HCLS1, HTRA1, LGALS7, LST1, MSR1, PIK3AP1, PSTPIP1, PTGER2, PTPN7, TAP1, TGM2, TREM2 and UBD*). MicroRNAs predicted by at least three databases were selected. The list was further refined by only selecting miRNAs that were in the signature miRNA list. These miRNAs were then used to generate a Venn diagram to identify common and unique genes from the list. Results showed that *MSR1* and *TGM2* were predicted to be targeted by at least three of the miRNAs in the further validation study (Figure 4.9). Interestingly, miR-200b was also predicted to target four of the patented genes (*MSR1, CXCL9, C1QTNF7* and *PTGER2*).

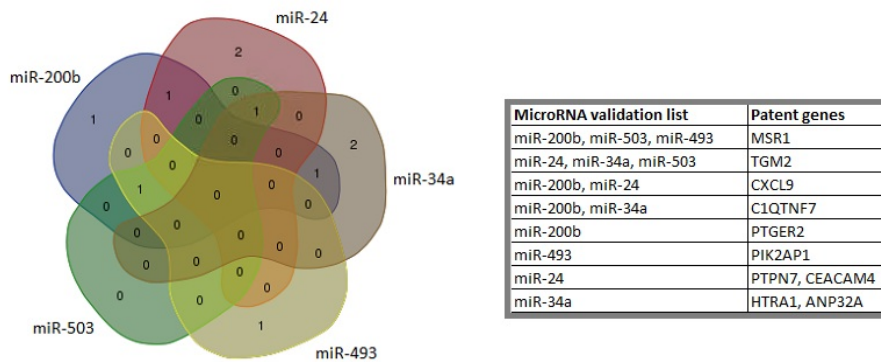


**Figure 4.9** Five miRNAs from the validation list were predicted to target the 18 genes (patent genes). The online database miRwalk (Dweep *et al.*, 2011) was used to perform the prediction analysis of miRNA target genes. The Venn diagram shows the number of common and unique genes that are predicted as targets per miRNA. The table on the right shows the miRNA genes. The Venn diagram was generated using an online program (<http://bioinformatics.psb.ugent.be/webtools/Venn/>).

#### **4.2.3.3 Twelve microRNAs were selected for further validation**

In summary, 12 miRNAs were selected for further validation by RT-qPCR. Eight miRNAs (miR-142-3p, miR-34a-5p, miR-503-5p, let-7c-5p, miR-21-3p, miR-365a-3p, miR-23b-3p and miR-24-3p) were selected based on their significant differential expression across the three groups (normal vs grade I vs grade II-III/IV) taking into consideration the two separate analyses performed using the two grades (overall clinical and skin histopathological grades). Two additional miRNAs (miR-2110 and miR-493-3p) were also included, because expression was only detected in the skin biopsies with overall clinical aGVHD grades II-IV and not in normal controls. A further miRNA, miR-200b-3p was also selected because of its known expression in epidermal homeostasis (Banerjee *et al.*, 2011). In the present experiment, miR-200b-3p expression was observed in the normal controls and only one aGVHD grade II skin biopsy. Therefore, it was considered biologically interesting to assess the expression of miR-2110, miR-493-3p and miR-200b-3p in order to evaluate whether these results were true positives or a technical error. Since miR-34a-5p expression was significantly over-expressed it was deemed biologically valuable to investigate its other strand miR-34a-3p in the same skin biopsies. MiR-155-5p and miR-155-3p were also investigated separately by Norden *et al* (unpublished data). MiR-21-5p and miR-125b-5p were not selected for further validation as they had been investigated previously (unpublished data) and no significant differential expression was observed between patients with and without aGVHD.

#### **4.2.4 Real-Time PCR based microRNA arrays and individual RT-qPCR assays agreed with each other**

Concordance between the RT-qPCR array and the individual RT-qPCR assays was evaluated using Bland-Altman method to measure agreement and Spearman's rho ( $r_s$ ) to assess correlation (Figure 4.10). In brief, for the qPCR array, normalization was carried out using the mean of the 186 detectable miRNAs while for the RT-qPCR results, the geometric mean of miR-103-3p and SNORD48 were used (see Chapter 2, Section 2.6.2). For Bland-Altman analysis the two methods agreed if the bias between them was equal to or less than one as this equated to less than one RT-qPCR cycle difference. For correlation, significance was set at  $p < 0.05$  and trend to significant set at  $p < 0.10$ . Only eight of the 12 miRNAs that were selected on the basis of their differential expression levels were included in this method comparison analysis. The additional four miRNAs were not assessed as either their expression was  $C_q \leq 35$  or absent from the array. MiR-24-3p expression was not included as its levels were detected using Taqman and not LNA chemistry.

In this analysis, results showed that the two RT-qPCR based methods agreed with each other for seven miRNAs (miR-503-5p, miR-23b-3p, 34a-5p/-3p, miR-142-3p, miR-365a-3p and let-7c-5p). The bias for miR-21-3p expression was greater than one so there was no statistical agreement between the two methods for this miRNA (Figure 4.10, E). The expression of only one miRNA (miR-142-3p) significantly correlated between the two RT-qPCR methods (Figure 4.10, F). The lack of correlation between the two methods showed that the detection methods are independent of each other.

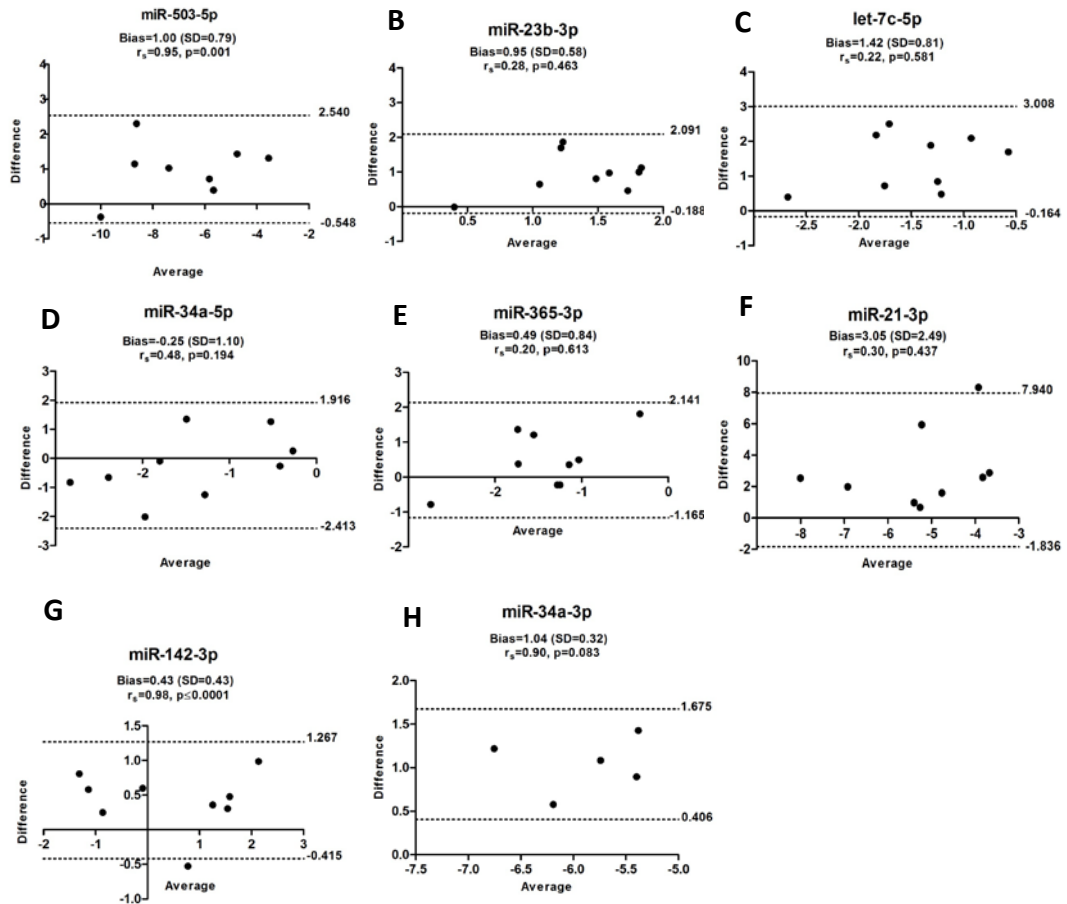


**Figure 4.10 Bland-Altman plots for the two RT-qPCR based methods.** (A) miR-503-5p, (B) miR-23b-3p, (C) let-7c-5p (D) miR-34a-5p, (E) miR-365-3p, (F) miR-21-3p, (G) miR-142-3p and (H) miR-34a-3p, expressions. The expression of seven miRNAs agreed between the two methods (plots: A, B, C, D, E, G and H). Correlation was only observed for miR-142-3p (plot G). Bias is the mean difference. Dashed lines show the 95% lower and upper limits of agreement. SD: Standard deviation. Correlation was assessed by Spearman rho ( $r_s$ ). Significance ( $p$ ) was set at  $p<0.05$  and trend to significant set at  $p<0.10$ . All results were  $\log_2$  transformed.

## **4.2.5 Validation of the Signature MicroRNA List**

### **4.2.5.1 Study cohort**

Skin biopsies were collected from patients (n=17) post-allo-HSCT during 2010-2012. These biopsies were taken before patients had received DLI and/or steroids (Figure 4.11). The biopsies were taken when the patients were free of viral infections and/or other underlying skin diseases such as psoriasis and eczema. In addition, in this validation study skin biopsies were also collected from patients prior to undergoing the allo-HSCT procedure. These skin biopsies were collected ideally seven days pre-transplant before the initiation of the conditioning regimen.

Patient characteristics for all the 17 patients used in this investigation are provided in Table 4.7. The cohort comprised of three females and 14 males. The median age was 47 years (range: 19-65). Only one patient had bone marrow infusion while the rest (n=16) had PBSC for graft infusion. Three patients had undergone total body irradiation. The patients with classic aGVHD were only included in the validation cohort. Median aGVHD onset was 23 days (range: 13-98) post allo-HSCT. When patients were categorized based on their overall clinical aGVHD grades, 41.2% had aGVHD grades 0-I (n=7) while 58.8% had been diagnosed with aGVHD grades II-IV (n=10). For histopathological aGVHD grading, the skin parameters are only considered as mentioned in Chapter 1. Thus, in this cohort 58.8% were diagnosed with grades 0-I skin histopathological aGVHD grade in contrast to 41.2% with grades II-III. In this cohort, 52.9% had developed cGVHD (no cGVHD: 23.5% and unassessed: 23.5%). In all, 29.4% of the patients had relapsed and 47.1% had died post allo-HSCT.



**Figure 4.11** Diagram showing the time of clinical skin biopsy collection from patient post allo-HSCT. Clinical biopsies were collected from patients at the time of query aGVHD onset. Patients with classic aGVHD onset were only included in this investigation. Therefore, the time period for biopsy collection was any day from the day of graft infusion up to 100 days post allo-HSCT. Skin biopsies were also collected from the patients at approximately seven days pre-transplant (Pre-Tx). D0 is the day that the patients had graft infusion.

Cohort Characteristics		aGVHD Histopathological Grades				Difference (p-value)
		0-I		II-III		
		No.	%	No.	%	
Patient age (median years)		47 (19-65)				1.000
Patient gender	Female	2	6.7	1	3.3	1.000
	Male	8	5.7	6	4.3	
Donor gender	Female	3	6.0	2	4.0	1.000
	Male	7	6.4	4	3.6	
Graft source	BM	1	10.0	0	0.0	1.000
	PBSC	9	5.6	7	4.4	
Underlying Disease	ALL	1	5.0	1	5.0	0.907
	AML	1	3.3	2	6.7	
	MDS	3	7.5	1	2.5	
	MF	0	0.0	1	10.0	
	NHL	3	6.0	2	4.0	
	CLL	1	10.0	0	0.0	
	MM	1	10.0	0	0.0	
Regimen	Myeloablative	1	3.3	2	6.7	0.537
	RIC	9	6.4	5	3.6	
Protocol	Cy TBI Alem	1	3.3	2	6.7	0.481
	Flu Bus Alem	1	3.3	2	6.7	
	Flu Mel Alem	8	7.3	3	2.7	
Campath	30 mg	3	6.0	2	4.0	1.000
	60 mg	6	6.0	4	4.0	
	90 mg	1	5.0	1	5.0	
Relationship	SIB	2	5.0	2	5.0	1.000
	MUD	8	6.2	5	3.9	
Patient CMV status	Negative	3	5.0	3	5.0	1.000
	Positive	6	6.0	4	4.0	
Donor CMV status	Negative	6	6.0	4	4.0	1.000
	Positive	3	5.0	3	5.0	
HLA class I compatibility	None	8	6.7	4	3.3	0.593
	One	2	4.0	3	6.0	
HLA class II compatibility	None	3	5.0	3	5.0	0.219
	One	3	4.3	4	5.7	
	Two	4	10.0	0	0.0	
Survival status	Alive	7	7.8	2	2.2	0.153
	Dead	3	3.8	5	6.3	
Relapse status	No	6	5.5	5	4.6	0.588
	Yes	4	8.0	1	2.0	
Disease status at Transplant	CR	1	10.0	0	0.0	0.394
	CR1	2	3.3	4	6.7	
	CR2	4	8.0	1	2.0	
	PR	1	3.3	2	6.7	

**Table 4.7 Patient characteristics for the validation of the miRNA signature list.**

Histopathological aGVHD grades were used for this grouping. Fisher's exact test was used to estimate the difference in frequencies between the aGVHD groups. Abbreviations:- BM: Bone marrow, PBSC: Peripheral blood stem cells, ALL: Acute lymphocytic leukaemia, AML: Acute myeloid leukaemia, CLL: Chronic lymphocytic leukaemia, MDS: Myelodysplastic syndrome, MM: Multiple myeloma, MPS: Multiple proliferative syndrome, NHL: Non-Hodgkin's lymphoma, RIC: Reduced intensity conditioning, Flu: Fludarabine, Mel: Melphalan, Bus: Busulfan, Cy: Cytrabine, TBI: Total body irradiation, Alem: Alemtuzumab, CsA: Cyclosporine, CMV: Cytomegalovirus, CR (1-3) Complete remission, PR: Progression, SIB: Sibling, MUD: Matched unrelated donor.

#### **4.2.5.2 Data analyses**

From the miRNA profiling investigation by RT-qPCR array, 12 miRNAs (miR-503-5p, let-7c, miR-365a-3p, miR-23b, miR-21-3p, miR-24-3p, miR-34a-5p/-3p, miR-142-3p, miR-493-5p, miR-200b-3p, and miR-2110) that were differentially expressed between the aGVHD skin biopsies and normal controls were selected for further validation. Normfinder was used to determine the most suitable miRNA for normalization of the validation data. MiR-103-3p was identified as the most suitable endogenous control. SNORD48 was also selected as the second endogenous control, as results from previous studies (unpublished data) had shown that this small nucleolar RNA has a stable expression profile across all skin specimens. Therefore, the geometric mean of the two endogenous controls was calculated for normalization of the expression results (see Chapter 2, Section 2.6.2). Taqman miRNA expression assays were used for the validation of miR-493, miR-200b, miR-24 and miR-2110 and Exiqon LNA miRNA assays for miR-503-5p, let-7c-5p, miR-365a-3p, miR-23b-3p, miR-21-3p, miR-142-3p, miR-34a-5p/-3p (see Chapter 2, Section 2.4.2, for explanation on the different chemistries between Taqman and LNA). These two different chemistries were used because the dissociation curves showed non-specific binding of the LNA primers for miR-493-3p and miR-24-3p as explained in Chapter 2 (Section 2.5.2).

#### **4.2.5.3 Five miRNAs were significantly differentially expressed between pre- and post allo-HSCT skin biopsies independent of aGVHD grading system**

The validation cohort was analysed separately using the overall clinical aGVHD grades (n=16) and the skin histopathological grade (n=17). One of the skin biopsies had no overall clinical aGVHD grade and was eliminated when the grouping was based on the clinical grade, hence n=16 for this group. Results showed that five miRNAs (let-7c-5p, miR-503-5p, and miR-365a-3p and miR-34a-5p /-3p) were significantly differentially expressed across all the four groups. The expression level of miR-365a-3p could be reduced as a consequence of the transplant procedure, regardless of the grading system. However, seven of the miRNAs (miR-493-3p, miR-142-3p, miR-21-3p, miR-24-

3p, miR-2110, miR-200b-3p and miR-23b-3p) did not retain their significance in this validation study (results presented in Appendix I, Figure 1).

#### **4.2.5.4 *Let-7c-5p, miR-503-5p and miR-365a-3p were differentially expressed in the skin biopsies post allo-HSCT***

Let-7c-5p, miR-503-5p and miR-365a-3p were all measured in the validation cohort using both the overall clinical aGVHD grades and the skin histopathological grade (Figure 4.12). Overall, let-7c-5p was differentially expressed across the different groups (Overall clinical aGVHD grade:  $p=0.013$ , Skin histopathological grade:  $p=0.037$ ). There was also a significant down-regulation in the pre-transplant biopsies in comparison to the normal controls ( $p<0.05$ ). Significant differential expression between pre-transplant biopsies and aGVHD grades II-IV was only observed when the overall clinical aGVHD grades were used for analysis ( $p<0.05$ ) (Figure 4.12, A and B). Similarly, miR-503-5p showed significant variation among normal controls, pre-transplant and post-allo-HSCT patients (Overall clinical aGVHD grade:  $p=0.042$ , Skin histopathological grade:  $p=0.021$ ) (Figure 4.12, C and D). However, miR-503-5p expression was only up-regulated in aGVHD patients in comparison to the pre-transplant group ( $p=0.021$ ) when the skin histopathological grades were used for analysis (Figure 4.12, D). Interestingly, miR-365a-3p was differentially expressed across all patient and normal group (Overall clinical aGVHD grade:  $p=0.016$ , Skin histopathological grade:  $p=0.015$ , Figure 4.12, E and F). When the overall clinical aGVHD grades were used, significant down-regulation of miR-365a-3p was observed between patients assessed with aGVHD grades II-IV in comparison to those pre-transplant ( $p<0.05$ ) (Figure 4.12, E). However, when the skin histopathological grades were used for analysis, miR-365a-3p was down-regulated in grade 0-I in comparison to the pre-transplant cohort ( $p<0.05$ ) (Figure 4.12, F).

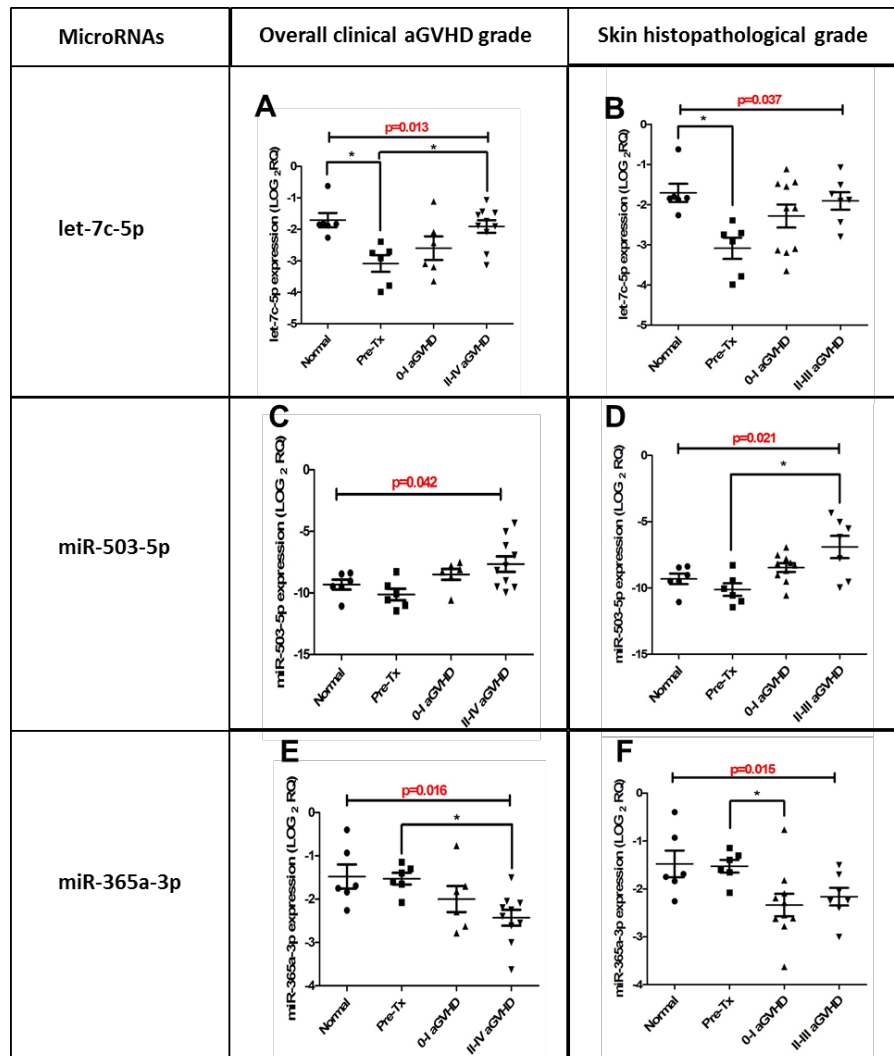


**Figure 4.12 Let-7c-5p, miR-503-5p and miR-365a-3p validated in skin biopsies.** MicroRNA expression results for (A, B) let-7c-5p, (C, D) miR-503-5p and (E, F) miR-365a-3p were used to perform analyses on the basis of overall clinical aGVHD grade (n=16) and the skin histopathological grade (n=17). Compared to pre-transplantation, significant overexpression was observed in let-7c-5p and miR-503-5p in the post allo-HSCT skin biopsies independent of the grading system used. MiR-365a-3p expression was down-regulated in post allo-HSCT skin biopsies compared to pre-transplantation. Kruskal-Wallis analysis of variance was used to determine the significance set at  $p \leq 0.05$  (\*). Scatter-plots show the mean and SEM. Each row shows the expression for a specific miRNA across all the skin biopsies. Each column shows the grading system used to perform the categorization of the skin biopsies. Normal: normal controls, Pre-Tx: Pre-transplant.

#### **4.2.5.5 *MiR-34a-5p was over-expressed post allo-HSCT and its expression positively correlated with miR-34a-3p expression in the skin biopsies***

Expression of miR-34a-5p was also investigated in the validation cohort (n=17). Interestingly, miR-34a-5p was differentially expressed across all groups in the cohort (overall clinical aGVHD grade:  $p=0.0006$ , skin histopathological grade:  $p=0.0005$ ). Data analyses using overall clinical aGVHD and histopathological grades demonstrated that miR-34a-5p was significantly up-regulated post allo-HSCT regardless of aGVHD grade ( $p<0.01$ ) (Figure 4.13).

Since recent literature on miRNA expression highlights that the passenger strand may not be degraded but may function independently; expression of miR-34a-3p was also investigated in the same cohort. Results showed that miR-34a-3p was expressed and not completely degraded in the skin biopsies. However, the mean miR-34a-5p expression (mean  $C_q=27.898$ ) was higher than miR-34a-3p (mean  $C_q=32.362$ ). It was also evident that miR-34a-3p expression was significantly varied across all groups in the cohort (overall clinical aGVHD grade:  $p=0.007$ , skin histopathological grade:  $p=0.013$ ). Based on the overall clinical aGVHD grade, miR-34a-3p was significantly up-regulated in the cohort with 0-I aGVHD in comparison to both normal and pre-transplant skin biopsies ( $p<0.05$ ) (Figure 4.13, C). No significant differential expression of miR-34a-3p was observed when the skin histopathological grades were used for analysis (Figure 4.13, D).

Therefore, correlation in miRNA expression was evaluated between miR-34a-5p and miR-34a-3p (Figure 4.13, E). Results demonstrated that the expression of miR-34a-5p and miR-34a-3p was significantly positively correlated in skin biopsies in this cohort ( $r_s=0.496$ ,  $p=0.006$ ).

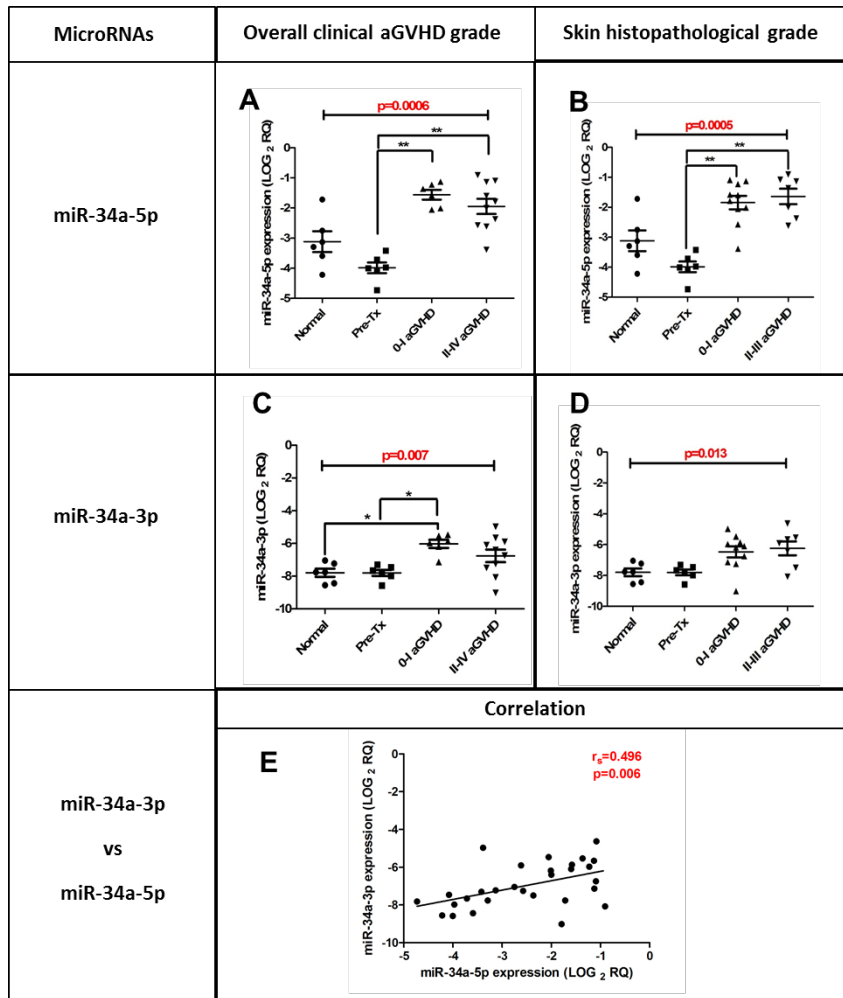


**Figure 4.13** MiR-34a-5p expression was significantly up-regulated post allo-HSCT in skin biopsies and its expression positively correlated with miR-34a-3p expression. There was a direct positive correlation between miR-34a-3p and miR-34a-5p expression. Scatter plots show (A, B) miR-34a-5p and (C, D) miR-34a-3p expression with error bars for SEM. Expression of both miRNAs was studied by RT-qPCR. Kruskal-Wallis analysis of variance was used to determine the significance set at  $p < 0.05$ . Normal: normal controls, Pre-Tx: Pre-transplant. (E) Spearman correlation was used to determine the correlation between the two miR-34a strands. Spearman's rho:  $r_s$ . Solid line represents regression. Significance was set at  $p \leq 0.05$  (\*) and  $p \leq 0.01$  (\*\*).

#### 4.2.5.6 *MiR-34a-5p showed the most significant trend with regards to aGVHD severity*

Jonckheere-Terpstra test was performed to assess for statistically significant trends. The cohort was arranged in an ordered pattern (pre-Tx, grade I, grade II). The patient with skin histopathological aGVHD grade III was eliminated from this analysis as for Jonckheere test, the number of variables per group should be approximately the same. Results demonstrated that miR-34a-5p had the highest statistically significant trend towards over-expression from pre to grade II aGVHD (Table 4.8).

MicroRNAs	Jonckheere's trend test
	P-value
miR-34a-5p	<b><u>0.001</u></b>
miR-503-5p	0.005
miR-142-3p	0.024
miR-21-3p	0.024
miR-34a-3p	0.029
miR-24-3p	0.029
let-7c-5p	0.034
miR-493-3p	0.04
miR-365a-3p	0.062
miR-200b-3p	0.082
miR-2110	0.528
miR-23b-3p	0.61

**Table 4.8** Eight miRNAs exhibited a significant trend in expression levels. Significant values are underlined and shown in bold.

#### 4.2.6 *Comparisons between MicroRNA Expression Levels, the Number of Necrotic Cells and Inflammatory Cell Infiltrates*

The number of inflammatory cell infiltrates and necrotic cells were semi-quantitated in the clinical skin biopsies (n=17) by two independent histopathologists. Necrotic cells were defined as dead cells with a degenerative nucleus and altered cytoplasm. Inflammatory cell infiltrates (lymphoid cells) were also counted and the mean of five fields of view per biopsy was calculated and used for this analysis.

#### 4.2.6.1 The number of necrotic cells positively correlated with skin histopathological aGVHD grade

There was no statistically significant correlation between the number of inflammatory cell infiltrates and the skin histopathological aGVHD grade ( $r_s=0.33$ ,  $p=0.190$ ) (Figure 4.14, A). However, there was significant positive correlation between the number of necrotic cells and the skin histopathological grade ( $r_s=0.66$ ,  $p=0.004$ ) (Figure 4.14, B). Results also showed borderline positive correlation ( $r_s=0.48$ ,  $p=0.052$ ) between the number of cell infiltrates and necrotic cells (Figure 4.14, C).

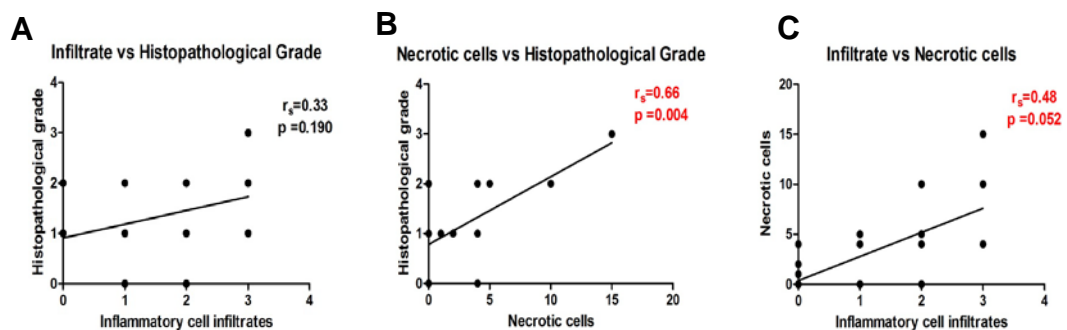


**Figure 4.14 Skin histopathological aGVHD grade correlated positively with the number of necrotic cells.** (A) Skin histopathological grade versus the number of inflammatory cell infiltrates, (B) Skin histopathological grade versus the number of necrotic cells and (C) Direct positive correlation between the number of necrotic cells and inflammatory cell infiltrates. The cells were counted per field at 400X magnification. The y-axis shows the mean of inflammatory cell infiltrates counted for five fields per biopsy. Spearman correlation was the test used, and significance was set at  $p<0.05$ . Spearman's rho:  $r_s$ .

Acknowledgments: Prof Anne Janin and Dr Philippe Ratajczak performed the semi-quantitative analyses.

#### 4.2.6.2 Three microRNA expression levels negatively correlated with the number of inflammatory cell infiltrates

Correlation statistics was performed to evaluate whether the miRNA expression levels were dependent on the number of inflammatory cell infiltrates and necrotic cells in the skin. The correlation was not statistically significant between any of 12 miRNAs in the validation cohort and the number of necrotic cells counted in the skin biopsies. However, miR-200b-3p ( $r_s=-0.53$ ,  $p=0.011$ ), miR24-3p ( $r_s=-0.60$ ,  $p=0.011$ ) and miR-23b-3p ( $r_s=-0.53$ ,  $p=0.031$ ) expressions negatively correlated with the number of inflammatory infiltrating cells in the skin biopsies ( $n=17$ ) (Figure 4.15).

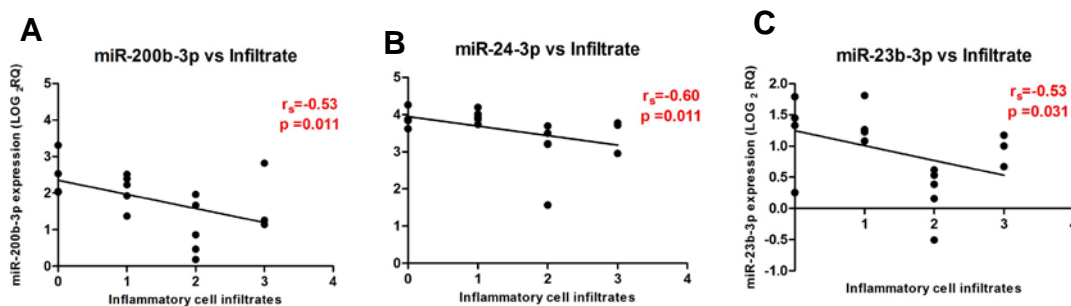


**Figure 4.15** Statistically significant negative correlations existed between miRNA expression levels and the number of inflammatory cells infiltrating the skin biopsies. (A) miR-200b-3p, (B) miR-24-3p and (C) miR-23b-3p expression versus inflammatory cell infiltrates. The cells were counted per field at 400X magnification. The y-axis shows the mean of inflammatory cell infiltrates counted for five fields per biopsy. Spearman correlation was the test used, and significance was set at  $p < 0.05$ . Spearman's rho:  $r_s$ .

#### **4.2.7 Association between MicroRNA Expressions with Overall Survival**

The aim of this Section was to evaluate whether the addition of miRNA expression levels could be predictive of other post allo-HSCT outcomes such as OS and relapse. There is limited research present on the role of miRNAs in predicting allo- HSCT survival outcomes and most of the existing knowledge relates to cancers and solid organ transplantations (Fan *et al.*, 2013; Han *et al.*, 2013; Zhu and Xu, 2014). In a meta-analysis study comprising of 25 independent investigations, it has been shown that higher levels of miR-21 was predictive of poor OS and disease-free survival (DFS) in cancer (Zhu and Xu, 2014). Likewise, it has been shown that down-regulation of miR-20a expression in hepatocellular carcinoma patients was predictive of poor OS (Fan *et al.*, 2013). In hepatocellular carcinoma patients who had undergone solid organ liver transplantation, higher miR-155 expression levels were associated with reduced survival (Han *et al.*, 2013). With the current research showing the association between miRNA expression level and allo-HSCT outcome, similar analyses were performed in this Section for survival.

##### **4.2.7.1 Study cohort**

The patient cohort (n=17) comprised of nine alive and eight deceased patients. The follow-up period was 19 months for all the patients. The cohort included patients that survived more than 4 months. . There was only one patient who had bone marrow infusion and had died. In all, 56% of patients infused with PBSC were alive while 44% were dead. Patients with skin histopathological aGVHD grades II-III had a high mortality percentage, 71%. This was in contrast to patients with grades 0-I of which 70% were still alive at the time of last follow-up. All ALL and MM patients had died, but this result must be interpreted with caution as the cohort size is small, and the underlying diseases are very heterogenous in this study. In all, 60% of patients who had disease relapse had died. Interestingly, all the female patients were alive in this cohort, in comparison to 35% of the males. Table 4.9 shows a frequency table with all the patient characteristics and OS grouping (alive/dead).

#### **4.2.7.2 Data analyses**

Variable selection for both clinical risk factors and miRNAs was performed using univariate analysis; either Kaplan-Meier log-rank test or Cox regression. Variables associated with outcome were entered in the multivariate analysis but only the significant variables were retained in the equation.

Cohort Characteristics (n=17)		Alive (%) (n=9)		Dead (%) (n=8)	
		No.	%	No.	%
Histopathological aGVHD grade	No aGVHD (Grade 0-I)	7	70	3	30
	Yes aGVHD (Grades II-III)	2	29	5	71
Patient gender	Female	3	100	0	0
	Male	6	43	8	57
Donor gender	Female	3	60	2	40
	Male	5	45	6	55
Graft source	BM	0	0	1	100
	PBSC	9	56	7	44
Underlying Disease	ALL	0	0	2	100
	AML	2	67	1	33
	MDS	2	50	2	50
	MF	1	100	0	0
	NHL	3	60	2	40
	CLL	1	100	0	0
	MM	0	0	1	100
Regimen	Myeloblative	1	33	2	67
	RIC	8	57	6	43
Protocol	Cy TBI	1	33	2	67
	Flu Bu	1	33	2	67
	Flu Mel	7	64	4	36
Campath	30 mg	2	40	3	60
	60 mg	6	60	4	40
	90 mg	1	50	1	50
Relationship	SIB	7	54	6	46
	MUD	2	50	2	50
Patient CMV status	Negative	2	33	4	67
	Positive	6	60	4	40
Donor CMV status	Negative	5	50	5	50
	Positive	3	50	3	50
HLA Class I mismatches	None	8	67	4	33
	One	1	20	4	80
HLA Class II mismatches	None	4	67	2	33
	One	3	43	4	57
	Two	2	50	2	50
Relapse status	No	7	64	4	36
	Yes	2	40	3	60
Disease status at Transplant	CR	1	100	0	0
	CR1	2	33	4	67
	CR2	3	60	2	40
	PR	1	33	2	67

**Table 4.9 Patient characteristics for the overall survival analysis.** Abbreviations:- BM: Bone marrow, PBSC: Peripheral blood stem cells, ALL: Acute lymphocytic leukaemia, AML: Acute myeloid leukaemia, CLL: Chronic lymphocytic leukaemia, MDS: Myelodysplastic syndrome, MM: Multiple myeloma, MPS: Multiple proliferative syndrome, NHL: Non-Hodgkin's lymphoma, RIC: Reduced intensity conditioning, Flu: Fludarabine, Mel: Melphalan, Bus: Busulfan, Cy: Cytrabine, TBI: Total body irradiation, Alem: Alemtuzumab, CsA: Cyclosporine, CMV: Cytomegalovirus, CR (1-3) Complete remission, PR: Progression, SIB: Sibling, MUD: Matched unrelated donor.

### **4.2.7.3 Lower miR-503-5p and miR-34a-3p expressions are associated with improved overall survival**

Clinical risk factors as well as miRNA expression levels from Section 4.4 were used to perform survival analysis. The expression of miR-34a-3p was also included as it positively correlated with its -5p strand. Since miRNA expressions were on a continuous scale, for OS, it was considered necessary to determine a decision threshold (cut-off) for each miRNA via ROC curve analysis. This enabled a threshold to be determined where the majority of patients above this value had a specific outcome and the majority of patients below this value had the alternative outcome (McNeil *et al.*, 1975). Thus, patients were dichotomised as having low or high miRNA expression levels (Table 4.10). For each value of specific miRNA sensitivity (True positivity) and specificity (false positivity) estimates were determined and these were used to plot the ROC curve. An area under the curve (A) of 0.5 signified that the miRNA had no diagnostic ability; an area under the curve of 1 signified that the miRNA had perfect diagnostic ability. The p-value accompanying the area under the curve tested the null hypothesis that the area under the curve was 0.5 (see Chapter 2, Section 2.14.2; for further details on ROC curve analysis). The ROC curve does not take into account the available time element. Thus, for improved cut-off accuracy, Kaplan-Meier analysis could have been employed incorporating the time factor. Subsequently, a survival curve would have been plotted for each of several divisions of the specific miRNA's full continuum; a dichotomy could hence have been established by observing how the survival curves naturally clustered together. However, such a Kaplan-Meier analysis is dependent on a very large sample size due to the large number of divisions required; in this study n=17 and hence the analysis was not possible.

The expression values of all the 12 miRNAs (miR-503-5p, let-7c-5p, miR-365a-3p, miR-34a-5p, miR-34a-3p, miR-142-3p, miR-21-3p, miR-24-3p, miR-2110, miR-200b-3p, miR-493-3p and miR-23b-3p) were used to perform the survival analysis. The ROC curve showed that the expression levels of miR-503-5p (A=0.833, p=0.021) and miR-34a-3p (A=0.931, p=0.003) were diagnostically significant in predicting the dead and alive patients (Table 4.10, Figure 4.16, A and C).

MicroRNAs	Cut-off value	Sensitivity	Specificity	AUC (95% CI)	P-value for AUC
miR-503-5p	>-7.79	<u>0.75</u>	<u>0.89</u>	<u>0.83(0.63-1.03)</u>	<u>0.021</u>
miR-34a-3p	>-6.04	<u>0.88</u>	<u>0.89</u>	<u>0.93(0.81-1.05)</u>	<u>0.003</u>
miR-34a-5p	<-1.13	0.88	0.33	0.57(0.28-0.86)	0.63
miR-23b-3p	>0.21	1.00	0.22	0.51(0.23-0.80)	0.923
miR-21-3p	>5.51	0.63	0.67	0.56(0.26-0.85)	0.7
miR-142-3p	>-1.78	1.00	0.33	0.74(0.49-0.98)	0.102
let-7c-5p	>-3.11	0.88	0.22	0.54(0.26-0.83)	0.773
miR-365a-3p	>-2.47	0.88	0.56	0.65(0.37-0.93)	0.29
miR-493-3p	>-8.54	0.88	0.22	0.57(0.26-0.85)	0.7
miR-200b-3p	<-2.45	0.88	0.33	0.51(0.23-0.80)	0.923
miR-24-3p	>-2.26	1.00	0.11	0.53(0.24-0.82)	0.847
miR-2110	<-7.55	1.00	0.22	0.60(0.32-0.87)	0.501

**Table 4.10 ROC curve analysis of miRNA expression with overall survival.** Log-transformed miRNA expression values were used to derive the cut-off value for dichotomising the expression as low or high. Significant values are underlined and shown in bold. <: lower values signify patient more likely to die; higher values signify patient more likely to live. >: higher values signify patient more likely to die; lower values signify patient more likely to live. Significant values are underlined and shown in bold.

To reinforce the ROC's dichotomy, the Kaplan-Meier log-rank-test (incorporating the time element) was then performed to compare the resulting two different levels (low and high) of miRNA expression with regards to OS. Only two miRNA dichotomies proved significantly associated with survival (Table 4.11): miR-503-5p (log-rank test,  $p = 0.003$ ) and miR-34a-3p (log-rank test,  $p = 0.004$ ) (Figure 4.16, B and D).

MicroRNAs	Log-Rank P-value
	(Alive n=9, Dead n=8)
miR-503-5p	<b><u>0.003</u></b>
miR-34a-3p	<b><u>0.004</u></b>
miR-34a-5p	0.777
miR-23b-3p	0.218
miR-21-3p	0.213
miR-142-3p	0.114
let-7c-5p	0.731
miR-365a-3p	0.109
miR-493-3p	0.502
miR-200b-3p	0.448
miR-24-3p	0.404
miR-2110	0.218

**Table 4.11 Univariate Kaplan-Meier analysis of miRNA expression with overall survival.** Significant values are underlined and shown in bold.

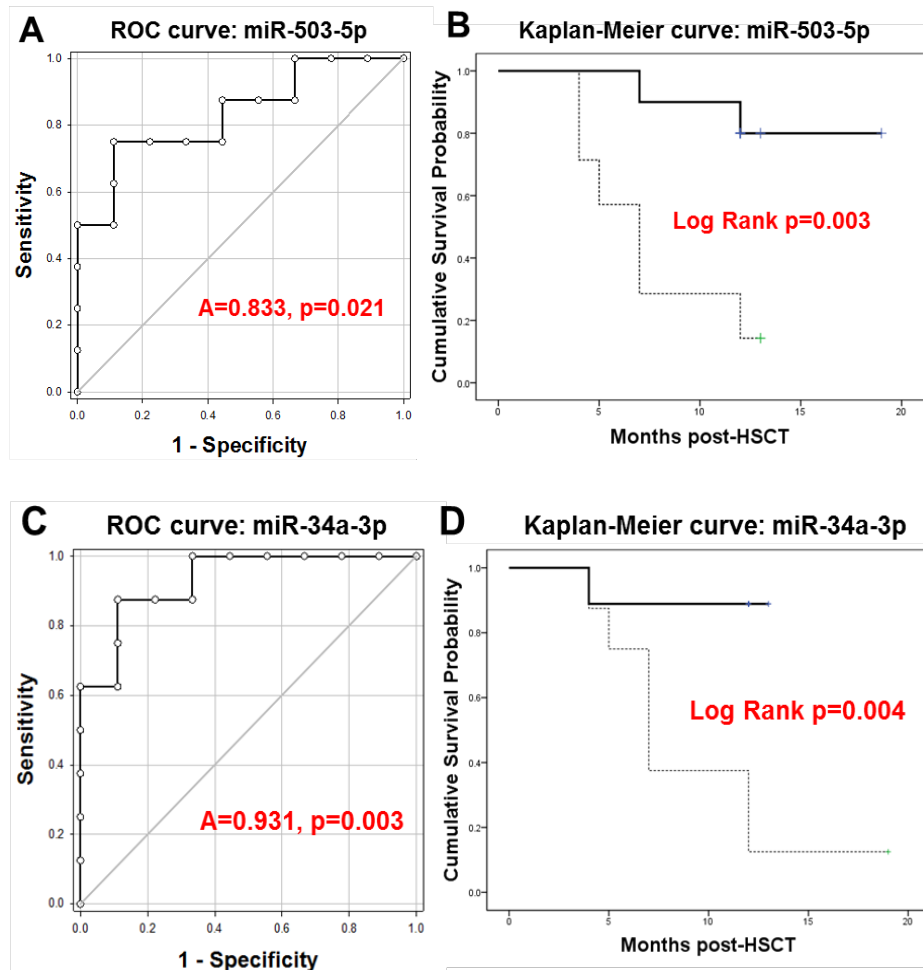


**Figure 4.16 ROC and Kaplan-Meier survival analysis for miR-503-5p and miR-34a-3p expression.** The cut-off value determined from the ROC test was used to dichotomise the miRNA expression for the log-rank test. (A) The dichotomy for miR-503-5p at the time in which aGVHD was clinically assessed significantly ( $p=0.021$ ) discriminated the patients that went on to survive ( $n=9$ ) from those who died ( $n=8$ ). (B) The clear separation of the Kaplan-Meier curves showed that the dichotomy for miR-503-5p expression could be used to predict OS post-HSCT ( $p=0.003$ ). (C) The dichotomy for miR-34a-3p at the time in which aGVHD was clinically assessed significantly ( $p=0.003$ ) discriminated the patients that went on to survive ( $n=9$ ) from those who died ( $n=8$ ). (D) The clear separation of the Kaplan-Meier curves showed that the dichotomy for miR-34a-3p expression could be used to predict OS post-HSCT ( $p=0.004$ ). Dashed lines (---) = high miRNA expression and solid black line (—) = low miRNA expression levels.

The chi-square statistic was employed to establish if the dichotomy used for each miRNA was sufficient to differentiate between patients who were dead and patients who were alive (Table 4.12). Overall there were eight dead (events) and nine alive (censored) cases. Exact p-values for the chi-square test were used to ensure accuracy regardless of the size, distribution, sparseness, or balance of the data. These results agreed with those of the log rank tests from the Kaplan-Meier analysis: miR-503-5p (p =0.003) miR-34a-3p (p=0.004). Low miRNA expression level was shown to be indicative of higher cumulative survival probability for both miR-503-5p and miR-34a-3p.

MicroRNAs	Expression level <sup>a</sup>	Total	No. Dead	No.Alive		Fisher's Exact
		N	N	N	Percent alive	p-value
miR-503-5p	Low expression	10	2	8	80.0%	<b><u>0.015</u></b>
	High expression	7	6	1	14.3%	
miR-34a-3p	Low expression	9	1	8	88.9%	<b><u>0.003</u></b>
	High expression	8	7	1	12.5%	
miR-34a-5p	Low expression	14	7	7	50.0%	1.000
	High expression	3	1	2	66.7%	
miR-23b-3p	Low expression	2	0	2	100.0%	0.471
	High expression	15	8	7	46.7%	
miR-21-3p	Low expression	9	3	6	66.7%	0.347
	High expression	8	5	3	37.5%	
miR-142-3p	Low expression	3	0	3	100.0%	0.206
	High expression	14	8	6	42.9%	
let-7c-5p	Low expression	3	1	2	66.7%	1.000
	High expression	14	7	7	50.0%	
miR-365a-3p	Low expression	6	1	5	83.3%	0.131
	High expression	11	7	4	36.4%	
miR-493-3p	Low expression	3	1	2	66.7%	1.000
	High expression	14	7	7	50.0%	
miR-200b-3p	Low expression	13	7	6	46.2%	0.577
	High expression	4	1	3	75.0%	
miR-24-3p	Low expression	1	0	1	100.0%	1.000
	High expression	16	8	8	50.0%	
miR-2110	Low expression	15	8	7	46.7%	0.471
	High expression	2	0	2	100.0%	

**Table 4.12 Case processing summaries for all the 12 validated miRNAs showing the number of events and censored cases per group.** All patients had the same follow-up period of 19 months. <sup>a</sup> grey shade: level containing larger proportion of patients who died. Significant values are underlined and shown in bold.

#### 4.2.7.4 Association of clinical risk factors with overall survival

To increase the accuracy of the multivariate model, variable selection was performed for both the clinical risk factors and miRNAs. The association of the clinical risk factors with OS was first assessed by either Kaplan-Meier log-rank test or univariate Cox regression with appropriate coding for categorical variables. Risk factors that had p-values less than 0.2 were selected for inclusion in the Cox regression variable selection procedure. Kaplan-Meier survival analysis was performed to assess the association of donor type, source, conditioning regimen, patient gender, donor gender, patient CMV status and donor CMV status with OS (Table 4.13). Patient gender (p=0.114) and CMV status (p=0.110) were chosen as candidate variables for subsequent variable selection in multivariate Cox regression modelling as their log-rank p-values were less than 0.2.

Clinical Risk Factors	Log-Rank P-value
Donor type	0.767
Source	0.546
Conditioning regimen	0.678
Donor gender	0.56
Patient gender	<b><u>0.114</u></b>
Donor CMV status	0.67
Patient CMV status	<b><u>0.11</u></b>

**Table 4.13 Univariate Kaplan-Meier analysis of clinical risk factors with survival.** Factor with  $p \leq 0.2$  were considered significant for inclusion in the multivariate analysis. Significant values are underlined and shown in bold.

The significance of the following clinical risk factors with OS were assessed by performing univariate Cox regression; Diagnosis (ALL, AML, MDS, MF, CLL, MM and NHL) patient age, type of protocol (Cy TBI/ Flu Bu/ Flu Mel), dosage of alemtuzumab (30/ 60/ 90), status at transplant (CR/ CR1/ CR2/ PR), HLA Class I and HLA Class II mismatches, skin histopathological aGVHD status (with/ without aGVHD). Mismatches in HLA Class I ( $p=0.171$ ) and skin histopathological aGVHD grade ( $p=0.096$ ) were the only variables selected for entry into the multivariate model (Table 4.14). Univariate Cox regression analysis was also performed for all the 12 miRNAs to select the significant ones for the final multivariate analysis (Table 4.14). The analysis showed that miR-503-5p ( $p=0.008$ ), miR-34a-3p ( $p=0.015$ ) and miR-142-3p ( $p=0.099$ ) were significantly ( $p\leq 0.2$ ) associated with OS and were therefore included in the multivariate Cox regression model.

Factors	P-value
Diagnosis	0.809
Patient age	0.729
Alemtuzuman dosage	0.678
Status at transplant	0.533
HLA Class I mismatches	<b><u>0.171</u></b>
HLA Class II mismatches	0.603
Skin histopathological aGVHD grade	<b><u>0.096</u></b>
miR-503-5p	<b><u>0.008</u></b>
miR-34a-3p	<b><u>0.015</u></b>
miR-34a-5p	0.694
miR-23b-3p	0.918
miR-21-3p	1.000
miR-142-3p	<b><u>0.099</u></b>
let-7c-5p	0.884
miR-365a-3p	0.748
miR-493-3p	0.586
miR-200b-3p	0.918
miR-24-3p	0.610
miR-2110	0.385

**Table 4.14 Univariate Cox regression analysis of clinical risk factors and miRNAs with survival.** Factors with  $p\leq 0.2$  were considered significant for inclusion in the multivariate analysis. Significant values are underlined and shown in bold.

Subsequently, multivariate Cox regression analysis was performed to estimate the predictive value of miRNA expression with OS post-HSCT. Data from a total of 17 patients was used for modelling; eight patients had died (event) and nine were alive (censored). There was no missing data in this analysis. The following were entered into the stepwise forward LR, multivariate Cox regression analysis: clinical risk factors (Patient gender and CMV status, mismatches in HLA Class I and skin histopathological aGVHD grade) and selected miRNAs (miR-503-5p, miR-34a-3p and miR-142-3p).

Interestingly, miR-503-5p [p=0.042, HR= 1.73 (95% CI: 1.02-2.94)] and miR-34a-3p [p=0.036, HR= 4.88 (95% CI: 1.11-21.53)] were the only variables that were entered in the Cox regression equation (Table 4.15). When both miR-503-5p and miR-34a-3p were entered into the equation, the significance and hazard ratio (HR) of miR-503-5p declined. MiR-503-5p alone was highly significant in predicting the patients that were at risk of death [p=0.011, HR=1.95 (95% CI: 1.16-3.26)]. The results showed that the hazard of dying increased (miR-503-5p: HR=1.73, miR-34a-3p: HR=4.88) with every unit increase in miR-503-5p and miR-34a-3p expression (Table 4.15). Thus, both the Kaplan-Meier log-rank test and the Cox regression model showed that low miR-503-5p and miR-34a-3p was associated with longer OS in this cohort.

Variables in the equations		Hazard Ratio (95% CI)	P-value
Step 1	miR-503-5p	1.95 (1.16-3.26)	<b><u>0.011</u></b>
Step 2	miR-503-5p	1.73 (1.02-2.94)	<b><u>0.042</u></b>
	miR-34a-3p	4.88 (1.11-21.53)	<b><u>0.036</u></b>

**Table 4.15** MiR-503-5p and miR-34a-3p were significant in predicting overall survival

## **4.2.8 Association of MicroRNA Expression with Relapse**

### **4.2.8.1 Study cohort**

The same patient cohort (n=17) was grouped into; no relapse and relapsed. The patient characteristic in each group is mentioned in Table 4.16. In all, 40% of the patients with skin histopathological aGVHD grades 0-I relapsed while only 16.7% patients with aGVHD grades II-III relapsed. Percentage of relapse was higher in female (66.7%) patients when compared to males (23.1%). The two patients who had been treated with 90 mg Campath (Alemtuzumab) did not relapse. The percentage of relapse in patients undergoing MUD or HLA-matched sibling transplants was almost equal. There was 50% relapse in allo-HSCT procedures where there were two mismatches in HLA class II in patient-donor pair.

### **4.2.8.2 Data analyses**

As in the previous Section 4.6.2, univariate analysis was performed to identify clinical risk factors and miRNAs associated individually with relapse for inclusion in the multivariate Cox regression analysis. There was no missing data in these analyses. Evidently, patients with PR status at transplant had relapsed. Patient gender ( $p=0.192$ ), CMV status ( $p=0.185$ ) and graft source ( $p=0.070$ ) were also selected as candidate variables for the subsequent variable selection in the multivariate Cox regression modelling as their log-rank  $p$ -values were less than 0.2 (Table 4.16). The univariate Cox regression analysis showed that Status at transplant ( $p=0.201$ ) and mismatches in HLA class II ( $p=0.198$ ) were significant variables associated with relapse and were thus included for entry in the multivariate Cox regression model (Table 4.16).

Cohort Characteristics (n=17)		No relapse (%) (n=11)		Relapse (%) (n=5)		P-value
		No.	%	No.	%	
Patient age		47 (19-65)				0.564†
Histopathological aGVHD grade	No aGVHD (Grade 0-I)	6	60	4	40	0.535*
	Yes aGVHD (Grades II-III)	5	83	1	17	
Patient gender	Female	1	33	2	67	<u>0.192*</u>
	Male	10	77	3	23	
Donor gender	Female	4	80	1	20	0.588*
	Male	6	60	4	40	
Graft source	BM	0	0	1	100	<u>0.07*</u>
	PBSC	11	73	4	27	
Underlying Disease	ALL	1	50	1	50	0.315†
	AML	2	67	1	33	
	MDS	2	50	2	50	
	MF	1	100	0	0	
	NHL	3	75	1	25	
	CLL	1	100	0	0	
	MM	1	100	0	0	
Regimen	Myeloblative	2	67	1	33	0.862*
	RIC	9	69	4	31	
Protocol	Cy TBI	2	67	1	33	0.437†
	Flu Bu	1	33	2	67	
	Flu Mel	8	80	2	20	
Campath	30 mg	2	50	2	50	0.264†
	60 mg	7	70	3	30	
	90 mg	2	100	0	0	
Relationship	SIB	9	69	4	31	0.969*
	MUD	2	67	1	33	
Patient CMV status	Negative	3	60	2	40	<u>0.185*</u>
	Positive	8	80	2	20	
Donor CMV status	Negative	6	67	3	33	0.718*
	Positive	4	67	2	33	
HLA Class I mismatches	None	8	73	3	27	0.568†
	One	3	60	2	40	
HLA Class II mismatches	None	4	80	1	20	<u>0.198†</u>
	One	5	71	2	29	
	Two	2	50	2	50	
Disease status at Transplant	CR	1	100	0	0	<u>0.201†</u>
	CR1	5	83	1	17	
	CR2	3	60	2	40	
	PR	1	50	1	50	

**Table 4.16 Patient characteristics for patients with no relapse and relapse.**

Abbreviations: - \*Univariate Kaplan-Meier log-rank test and †univariate Cox regression for variable selection. BM: Bone marrow, PBSC: Peripheral blood stem cells, ALL: Acute lymphocytic leukaemia, AML: Acute myeloid leukaemia, CLL: Chronic lymphocytic leukaemia, MDS: Myelodysplastic syndrome, MM: Multiple myeloma, MPS: Multiple proliferative syndrome, NHL: Non-Hodgkin's lymphoma, RIC: Reduced intensity conditioning, Flu: Fludarabine, Mel: Melphalan, Bus: Busulfan, Cy: Cytarabine, TBI: Total body irradiation, Alem: Alemtuzumab, CsA: Cyclosporine, CMV: Cytomegalovirus, CR (1-3) Complete remission, PR: Progression, SIB: Sibling, MUD: Matched unrelated donor

#### 4.2.8.3 *Let-7c-5p expression may have a protective role against relapse*

As in the previous Section 4.6.2, univariate Cox regression analyses were also performed for all the 12 miRNAs to select the ones significantly associated with relapse (Table 4.17). The analysis showed that miR-34a-3p ( $p=0.060$ ), miR-23b-3p ( $p=0.061$ ), let-7c-5p ( $p=0.000$ ) and miR-2110 ( $p=0.050$ ) were significantly ( $p\leq 0.2$ ) associated with relapse and were therefore included in the multivariate Cox regression model.

Clinical Risk Factors	P-value
miR-503-5p	0.811
miR-34a-3p	<b><u>0.060</u></b>
miR-34a-5p	0.737
miR-23b-3p	<b><u>0.061</u></b>
miR-21-3p	0.864
miR-142-3p	0.656
let-7c-5p	<b><u>0.000</u></b>
miR-365a-3p	0.343
miR-493-3p	0.382
miR-200b-3p	0.822
miR-24-3p	0.310
miR-2110	<b><u>0.050</u></b>

**Table 4.17 Univariate Cox regression analysis of miRNAs with relapse.** Significant values are underlined and shown in bold.

Multivariate Cox regression analysis was performed to estimate the predictive value of miRNA expression with relapse. The following were entered into the stepwise forward LR, multivariate Cox regression analysis: clinical risk factors (Patient gender and CMV status, graft source, status at transplant and mismatches in HLA Class II) and selected miRNAs (miR-34a-3p, miR-23b-3p, let-7c-5p and miR-2110).

The multivariate Cox regression analysis showed that let-7c-5p [ $p=0.051$ , HR= 0.01 (95% CI: 0.00- 1.03)] was the only variable entered in the Cox regression equation. This indicated that for every unit increase in let-7c-5p expression the patient risk of relapse declined by 0.01. Thus, let-7c-5p expression had a protective effect against relapse. Interestingly, quasi-complete separation was also identified for let-7c-5p expression

between the relapse and non-relapse group of patients. Only one patient with low let-7c-5p expression did not relapse, and this has been shown clearly in Table 4.18.

let-7c-5p expression	Event free Survival (months)	Relapse
		(Yes=1, No=0)
-3.65	2	1
-3.2	8	1
-3.14	3	1
-3.1	5	1
-2.8	12	0
-2.44	10	1
-2.09	13	0
-2.09	19	0
-1.91	4	0
-1.89	12	0
-1.73	7	0
-1.55	13	0
-1.51	4	0
-1.48	7	0
-1.44	12	0
-1.12	12	0
-1.07	7	0

**Table 4.18** Quasi-complete separation for let-7c-5p expression ( $\log_2$  fold change). The box indicates the only patient that did not relapse but had low let-7c-5p expression.

## **4.2.9 Model for MicroRNA Expression Levels**

### **4.2.9.1 Significant interaction between miR-503-5p and miR-34a-3p**

Almost all biological processes are dependent on interactions between different molecules. Interactions between all the 12 miRNAs were also assessed in this research. Ordinal logistic regression analysis was performed encompassing both the main effect and interaction of all the validated miRNAs in a step-wise manner. The skin histopathological aGVHD grade was selected as the response outcome. Results showed that there was a statistically significant interaction between miR-503-5p and miR-34a-3p expression ( $p=0.016$ ) with miR-503-5p had the most significant main effect ( $p=0.011$ ) and miR-34a-3p was the moderator ( $p=0.020$ ) in this interaction (See Chapter 2, Section 2.14.4; for detailed explanation on main effect and interactions). There existed a conditional relationship between miR-503-5p and miR-34a-3p such that when high levels of miR-34a-3p were expressed, higher levels of miR-503-5p were more clearly associated with severity of skin histopathological aGVHD grade (Figure 4.17, A). However, the relationship between miR-503-5p and skin histopathological aGVHD severity was less clear when low levels of miR-34a-3p were expressed and this needs further investigation to elucidate either the clinical or biological reason for this change in trend (Figure 4.17, B). To further understand the conditional interaction between miR-503-5p and miR-34a-3p, rotational 3D scatterplots were generated (Figure 4.18). Since miR-503-5p and miR-34a-3p were significantly associated with OS; non-parametric density contours based on the patient survival status were also added to the scatterplots to aid visualisation. The plots demonstrated the conditional interaction between miR-503-5p and miR-34a-3p expression visually.

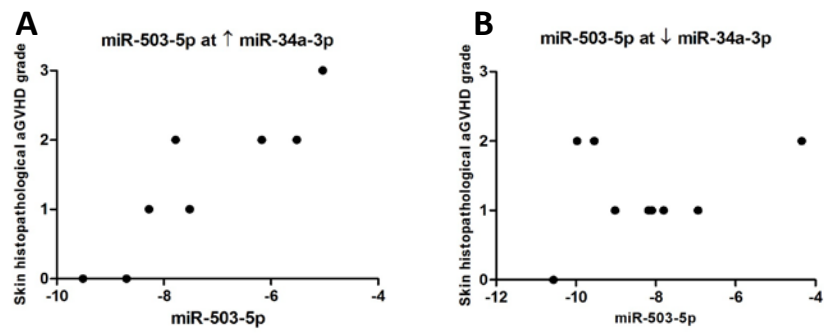


**Figure 4.17** MiR-503-5p expression is associated with aGVHD severity. (A) miR-503-5p expression was associated with skin histopathological aGVHD severity when high levels of miR-34a-3p were expressed. (B) MiR-503-5p expression was not clearly associated with skin aGVHD severity when low miR-34a-3p levels were expressed.

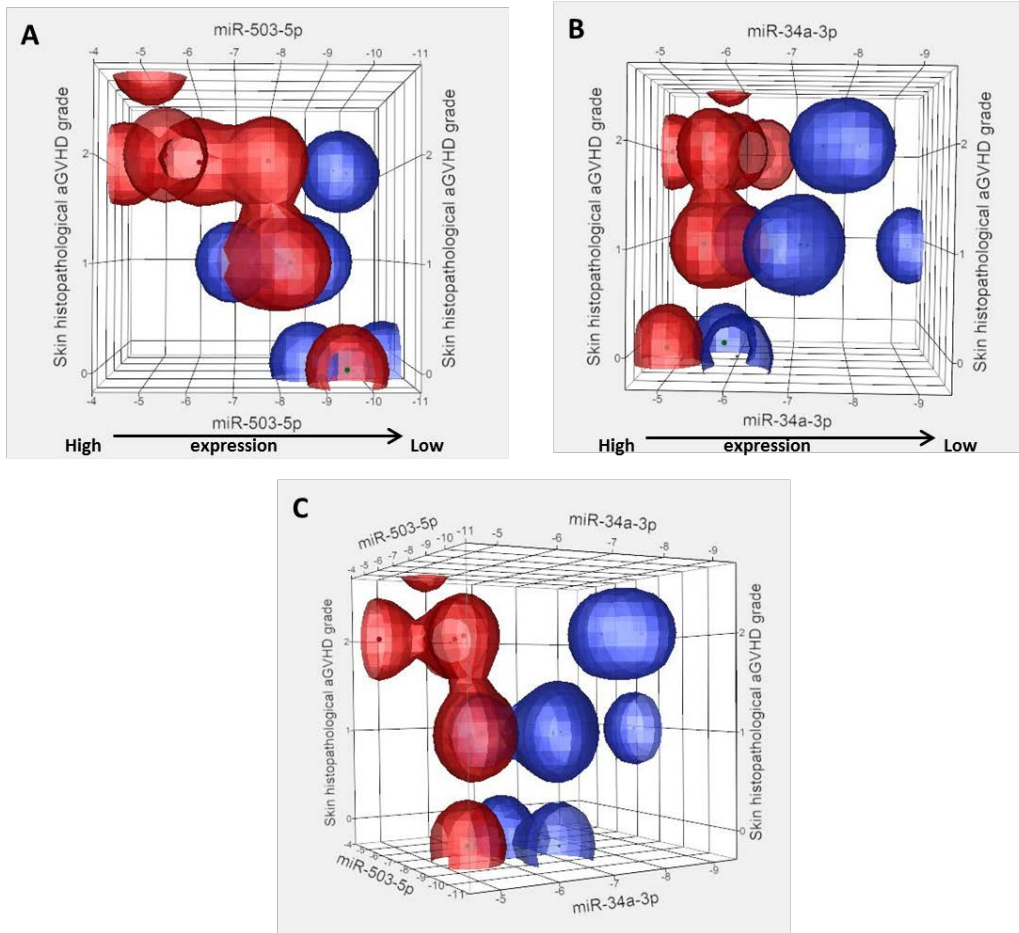


**Figure 4.18 Rotational 3D scatterplots demonstrating miR-503-5p and miR-34a-3p conditional interaction.** (A) Higher miR-503-5p expression was associated with skin histopathological aGVHD severity (B) lower miR-34a-3p expression was also associated with skin aGVHD severity and (C) Distinct separation between the dead and alive patients based on their miRNA expression levels in particular with low miR-34a-3p expression showing improved OS. The plot shows three axes: miR-34a-3p, miR-503-5p and cutaneous histopathological aGVHD grades. Red=dead, blue= alive patients. Each dot represents a patient. Non-parametric density contours were drawn based on the patient survival status (dead or alive). The arrow shows the expression scale from high to low.

### 4.3 Discussion

Currently, more than 1900 miRNAs (Kozomara and Griffiths-Jones, 2011) have been identified in humans, and it is well known that a single miRNA can target more than 200 mRNAs (Bartel, 2004b). The critical role of miRNA in disease pathology and development has been highlighted in numerous studies to-date (Lu *et al.*, 2005). MicroRNAs are cell-specific, stable and therefore ideal biomarkers (Culpin *et al.*, 2013). This study aimed to identify a signature list of miRNAs that could discriminate mild (Grade I) from moderate/severe (Grade II-III) aGVHD. Global miRNA profiling by RT-qPCR was carried out, 12 miRNAs that were either differentially expressed across the groups (miR-142-3p, miR-34a-5p, miR-503-5p, let-7c-5p, miR-21-3p, miR-365a-3p, miR-23b-3p and miR-24-3p) or could have an important role in disease biology (miR-493-3p, miR-2110 and miR-200b-3p) were selected and then individually validated by RT-qPCR in normal controls, pre- and post-transplantation skin biopsies. MiR-34a-3p expression was also investigated as its expression correlated with miR-34a-5p, and it was biologically interesting to further investigate its association with allo-HSCT in particular aGVHD.

Global miRNA profiling by RT-qPCR was considered the most appropriate technique for this investigation as the quantity of total RNA extracted (concentration < 100 ng/μl) from skin biopsies was below the acceptable concentration for both microarrays (100 ng/μl) and Nanostring (100 ng) profiling technologies. As the total RNA concentrations were low, prior to profiling every sample was quality control checked by RT-qPCR to detect for any PCR inhibitors. All samples had RIN > 7.0 that was indicative of purity and gel analysis showed no degradation.

Allogeneic HSCT is a complicated process with a high mortality rate, and GVHD is one of its major complications. Acute GVHD is assessed by considering the onset of characteristic clinical symptoms in any of the target organs (skin, liver and gut) as outlined in Chapter 1. Histopathological changes are also examined in skin and gut to rule out infections or adverse drug reactions. Skin is the first and most frequently affected GVHD target organ when compared to the gut and liver. Liver is the most difficult target organ to study as liver biopsies are rarely taken due to the invasiveness

of the procedure that can increase the risk of internal bleeding. On the other hand, gut biopsies are more common than liver and are performed if the patient is suspected of gastrointestinal aGVHD with characteristic clinical symptoms as classified by Glucksberg (Przepiorka *et al.*, 1995). However, at the Newcastle Transplantation centre, gut biopsies are rarely taken from the patients. GVHD gut involvement is mainly assessed based on the patient's clinical symptoms. Thus, the skin was the ideal target organ to investigate both pathophysiologically and also due to its accessibility.

As mentioned earlier, skin biopsies are more often taken from the patients than gut, yet treatment usually starts prior to skin histopathological grading. This is due to the fact that clinical symptoms do not frequently correlate with the skin histopathological aGVHD grade and therefore, treatments are based on the severity of clinical symptoms (percentage coverage of skin rash) rather than histological changes. All the patients in this study had been administered Cyclosporine A as standard GVHD prophylaxis but not steroids.

Since clinical aGVHD grades are necessary with regards to patient treatment, in this investigation all results were analyzed by grouping patients based on the overall clinical aGVHD grade and also on the skin histopathological grade for comparison. As such, the overall clinical aGVHD grade and the skin histopathological grade did not correlate as demonstrated extensively in the literature and also again confirmed in this study (Zhou *et al.*, 2000).

Several recent investigations have highlighted the impact of aging on the expression levels of specific miRNAs such as miR-151-5p, miT-181a-5p and miR-1248 (Noren Hooten *et al.*, 2013). However, none of these miRNAs were significantly differentially expressed between the 0-I aGVHD and II-III aGVHD histopathological grades. All the patients in this cohort were older than 50 years except the single patient in the profiling experiment (19 years old). Therefore, the patients investigated were an older population hence the differential expression observed was independent of age.

Unsupervised hierarchical clustering of the global miRNA expression levels showed that there were two distinct clusters among the skin biopsies. One cluster comprised of only the allo-HSCT patients while the other, the normal controls. There were also

three distinguishable microRNA clusters on the basis of their expression levels; over-expressed, intermediate and under-expressed miRNAs. In fact, majority of the miRNAs in the clusters were under-expressed. The clustering analyses supported the hypothesis that normal controls and allo-HSCT patients have different miRNA expression patterns.

Discriminatory analyses were then performed to identify which miRNAs were deregulated in allo-HSCT patients with an emphasis on aGVHD. Twelve miRNAs were determined for further validation. The investigation showed that five miRNAs (let-7c-5p, miR-503-5p, miR-365a-3p and miR-34a-5p/-3p) were significantly differentially expressed between pre- and post allo-HSCT skin biopsies independent of aGVHD grading system (overall clinical or skin histopathological aGVHD grade). The findings suggested that miRNAs could be deregulated as a result of both, the allo-HSCT procedure and aGVHD disease onset. Additionally, a positive correlation was observed between miR-34a guide (-5p) and passenger (-3p) strands.

The next hypothesis to test was whether miRNA expression patterns reflected aGVHD severity. Extreme aGVHD cases are rare in the Newcastle Transplantation facility due to the controlled conditioning and prophylaxis treatments administered to patients. Almost every patient in this centre is administered alemtuzumab (Campath) which is an antibody against CD25 lymphocytes. Thus, all the patients undergo T-cell depletion, this is one of the reasons for the limited number of severe aGVHD patients. In this study, only one patient had an overall clinical aGVHD grade IV with skin histopathological grade III. The remaining patients had either been assessed with aGVHD grade I (mild) or II (moderate). Therefore, finding a set of miRNAs that could clearly discriminate the severe aGVHD patients with grades III-IV from those with grades I was not feasible experimentally. Statically, it was possible to test for trends that showed miRNA deregulation could be characteristic of aGVHD severity.

It is well known that inflammatory lymphocyte infiltrates and necrosis are the immune system hallmarks of cutaneous aGVHD. Keratinocyte apoptosis is also one of the main distinguishing factors. It has been shown in a single centre; homogeneous underlying

disease population (Fanconi anemia) that increased apoptosis was related with aGVHD severity. Not surprisingly, miR-34a-5p showed the most significant trend towards over-expression with regards to aGVHD severity. The authors also showed that it was miR-34a expression that was linked to higher epithelial apoptosis.

In contrast to the study mentioned above, it was thought appropriate to test the relationship between the number of necrotic cells, inflammatory cells infiltrates, cutaneous aGVHD severity and miRNAs. There was no direct positive correlation between any of the miRNAs and the number of cell infiltrates or necrotic cells. But, there was direct negative correlations between miR-24a (interfollicular keratinocyte differentiation), miR-200b (fibroblast proliferation) and miR-23b (keratinocyte differentiation), all of which have been shown to exhibit extensive roles in skin morphology (Hildebrand *et al.*, 2011; Amelio *et al.*, 2013; Li *et al.*, 2014a). MiR-24 is a polycistronic miRNA and is localized on two chromosomes 9 (miR-23b, miR-27a and miR-24-1) and 19 (miR-23a, miR-27a and miR-24-2) (Amelio *et al.*, 2013; Kozomara and Griffiths-Jones, 2014). However, its mature passenger strand miR-24-3p has the same sequence when produced from either of the clusters. This finding further supports the hypothesis that miR-24-3p and miR-23b are reflecting the inflammatory skin status through the imbalance in keratinocyte differentiation or apoptosis. To confirm this hypothesis, it might be interesting to detect keratinocyte apoptosis. Interestingly, the number of necrotic cells positively correlated with skin histopathological aGVHD grade which might be as a consequence of the conditioning and prophylaxis treatments as well as GVH reaction. There was also borderline significant positive correlation between the number of necrotic and inflammatory cell infiltrates. Infiltration of lymphocytes is indicative of inflammation or infection; however, none of the patients had infection at the time of biopsy collection. This could be due to the lymphocytes infiltrating the skin tissue post allo-HSCT during the GVH reaction and undergoing apoptosis.

Three of the miRNAs in the validation cohort are polycistronic with more than one miRNA being encoded by the same gene. Let-7c-5p is both part of the let-7c family and let-7c-mir-99a cluster, and its gene localized to chromosome 21 (Griffiths-Jones *et al.*,

2006; Kozomara and Griffiths-Jones, 2014). MiR-503 is also a polycistronic (mir-424, mir-503, mir-542, 450a-1/2, 450b) miRNA and derived from the mir-424-503 precursor miRNA. The gene for the miR-424-503 cluster is located on chromosome X (Griffiths-Jones *et al.*, 2006; Kozomara and Griffiths-Jones, 2014). Chromosome 16 encodes the gene for miR-365a which is again a polycistronic miRNA (mir-365a and mir-193b) (Griffiths-Jones *et al.*, 2006; Kozomara and Griffiths-Jones, 2014). MiR-34a was the only monocistronic miRNA and a member of the miR-34 family and its gene located on chromosome 1 (Griffiths-Jones *et al.*, 2006; Kozomara and Griffiths-Jones, 2014).

This study has shown that let-7c-5p expression increases after transplantation. But it was surprising to find out that its levels were approximately the same as that of normal controls in skin biopsies with histopathological grades II-III. Survival analysis also showed that let-7c-5p expression was protective against relapse. To better understand its role in transplantation, the patient characteristics was studied, and it was found that only one out of six patients with skin histopathological grade II-III had relapsed. Thus, let-7c-5p might be a marker for GVT effect rather than GVHD both because of its normal levels in moderate-severe aGVHD patients and also its protective role against relapse. Studies have shown that let-7c-5p is highly expressed in CD4<sup>+</sup>T cells in healthy individuals (Swaminathan *et al.*, 2011). Results in the normal controls were, therefore, in concordance with this study, despite studying let-7c-5p expression in the whole skin rather than a subset of cells. Swaminathan *et al.*, (2011) have shown that the expression of IL-10 protein could be modulated by let-7c-5p. IL-10 is an anti-inflammatory cytokine that has been extensively studied in GVHD (Lin *et al.*, 2005). At this stage, it could be postulated that let-7c-5p might play a role in immunoregulation rather than GVHD.

In this study, miR-503-5p was also overexpressed in the skin with histopathological aGVHD grades II-III in comparison to pre-transplant biopsies. Interestingly, its expression levels had a direct impact on OS, with lower expression of this miRNA improving survival. MiR-503 has been shown to regulate CD40 gene expression negatively when malignant human monocyte-derived cells (U937 cells) were irradiated (Cheng *et al.*, 2012). The function of CD40-CD40 ligand (CD40L) pathway has been investigated in GVHD models (Durie *et al.*, 1994). T and NK cells are activated when

CD40 and CD40L ligate as this results in the release of established pro-inflammatory cytokines such as IFN- $\gamma$ , IL-2 and IL-12 (Briones *et al.*, 2011). Studies have shown that anti-CD40L antibodies can decrease GVHD severity (Durie *et al.*, 1994). Activated CD4<sup>+</sup> T-cells express CD40L that can be targeted by anti-CD40L antibodies. These antibodies block CD4<sup>+</sup> T-cells, thus making them tolerant to host antigens and result in lower GVHD (Blazar *et al.*, 1998). Moreover, CD40 is also expressed in human keratinocytes in the skin (Denfeld *et al.*, 1996). Since, miR-503 and miR-424 are polycistronic they have very similar seed sequences. As a result, they have been shown to target the same genes and also be involved in the monocyte to macrophage differentiation in an AML cell line study (Forrest *et al.*, 2010). In a GVHD related study, the investigators showed that miR-424 levels are higher in cord blood CD4<sup>+</sup> and CD8<sup>+</sup> cells when compared to adult peripheral blood cells (Takahashi *et al.*, 2012). The authors also showed that miR-424 was over-expressed in adult blood CD14<sup>+</sup> monocytes when compared to CD4<sup>+</sup> and CD8<sup>+</sup> T cells (Takahashi *et al.*, 2012). It is known that during inflammation monocytes are recruited to the affected site and differentiate to either macrophages and/or DCs (as reviewed by (Ginhoux and Jung, 2014)). Several mechanisms of action could be proposed for miR-503-5p and its role in allo-HSCT and GVHD. Firstly, it could be overexpressed to target CD40 gene expression and thus inhibit T cell activation. Secondly, miR-503-5p expression levels might be up-regulated as more monocytes are recruited from the blood to host skin tissue.

Likewise, miR-365a-3p was under-expressed post-transplantation. Xu *et al.* (2010) have shown that miR-365a-3p is a negative regulator of IL-6, which is a cytokine involved in the control of immune responses (Akira *et al.*, 1990; Xu *et al.*, 2011). Studies have demonstrated that IL-6 levels are elevated at the time of aGVHD onset in the sera of patients (Symington *et al.*, 1992). Skin fibroblasts have also been shown to express IL-6 under inflammatory conditions (Koch *et al.*, 1993). It may be possible that because miR-365a-3p decline post-transplant, IL-6 levels increase in the aGVHD patients.

MiR-34a-5p was significantly differentially expressed between pre-transplant and Grade 0-I as well as Grade II-III skin biopsies ( $p < 0.01$ ). However, no significant difference was observed between mild and moderate aGVHD independent of the aGVHD grading system (overall clinical or skin histopathological) used for the analyses.

Results suggested that miR-34a-5p was up-regulated as a result of the allo-HSCT as well as inflammation due to GVHD. MiR-34a-5p was selected as the most suitable candidate for further investigation in order to determine its function in allo-HSCT and skin GVHD as; (1) results from the validation study of miR-34a-5p were promising in this cohort, (2) it was determined by miRwalk miRNA target prediction databases to target the GVHD associated genes previously identified by Norden et al (unpublished data) and (3) it is reported in the literature to be involved in GVHD severity of the gut (Wang *et al.*, 2013).

The penultimate hypothesis was that the miRNA expression in post allo-HSCT patients is associated with survival outcome. Therefore, to test it, validated miRNA expression levels from all the 12 miRNAs were included as variables in predicting post allo-HSCT outcomes (OS and relapse) in addition to the clinical risk factors that were identified as significant from univariate analysis.

The relationship between graft source (PBSC/BM) has been studied previously with reports indicating higher aGVHD risk for patients who had received PBSC with no improvement on survival outcome (Eapen *et al.*, 2007). Currently, PBSC is the most common graft source, and this was reflected in the patient cohorts evaluated in the skin survival study. In this study also there was no association between graft source and allo-HSCT outcome in particular since the majority had received PBSC. Historically, patient age has been associated with poor survival outcome (Lowenberg *et al.*, 1999) but with the changes in the transplant protocol more elderly patients are transplanted. In this study, the median age was greater than 45 years that by default scored the patients as high risk. Therefore, the age range of the EBMT risk score was not applicable in this cohort.

The comprehensive survival study supported the hypothesis as it showed that low expression levels of miR-503-5p and miR-34a-3p was indicative of improved OS outcome. Additionally let-7c-5p was associated with relapse and its expression had a protective effect. Quasi-complete separation was also observed in the expression levels of let-7c-5p that re-iterated its association with relapse. Competing risks analysis is performed to determine the probability of failure for a particular cause (event) in the

presence of other causes at a specific time-point post-HSCT. It was not feasible to perform competing risk analysis due to the few cases present per group.

To test the final hypothesis that miRNAs' interactions exist under pathophysiological conditions, all the miRNA expression levels were analyzed with advanced statistical tests (ordinal logistic regression, GLM). The finding that a significant interaction was present between miR-503-5p and miR-34a-3p and that it was distinctly evident when survival status was added onto 3D plots for visualization further supported the last hypothesis.

Studies have reported global profiling of miRNAs in plasma of patients with various aGVHD grades. The signature list of miRNAs identified in the study by Xiao *et al.* (Xiao *et al.*, 2013) in the plasma of allo-HSCT patients do not correspond with the list of miRNAs differentially expressed in this research (miR-423, miR-199a-3p, miR-93\*, and miR-377). Numerous investigations have shown that miRNAs are cell and tissue specific (Allantaz *et al.*, 2012). Thus, the lack of overlap between the two miRNA studies in skin and plasma support the cellular specificity of miRNAs. To my knowledge this is the only study that has investigated the expression of miRNA in the skin biopsy of aGVHD patients.

Skin is comprised of several different cellular layers. The uppermost layer is the epidermis that protects the body from harmful external attacks. Below is the dermis which contains APCs and lymphatic vessels. In this study whole skin biopsies were used for miRNA expression analysis (Pasparakis *et al.*, 2014). However, aGVHD mainly attacks the epidermal layer of the skin (Hofmeister *et al.*, 2004). Thus, the miRNA expressions observed are collective and may decrease the discriminatory specificity of the results. In addition, the proportion and types of cells in the epidermis and dermis are different. Disperse treatment is required to separate the epidermis from dermis. The effect of the disperse treatment on miRNA expression is unknown. Thus, it may be essential to assess the miRNA expression levels separately in each of the layers as well as the whole skin but to take into consideration the impact of disperse on the miRNA levels.

Furthermore, some of the patients in this cohort had sex-mismatched allo-HSCTs. The current finding of this study is not able to demonstrate whether miRNA expressions in the skin cells are recipient or donor origin. This issue may be partially addressed by a follow-up study showing the chimerism in skin sections and comparing it to miRNA expression results. However, the level of chimerism would only represent haematopoietic cells and their contribution to the overall miRNA expression.

In summary, this research has shown that miR-34a-5p, miR-503-5p, let-7c-5p and miR-365a-3p expression levels may be deregulated as a consequence of the transplant procedure (treatment) and the pathogenesis of aGVHD. Further investigation into the experimentally validated targets of miR-503-5p, let-7c-5p and miR-365a-3p may shed light on their impact at the protein level and their immunoregulatory roles in maintaining skin homeostasis. The targets of miR-503-5p, let-7c-5p and miR-365a-3p were not studied in this project due to time constraints. Thus, measuring the protein targets IL-10, IL-6 and CD40 were out of the scope of this investigation. MiR-34a-5p was the most significant miRNA in this investigation and selected for protein target investigation to elucidate its pro-apoptotic role in aGVHD, as pointed out in a recent literature (Ebner and Selbach, 2014). These preliminary results on allo-HSCT outcome based on the expression of miR-503-5p, miR-34a-3p and let-7c-5p are promising.

Overall, the result from the miRNA expression in the skin study is preliminary and is, therefore, only suggestive of their associations with allo-HSCT outcome. The results need to be validated in a larger, multicentre cohort to eliminate the impact of peri-transplant risk factors on the significance of the results. Also, access to cutaneous biopsies with severe aGVHD grades can further elucidate the role of the validated miRNAs in GVHD.

## **Chapter 5. The functional role of miR-34a in allogeneic haematopoietic stems cell transplantation**

“The journey of a thousand miles begins with one step.”

**-Lao Tzu**

## 5.1 Introduction

In Chapter 4, a global miRNA profiling experiment was performed to identify miRNAs associated with aGVHD incidence and severity. A signature miRNA list was identified and then validated by RT-qPCR. Results showed that miR-34a had the highest association with aGVHD severity based on the results of Chapter 4 and thus, was selected as the candidate miRNA for further downstream investigations.

MiR-34a has been extensively studied in numerous diseases and has established roles in cancers of the colon, lung, liver, myeloma and leukaemia (as reviewed by (Li *et al.*, 2014b)). Currently, a phase I clinical trial (NCT01829971) that aims to restore miR-34a levels in liver cancer is ongoing. MiR-34a is a member of the highly conserved miR-34 family which comprises of two other miRNAs; miR-34b and miR-34c. However, miR-34a is transcribed from a single gene (monocistronic) encoded on Chromosome 1, whereas miR-34b and miR-34c are transcribed from the same gene (polycistronic) on Chromosome 11 (Li *et al.*, 2014b) (Figure 1). All three members have the same miRNA seed sequence. Thus, they may regulate the same protein targets. The promoter regions of both miR-34 genes have a binding site for the tumour suppressor protein p53 (He *et al.*, 2007). In addition, CpG regions lie upstream of miR-34 genes and comprise areas of linear sequences wherein the cytosine and guanine nucleotides are separated from one another by just one phosphate molecule. Studies have shown that miR-34a is regulated in various ways; (i) genomic deletion (Attiyeh *et al.*, 2005), (ii) methylation of the CpG region (Lodygin *et al.*, 2008) and (iii) by transcription factors (Raver-Shapira *et al.*, 2007).

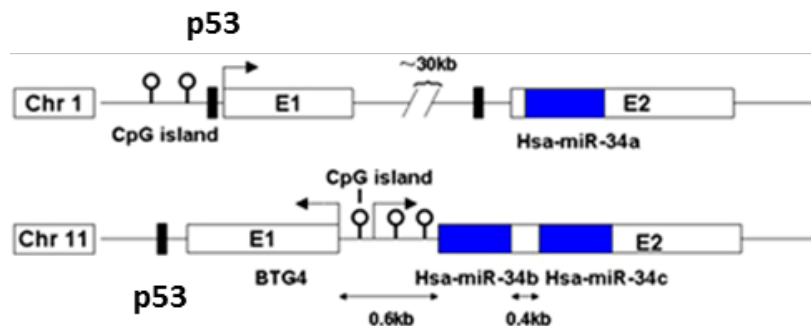


**Figure 5.1 Chromosomal location of miR-34 family** (adopted from (Li *et al.*, 2014b)). MiR-34a is transcribed from its gene on Chromosome 1 while miR-34b/c is encoded on Chromosome 11. The genomic loci of all the three members are Exon 2 (E2). The CpG regions are present prior to Exon 1 (E1) on Chromosome 1 while between E1 and E2 on Chromosome 11. Blue represents the miRNA hairpins. The p53 binding site is denoted by the black line which is upstream of E1.

A well-established transcriptional factor that regulates the miR-34 family is p53 (Raver-Shapira *et al.*, 2007). This is due to the p53 binding site present upstream of the miR-34 family genes (Raver-Shapira *et al.*, 2007). Reduced expression of miR-34a is commonly reported in cancers (lymphoma, colorectal) (Roy *et al.*, 2012; He *et al.*, 2013). Both miR-34a and p53 are proapoptotic and therefore may play a crucial role in the prevention of cancer (Raver-Shapira *et al.*, 2007; Wiggins *et al.*, 2010). P53 is central to the apoptotic pathway as it stops cells in the G1 phase of the cell cycle to prevent extension of DNA damage (Yonish-Rouach *et al.*, 1991). P53-mediated apoptosis occurs when the DNA damage cannot be repaired (Levine, 1997). It activates the miR-34 family, and this contributes to the promotion of apoptosis (Raver-Shapira *et al.*, 2007). In addition to activating miRNAs, p53 also plays a central role in the miRNA biogenesis pathway. In embryonic fibroblasts loss of Dicer1 (the enzyme essential for the production of the mature form of microRNAs), results in the development of p53 expression (Mudhasani *et al.*, 2008). P63 that is also a member of the p53 family regulates the expression of Dicer1 (Su *et al.*, 2010). P63 is

overexpressed in the epithelial cells of the skin and is required for the proliferative function of epithelial stem cells (Senoo *et al.*, 2007). In all, p53 is reported to control miRNA transcription, processing as well as miRNA target selection, as reviewed by (Rokavec *et al.*, 2014). In a study focused on aGVHD, miR-34a was shown to have a proapoptotic potential (Wang *et al.*, 2013). Patients with severe aGVHD had overexpression of miR-34a that correlated with the number of apoptotic cells counted in the patients gut tissues (Wang *et al.*, 2013). Moreover, miR-34a triggers the expression of p53 and Sirt1 (Yamakuchi and Lowenstein, 2009). Therefore, the convincing results of the afore mentioned (Wang *et al.*, 2013) study and the overexpression of miR-34a observed in Chapter 4, prompted further protein investigation of p53 by immunohistochemistry. The protein expression was, therefore, investigated in the same cohort discussed in Chapter 4, both in the pre- (n=5) and post allo-HSCT subjects (n=17). The skin FFPE block for one of the pre-transplant specimens was absent, hence sample size was reduced to five.

As mentioned earlier, p53 activates miR-34a and they both have proapoptotic functions. A recent proteomic study had shown that miR-34a suppresses c-MYC expression (Ebner and Selbach, 2014), this targeting can also be found by looking at the alignment sequence of the MYC gene on micrn.org. Interestingly, c-Myc has numerous functions in haematopoiesis such as regulating the HSCs regeneration and differentiation (Wilson *et al.*, 2004). c-Myc protein is a transcription factor that is constitutively expressed in many tumours (Jackstadt and Hermeking, 2014). c-Myc also impacts miRNA biogenesis steps in the nucleus (Jackstadt and Hermeking, 2014). It directly binds upstream of the miRNA gene, in the promoter region and regulates the transcription of the primary miRNA (Jackstadt and Hermeking, 2014). It can also repress miRNA generation via activating genes, such as Lin28, that inhibit the enzymatic processing of the miRNA (Chang *et al.*, 2009). Transcription of Drosha can be impaired by c-Myc that again impacts on miRNA processing (Wang *et al.*, 2013). Interestingly, c-Myc, p53 and miR-34a are all involved in the p53 pathway and the epithelial-mesenchymal transition network (Hahn *et al.*, 2013). To better understand the role of miR-34a in post allo-HSCT outcome, c-Myc protein expression was also investigated via immunohistochemistry. Figure 5.2 summarizes the interlinked regulation mechanisms of p53, miR-34a and c-Myc. In the context of allo-HSCT, p53

deficient mice that develop aGVHD have a better overall survival when compared to mice with at least one copy of the gene (Yada *et al.*, 2005). In this study, p53 promoted the activation of the death cell receptor, Fas that resulted in cellular toxicity and death in mice (Yada *et al.*, 2005).

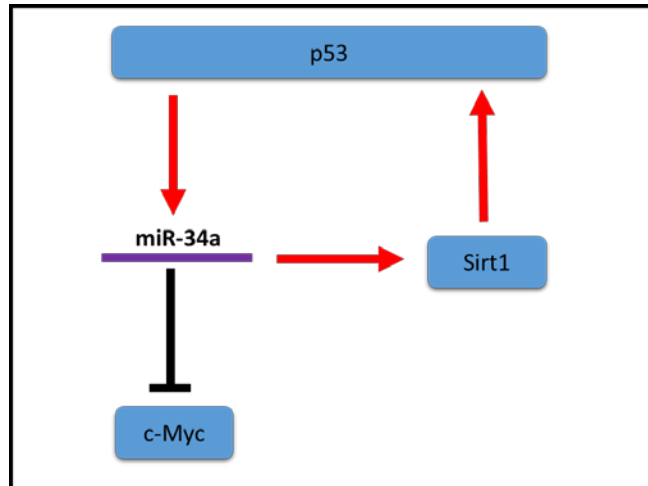


**Figure 5.2** **MiR-34a interactions with p53 and cMyc** (adopted from (Ebner and Selbach, 2014)). P53 activates miR-34a expression that targets c-Myc. MiR-34a can also activate p53 expression via Sirt1 (Yamakuchi and Lowenstein, 2009). Activation: ↑ and inhibition: —| .

### 5.1.1 Study hypothesis

MicroRNA targets are usually predicted using online databases such as [microrna.org](http://microrna.org) (Betel *et al.*, 2008) as mentioned in Chapter 1. The mRNA target levels may be determined using RT-qPCR and the corresponding protein levels by ELISAs (serum), immunocytochemistry (cells) or immunohistochemistry (tissues) depending on the target site (Bentwich, 2005).

In this Chapter, the expression levels of both miR-34a-5p and miR-34a-3p were tested for association with p53 and c-Myc protein expression (Figure 5.3, A). MicroRNA passenger strands (-3p) also share the same seed sequence as the guide strands (-5p) and this may lead to co-regulation of the target mRNAs (Ebner and Selbach, 2014). Therefore it was essential when assessing the relationships between miRNAs and protein targets, to test for both miR-34a (-5p and -3p) strands. MiR-34a expression levels were up-regulated post allo-HSCT and there was a significant trend with regards to aGVHD severity (Chapter 4). GVHD is mediated by the triggering of alloreactive T

cells and their proliferation that initially occurs in the lymphoid organs and their subsequent translocation into tissues such as the skin (Reddy and Ferrara, 2003). It was hypothesized that inhibition of miR-34a expression using miRNA inhibition approach in an allogeneic MLR may result in lower T cell proliferation and that this could be indicative of miR-34a involvement in aGVHD development and severity (Figure 5.3, B). Thus, miRNA inhibitors were used to compete with the endogenous miRNA in the RISC complex for binding to the 3' UTR of the mRNA target.

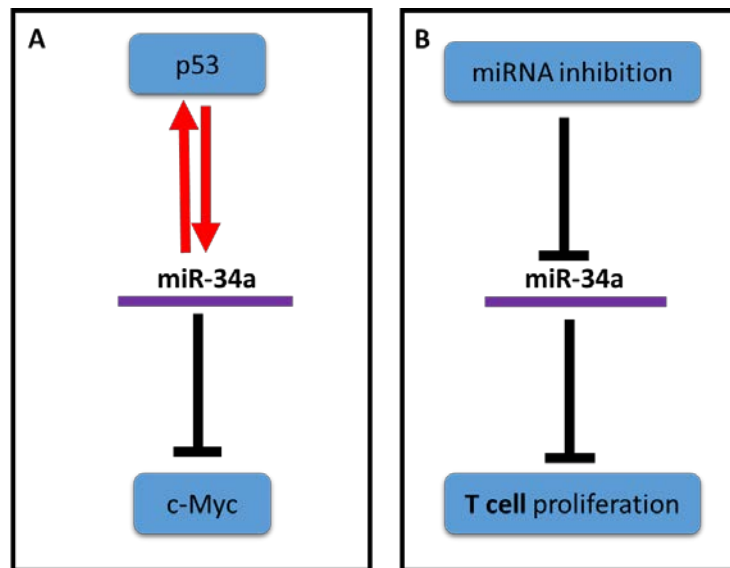


**Figure 5.3 Chapter 5 study hypothesis.** (A) P53 and c-myc protein expression levels are regulated by miR-34a expression. P53 and c-Myc expression levels were detected in skin by immunohistochemistry (B) T-cells proliferation is lowered by miR-34a inhibition. MiRNA inhibitors that competed with miR-34a levels were used for the inhibitory experiments. T-cell proliferation was detected by  $^3\text{H}$  Thymidine assay. Activation:  $\uparrow$  and inhibition:  $\text{—}|$ .

### **5.1.2 Specific study aims**

The aims of this investigation were as follows;

1. To test whether miR-34a expression correlated with p53 and/or c-Myc protein expressions.
2. To test whether miR-34a expression is involved in alloimmune response.
3. To conduct a preliminary investigation into the influence of miR-34a inhibition.

## 5.2 Results

### 5.2.1 Study cohort

MiR-34a protein targets; c-MYC and p53 were quantified in the aGVHD clinical skin biopsies with grades 0-III (n=17), as well as pre-transplant samples (n=5), via immunohistochemical methods.

In brief, for miR-34a inhibition experiments, transfection was initially optimised using a miRNA inhibitor hairpin transfection control (*C. elegans* non-targeting sequence) conjugated to a fluorescent tag (Dy547) to monitor levels of transfection efficiency. The miRNA inhibitor is complimentary to the endogenous miRNA sequence and therefore binds to the strand and prevents its loading onto the RISC complex. Electroporation was used for the transfection of PBMCs with the miRNA inhibitors and the negative control (for more details, see Chapter 2, Section 2.9.4).

### 5.2.2 Data analyses

The miR-34a-5p and miR-34a-3p expression values that were determined by RT-qPCR in the previous chapter (Chapter 4) were used for the correlation statistics. For details on the patient's characteristics, please see Chapter 4, Table 4.7.

The 'quick score' which is a semi-quantitative method was used for assessing the percentage of positively stained cells for both p53 and c-Myc proteins and a consensus score (average of two assessments) calculated as each section was assessed by two independent researchers, who were blinded to the origin of the samples.. The score for each biopsy was calculated by considering both the intensity and the proportion of cells within that intensity (for more details see Chapter 2, Section 2.12.2). The whole section was used for calculating the percentage positivity scores. Since miR-34a expression was quantified in both the epidermis and dermis, quick scores were calculated (1) for the entire section regardless of the layer and (2) in each layer individually.

### **5.2.3 Immunohistochemical analyses of c-Myc and p53 proteins**

#### **5.2.3.1 c-Myc and p53 positive-cells were present in cutaneous biopsies of allo-HSCT patients**

Immunohistochemical analysis was performed to test whether c-Myc and p53 proteins were expressed in cutaneous biopsies from allo-HSCT patients pre- and post-transplantation. Levels were associated with different skin histopathological aGVHD grades. Imaging and analysis of the skin sections showed that the majority of c-Myc-positive cells particularly those with high c-Myc intensity were present in the basement membrane of Grade 0 and Grade I aGVHD biopsies. In Grade II and Grade III, the complete epidermis was stained positive for c-Myc and very few negative ones. A limited number of cells demonstrated cytoplasmic only staining for c-Myc, while majority showed both cytoplasmic and nuclear staining. In general, the percentage of cells (positive and negative stained) that were present in the dermis was very low (4%) but as aGVHD severity increased from no aGVHD to Grade III, more cells were observed to be infiltrating the dermis (Figure 5.4).

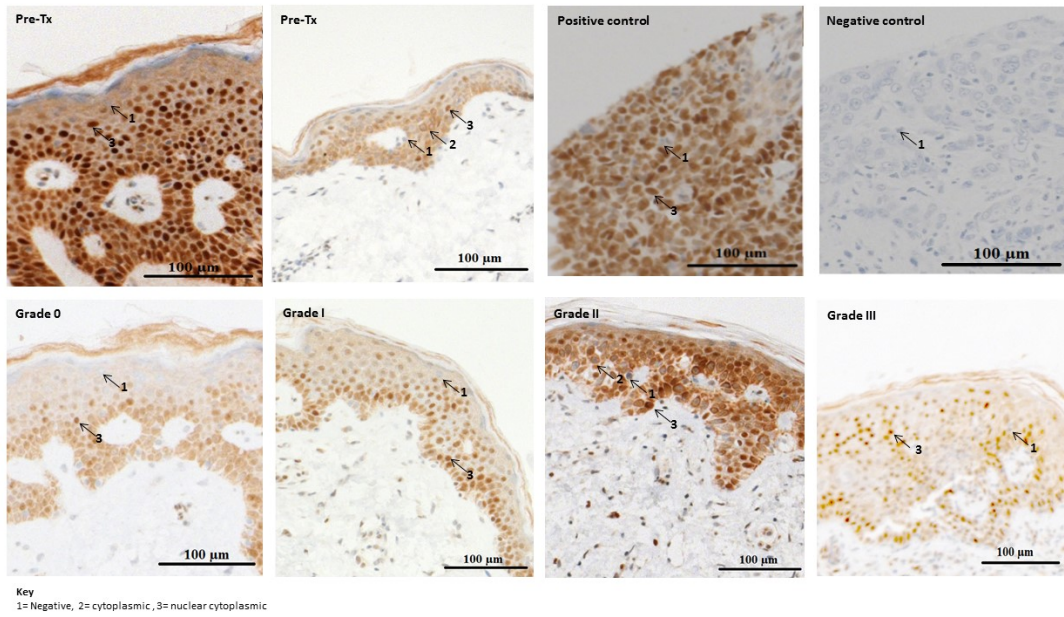


**Figure 5.4 Skin sections positively stained for c-Myc protein.** c-Myc- positive cells had variable expression intensities (low, moderate and high). No aGVHD biopsies had high intensity c-Myc-positive cells in the basement membrane, while in grades II-III aGVHD positivity c-Myc was observed throughout the entire epidermis. Positive-c-Myc proteins were also present in the pre-transplantation cutaneous biopsies. The first row shows the two pre-transplantation skin sections that were taken from the individuals assessed with cutaneous histopathological aGVHD Grade 0 and Grade I (second row), respectively. Breast carcinoma tissues were used as negative and positive controls. Grade III skin section exhibited the hallmark signs of severe cutaneous aGVHD with the initiation of separation between the epidermis and dermis. The number of cells that infiltrated the dermis gradually increased from no GVHD (Grade 0) to severe aGVHD (grade III). The images were taken at 20X magnification using AxioCamMR3.

Likewise, cells that positively stained for p53 protein were also analysed for observable differences between pre- and post allo-HSCT skin biopsies. Visualization of the sections showed positive cytoplasmic-nuclear staining for p53 under all histopathological conditions (pre-transplantation to Grade III aGVHD). P53-positive cells were localized in the epidermis (Figure 5.5). Under normal conditions p53-positive cells are confined to the basement membrane (Baran *et al.*, 2005). There was only an occasional cell in the dermis that was p53-positive. The majority of p53-positive cells stained with strong to moderate intensity.

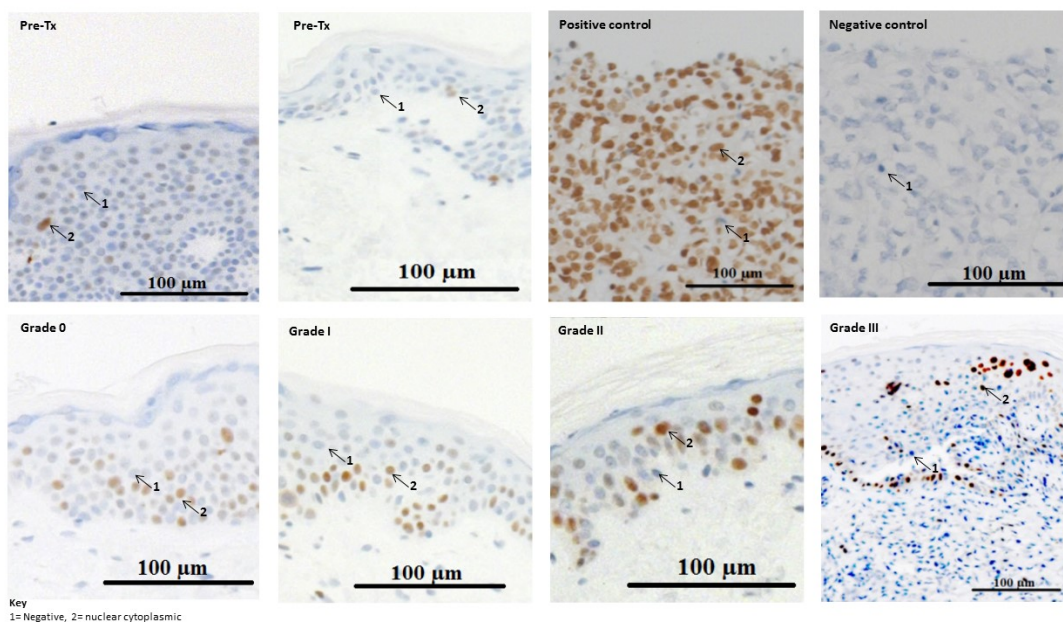


**Figure 5.5 Skin sections positively stained for p53 protein.** P53-positive cells were present in pre-transplantation skin biopsies but were limited in number. Strong positive signal was observed with aGVHD severity. The first row shows the two pre-transplantation skin sections that were taken from the individuals assessed with cutaneous histopathological aGVHD Grade 0 and Grade I (second row), respectively. Breast carcinoma tissues were used as a negative and positive control. Grade III skin section exhibited the hallmark signs of severe cutaneous aGVHD with the initiation of separation between the epidermis and dermis. The number of cells that infiltrated the dermis gradually increased from no GVHD (Grade 0) to severe aGVHD (grade III). The images were taken at 20X magnification using AxioCamMR3.

### **5.2.3.2 P53 positively correlated with miR-34a-5p expression**

The quick scores for c-Myc and p53 cell positivity and the miR-34a (-5p and -3p) expression levels were used to perform the Spearman correlation statistics. The total allo-HSCT cohort was used for the analyses (n=22). As mentioned earlier, the analyses were performed by firstly considering the proportion of positive cells in the entire section, followed by the dermis alone and finally the epidermis only.

In all the studies, results showed that there was no statistically significant correlation between miR-34a (-5p and -3p) expression levels and the proportion of c-Myc-positive cells ( $r_s=0$ ,  $p>0.05$ ). There was also no trend in the percentage of c-Myc-positive cells and this was confirmed by performing Jonckheere's trend test ( $p=0.988$ ).

The dermis had less than 4% p53-positive cells and was, therefore, considered as p-53 negative. Thus, for p53, the quick score was calculated only based on the epidermis. Interestingly, in the entire cohort (n=22) that included pre-transplant subjects, miR-34a-5p expression alone positively correlated with the percentage of p53-positive cells ( $r_s=0.44$ ,  $p=0.039$ ) in the epidermis (Figure 5.6, A). In post-allo-HSCT skin biopsies only (n=17), there was no significant correlation present between p53-positive cells and miRNAs. Non-parametric analysis of variance also showed borderline significant difference ( $p<0.5$ ) between the percentage p53-positive cells pre-transplantation and skin histopathological grades II-III. Jonckheere's trend test confirmed the significant ( $p=0.009$ ) trend towards higher p53-positive cells with aGVHD severity post allo-HSCT.

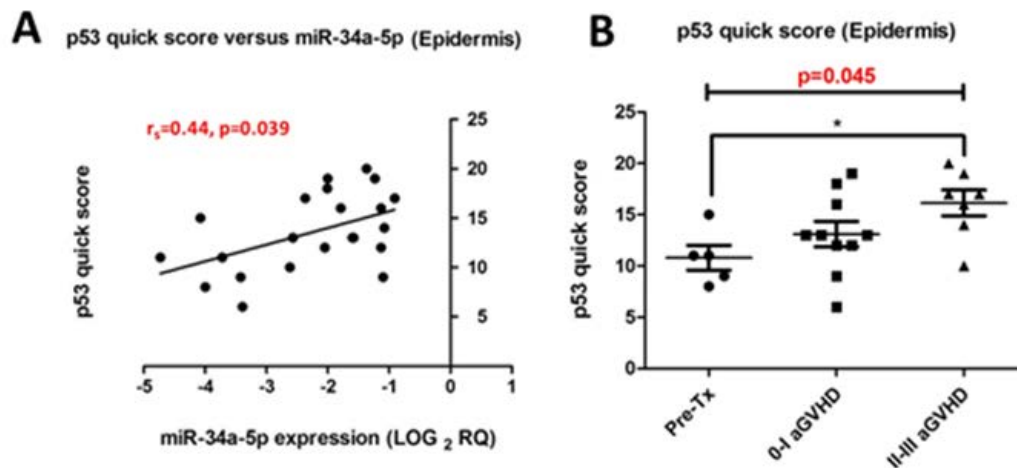


**Figure 5.6 p53 expressions in the epidermis positively correlated with miR-34-5p expression.** The proportion of cells positively stained for p53, (A) correlated in the epidermis with miR-34a-5p expression in the clinical skin biopsies (n=22), (B) p53-positive cells were significantly higher in the epidermis of skin biopsies with severe skin histopathological aGVHD grades (II-III) in comparison to pre-transplantation. Spearman correlation was used to calculate the coefficient of correlation ( $\rho = r_s$ ). Kruskal-Wallis analysis of variance was performed to determine the difference between the three groups. Significance was set at  $p < 0.05$ .

#### **5.2.4 Silencing the expression of miR-34a in primary peripheral blood mononuclear cells**

MiR-34a-5p expression results in Chapter 4 demonstrated an increased expression in cutaneous clinical biopsies post allo-HSCT in comparison to pre-transplantation. Therefore, to investigate the role of miR-34a its expression levels were inhibited in cryopreserved PBMCs using commercially available miR-34a-5p and miR-34a-3p specific inhibitors. Since miR-34a is expressed in several T cell subsets, PBMCs were the ideal source to perform the transfection study as it permitted the impact of inhibition to be investigated at a larger magnitude rather than a particular cell subset. In addition, current literature has shown that both fresh and cryopreserved PBMCs conserve their immune responses when the electroporation is used for transfection (Van Camp *et al.*, 2010).

The experiments in this section aimed to optimise the transfection technique that is required for functional confirmation of the findings of this thesis using *in vitro* techniques. For *in vitro* functional investigations, miRNA transfections were optimised, and their knockdown impact on T-cells investigated. The *in vitro* skin explant model was also evaluated, to test whether it could be employed for extended functional studies.

##### **5.2.4.1 PBMCs were viable post-transfection**

PBMCs were electroporated using three different voltages (330, 340 and 350 V) for transfection with the negative miRNA control. To ascertain that the PBMCs were not affected by electroporation, viability was assessed by standard cell counting methods (Trypan-blue exclusion) every 24 hours after transfection for up to six days. Cell viability was  $\geq 89.9\%$  in the transfected PBMCs (Figure 5.7). Pre-B 697 (leukemic cell line) was used as the positive transfection control and had a mean viability of 80.4%. Post 96 hours their viability had a sharp decline as the cells had reached post-confluence stage. PBMCs that were not electroporated were also cultured for six days as the microenvironment control and had a mean viability of 87.7%. Results showed that PBMCs electroporated at 330Vs had the highest viability.

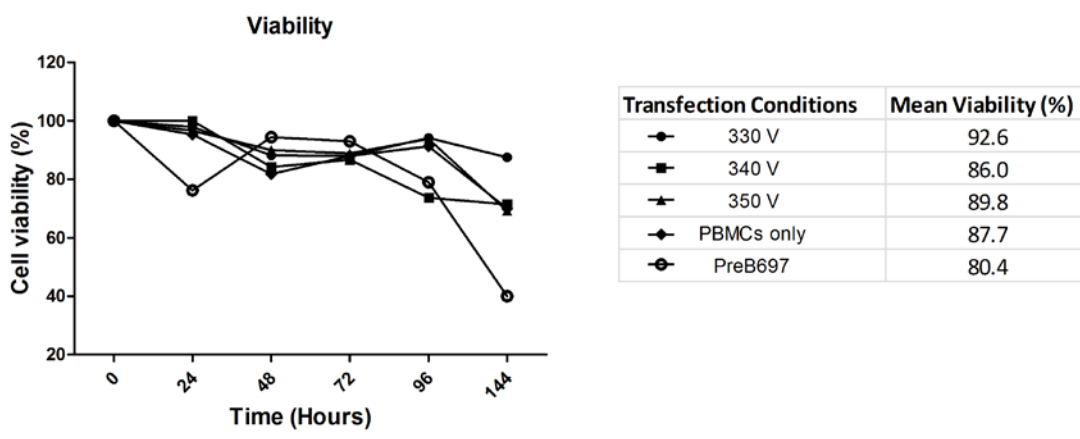


**Figure 5.7 PBMCs were viable post- transfection.** PBMCs were electroporated at three different voltages and cultured for six days to determine their percentage viability after electroporation and transfection. PBMCs were also cultured alone as a microenvironment control, and PreB697 was used as a positive control. The mean viability in the six days period is shown in the table and was highest for cells electroporated at 330 Vs.

**5.2.4.2 PBMCs had the optimal transfection when electroporated at 350Vs**

The optimal voltage for electroporation of the PBMCs was determined based on the percentage of cells transfected at three different voltages (330, 340 and 350 Vs). Transfection efficiency was determined based on the percentage of cells-positive per field of view. At 330 V and 340V, the transfection efficiencies were 40 and 38.7%, respectively. The optimal voltage was assessed as 350 Vs as the transfection efficiency was the highest at 60% (Figure 5.8).

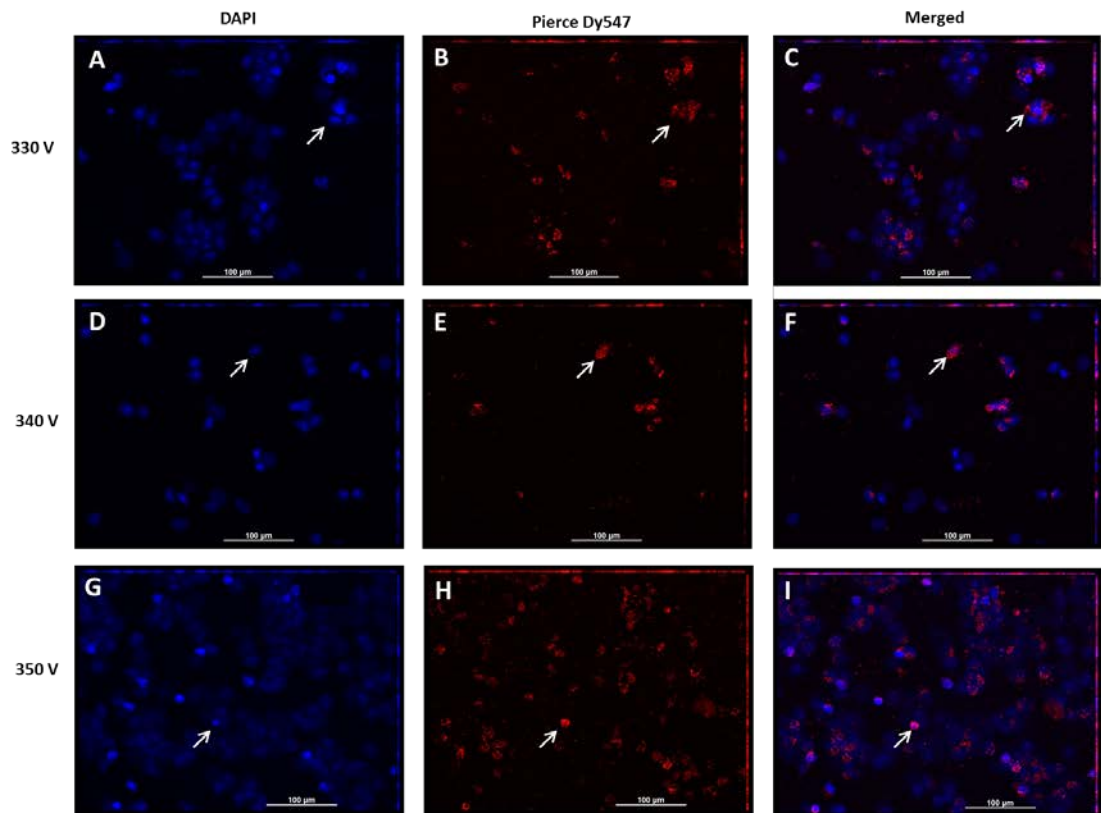


**Figure 5.8 Optimisation of the electroporation using different voltages.** PBMCs were transfected using miRNA inhibitor transfection control (500 nM) labelled with Pierce Dy547. Three different voltages were used for electroporation. Transfection efficiency at each voltage setting (A-C) 40% at 330 V, (D-F) 38.7 % at 340 V and (G-I) 60% at 350 V. The highest transfection was achieved at 350 Vs. The images were acquired using two filters after 24 hrs of transfection. The blue colour showed the staining with DAPI and the red colour for Pierce Dy547. The merged images show the transfected cells in pink and the blue nuclei. All the images were acquired at 20X magnification. The arrows show the representative transfected cells.

### 5.2.4.3 PBMCs had the highest transfection when 500 nM of miRNA inhibitor was used

The optimal concentration of miRNA inhibitor for transfection was also determined by using three different set concentrations of the inhibitor control (250, 500 and 750 nM). Using 250 nM and 750 nM of inhibitor, the transfection efficiencies were 10 and 30%, respectively. The optimal concentration was assessed as 500 nM as the transfection efficiency was 45% (Figure 5.9). There were a lot of background when using 700 nM that were due to the non-transfection of the inhibitor control.

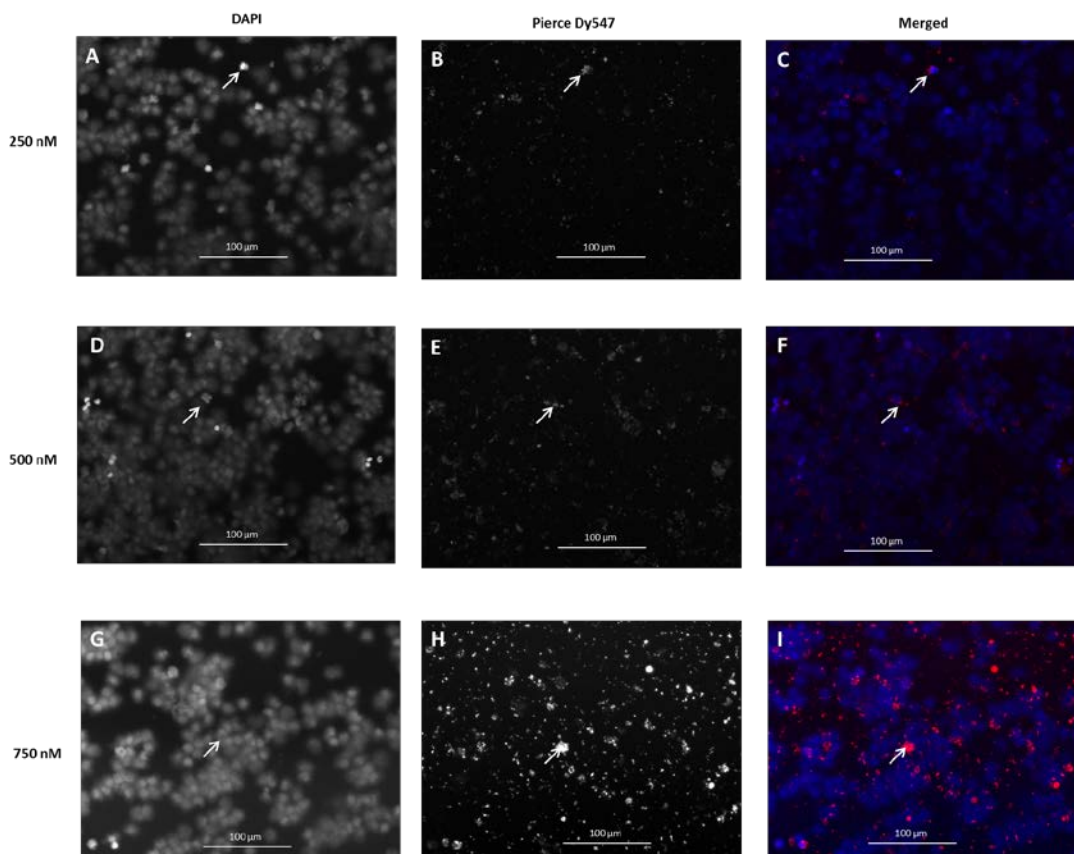


**Figure 5.9** Optimisation of the transfection using different concentrations of the inhibitor. Optimal transfection was achieved with 500 nM of miRNA inhibitor control. PBMCs were transfected using miRNA inhibitor transfection control (350 V) labelled with Pierce Dy547. Three different concentrations were used for transfection; (A-C) 250 nM, (D-F) 500 nM and (G-I) 750 V. The highest transfection was achieved at 500 nM. The images were taken using two filters after 24 hrs of transfection. The blue colour showed staining with DAPI and the red colour for Pierce Dy547. The merged images show the transfected cells in pink and the blue nuclei. All the images were taken at 20X magnification. The arrows show the transfected cells.

#### 5.2.4.4 Preliminary miR-34a knockdown results

Both miR-34a-5p and miR-34a-3p were inhibited in responder PBMCs using the optimised settings: 500 nM concentration of miR inhibitor and 350 V. Cells were harvested after 24 hours, RNA extracted and miR-34a levels assessed by RT-qPCR. Results showed that miR-34a-5p had a significantly higher level of knockdown relative to that of a non-targeting miRNA-construct, with 17.43%, SEM  $\pm$  3.4% ( $p < 0.0001$ ; paired t-test) residual miR-34a-5p remaining (Figure 5.10, A). By contrast, using the same optimised settings, miR-34a-3p failed to be knocked down significantly with 71.95%  $\pm$  10.92% (SEM) residual miR-34a-3p remaining when compared to that of the negative control. These results are preliminary and showed that miR-34a-5p could be inhibited significantly in PBMCs using a miRNA-specific inhibitor that competes with the endogenous miRNA. However, miR-34a-3p-knockdown in PBMCs requires further work to achieve optimal miRNA-reduction for future functional work.

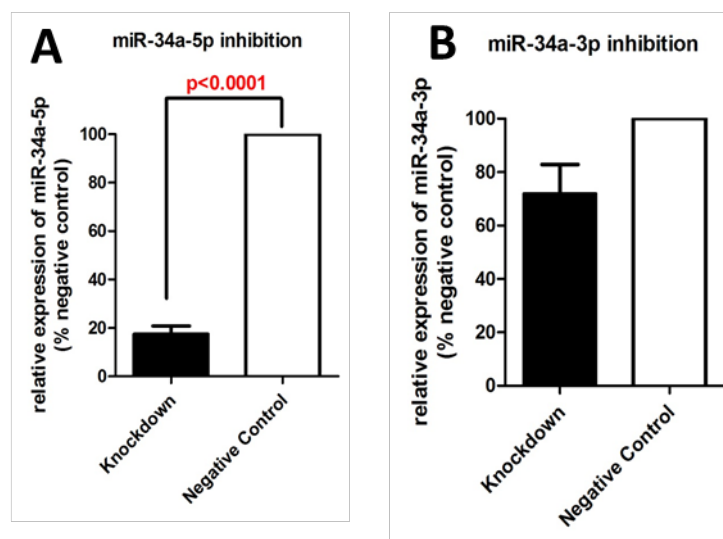


**Figure 5.10 MiR-34a-5p was significantly inhibited in primary PBMCs.** PBMCs were seeded at  $1 \times 10^7$  cells/ml and electroporated at 350 V with a miR-inhibitor concentration of 500 nM. Both strands of miR-34a (-5p and -3p) were knocked-down separately, using strand-specific miRNA inhibitors. Following a 24 hr incubation, cells were harvested, RNA extracted and RT-qPCR performed to assess the miR-34-5p and miR-34-3p expression. Data shows mean levels of expression  $\pm$ S.E.M of miR-34-5p (n=5; A) and miR-34-3p (n=2; B) expressed relative to the negative, inhibitor control.

#### ***5.2.4.5 Preliminary miR-34a-5p functional impact on T cell proliferation***

To assess the functional ability of responder cells when endogenous miR-34a-5p incorporation into the RISC complex was inhibited, mis-matched MLRs (n=2) were established and T cell proliferation was measured using the standard <sup>3</sup>H-thymidine T proliferation assay (Figure 5.11). Briefly, the <sup>3</sup>H-thymidine works by incorporating radioactive nucleoside thymidine into the DNA of dividing cells during cell division and the amount of radioactivity is proportional to the number of proliferating cells. Auto-MLRs were also set-up as the negative control for the MLRs. PBMCs were transfected as described above, using either the miR-34a-5p inhibitor or the non-targeting miRNA, and allowed recovery for 24 hours before co-incubation with an irradiated stimulator PBMC. After four days incubation, <sup>3</sup>H-thymidine was added and 18 hours later, the 96-well plate was harvested and each well was measured using a scintillation beta-counter. The preliminary results showed that the miR-34a-5p knockdown in responder PBMCs had the potential to reduce T cell proliferation in an allogeneic reaction, when compared to PBMCs transfected with a non-targeting miRNA inhibitor. It was not possible to calculate an accurate percentage of T cell inhibition as the sample size was very small (n=2).

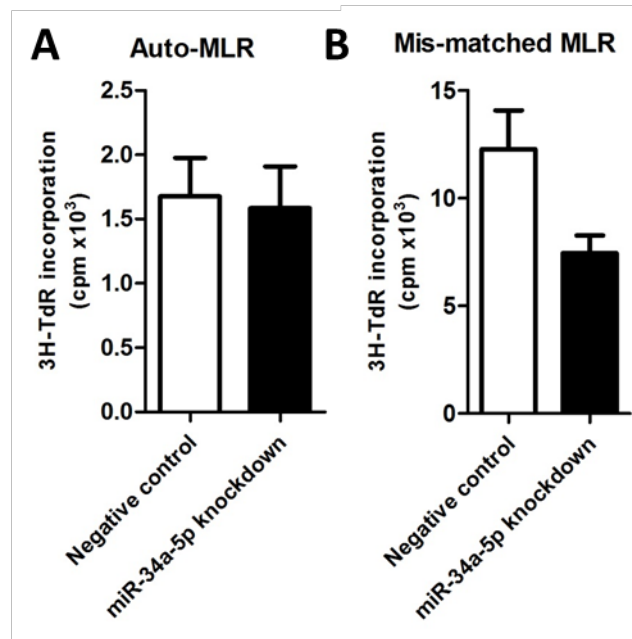


**Figure 5.11** MiR-34a-5p knockdown may result in lower T cell proliferation. T cells were tested for their proliferation ability when responder T cells were knocked-down in mismatched (n=2) and auto-MLRs, respectively. PBMCs were seeded at  $1 \times 10^7$  cells/ml and electroporated at 350 V with a miR-inhibitor concentration of 500 nM. MiR-34a-5p was knocked-down using strand-specific miRNA inhibitor.

#### 5.2.4.6 *MiR-34a* expression was not differential in the *in vitro* skin explant model with regards to GVHR severity

The *in vitro* human skin explant assay is a very useful research tool for investigating the expression of miRNAs, genes and/or the impact of drugs on the allogeneic response and the influence on GVHR severity. To test whether miR-34a expression was due to the MLR or the severity of the GVH reaction, the levels of both miR-34a strands (-5 and -3p) were quantified in time-course *in vitro* skin explant experiments (n=3-6). Results showed that both miR-34a strands were not significantly differentially expressed in the skin with GVHR grades II-III. The mean expression level of miR-34a-5p (-2.9) was higher when compared to miR-34a-3p (-9.4) levels in the *in vitro* skin explant assay. The same pattern of expression was also observed in the post allo-HSCT skin biopsies (mean expression of miR-34a-5p= -1.8 and miR-34a-3p=-6.4).

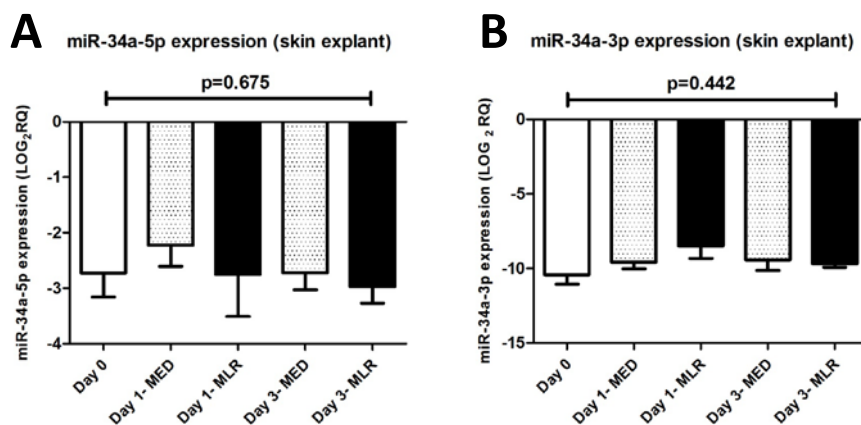


**Figure 5.12 MiR-34a expressions in the skin explant model.** Mis-matched *in vitro* skin explants were set up (n=3-6) for three days. MiR-34a expression was quantified by RT-qPCR on skin that was taken from the patient directly (Day 0) and added to the skin explant model. Skin biopsies were graded for GVHR by two independent researchers, blindly. Skin in medium only (MED) was the experimental control. All Day 1 skin biopsies (n=3) had grade I GVHR, and Day 3 (n=6) were assessed as grade 3 GVHR. Both (A) miR-34a-5p and (B) miR-34a-3p did not show any deregulation in expression under any condition. Kruskal-Wallis ANOVA was performed for all expression analyses.

#### **5.2.4.7 Stimulation with Cyclosporine A had no direct impact on miR-34a expression levels**

Since no difference in miR-34a expression levels were found in the *in vitro* skin explant model between biopsies collected pre-transplantation (Day 0), GVHR grade I (Day 1) and GVHR grades II-III (Day 3), it was hypothesized that the deregulation observed in patient biopsies might be due to Cyclosporine A. This is a GVHD prophylaxis treatment and routinely administered to allo-HSCT 1-2 days prior to transplantation and continues up to several months post-transplantation. Thus, the effect of Cyclosporine A on miR-34a expression levels was assessed by setting up mis-matched MLRs co-cultured with four different concentrations of Cyclosporine A over 96 hrs time-period. Mis-matched MLRs were the experiment and unstimulated auto-MLR acted as a control for allogeneic response. The set concentrations were selected based on a previous study (Petropoulos and University of Newcastle upon Tyne. Institute of Cellular Medicine, 2010) that had shown the inhibitory effect of Cyclosporine A on T cells using 10 different Cyclosporine A concentrations (2-1000 ng/ml). This study showed that using 50 ng/ml approximately inhibited T cell proliferations by 70% and incubation with 200 ng/ml resulted in almost 90% inhibition. To try and increase inhibition to 100%, Cyclosporine A concentration of 300 ng/ml was included in this test. Allo-HSCT patients have their target Cyclosporine A trough concentration at ~200-250 ng/ml and therefore this was included as one of the doses in this experiment. Unstimulated MLRs were also setup without any Cyclosporine A (0 ng/ml) as a negative control. Results showed that there was no statistically significant difference in both miR-34a-5p and miR-34a-3p expression level with any Cyclosporine A dose (Figure 5.13).

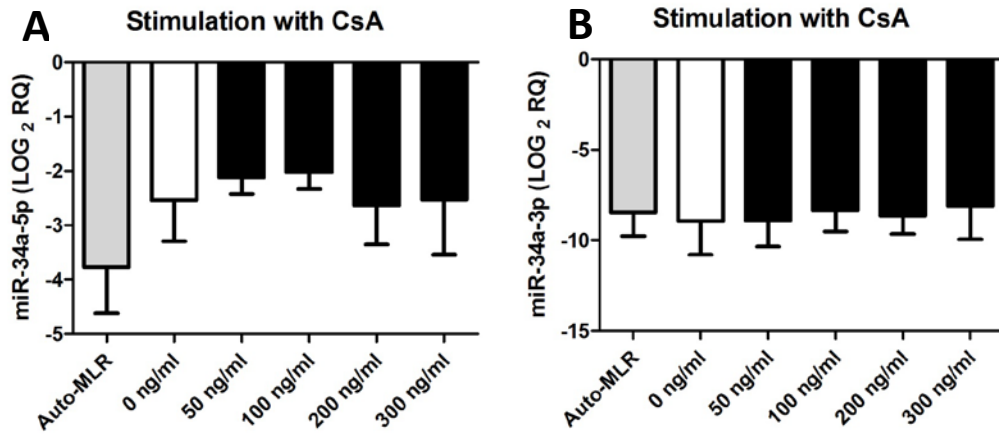


**Figure 5.13 MiR-34a expression is not influenced by Cyclosporine A.** Standard MLRs (n=3) were set up co-cultured with different doses of Cyclosporine A (50-300 ng/ $\mu$ l) for 96 hrs. Mis-matched MLRs were the experiments while auto-MLRs acted as the negative controls (A) miR-34a-5p expression was not altered by different concentration of Cyclosporine A in the MLR reaction (Kruskal-Wallis p=0.909) and (B) miR-34a-3p was also not effected by Cyclosporine A (Kruskal-Wallis p=0.980). Allo-MLR: mis-matched MLRs.

### 5.3 Discussion

The epidermal layer of the skin is the primary target site for GVHD-mediated damage in particular the basal cells that line the basement membrane. MiRNA target protein detection experiments were performed using immunohistochemistry, to understand the impact of miR-34a in allo-HSCT procedure and GVHD. Studies have shown the existence of a positive feedback loop between p53 and miR-34a (Yamakuchi and Lowenstein, 2009). Likewise, c-Myc expression is regulated by miR-34a expression (Ebner and Selbach, 2014).

Thus, both p53 and c-Myc positive-cells were scored in the skin biopsies of patients pre- and post allo-HSCT. This study showed that c-Myc and p53 positive-cells were present in cutaneous biopsies of allo-HSCT patients. The proto-oncogene c-Myc is involved in numerous processes such as differentiation, apoptosis and cellular proliferation (Schuhmacher *et al.*, 1999; Pelengaris *et al.*, 2002). However, in this study no significant correlation or association was determined between miR-34a and c-Myc-positive cells.

P53 has a very short half-life and for this reason immunohistochemical methods are mainly able to detect its stimulated or mutated form only (Hainaut and Hollstein, 2000). Constitutive expression of p53 is present in most cells (Hainaut and Hollstein, 2000) and it is usually activated only when there is (1) DNA damage, (3) cellular stress due to oncogenic proliferation signals that result in the expression of Myc and (4) therapeutics (chemotherapy drugs, irradiation) (Lowe and Lin, 2000; Vogelstein *et al.*, 2000). There was significant positive correlation between p53-positive cells and miR-34a-5p expression levels only. This result is in support of the p53 positive feedback loop with miR-34a (Yamakuchi and Lowenstein, 2009). P53-positive cells were observed even in pre-transplantation skin biopsies, and there was a significant trend in the score of positive-cells with aGVHD severity. Taken together, these results may suggest that pre-transplant activation of p53 is due to the conditioning regimen, which is not sufficient to trigger miR-34a-5p overexpression. In the post allo-HSCT skin p53 is over-expressed due to the therapeutics as well as the GVH reaction, which leads to higher miR-34a-5p expression and therefore their positive correlation. This may also be suggestive of the higher incidence of apoptosis observed in severe aGVHD skin.

Moreover, miR-34a is also regulated by p63 that is an additional member of the p53 family. In the skin, p63 is essential for the proliferation of keratinocytes (Senoo *et al.*, 2007). A study has shown that miR-34a expression is up-regulated in epidermal cells when p63 expression is repressed (Antonini *et al.*, 2010). The same study highlighted that in murine skin, there was lower miR-34a expression in the hair follicles in comparison to the epidermal layer (Antonini *et al.*, 2010). P63 is targeted by another skin related miRNA, miR-203 (Lena *et al.*, 2008). This may suggest a stepwise distinct regulatory mechanism in the skin whereby miR-203 and miR-34a expression control keratinocyte proliferation (Antonini *et al.*, 2010). However, in the cutaneous miRNA study in Chapter 4, miR-203 was not differentially expressed. In addition, excessive keratinocyte proliferation is not an attribute of cutaneous aGVHD. This further supports that miR-34a-5p overexpression may be due to the activation of p53 apoptosis pathway rather than p63.

In the context of allo-HSCT and GVHD, TCR are stimulated during the GVH cycle when the HLA mismatches are recognized. This results in partial activation of the T-cells (Baxter and Hodgkin, 2002). Recently, it has been shown that overexpression of miR-34a is related to higher T cell activation by TCR. The positive correlation between miR-34a expression and TCR stimulation has been linked to diacylglycerol kinase-zeta (DAGK-  $\zeta$ ), which is an enzyme responsible for metabolising DAG (Shin *et al.*, 2013). Lower DAGK-  $\zeta$  results in higher T cell activation as the cells become sensitive to TCR triggers. It has been demonstrated that miR-34a directly targeted DAGK-  $\zeta$  mRNA and therefore this leads to more un-metabolised DAG, which stimulated TCRs leading to enhanced T cell activation (Shin *et al.*, 2013). Phorbol myristate acetate (PMA) is an analogue of DAG and has been extensively used for the stimulation and activation of TCR. To test whether the miR-34a overexpression is also due to TCR activation in addition to the overexpression of p53, it would be interesting to use PMA as the stimulator and then measure both miR-34a expressions by RT-qPCR and TCR activation (CD25+) by flow cytometry.

To address the question of whether miR-34a inhibition had an influence on T-cell proliferation, preliminary optimisation experiments were performed to silence the expression of miR-34a in PBMCs. PBMC viability was checked post transfection and showed that the introduction of the inhibitors did not increase cell death. PBMCs were

shown to be successfully transfected with 500 nM miR-34a-5p inhibitors using electroporation methods set at 350Vs. Preliminary T cell proliferation results also looked promising as they showed a trend to lower T cell proliferation when miR-34a-5p was inhibited. However, additional supplementary tests are required in order to enable statistical analysis of the percentage T cell inhibition.

Moreover, miR-34a expression was also tested in an *in vitro* skin explant model to test for differential expression levels as a result of GVHR severity. The results showed that the miR-34a expression was not deregulated in the *in vitro* skin explant model with regards to GVHR severity. This result may be suggestive that the deregulated miR-34a expression that was observed in the clinical skin biopsies was not due to the allogeneic GVH reaction alone, but due to a cumulative effect of the transplantation procedure, the GVH reaction and prophylaxis. In all, it may suggest that in order to use the *in vitro* skin explant model to investigate miRNA functional mechanisms, the assay would need to be optimised for the respective applications such that it reflects more accurately the *in vivo* conditions.

As miRNAs are very sensitive and may be affected by prophylactic therapy, MLRs stimulated with different doses of Cyclosporine A were set-up. Interestingly, miR-34a expression was not influenced by the different doses of Cyclosporine A even though high doses are indicative of increased T cell inhibition which was hypothesized to result in lower miR-34a expression. The influence of drugs on miR-34a expression would need to be further studied to better understand the metabolism of action in such instances.

In order to better understand the function of miR-34a with regards to T cells, the functional work needs to be further extended. This requires the optimisation of miR-34a-3p such that higher knocked-down percentages are obtained as well as setting up assays where both the strands of miR-34a are inhibited. In addition, the miR-34a target, p53 needs to be assessed pre- and post-inhibition of miR-34a-5p using RT-qPCR to elucidate the downstream impact of inhibition. Luciferase reporter assays could also be incorporated into the study to show the direct targeting of p53 by miR-34a-5p.

In summary, results of this Chapter have shown that miR-34a-5p expression is positively correlated with p53-positive cells and that c-Myc may not be a direct target

of miR-34a under allo-HSCT condition. The miRNA inhibition experiments have established the optimal conditions required for future transfection studies involving miRNA inhibitions for allogeneic experimental conditions.

## **Chapter 6. Expression of MiRNAs with Specific Immune Functions in the Whole Blood of Allo-HSCT Patients**

“Science is a way to teach how something gets to be known; what is not known; to what extent things are known (for nothing is known absolutely); how to handle doubt and uncertainty; what the rules of evidence are; how to think about things so that judgements can be made; how to distinguish truth from fraud and from show.”

**-Richard Feynman**

## 6.1 Introduction

Body fluids such as serum (Mitchell *et al.*, 2008), plasma (Liu *et al.*, 2012), urine (Wang *et al.*, 2010), bone marrow (Dostalova Merkerova *et al.*, 2011) and whole blood (Viprey *et al.*, 2012) have extensive miRNA profiles that directly pertain to the type of disease, its progression and outcome. Moreover, miRNA investigations have identified miRNA signatures for numerous diseases such as breast cancer, lymphomas and rheumatoid arthritis as well as more recently for GVHD (murine models) (Ranganathan *et al.*, 2012; Xiao *et al.*, 2013; Stickel *et al.*, 2014) (for more detail on miRNA-based GVHD biomarkers see Chapter 1). Thus, identifying miRNAs that play a significant role in the onset and severity of GVHD can assist the monitoring and prognosis of this potentially fatal complication. Additionally, finding a signature list of miRNAs to predict GVHD onset can help treatment strategies for improved outcomes and reduce healthcare costs. Since miR-146a and miR-155 are both involved in the adaptive and innate immune system (Lindsay, 2008; Pauley *et al.*, 2008) it was discerned of great interest to assess their dual function in allo-HSCT and in particular, aGVHD. The aim was to provide a more meaningful picture of their involvement in this pathophysiologically complex disease condition. In this investigation, miRNA expression levels were detected in whole blood collected in PAXgene tubes. Whole blood study can be easily extended for clinical applications due to less invasiveness of the procedure and the reduced sample processing time. Since miRNAs are present in almost every cell type and even in extracellular vesicles, such as, the exosomes, whole blood studies provide a more complete picture of the deregulation present under normal and diseased conditions.

### 6.1.1 Immune specific miRNAs: miR-146a and miR-155

MiR-146 plays a role in the immune system. This miRNA is monocistronic, and two copies of its genes are present; miR-146a and miR-146b (Labbaye and Testa, 2012). MiR-146a gene is located on chromosome 5 while the gene encoding miR-146b is located on chromosome 10 (Griffiths-Jones *et al.*, 2006; Kozomara and Griffiths-Jones, 2014). MiR-146a and miR-146b only differ by two nucleotides which makes them structurally similar. MiR-155 is monocistronic and encoded by the *bic* gene on

chromosome 21 (Griffiths-Jones *et al.*, 2006; Lindsay, 2008; Kozomara and Griffiths-Jones, 2014). There exists comprehensive literature on both miRNAs, as they have been studied extensively in numerous biological processes and diseases. This section aims to cover the most relevant literature with an emphasis on the mechanisms of action that have been thoroughly investigated to-date.

#### **6.1.1.1 *MiR-146a function and known mechanism of action***

MiR-146a is essential for Treg function (Lu *et al.*, 2010). Studies in psoriasis showed that the miR-146a indirectly affected the tumor-necrosis factor-alpha (TNF- $\alpha$ ) pathway (Taganov *et al.*, 2006) leading to disease development. MiR-146a has been demonstrated to target several genes: IRAK1, TRAF6, IL8, IL6, and CXCR4 (Taganov *et al.*, 2006; Bhaumik *et al.*, 2008; Labbaye *et al.*, 2008). TRAF6 and IRAK1 have been reported as the primary targets of miR-146a (Taganov *et al.*, 2006) and regulates their expression in a negative feedback-loop via the TLR-4 signaling pathway and NF $\kappa$ B activation (Taganov *et al.*, 2006; Taganov *et al.*, 2007) (Figure 6.1). TRAF6 exhibits important functions in the development and role of various haematopoietic cells (Choi, 2005) while IRAK1 plays a role in autoimmunity via miR-146a (Deng *et al.*, 2003).

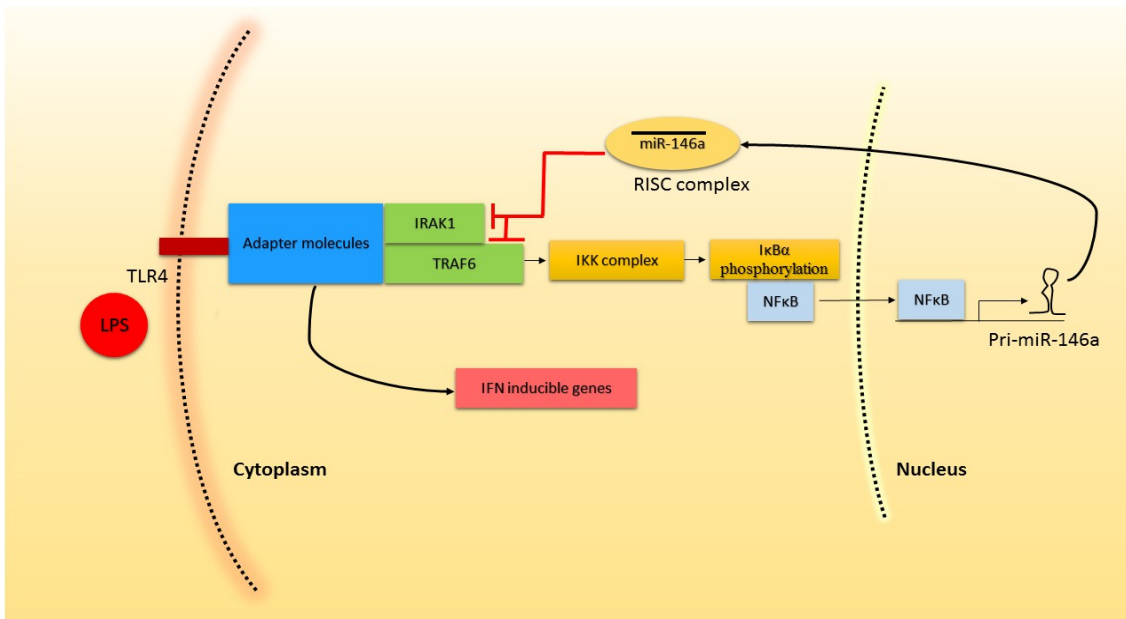


**Figure 6.1** **MiR-146a negatively regulates TRAF6 and IRAK via the TLR4 signalling pathway and NFκB activation** (adopted from (Rusca and Monticelli, 2011) and (Taganov *et al.*, 2007)). LPS stimulates TLR4 receptor which leads to a subsequent activation and expression of adaptor molecules, IRAK1 and TRAF6. This results in the activation of the IκB kinase (IKK complex) that promotes phosphorylation of the inhibitor of kappa B (IκBα). NFκB is then activated and translocates into the nucleus propagating miR-146a gene transcription. The pri-miR-146a then undergoes several enzymatic processes both in the nucleus and cytoplasm via its biogenesis pathway. The mature miR-146a then binds to the RISC complex that directs it to its targets TRAF6 and IRAK1. Binding of miR-146a either causes mRNA degradation or translational inhibition of both targets depending on the particular inflammatory condition (Rusca and Monticelli, 2011). In parallel to this negative feedback regulation, the activation of adaptor molecules also leads to the transcription of IFN-inducible genes such as CXCL10 and CCL5 (Hirotsani *et al.*, 2005). The triggering of the TLR signaling cascade can lead to control of inflammation as well as its exacerbation when multiple factors cease to function normally.

In addition, IFN regulatory factor 5 (IRF5) and signal transducer and activator of transcription 1 (STAT1) are known validated targets of miR-146a (Tang *et al.*, 2009). Tang *et al.*, showed that over-expression of miR-146a lowered STAT1 and IRF-5 both at the molecular and protein level which further confirmed the two genes as targets of miR-146a (Tang *et al.*, 2009). In a murine gene expression study of GVHD, it has been shown that the levels of Stat1 were elevated post-transplantation and it may be due to lower miR-146a expression (Sugerman *et al.*, 2004). Moreover, it has been shown in mice that miR-146a depleted Treg cells have high levels of Stat1 and this results in IFN- $\gamma$  mediated autoimmunity (Lu *et al.*, 2010) (Figure 6.2).

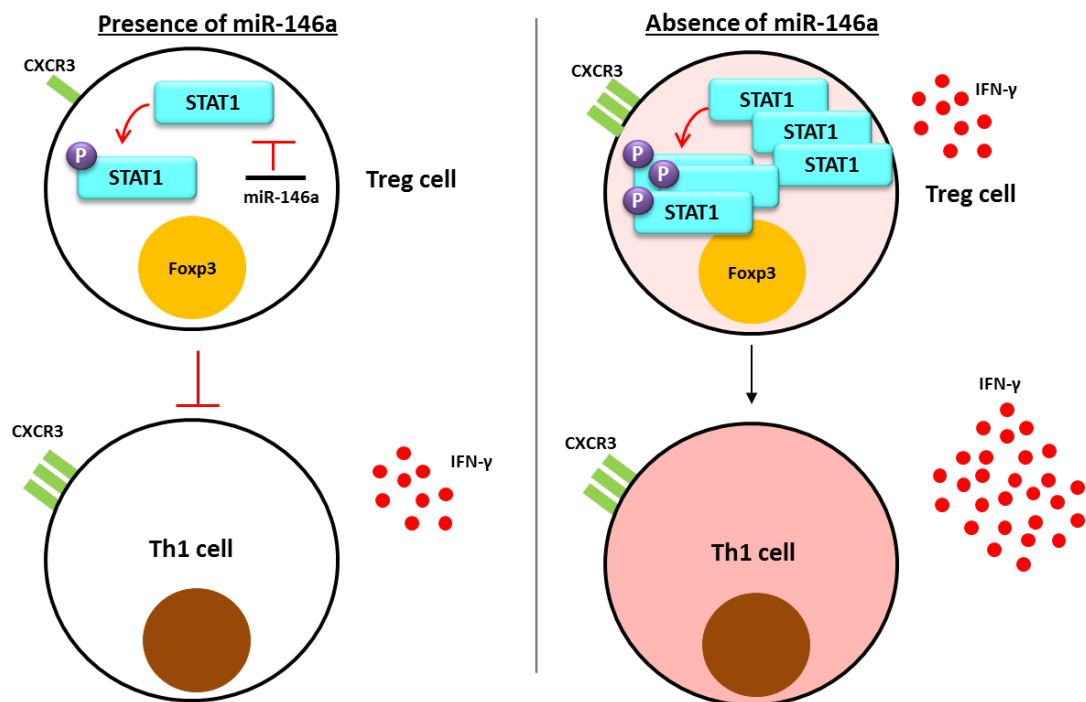


**Figure 6.2** MiR-146a is required to prevent Th1-mediated immune response (adopted from (Lu *et al.*, 2010)). Phosphorylation of STAT1 is essential for Th1 effector cells to differentiate. The effect of miR-146a presence is shown on the left and its absence on the right. In the presence of miR-146a in Treg cells, STAT1 expression is regulated, and this prevents Th1 mediated immune response. In the absence of miR-146a, STAT1 is overexpressed, and this propagates Th1 effector cells to differentiate excessively, which leads to inflammation in a Th-1 mediated manner. This deregulation results in high secretions of IFN- $\gamma$  both in the Treg cells as well as from Th1 effector cells (Lu *et al.*, 2010).

Further studies have also shown that IL-6 and IL-8 are negatively regulated by the expression of miR-146a (Perry *et al.*, 2008; Bhaumik D, 2009). MiR-146a also targets chemokine receptor CXCR4 (Labbaye *et al.*, 2008). In all, miR-146a has also been implicated in the pathogenesis of other autoimmune diseases (Sonkoly *et al.*, 2008) such as RA (Pauley *et al.*, 2008) and SLE (Tang *et al.*, 2009) as well more recently in mouse GVHD model (Stickel *et al.*, 2014). Table 6.1 shows a summary of the significant roles of miR-146a and its various immune-related functions. Hence, one of the primary focus of this investigation was on the expression of miR-146a and four of its validated targets (IRAK1, TRAF6, STAT1- $\alpha$  and TRAF6) because of their known functions in both the adaptive and innate immune system.

MiR-146a expression and function	Validated targets	References
Attenuated TLR4 signaling in monocytes	IRAK1, TRAF6	(Taganov <i>et al.</i> , 2006)
Contributed to the establishment of endotoxin tolerance in monocytes	IRAK1, TRAF6	(Nahid <i>et al.</i> , 2009)
Desensitized Langerhans cells to inappropriate TLR signaling		(Jurkin <i>et al.</i> , 2010)
Controlled megakaryopoiesis	CXCR4	(Labbaye <i>et al.</i> , 2008)
SNP in pre-miR-146a predisposes to papillary thyroid carcinoma		(Jazdzewski <i>et al.</i> , 2008)
In GVHD, regulation of TRAF6 in donor T cells	Traf6	(Stickel <i>et al.</i> , 2014)
Differential expression in Th1/Th2 cells		(Monticelli <i>et al.</i> , 2005)
Impaired Treg function in mice lacking miR-146a	Stat1	(Lu <i>et al.</i> , 2010)

**Table 6.1 Summary of miR-146a functions and relevant, validated targets** (adopted from (Rusca and Monticelli, 2011)).

### 6.1.1.2 MiR-155 functions and known mechanism of action

MiR-155 is required for the normal function of B and T lymphocytes in humans (Stauffer *et al.*, 2010). Macrophages and DCs also express miR-155 (O'Connell *et al.*, 2007). In a small cohort (n=5) it has been shown that it is overexpressed in the gut of aGVHD patients while expression is absent in normal gut (Ranganathan *et al.*, 2012). MiR-155 is necessary for CD8+ T cell proliferation and its deficiency can lead to the overexpression of STAT1, which has anti-proliferative functions in T cells (Tanabe *et al.*, 2005; Gracias *et al.*, 2013). Myeloid cell development encompasses several regulatory mechanisms, one of which is miRNA interactions (Figure 6.3). MiR-155 switches the differentiation and activation of the cells during this development cycle. It repress PU.1

that is a primary myeloid transcription regulator (Vangala *et al.*, 2003). Table 6.2 shows a summary of the major roles of miR-155 with various immune-related functions. Interestingly, this miRNA also prevents IFN- $\gamma$  signaling in CD4+T cells by targeting IFN- $\gamma$ Receptor alpha-chain (Banerjee *et al.*, 2010).

MiR-155 expression and function	Validated targets	References
B cell maturation, homeostasis and hematopoiesis	PU.1, SHIP1	<a href="#">(Thompson et al., 2011)</a>
CD4+ T cell differentiation	SOCS1	<a href="#">(Wu et al., 2012)</a>
Acts as oncogene by targeting pro-apoptotic transcripts		<a href="#">(Zhang et al., 2014)</a>
Overexpression in the gut of aGVHD patients		<a href="#">(Ranganathan et al., 2012b)</a>

**Table 6.2** Summary of mir-155 functions and relevant, validated targets adopted from (Tili *et al.*, 2009))

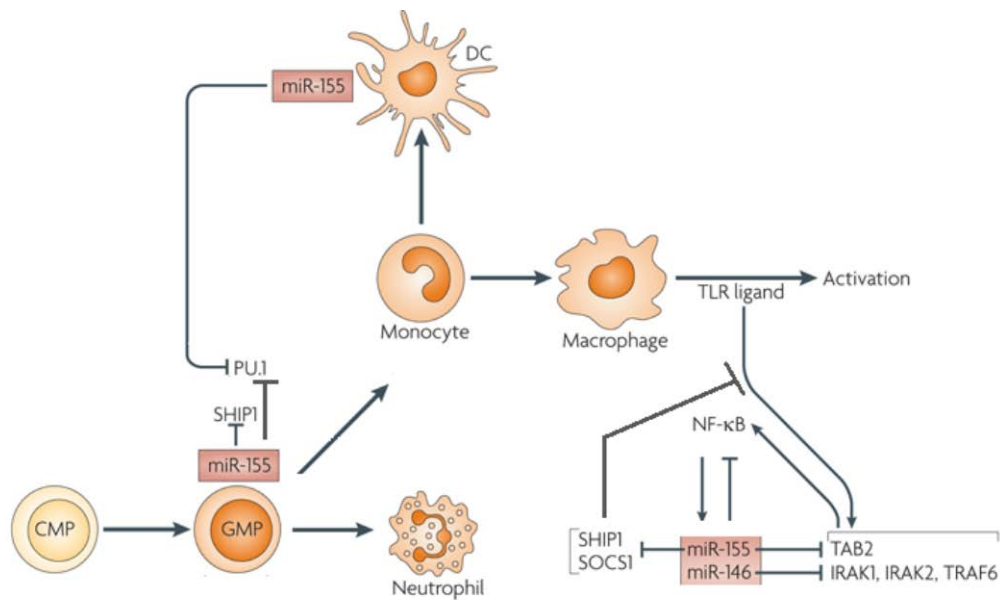


**Figure 6.3 MiR-155 is involved in myeloid cell development** (adopted from (O'Connell *et al.*, 2010)). Myeloid cell development is regulated by miRNAs and transcription factors such as PU.1. CMPs differentiate to GMP that produces monocytes and neutrophils. Monocytes then differentiate to macrophages and/DCs. MiR-155 targets SHIP1 and PU.1 thereby influencing the differentiation and activation of GMP and DCs. Likewise, it can both activate and repress the NFκB pathway. It also targets SOCS1 that represses the TLR activation. MiR-146a has a lower impact in myeloid cell development and is mainly involved in regulating inflammatory responses via TLR (O'Connell *et al.*, 2010). Abbreviations: - CMP: Common Myeloid Progenitors; GMP: Granulocyte-Monocyte Progenitors; SHIP (INPP5D): Inositol polyphosphate-5-phosphatase; PU.1 (SPI1): Spi-1 proto-oncogene; TLR: Toll-Like Receptors; SOCS1: Suppressor of cytokine signaling 1; TAB2: TGF-beta activated kinase 1/MAP3K7 binding protein 2. IRAK2: Interleukin-1 receptor-associated kinase 2.

### **6.1.2 Specific study aims**

In this investigation, the guide strands (-5p) of both miRNAs were studied; i.e. miR-146a-5p and miR-155-5p.

The aims of this study were to;

1. Assess whether the extensively studied immune related miRNAs; miR-146a and miR-155 were associated with aGVHD incidence and severity as well as other allo-HSCT outcomes such OS, relapse and NRM.
2. Determine a model for predicting aGVHD incidence and severity using the levels of miR-146a and miR-155 expression.
3. Investigate the impact of miR-146a on its validated targets (IRAK1, TRAF6, STAT1- $\alpha$  and IRF5) as well as miR-155 and its target PU.1

## 6.2 Results

### 6.2.1 Study cohort

In this study, the expression levels of both miR-146a-5p and miR-155-5p were determined in whole blood obtained from allo-HSCT patients at pre-transplant (Day-7) and post-transplant (Day+28 and three months). This aim of this study was to evaluate whether aGVHD incidence and severity could be predicted from pre and post-transplant miR-146a-5p and miR-155-5p expression values for patients who at the time of testing had no aGVHD but later on went on to develop aGVHD grades II-III.

In brief, whole blood samples were collected in PAXgene™ Blood RNA tubes; these stabilize the total RNA content of the blood including the miRNA population. PAXgene™ Blood RNA tubes are ideal for miRNA investigations as they provide the miRNA content in whole blood rather than distinct cell populations such as PBMCs (Viprey *et al.*, 2012). This is clinically relevant, as endosomes that also contain miRNAs and granulocytes are lost when PBMCs are collected but may present valuable disease signatures (Viprey *et al.*, 2012). Hence, for prognostic biomarker discoveries whole blood samples can be more informative than investigating in only specific cell populations. MicroRNA expression levels were quantified by RT-qPCR and results were log-transformed, both for the exponential nature of RT-qPCR results as well as for a normal distribution. The expression at pre-transplant and Day+28 post-transplant was used for building the predictive aGVHD model. Expression at three months was interesting as it depicted the overall microRNA expression pattern at the 100 days aGVHD cut-off period.

At three months some of the patients were on prophylactic steroids but most patients had their Cyclosporine A administration tapered by then. All patients had received Campath (anti-CD52) as part of their conditioning regimen. Clinicians assessed aGVHD outcome as per the NIH consensus (Grade 0: without, Grade I: mild, II: moderate and III: severe aGVHD). Patients that manifested aGVHD within the 100 days' time-period post-allo-HSCT were included in the analyses. At Day+28 none of the patients were on steroids nor had they developed aGVHD. The number of patients per time-point varied

as at times it was not feasible to collect blood due to the patient's clinical conditions. In this cohort, all the patients survived until day 100, and none had received DLI before the Day+28 whole blood collection. The study cohort comprised of whole blood collected from patients at seven days pre-transplantation (n=35), 28 days (n=54) and three months (n=34) post-transplantation. The cohort consisted of 48% with aGVHD (grade 0) and 52% with an incidence of aGVHD (grades I-III). Ten patients in this cohort had developed grade II aGVHD and only one patient had developed grade III aGVHD.

The cohort consisted of patients who had undergone allo-HSCT (2010-2013) from both siblings and matched unrelated donors, primarily those who had undergone a reduced intensity conditioning regimen (80%). The follow-up period was 44 months for all the patients in this study. The median age of patients was 54.5 years (Range: 19.9-67.6), and the majority was over 50 years of age. The median age for the controls (grade 0) was 57.2 (Range: 30-67.3) and for the cases (grade I-III) was 51.1 (Range: 19.9-67.3). There were only five patients with grade I who were below 30 years old. There were only seven cases with 'female donor-male recipient' in this study. The predominant underlying diseases were AML (28%) and MDS (26%). Cyclosporine A levels at Day+28 were measured with a median 159 ng/ml (Range: 68-333). Cyclosporine A levels were missing for 20 (36%) of the patients in this cohort. Incidence of relapse was 30%, and survival rate was 61% in the total cohort. Table 6.4 shows the frequency of patients as per the clinical characteristics.

### **6.2.2 Data analyses**

A multivariate generalized linear model (GLM: see Chapter 2, for more details) was used for the prediction of aGVHD incidence and severity in this investigation. Thus, a primary univariate analysis of the patient cohort using Fisher's exact test was performed to identify clinical risk factors associated with aGVHD incidence and severity. Clinical risk factors were selected based on the difference between the two groups and were entered into the model. Fisher's exact test was chosen as it ensured that the p-value was accurate regardless of the size, distribution, sparseness, or balance of the data. Clinical factors are considered for multivariate analysis when p-values are less than 0.1 or 0.2 but as per the EMBT 2013 statistical guideline the significance of the factor must be independently assessed (Iacobelli, 2013). After initial univariate analysis, potential predictors with a p-value < 0.2 were selected as candidates in the variable selection procedure. The p=0.2 criterion was chosen to reduce the exclusion of relevant factors (18).

#### **Acknowledgements:**

Mahid Ahmed contributed to the measurement of miR-155-5p expression levels in whole blood at pre- and post-transplantation (Day-7 and Day+8, respectively). This was part of his Wellcome Trust Summer Internship programme.

Hannah Smith contributed to the measurement of miR-146a-5p and miR-155-5p in whole blood of healthy volunteers (n=10) as part of her undergraduate research project.

### **6.2.3 Associations with aGVHD Incidence and Severity**

#### **6.2.3.1 Acute GVHD incidence was significantly predictable using miRNA expression levels**

To assess for associations between miRNA expression and aGVHD incidence, generalised linear model (GLM) were built (see Chapter 2). As mentioned earlier, univariate Fisher's exact test was performed and the following clinical risk factors were determined as significant in predicting aGVHD incidence; Patient's gender ( $p=0.155$ ), underlying disease ( $p=0.128$ ), transplantation conditioning regimen ( $p=0.179$ ) protocol ( $p=0.133$ ) and mismatches in HLA class II ( $p=0.096$ ) (Table 6.3). Chronic GVHD was also associated with aGVHD outcome ( $p=0.011$ ) but it was not included in the model as aGVHD develops prior to cGVHD or at the same time during overlap syndrome. There was no significant difference with the other clinical risk factors.

Cohort Characteristics (n=54)		No aGVHD (Grade 0) (%) (n=26)		Yes aGVHD (Grade I-III) (%) (n=28)		Difference (p-value)
		No.	%	No.	%	
Patient age (median years)		54.53 (19.85-67.63)				0.741
cGVHD	No	11	73	4	27	<b><u>0.011</u></b>
	Yes	8	31	18	69	
Patient gender	Female	12	63	7	37	<b><u>0.155</u></b>
	Male	14	40	21	60	
Donor gender	Female	8	57	6	43	0.533
	Male	16	44	20	56	
Graft source	BM	3	50	3	50	1.000
	PBSC	23	48	25	52	
Underlying Disease	ALL	3	43	4	57	<b><u>0.128</u></b>
	AML	4	27	11	73	
	CLL	2	100	0	0	
	CML	1	100	0	0	
	MDS	9	64	5	36	
	MM	2	67	1	33	
	MPS	2	100	0	0	
	NHL	3	33	6	67	
	SAL	0	0	1	100	
Regimen	Myeloblative	3	27	8	73	<b><u>0.179</u></b>
	RIC	23	53	20	47	
Protocol	Flu Mel Alem	22	55	18	45	<b><u>0.133</u></b>
	Flu Bus Alem	3	60	2	40	
	Cy Alem	1	17	5	83	
	FluAmCyCycloAlem	0	0	3	100	
CsA prophylaxis at Day+28 (ng/ml)		159 (68-333)				0.795
Campath	30 mg	13	52	12	48	0.497
	60 mg	12	43	16	57	
	90 mg	1	100	0	0	
Relationship	SIB	11	55	9	45	0.574
	MUD	15	44	19	56	
Patient CMV status	Negative	11	46	13	54	0.791
	Positive	15	50	15	50	
Donor CMV status	Negative	17	53	15	47	0.418
	Positive	9	41	13	59	
HLA Class I mismatches	None	24	47	27	53	0.604
	One	2	67	1	33	
HLA Class II mismatches	None	17	61	11	39	<b><u>0.096</u></b>
	One	7	41	10	59	
	Two	2	22	7	78	
Survival status	Alive	16	48	17	52	1.000
	Dead	10	48	11	52	
Relapse status	No	18	47	20	53	1.000
	Yes	8	50	8	50	
Disease status at Transplant	CR	2	100	0	0	0.437
	CR1	11	52	10	48	
	CR2	4	33	8	67	
	CR3	2	40	3	60	
	Unt	4	67	2	33	

**Table 6.3 Frequency of patient characteristics in patients with and without incidence of aGVHD grades I-III.** Fisher's exact test was used to estimate the difference in frequencies between the two different aGVHD groups. Significant p-values are in bold and underlined. Abbreviations:- cGVHD: chronic GVHD, BM: Bone marrow, PBSC: Peripheral blood stem cells, ALL: Acute lymphocytic leukaemia, AML: Acute myeloid leukaemia, CLL: Chronic lymphocytic leukaemia, CML: Chronic myeloid leukaemia, HD: Hodgkin's Disease, MDS: Myelodysplastic syndrome, MM: Multiple myeloma, MPS: Multiple proliferative syndrome, NHL: Non-Hodgkin's lymphoma, SAL: Secondary Acute Leukaemia, RIC: Reduced intensity conditioning, Flu: Fludarabine, Mel: Melphalan, Bus: Busulfan, Cy: Cytrabine, Cyclo: Cyclophosphamide, TBI: Total body irradiation, Alem: Alemtuzumab, Cyclosporine A: Cyclosporine, CMV: Cytomegalovirus, CR (1-3) Complete remission, Unt: Untreated, SIB: Sibling, MUD: Matched unrelated donor.

### 6.2.3.2 Variance was equal and multicollinearity absent across all groups

The test of homogeneity of variance was performed to identify if there was any variation between the continuous variables in the groups. A difference equal to or greater than 0.05 is indicative of equal variance. The test showed that the variance between all the groups was equal which indicated that assumptions of Levene's test were satisfied (Table 6.4). Therefore, the scale function in GLM was set to default, i.e. one as it was not necessary to adjust the model for variance. The response distribution for GVHD outcome (response) was binary and therefore a generalised binary logistic regression was run. Multicollinearity was also absent between all the independent variables which was indicative by the tolerance values that were all greater than or equal to 0.1 (Table 6.5).

Covariates	p-value
Pre-Tx: miR-146a-5p	0.09
Pre-Tx: miR155-5p	0.77
Day+28: miR-146a-5p	0.91
Day+28: miR-155-5p	0.52
3m: miR146a-5p	0.08
3m: miR-155-5p	0.29
Patient Age at Tx	0.05
CsA concentration at Day+28	0.33

**Table 6.4 Test of homogeneity of variances for all the continuous covariates used in the generalized linear model**

Independent variables	Collinearity Statistics
	Tolerance
Pre-Tx: miR-146a-5p	0.7
Pre-Tx: miR155-5p	0.5
Day+28: miR-146a-5p	0.7
Day+28: miR-155-5p	0.5
Patient Sex	0.9
Underlying disease	0.8
Regimen	0.1
Protocol	0.1
HLA class II mismatches	0.9

**Table 6.5 Test of multicollinearity.** (Tolerance value greater than or equal to 0.1 indicated absence of multicollinearity)

### 6.2.3.3 *The interaction between miR-146a-5p and miR-155-5p was significant in predicting aGVHD incidence at day+28 post allo-HSCT*

Acute GVHD incidence was predicted in a stepwise manner. The first model comprised of miR-146a-5p and miR-155-5p expression both at pre- and at Day+28 post allo-HSCT and the clinical risk factors (patient sex, underlying disease, transplant regimen and protocol, HLA class II mismatches). The model only included cases without missing values. Thus in the first analysis only 35 of the cases were included [pre-transplant (n=35) and at Day+28 (n=54)]. Results showed that in this model the clinical risk factors and miRNA expression levels at pre- allo-HSCT were not significantly associated with aGVHD incidence.

However, in the same model, the main effect of miR-146a-5p expression and its interaction with miR-155-5p at Day+28 were significant in predicting aGVHD incidence. An increase in miR-146a-5p expression was associated with a decrease in the odds of patients developing aGVHD [odds ratio= 0.023 (95% CI: 0.001-0.588)] which was a statically significant main effect (p=0.023). The interaction between miR-146a-5p and miR-155-5p expression at Day+28 was also statistically significant, odds ratio=0.516 (95% CI: 0.292-0.911), p=0.022. The main effect of miR-155-5p had a trend towards significance [odds ratio=0.336 (95% CI: 0.104-1.088) p=0.069]. Together, the GLM fitted was significantly able to predict the incidence of aGVHD (p=0.043). A confusion matrix was created based on the overall adjusted model and showed that 73% of the patients were accurately classified as without aGVHD and 86% as with aGVHD incidence (Table 6.6).

Confusion matrix		Predicted aGVHD grade	
		0	I-III
Observed aGVHD grade: Count (%)	0	11 (73.3%)	4 (26.7%)
	I-III	3 (14.3%)	18 (85.7%)

**Table 6.6** Confusion matrix based on the observed aGVHD and predicted aGVHD grades.

#### **6.2.3.4 Acute GVHD severity was not predictable when using miRNA expression levels**

Next, the same miRNA expression levels were tested to see if they could also predict aGVHD severity. Therefore, the patient cohort (n=54) was dichotomised to those with grades 0-I and others who went on to develop aGVHD grades II-III later. The majority of the patients had none or grade I aGVHD (79.6%) while only 20.4% had developed grades II-III aGVHD post Day+28. As in the previous Section 5.2.2, a univariate Fisher's exact test was performed to select the significant clinical risk factors for inclusion in building the GLM (Table 6.7). Graft source, the relationship of donor to patient, donor CMV status and mismatches in HLA Class II were determined significant ( $p < 0.02$ ) and were included for building the GLM model in a stepwise manner in addition to the miRNA expression levels. However, none of the variables were significant in predicting aGVHD severity and therefore no GLM was fitted.

Cohort Characteristics (n=54)		Grades 0-I aGVHD (%) (n=43)		Grades II-III aGVHD (%) (n=11)		Difference (p-value)
		No.	%	No.	%	
Patient age (median years)		54.53 (19.85-67.63)				0.895
cGVHD	No	12	80	3	20	1.000
	Yes	20	77	6	23	
Patient gender	Female	17	89	2	11	0.292
	Male	26	74	9	26	
Donor gender	Female	12	86	2	14	0.705
	Male	27	75	9	25	
Graft source	BM	3	50	3	50	<b><u>0.091</u></b>
	PBSC	40	83	8	17	
Underlying Disease	ALL	11	73	4	27	1.000
	AML	6	86	1	14	
	CLL	11	79	3	21	
	CML	7	78	2	22	
	MDS	2	100	0	0	
	MM	2	67	1	33	
	MPS	2	100	0	0	
	NHL	1	100	0	0	
Regimen	Myeloblative	9	82	2	18	1.000
	RIC	34	79	9	21	
Protocol	Flu Mel Alem	32	80	8	20	0.914
	Flu Bus Alem	4	80	1	20	
	Cy Alem	5	83	1	17	
	FluAmCyCycloAlem	2	67	1	33	
CsA prophylaxis at Day+28 (ng/ml)		159 (68-333)				0.973
Campath	30 mg	21	84	4	16	0.609
	60 mg	21	75	7	25	
	90 mg	1	100	0	0	
Relationship	SIB	18	90	2	10	<b><u>0.181</u></b>
	MUD	25	74	9	26	
Patient CMV status	Negative	18	75	6	25	0.510
	Positive	25	83	5	17	
Donor CMV status	Negative	28	88	4	13	<b><u>0.100</u></b>
	Positive	15	68	7	32	
HLA Class I mismatches	None	41	80	10	20	0.502
	One	2	67	1	33	
HLA Class II mismatches	None	25	89	3	11	<b><u>0.074</u></b>
	One	13	76	4	24	
	Two	5	56	4	44	
Survival status	Alive	27	82	6	18	0.733
	Dead	16	76	5	24	
Relapse status	No	29	76	9	24	0.474
	Yes	14	88	2	13	
Disease status at Transplant	CR	2	100	0	0	0.712
	CR1	18	86	3	14	
	CR2	10	83	2	17	
	CR3	3	60	2	40	
	Unt	5	83	1	17	

**Table 6.7 Frequency of patient characteristics in patients with aGVHD grades 0-I and II-III.** Fisher's exact test was used to estimate the difference in frequencies between the four different aGVHD groups. Significant p-values are in bold and underlined. Abbreviations:- cGVHD: chronic GVHD, BM: Bone marrow, PBSC: Peripheral blood stem cells, ALL: Acute lymphocytic leukaemia, AML: Acute myeloid leukaemia, CLL: Chronic lymphocytic leukaemia, CML: Chronic myeloid leukaemia, HD: Hodgkin's Disease, MDS: Myelodysplastic syndrome, MM: Multiple myeloma, MPS: Multiple proliferative syndrome, NHL: Non-Hodgkin's lymphoma, SAL: Secondary Acute Leukaemia, RIC: Reduced intensity conditioning, Flu: Fludarabine, Mel: Melphalan, Bus: Busulfan, Cy: Cytrabine, Cyclo: Cyclophosphamide, TBI: Total body irradiation, Alem: Alemtuzumab, CsA: Cyclosporine, CMV: Cytomegalovirus, CR (1-3) Complete remission, Unt: Untreated, SIB: Sibling, MUD: Matched unrelated donor.

## **6.2.4 Associations with Relapse, OS and NRM**

### **6.2.4.1 *MiR-146a-5p and miR-155-5p expression in whole blood was not associated with relapse***

Subsequently, tests were performed to assess whether the clinical factors, as well as miR-146a-5p and miR-155-5p expression levels in whole blood at Day+28 post allo-HSCT, were associated with OS, relapse and NRM. The finding of Section 5.2.2 showed that the Day+28 time-point was highly significant in predicting aGVHD incidence, and thus the expression values at this time were used for all subsequent analyses.

The association between various clinical risk factors and relapse was evaluated using Kaplan-Meier log-rank test for dichotomized variables and univariate Cox regression for continuous variables (Table 6.8). In addition to the miRNA expression levels, patient gender, transplant protocol, donor CMV status and mismatches in HLA Class I were determined significant ( $p < 0.02$ ) and were included for performing the multivariate Cox regression analysis using the stepwise, Forward-LR method. Cox regression model showed that only mis-matches in HLA class I was marginally predictive of patient risk of relapse [ $p = 0.048$ , HR=4.744 (95% CI: 1.016-22.154)]. Neither the miRNA expression levels nor other clinical risk factors were associated with relapse.

Cohort Characteristics (n=54)		No Relapse (%) (n=43)		Relapse (%) (n=11)		Difference (p-value)
		No.	%	No.	%	
Patient age (median years)		54.53 (19.85-67.63)				0.847†
cGVHD	No	9	60	6	40	0.543*
	Yes	17	65	9	35	
aGVHD incidence	No aGVHD (Grade 0)	18	69	8	31	0.914*
	Yes aGVHD (Grades I-III)	20	71	8	29	
Patient gender	Female	16	84	3	16	<b><u>0.094*</u></b>
	Male	22	63	13	37	
Donor gender	Female	11	79	3	21	0.538*
	Male	23	64	13	36	
Graft source	BM	3	50	3	50	0.294*
	PBSC	35	73	13	27	
Underlying Disease	ALL	5	71	2	29	0.929†
	AML	9	60	6	40	
	CLL	1	50	1	50	
	CML	1	100	0	0	
	MDS	10	71	4	29	
	MM	3	100	0	0	
	MPS	2	100	0	0	
	NHL	6	67	3	33	
Regimen	Myeloblastic	7	64	4	36	0.647*
	RIC	31	72	12	28	
Protocol	Flu Mel Alem	28	70	12	30	<b><u>0.198†</u></b>
	Flu Bus Alem	5	100	0	0	
	Cy Alem	4	67	2	33	
	FluAmCyCycloAlem	1	33	2	67	
CsA prophylaxis at Day+28 (ng/ml)		159 (68-333)				<b><u>0.132†</u></b>
Campath	30 mg	16	64	9	36	0.648†
	60 mg	21	75	7	25	
	90 mg	1	100	0	0	
Relationship	SIB	13	65	7	35	0.634*
	MUD	25	74	9	27	
Patient CMV status	Negative	15	63	9	38	0.401*
	Positive	23	77	7	23	
Donor CMV status	Negative	20	63	12	38	<b><u>0.166*</u></b>
	Positive	18	82	4	18	
HLA Class I mismatches	None	37	73	14	28	<b><u>0.027*</u></b>
	One	1	33	2	67	
HLA Class II mismatches	None	17	61	11	39	0.410†
	One	13	77	4	24	
	Two	8	89	1	11	
Survival status	Alive	27	82	6	18	<b><u>0.001*</u></b>
	Dead	11	52	10	48	
Disease status at Transplant	CR	1	50	1	50	0.932†
	CR1	14	67	7	33	
	CR2	9	75	3	25	
	CR3	4	80	1	20	
	Unt	4	67	2	33	

**Table 6.8 Frequency of patient characteristics for those who did not relapse and those that relapsed.** \*To estimate the difference in frequencies between the no relapse and relapse group, Kaplan-Meier log-rank test was used for the binary variables and †univariate Cox regression for continuous variables. Significant p-values are in bold and underlined. Abbreviations:- cGVHD: chronic GVHD, BM: Bone marrow, PBSC: Peripheral blood stem cells, ALL: Acute lymphocytic leukaemia, AML: Acute myeloid leukaemia, CLL: Chronic lymphocytic leukaemia, CML: Chronic myeloid leukaemia, HD: Hodgkin's Disease, MDS: Myelodysplastic syndrome, MM: Multiple myeloma, MPS: Multiple proliferative syndrome, NHL: Non-Hodgkin's lymphoma, SAL: Secondary Acute Leukaemia, RIC: Reduced intensity conditioning, Flu: Fludarabine, Mel: Melphalan, Bus: Busulfan, Cy: Cytarabine, Cyclo: Cyclophosphamide, TBI: Total body irradiation, Alem: Alemtuzumab, CsA: Cyclosporine, CMV: Cytomegalovirus, CR (1-3) Complete remission, Unt: Untreated, SIB: Sibling, MUD: Matched unrelated donor.

### **6.2.4.2 Low miR-146a-5p expression was associated with better overall survival**

Both miR-146a-5p and miR-155-5p expressions were measured on a continuous scale. To reduce observer bias and lack of the decision threshold (cut-off) present in the literature for both miRNAs, it was deemed useful to determine a cut-off for each miRNA via ROC curve analysis.

Thus, ROC curve analyses showed that the expression of miR-146a-5p (A=0.623, p=0.129) and miR-155-5p (A=0.530, p=0.716) were diagnostically not significant in classifying patients who were alive from those that died (Table 6.9, Figure 6.4, A). However, the cut-off value calculated for dichotomising miR-146a-5p expression was considered as valid as the sensitivity (true positive) was 90% (Table 6.9).

MicroRNAs	Cut-off value	Sensitivity	Specificity	AUC (95% CI)	p-value for AUC
miR-146a-5p	>4.69	0.91	0.42	0.62 (0.47-0.77)	0.129
miR-155-5p	<0.01	1.00	0.03	0.53 (0.37-0.69)	0.716

**Table 6.9 ROC curve analysis of miRNA expression with overall survival.** Log-transformed miRNA expression values were used to derive the cut-off value for dichotomising the data. <: lower values signify patient more likely to die; higher values signify patient more likely to live. >: higher values signify patient more likely to die; lower values signify patient more likely to live.

To reinforce the ROC's dichotomy, the Kaplan-Meier log-rank-test (incorporating the time element) was then performed to compare the resulting two different levels (low and high) of miRNA expression with regards to OS. MiR-146a-5p expression, when dichotomised, was statistically significant in predicting patient OS (log-rank p=0.015) (Figure 6.4 B). MiR-155-5p could not be dichotomised based on the cut-off value determined as per the ROC curve analysis. Thus, Kaplan-Meier log-rank test could not be performed as there was only one value for the survival factor (dead).

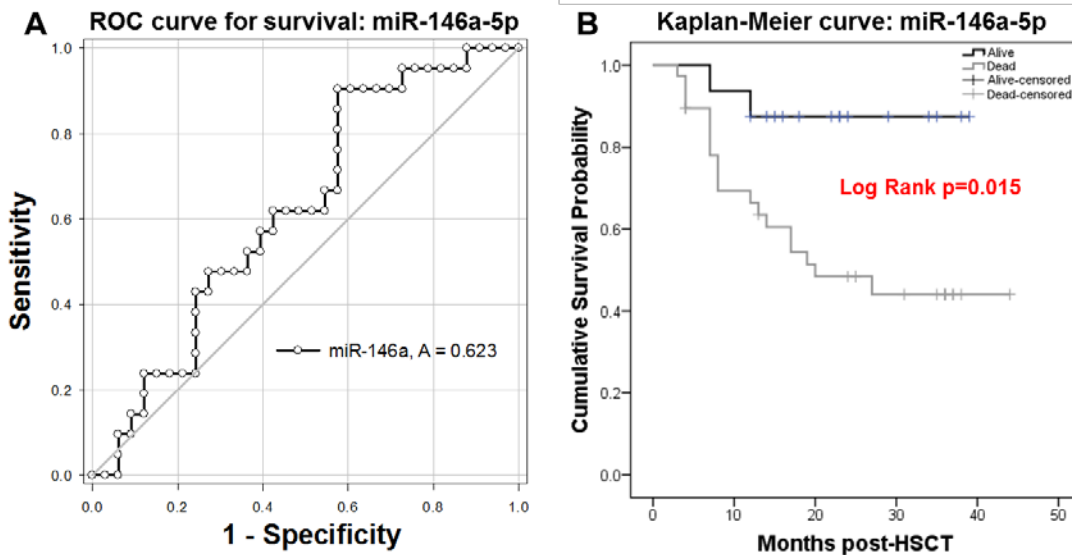


**Figure 6.4 ROC curve and Kaplan-Meier survival analysis for miR-146a-5p.** (A) The cut-off value was determined from the ROC test and used to dichotomise miR-146a-5p expression for the log-rank test. (B) The clear separation of the Kaplan-Meier curves showed that the dichotomy for miR-146a-5p expression could be used to predict OS post-HSCT ( $p=0.015$ ). Black line = low miRNA expression and grey line= high miRNA expression.

The chi-square statistic was employed to establish if the dichotomy used for each miRNA was sufficient to differentiate between patients who were deceased and patients who were alive. Overall there were 21 dead (events) and 33 alive (censored) cases. Exact p-values for the chi-square test were used to ensure the accuracy regardless of the size, distribution, sparseness, or balance of the data. Only miR-146a-5p dichotomy proved significantly associated with survival [ $p=0.000$ ] (Table 6.10). This result agreed with those of the log-rank tests from a Kaplan-Meier analysis: miR-146a-5p [ $p=0.015$ ] (Figure 6.4). Together, low miRNA expression level was shown to be indicative of higher cumulative survival probability for miR-146a-5p only.

microRNAs	Expression level <sup>a</sup>	Total	Dead	Alive		Chi-Square
		N	N	N	%	Exact p-values
miR-146a-5p	Low expression	16	2	14	87.5	0.000
	High expression	38	19	19	50	

**Table 6.10 Case processing summaries for all the 11 validated miRNAs showing the number of events and censored cases per group.** <sup>a</sup> grey shade: level containing a larger proportion of patients who died.

### 6.2.4.3 HLA class I mismatches was associated with risk of death

Subsequently, multivariate Cox regression analysis was performed to estimate the predictive value of miRNAs when expression levels were used on a continuous scale to perform the analysis. This would reinforce the accuracy of the dichotomy used in for the Kaplan-Meier log-rank test. It would also test whether the miRNA expression levels retained their significance when clinical risk factors were included in the study. Hence, miRNA expression values were entered as continuous variables and significant clinical risk factors were either selected by performing Kaplan-Meier log-rank test or univariate Cox regression as mentioned, previously. The following clinical risk factors were entered for performing the stepwise Forward-LR method for variable selection procedure in addition to the miRNA expression values: Patient and donor gender, underlying disease, transplant protocol, dose of Campath and mismatches in HLA class I (Table 6.11).

Interestingly, mis-matches in HLA class I was the only variable that was associated with patient risk of death and was entered into the Cox regression equation [p=0.004, HR=6.667 (95% CI: 1.837-24.202)]. For every single mis-match in HLA class, I between the patient-donor pair the risk of dying increased by 6.7 folds. These results showed that the miRNA-146a-expression was not significantly associated with improved OS when clinical risk factors such as mis-matches in HLA class I were included as variables in the analysis

Cohort Characteristics (n=54)		Alive (%) (n=33)		Dead (%) (n=21)		Difference (p-value)
		No.	%	No.	%	
Patient age (median years)		54.53 (19.85-67.63)				0.990
cGVHD	No	10	67	5	33	0.640
	Yes	14	54	12	46	
aGVHD incidence	No aGVHD (Grade 0)	16	62	10	38	0.986
	Yes aGVHD (Grades I-III)	17	61	11	39	
Patient gender	Female	14	74	5	26	<b><u>0.128</u></b>
	Male	19	54	16	46	
Donor gender	Female	6	43	8	57	<b><u>0.123</u></b>
	Male	23	64	13	36	
Graft source	BM	5	83	1	17	0.284
	PBSC	28	58	20	42	
Underlying Disease	ALL	3	43	4	57	<b><u>0.027</u></b>
	AML	10	67	5	33	
	CLL	1	50	1	50	
	CML	1	100	0	0	
	MDS	8	57	6	43	
	MM	1	33	2	67	
	MPS	2	100	0	0	
	NHL	7	78	2	22	
Regimen	Myeloblative	6	55	5	45	0.661
	RIC	27	63	16	37	
Protocol	Flu Mel Alem	24	60	16	40	<b><u>0.023</u></b>
	Flu Bus Alem	5	100	0	0	
	Cy Alem	4	67	2	33	
	FluAmCyCycloAlem	0	0	3	100	
CsA prophylaxis at Day+28 (ng/ml)		159 (68-333)				0.728
Campath	30 mg	15	60	10	40	<b><u>0.147</u></b>
	60 mg	18	64	10	36	
	90 mg	0	0	1	100	
Relationship	SIB	11	55	9	45	0.641
	MUD	22	65	12	35	
Patient CMV status	Negative	14	58	10	42	0.908
	Positive	19	63	11	37	
Donor CMV status	Negative	18	56	14	44	0.579
	Positive	15	68	7	32	
HLA Class I mismatches	None	33	65	18	35	<b><u>0.001</u></b>
	One	0	0	3	100	
HLA Class II mismatches	None	16	57	12	43	0.731
	One	13	76	4	24	
	Two	4	44	5	56	
Relapse status	No	27	71	11	29	<b><u>0.079</u></b>
	Yes	6	38	10	63	
Disease status at Transplant	CR	1	50	1	50	0.789
	CR1	11	52	10	48	
	CR2	9	75	3	25	
	CR3	3	60	2	40	
	Unt	4	67	2	33	

**Table 6.11 Frequency of patient characteristics which were alive and those who were deceased.** To estimate the difference in frequencies between the alive and dead group, Kaplan-Meier log-rank test was used for the binary variables and univariate Cox regression for continuous variables. Significant p-values are in bold and underlined. Abbreviations:- cGVHD: chronic GVHD, BM: Bone marrow, PBSC: Peripheral blood stem cells, ALL: Acute lymphocytic leukaemia, AML: Acute myeloid leukaemia, CLL: Chronic lymphocytic leukaemia, CML: Chronic myeloid leukaemia, HD: Hodgkin's Disease, MDS: Myelodysplastic syndrome, MM: Multiple myeloma, MPS: Multiple proliferative syndrome, NHL: Non-Hodgkin's lymphoma, SAL: Secondary Acute Leukaemia, RIC: Reduced intensity conditioning, Flu: Fludarabine, Mel: Melphalan, Bus: Busulfan, Cy: Cytarabine, Cyclo: Cyclophosphamide, TBI: Total body irradiation, Alem: Alemtuzumab, CsA: Cyclosporine, CMV: Cytomegalovirus, CR (1-3) Complete remission, Unt: Untreated, SIB: Sibling, MUD: Matched unrelated donor.

#### 6.2.4.4 *Clinical risk factors were associated with relapse and non-relapse mortality*

Competing risk analysis was performed using R (version 3.0.1) for all the 54 patients to estimate the cumulative incidence of NRM and disease relapse (relapse and death act as competing risks). Gray's test (Gray, 1988) was performed to test for equality of cumulative incidence functions across the different clinical risk factor groups. Results showed that the cumulative incidence curves were not statistically significant for NRM, but there were sometimes trends toward significance (Table 6.12). Mismatches in HLA class I showed borderline significance ( $p=0.051$ ) towards a greater incidence of relapse for those with one HLA mismatch when compared to those with no mismatch (Figure 6.5, A). However, this result must be interpreted with caution as there were only three transplantations with HLA I class mismatches. Likewise, transplantations with mismatches in the HLA class II had a trend ( $p=0.077$ ) towards more incidence of NRM (Figure 6.5, B). Patient gender showed a trend ( $p=0.084$ ) towards higher incidence of relapse in males compared to females (Figure 6.5, C) while in donor gender there was a trend ( $p=0.109$ ) towards significance of NRM in patients with female donors compared to those with male donors (Figure 6.5, D).

Clinical risk factors	Relapse (p-value)	Non-Relapse Mortality (p-value)
Transplant type	0.601	0.827
Patient CMV status	0.354	0.453
Donor CMV status	0.161	0.61
HLA class I mismatches	<b><u>0.051</u></b>	0.469
HLA class II mismatches	0.259	<b><u>0.077</u></b>
Conditioning regimen	0.688	0.88
Graft source	0.2	0.216
Patient gender	<b><u>0.084</u></b>	0.543
Donor gender	0.425	<b><u>0.109</u></b>
Patient age	0.743	0.276

**Table 6.12** Gray's test summary for relapse and non-relapse mortality (difference indicated by p-values).

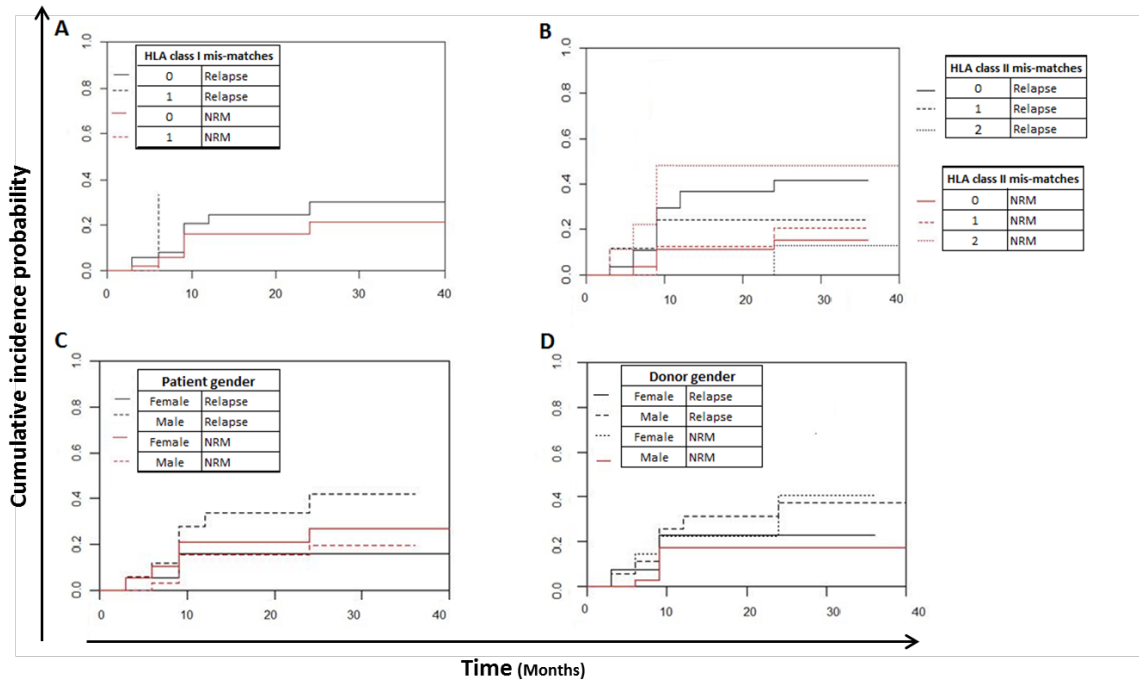


**Figure 6.5** Estimated cumulative incidence curves for NRM and relapse. (A) HLA class I mismatches (B) HLA class II mismatches (C) Patient gender and (D) Donor gender.

## **6.2.5 Correlation assessment between the miRNAs and their targets**

### **6.2.5.1 Positive correlation was present among miR-146a targets at the mRNA level both at pre and post allo-HSCT time-points**

Both miR-146a-5p and miR-155-5p have been shown to have increased expression levels upon exposure to LPS that results in the activation of Toll-like receptor 4 (TLR4) and in turn in the NFκB signalling pathway (Taganov *et al.*, 2006; Rai *et al.*, 2008). As shown earlier, miR-146a-5p is the main miRNA involved in predicting the incidence of aGVHD and improving OS, thus in order to better understand its role in the disease pathway and inflammation, its established targets (*TRAF6*, *IRAK1*, *STAT1-α* and *IRF-5*) were quantified both at the mRNA and protein levels, respectively. Analysis was performed by segregating the cohort into two groups (Grade 0 and Grades I-III) and then testing for correlation between the miRNA expression levels and their respective mRNA targets at pre-transplant, Day+28 and three months.

MiRNA expression levels that were quantified in the Section 5.2 were used for performing correlation statistics. The correlation was performed separately for those who never developed aGVHD (grade 0) by the time of the last follow-up and those who went on to develop grade II-III aGVHD post Day+ 28 time-points (for all the correlation tables, please see Appendix B, tables 1-8).

In the patients with no aGVHD (grade 0), results showed that the mRNA expression levels of *TRAF6*, *IRAK1*, *STAT1-α* and *IRF-5* did not significantly correlate with miR-146a-5p expression levels in whole blood obtained from the patients' pre- allo-HSCT. As all the targets are involved together in the same pathways, it was interesting to assess whether their levels correlated with each other or not at every time-point. Not surprisingly, there was a significant positive correlation between *TRAF6* and *IRAK1* ( $r_s=0.79$ ,  $p=0.001$ ) as well as *TRAF6* and *STAT1-α* ( $r_s=0.59$ ,  $p=0.027$ ). Whole blood samples collected at Day+28 were then assessed for target correlation and results showed that there was no correlation between miR-146a-5p and its targets at this time-point. However, there was a trend towards the negative correlation between miR-146a-5p and *TRAF6* mRNA expression ( $r_s=-0.37$ ,  $p=0.061$ ). Statistically significant ( $p\leq 0.002$ ) positive correlation was present between all the targets. In whole blood

collected at three months post-transplantation, there was no relationship between miR-146a-5p expression and its mRNA targets or among the targets.

Likewise, correlation between miR-146a-5p and its targets was also assessed in the aGVHD patient cohort (Grades I-III). Measurements at Day+28 showed that there was no correlation between miR-146a-5p and its targets, but there was statistically significant ( $p \leq 0.02$ ) positive correlation present between all the targets. At 3 months post-transplantation there was a significant negative correlation ( $r_s = -0.69$ ,  $p = 0.019$ ) between miR-146a-5p and *IRF5* mRNA expression. At the same time-point, *TRAF6* and *IRAK1* expression positively correlated with each other ( $r_s = 0.86$ ,  $p = 0.001$ ).

#### **6.2.5.2 *IRF5* mRNA expression positively correlated with its protein levels measured in whole blood at Day+28 in aGVHD patients**

Subsequently, the protein levels of the targets were quantified using commercially available ELISA kits in a representative subset of the cohort (Grade 0,  $n=5$ ; Grades I-III,  $n=10$ ). However, only STAT1- $\alpha$  and IRF5 proteins were detectable by the assays. Therefore, it was concluded that the biological protein levels of TRAF6 and IRAK1 were below the sensitivity of the assay, as the standards for each of the proteins quantified as per the manufacturer's guidelines.

The pre-transplant protein levels of STAT1- $\alpha$  and IRF5 neither correlated with their mRNA expression nor with miR-146a-5p expression levels ( $p > 0.05$ ). The Day+28 protein levels of STAT1- $\alpha$  and IRF5 in the no aGVHD cohort significantly positively correlated with each other ( $r_s = 0.90$ ,  $p = 0.037$ ). At three months post-transplantation, there was no correlation between miR-146a-5p and its protein targets. Similarly, miR-146a-5p correlation with its protein targets was also assessed in the aGVHD patient group (Grades I-III). At Day+28, there was a trend towards a positive correlation between miR-146a-5p and STAT1- $\alpha$  protein levels ( $r_s = 0.53$ ,  $p = 0.092$ ). Likewise, there was also a trend towards *STAT1- $\alpha$*  mRNA and protein levels ( $r_s = 0.57$ ,  $p = 0.068$ ). Results showed a significant positive correlation ( $r_s = 0.71$ ,  $p = 0.009$ ) between IRF5 mRNA and its protein levels. At 3 months post-transplantation there was a significant negative correlation ( $r_s = -0.69$ ,  $p = 0.019$ ) between miR-146a-5p and IRF5. However, some patients at three months were receiving prophylactic steroids so this result must be interpreted with caution.

### 6.2.5.3 *In the whole blood of aGVHD patients at Day+28, MiR-155-5p and miR-146a expression correlated with the transcription factor, SPI1*

SPI1 (PU.1) is an important transcription factor in haematopoietic differentiation (Rosenbauer *et al.*, 2006) and has been shown to regulate the expression of miR-146a-5p and miR-155-5p. In a murine study, it was demonstrated that Spi1 binds to pre-miR-146a-5p locus permanently to regulate its expression. In the same study, SPI1 bound to the miR-155-5p locus only during HSC differentiation (Ghani *et al.*, 2011). Thus, miR-155-5p expression was tested against its target *SPI1* in whole blood samples at Day+28 and results showed that there was a significant negative correlation ( $r_s=-0.534$ ,  $p=0.004$ ) in the aGVHD patient cohort (Grades I-III) only (Figure 6.6, A). Interestingly, in the same cohort there was a significant negative correlation between miR-146a-5p and *SPI1* ( $r_s=-0.45$ ,  $p=0.016$ ) (Figure 6.6, B).

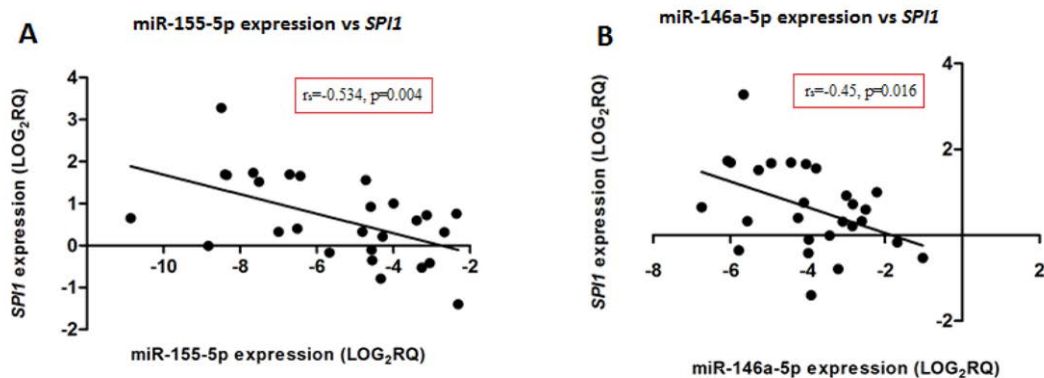


**Figure 6.6 MiR-155-5p and miR-146a-5p expression directly correlated with SPI1 mRNA levels.** There was a significant negative correlation for both (A) miR-155-5p and (B) miR-146a-5p expression. The correlation was only significant in aGVHD patients with grades I-III (n=26). The x-axis shows the miRNA expression levels and the y-axis the *SPI1* mRNA levels. Spearman correlation was used to test for correlation. Spearman rho:  $r_s$ . Significance was set as  $p < 0.05$ .

### 6.2.6 MicroRNA expression levels between normal volunteers and transplant patients

To find if there was any difference in miRNA expression levels between normal and diseased populations, whole blood samples were tested across three groups; normal volunteers, pre-transplant patients and post allo-HSCT patients. Surprisingly, miR-146a-5p expression levels were not significantly different between any of the groups (Figure 6.7, A). However, miR-155-5p expression varied between the pre-transplant patients and normal samples as well as post allo-HSCT patients (Figure 6.7, B). This further highlight that the main effect and interaction identified between miR-146a-5p and miR-155-5p expression may be as a result of the disease state.

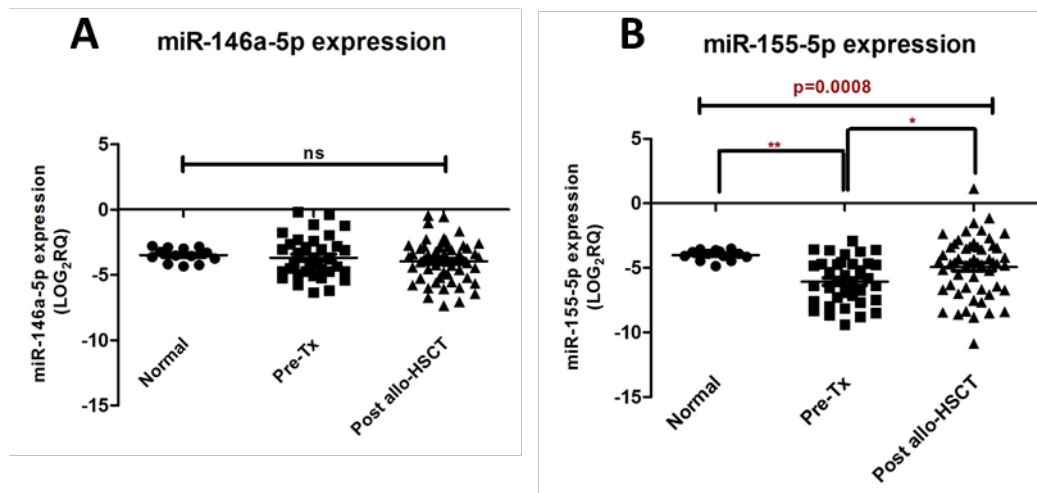


**Figure 6.7 MiRNA expression levels in the whole blood of normal volunteers and transplant patients.** (A) MiR-146a-5p expression was not varied between normal volunteers, pre-transplant patients and those who underwent allo-HSCT (B) Normal volunteers had significantly higher miR-155-5p expression levels compared to the pre-transplant patients. Kruskal-Wallis analysis of variance was used to calculate the difference. Significance was set at  $p < 0.05$ . Pre-Tx: pre-transplant; ns: not significant

## **6.2.7 *In Vitro* Stimulation Studies assessing the impact of miRNA expression levels**

### **6.2.7.1 *MiR-146a-5p* expression declines upon stimulation with IFN- $\gamma$**

All the patients in this study had no GVHD at Day+28, yet it was possible to predict aGVHD incidence. Thus, it was hypothesized that the miRNA expression levels were a marker of inflammation in phase II of aGVHD development cycle before aGVHD had a clinical or histological manifestation in the target organs. IFN- $\gamma$  is one of the main proinflammatory cytokines secreted during phase II of aGVHD development (Ferrara *et al.*, 1999). Thus, to test this hypothesis, PBMCs were challenged with two different concentrations of IFN- $\gamma$  to see whether this inflammatory cytokine had any impact on miR-146a-5p and miR-155-5p expression levels in a more diverse population of cells that was more representative of the whole blood population. The cells were stimulated with 50 ng/ml and 100 ng/ml IFN- $\gamma$  for 24 and 48hrs. For both miRNAs, IFN- $\gamma$  stimulation for 24 hrs had no effect on their expression levels when compared to the unstimulated PBMCs (0 ng/ml) (Figure 6.8, A). Interestingly; miR-146a-5p expression was significantly reduced upon stimulation after 48 hrs with 50 ng/ml and 100 ng/ml IFN- $\gamma$  while miR-155-5p expression remained still unaltered. However, there was a trend towards the reduction of miR-155-5p expression after 48 hrs IFN- $\gamma$  stimulation (Figure 6.8, B).

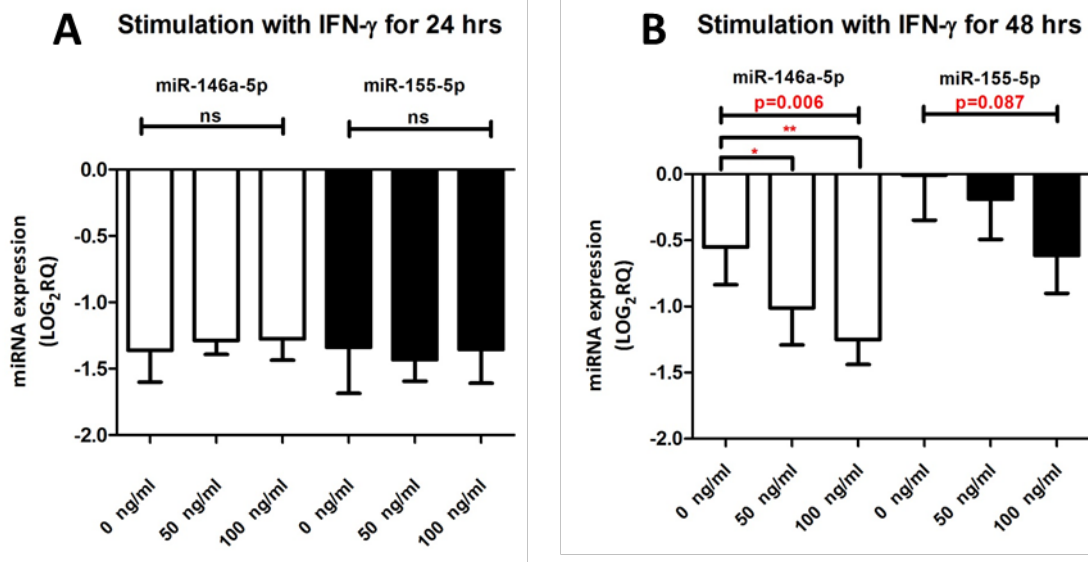


**Figure 6.8** PBMCs stimulated with IFN- $\gamma$  for 48 hrs showed significantly reduced miR-146a-5p expression. PBMCs (n=4) from healthy volunteers were stimulated with IFN- $\gamma$  (50 and 100 ng/ml) for 24 and 48 hrs prior to total RNA extraction. MiR-146a-5p and miR-155-5p expression levels were quantified using RT-qPCR. IFN- $\gamma$  stimulation for (A) 24 hrs and (B) 48 hrs. Repeated measures ANOVA was used to calculate the statistical difference between unstimulated controls (0 ng/ml) and samples stimulated with 50ng/ml and 100 ng/ml of IFN- $\gamma$ .

### **6.2.7.2 Stimulation with Cyclosporine A had no direct impact on miRNA expression levels**

Cyclosporine A is one of the calcineurin inhibitors administered routinely to post allo-HSCT patients at the Newcastle Transplantation centre. Cyclosporine A inhibits IFN- $\gamma$  secretion (Kalman and Klimpel, 1983; Sica *et al.*, 1997) so theoretically, it should indirectly up-regulate miR-146a-5p expression levels. In the patient cohort, it was found that Cyclosporine A concentrations at Day+28 did not correlate with either of the miRNA expression levels ( $r_s \leq 1.00$ ,  $p \geq 0.05$ ). To confirm that Cyclosporine A had no impact on miR-146a-5p and miR-155-5p expression levels, *in vitro* experiments were set-up. Cyclosporine A was co-cultured at various doses in mis-matched MLRs for 96 hours. In parallel, unstimulated auto-MLRs were also set up as a control for allogeneic response. Unstimulated mis-matched MLR was set up as a control for the different Cyclosporine A doses used in the experiment. Results showed that miR-146a-5p and miR-155-5p expressions were unaffected by the different doses of Cyclosporine A, and direct correlation was absent (Figure 6.9). However, an interesting observation was that the miR-155-5p expression was almost unaffected by the MLR response.

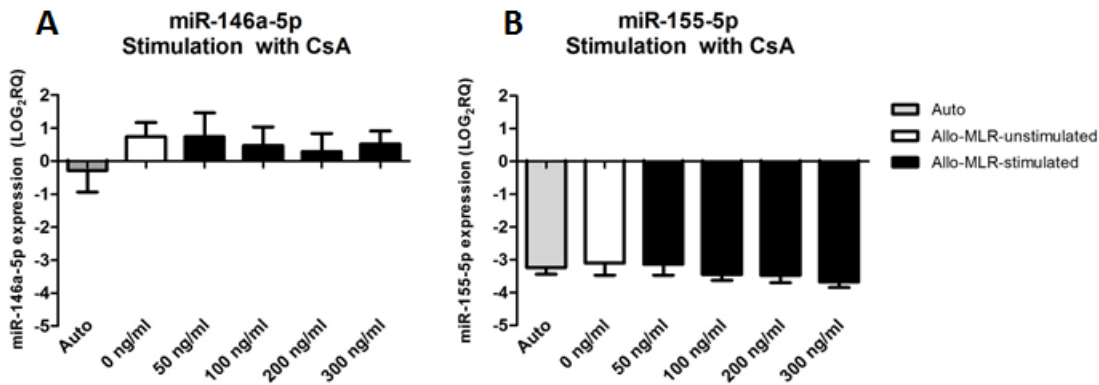


**Figure 6.9 Cyclosporine A had no impact on the expression of miR-146a-5p and miR-155-5p.** Cyclosporine A was co-cultured at different doses with mis-matched MLRs (n=3) for 96 hours (A) MiR-146a-5p expression was higher in mis-matched MLRs, but it was not statistically significant. MiR-146a-5p expression did not vary when low to high concentrations of Cyclosporine A were co-cultured with the MLRs. (B) MiR-155-5p expression was unaffected by both the allogeneic response in the mismatched MLRs as well as the different doses of Cyclosporine A used in the experiment. Auto-MLRs were set up as controls for the allogeneic response and unstimulated mis-matched MLRs as controls for the stimulated MLRs. Repeated-measures ANOVA was used to test for statistical significance.

## 6.3 Discussion

Both miR-146a and miR-155 have been experimentally shown to be indispensable in regulating several immune-related pathways under steady and diseased conditions (Pauley *et al.*, 2008; Nahid *et al.*, 2009; Banerjee *et al.*, 2010; Lu *et al.*, 2010). They have also been shown to be prognostic biomarkers of aGVHD state, SLE and RA (Pauley *et al.*, 2008; Wang *et al.*, 2010; Ranganathan *et al.*, 2012). It is known in HSCT that miR-155 expressions are overexpressed when target organ damage has already occurred in the patient (Ranganathan *et al.*, 2012). It is also known that GVT effect is required to prevent disease relapse (Bleakley and Riddell, 2004). Tailoring treatments to maintain a balance between GVHD and GVT/GVL is, therefore, important in the clinic. This study aimed to assess whether the expression of both miRNAs could be used to predict aGVHD incidence and/or severity prior to histological and clinical disease manifestations. This knowledge could make clinical interventions possible prior to disease onset and, therefore, prevent the complications associated with aGVHD severity. Understanding the miRNA regulation involved in the pathophysiology of aGVHD could also be reflective of the GVH reaction and in particular the essential GVT effect. It could, therefore, be used for monitoring the GVH reaction and could direct therapies for more enhanced GVT effect. Thus, for prediction analyses all the patients in this cohort were aGVHD-free at the 28 days post-transplantation time-point.

This study also applied a new approach to statistical model fitting, as it looked at both the main effects and the interactions between miR-146a-5p and miR-155-5p with regards to predicting aGVHD outcome (incidence and severity). An appropriate model can aid researchers in interpreting quantitative data and finding the impact of the biological deregulation of molecules/genes or miRNAs in both health and disease. There are two main elements that need to be considered in model fitting, (1) selecting an appropriate model that fits with the type of data and complexity of condition as well as (2) selecting factors that are necessary for the prediction of outcomes and probabilities. Inclusion of nonessential variables in the model increases variability of predictions. For this reason, candidate selection was carried out for the model building in this investigation to eliminate imprecise probability estimates. In many biological investigations, in particular in the field of allo-HSCT, interactions are often overlooked

even though they are one of the keys to better understanding the biological relationships and combinations.

Therefore, the expression levels of both miR-146a-5p and miR-155-5p were used for model fitting that showed that miR-146a-5p had the main role in the prediction of aGVHD incidence when it interacted with miR-155-5p expression. The interaction observed is in support of the differential 'check-point' mechanism of action shown by Schulte et al., (Schulte *et al.*, 2012). Lipopolysaccharides trigger the expression of miR-146a (Taganov *et al.*, 2006). Using various immune system stimulators such as LPS, they showed that miR-146a was the initial player in exhibiting an inflammatory response and that miR-155 expression was only altered when miR-146a levels of inflammatory tolerance had been surpassed. This may explain why higher miR-155 expression levels have been observed in both serum and gut of patients at the time of aGVHD onset, which is the effector phase in the GVHD cycle (Ferrara, 1993; Ranganathan *et al.*, 2012; Xie *et al.*, 2014).

Additionally, this study has shown that lower expression of both miRNAs was predictive of aGVHD incidence. This is in support of the very recent aGVHD study in mouse that showed that miR-146a expression levels were lower in aGVHD mice (Stickel *et al.*, 2014). Nahid et al., also showed that over-expression of miR-146a prevents an inflammatory response and thus, has a protective role in innate immunity (Nahid *et al.*, 2009).

MiR-146a had the main role when detected in pre- aGVHD onset samples at Day+28 in this study. To understand the miR-146a-5p regulatory mechanism of action, its four highly cited and experimentally validated targets were investigated both at the mRNA and protein level. There was no correlation between miR-146a-5p expression levels and its mRNA targets at pre-transplant, Day+28 and three months post allo-HSCT. Boldin et al., have shown that miR-146a expression affects the expression of TRAF6 and IRAK1 at the protein level rather than at the mRNA-level (Boldin *et al.*, 2011). But in this study using ELISAs, the protein level of IRAK1 and TRAF6 were not undetectable in the sera of normal volunteers as well as allo-HSCT patients. IRF5 and STAT1- $\alpha$  proteins were detected in the allo-HSCT patients, but they did not correlate with miR-146a-5p expression levels. Human IRF5 belongs to a family of genes that functions both in the IFN signalling and the immune system. IFN- $\alpha$ , TNF- $\alpha$ , IL-6, IL-12 and IL-23

are all stimulated by IRF5. Recently, IRF5 has been shown to be involved in inflammation and in humans, higher expression of IRF5 as a consequence of polymorphisms in the gene has been implicated with autoimmune diseases (SLE and RA) (Graham *et al.*, 2006; Dieguez-Gonzalez *et al.*, 2008). Low expression of IRF5 results in up-regulation of IL-10 (Krausgruber *et al.*, 2010). IL-10 is an anti-inflammatory cytokine which is also associated with autoimmune diseases, due to its ability to lower the expression of TNF and other inflammatory cytokines (Fiorentino *et al.*, 1991). The findings of this study showed that *IRF5* mRNA expression positively correlated with its protein levels measured in whole blood at Day+28 in patients who went on to develop aGVHD and not in patients who did not develop aGVHD. However, there was no correlation between miR-146a-5p expression and IRF5 levels at both the mRNA and protein level. Not surprisingly, positive correlation was present among miR-146a-5p targets at the mRNA level both at pre and post allo-HSCT time-points. This showed that their expressions were dependent on one another. These results may suggest that miR-146a-5p and miR-155-5p act as 'paramedics' in the initial phases of inflammation due to their characteristic sensitivity. Thus, their levels are deregulated pre- aGVHD onset. However, once the limit of miR-146a-5p tolerance is breached, and miR-155 is overexpressed to compensate, the immune system is alarmed (Schulte *et al.*, 2012). It is at heightened inflammatory stage that their expression reaches a level that impacts the expression levels of their targets. This may be the reason why no correlation was seen between miR-146a-5p and its targets pre- aGVHD onset while the same miRNA has been shown to regulate TRAF6 expression at the time of aGVHD onset (Stickel *et al.*, 2014). This also explains the significant main effect of miR-146a-5p and its interaction with miR-155-5p observed in this study pre- aGVHD disease onset.

Mice deficient in miR-146a develop autoimmune disorders and die prematurely (Boldin *et al.*, 2011). The mutant mice had a loss of peripheral T cells as a result of the absence of miR-146a. Thus, a low expression of miR-146a could result in an inflammatory phenotype as noted in mice and impact survival (Luo *et al.*, 2010). Next, the impact of miRNA expression levels on survival was tested, and results showed that higher miR-146a-5p expression was indicative of poor survival outcome. This may suggest that patients with lower miR-146a-5p expression have more GVT effect due to exacerbated GVH reaction, and this eventually leads to GVHD. When the important clinical risk factors were included in the study, results showed that mismatches in HLA

class I were associated with risk of death. This finding shows that the miR-146a-5p expression is not associated with survival outcome when clinical risk factors are included in the analysis.

Interferons and TNF- $\alpha$  have been found to function in pathogenesis of GVHD (Klimpel *et al.*, 1990; Cooke *et al.*, 1998). The IFNs play an integral role in the regulation of both innate and adaptive immune reactions. Even though there have been investigations to determine the role of type I and II IFNs in GVHD, this yet remains unclear. IFN- $\gamma$  (Type II) has been shown to either reduce or escalate the disease (Welniak *et al.*, 2000; Lu and Waller, 2009). In contrast, very limited studies have focused on the role of IFN- $\alpha$  (Type I) in the pathogenesis of GVHD (Reyes and Klimpel, 1987; Pavord *et al.*, 1992). Reyes and Klimpel, were able to show that the serum level of IFN- $\alpha$  correlates with GVHD severity (Reyes and Klimpel, 1987) and other studies have shown that STAT1 is the main signal transducer for both IFN- $\alpha$  and IFN- $\gamma$  (Schindler and Plumlee, 2008). Recently in murine models, higher expression of Stat1 and Stat1-dependent cytokines (Cxcl10, Cxcl9) have been shown to be involved in the development of GVHD (Ma *et al.*, 2011).

Using the available online database, [microrna.org](http://microrna.org) it was found that miR-146a-5p and miR-155-5p only bind to STAT1- $\alpha$  rather than STAT1- $\beta$ . It is STAT1- $\alpha$  which is responsible for IFN- $\gamma$  induction (Lee and Benveniste, 1996). However, in this investigation STAT1- $\alpha$  did not correlate with the expression of either miRNAs. As part of their conditioning regimens, 88% of allo-HSCT patients in this study had been administered fludarabine as part of their conditioning regimen. It reduces the levels of both variants of STAT1 (STAT1- $\alpha$  and STAT1- $\beta$ ). In fact the study by Frank *et al.*, has shown that PBMCs exposed to fludarabine for only 24 hrs and then washed and stimulated with phytohemagglutinin (PHA) have significantly lower levels of IFN- $\gamma$  secretion (Frank *et al.*, 1999). The authors suggested that the fludarabine does not have a transient impact on lymphocytes (LoVecchio *et al.*, 1999). A major criticism of the work is that the cells were only washed after exposure with fludarabine and then stimulated with PHA. The half-life of fludarabine is 20 hrs thus; when the cells were triggered with PHA the effect of fludarabine was still present. Also, under allogeneic conditions the impact of fludarabine might be less pronounced as the patients are infused with donor lymphocytes that have not been exposed to fludarabine. As a

future study, it might be interesting to set up a dose-response experiment with fludarabine in MLR and check for differences in the expression levels of the miRNAs. However, the terminal life of the drug should be considered in the experimental design.

The master transcription factor *SPI1* (PU.1) (Vangala *et al.*, 2003) controls miR-155 expressions (Ghani *et al.*, 2011). Both miRNAs are predicted to target *SPI1* according to microrna.org. Experiments have also shown that this transcription factor controls the expression of both miRNAs in HSCs (Ghani *et al.*, 2011). To test whether this critical transcription factor had any role in allo-HSCT, its levels were quantified in patients who went on to develop aGVHD (grades I-III) after Day+28. Interestingly, miR-155-5p and miR-146a-5p expression levels negatively correlated with *SPI1* mRNA levels. This may suggest that during GVH reaction the miRNAs are triggered by chemokines and cytokines which results in their regulation of *SPI1* rather than their activation by it (Ghani *et al.*, 2011; Joyce and Novina, 2013).

The normal or steady-state levels of both miRNAs were detected in the whole blood of healthy volunteers. MiR-146a-5p expression was not altered between normal volunteers, pre- and post allo-HSCT while the levels of miR-155-expression were under-expressed between normal and pre-transplantation. In addition, there was a difference in the levels of miR-155-expression between pre- and post allo-HSCT. This further confirmed that the main effect and interaction identified between miR-146a-5p and miR-155-5p expression was a result of the disease state.

Additionally, PBMCs were stimulated with IFN- $\gamma$  and miRNA expression levels detected after 24 and 48hrs. Interestingly, exposure of PBMC for 24hrs with IFN- $\gamma$  had no influence on the miRNA expression levels. However, after 48hrs there was a significant reduction in miR-146a-5p expression levels in comparison to the unstimulated cells. Experiments have shown that IFN- $\gamma$  can reduce miR-146a expression levels in CD14+ monocytes present in both cord blood and adult peripheral blood (Takahashi *et al.*, 2012). In contrast, miR-155-5p expression only showed a trend in reduction and this might mean that higher doses, as well as longer exposure periods, are needed for miR-155-5p expression to be significantly repressed. This finding is also supported by the differential 'check-point' hypothesis mentioned earlier and also shows that miR-146a-5p is more sensitive to the dose of IFN- $\gamma$  and its exposure time.

In SLE patients, no association was observed between miR-146a expression and high levels of steroids (Tang *et al.*, 2009). In the present study, all the patients were steroids-free at Day+28. In Jurkat cell lines Cyclosporine A reduces miR-146a and IL-2 levels (Curtale *et al.*, 2010). Cyclosporine A is prescribed to patients routinely one day before transplantation with a target dose of 250 ng/ml, for up to nearly 3-6 months post-transplantation. However, the dose may vary depending on the type of transplant (HLA-matched), risk of GVHD and other HSCT complications that might arise post-transplantation. To address the question of whether Cyclosporine A had any direct impact on miRNA expression levels both correlation statistics was performed as well as *in vitro* experiments using MLR reactions as the allogeneic response. Results showed that there was no significant correlation between either of the miRNAs and Cyclosporine A concentration in the peripheral blood at Day+28. Stimulation with low and high doses of Cyclosporine A had no impact on the miRNA expression levels in the MLR.

MiR-146a-5p is located on 5q33.33. Chromosome 5q is significant in MDS in which subgroups of patients develop 5q deletions and significantly lower miR-146a-5p expression (Starczynowski *et al.*, 2009). Even though 26% patients in this cohort had MDS as their underlying disease they were all in complete remission on transplantation. In addition, karyotype reports showed that only two out of the 14 patients had 5q deleted regions. One patient had deletion of both 5q31 and 5q33 while the other had both copies of 5q33 deleted regions. This further shows that the lower miR-146a-5p expression associated with aGVHD incidence is not due to the prior underlying diseases.

In summary, the results of this Chapter have shown that miR-146a-5p and miR-155-5p are lower in patients who go on to develop aGVHD (grade I-III). Results have also shown that *SPI1* is regulated by both miRNAs during the early stages of inflammation and that there is no detectable difference between the miRNA target levels and the respective miRNAs. It has also been shown that Cyclosporine A has no impact on the expression levels of both miRNAs while IFN- $\gamma$  reduces miR-146a expression levels significantly after 48 hr exposure. Figure 6.10 summarises the findings and postulations of this Chapter. However, the results need to be validated in a larger cohort with more severe aGVHD grades III-IV to be able to discern whether both miRNAs can be used as

predictive biomarkers for severity. This study has shown that their interaction with the response may be used as a predictive biomarker of incidence of aGVHD and this provides further insight into both the biology of the miRNAs and their targets in aGVHD disease biology.

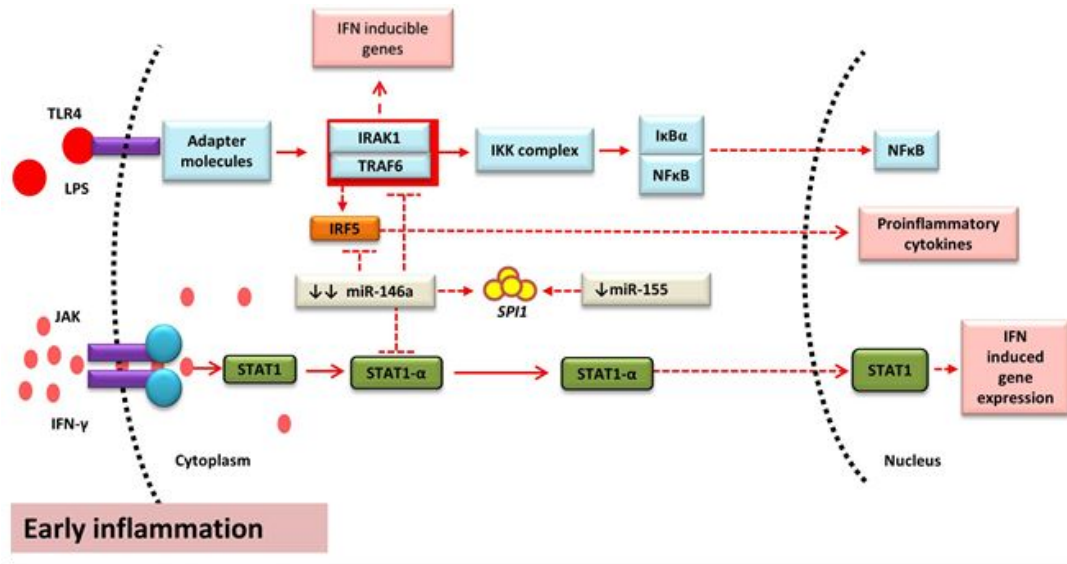


**Figure 6.10 MiR-146a-5p and miR-155-5p mechanism of action during early stages of inflammation** (adopted from (Taganov *et al.*, 2007; Rusca and Monticelli, 2011; Shen *et al.*, 2012). During the early stages of inflammation in GVHD, the TLR and Janus Kinase (JAK)-STAT1 pathway are activated by LPS and IFN-γ respectively. Both miR-146a-5p and miR-155-5p have reduced expression levels. This results in minor changes in the miRNA target levels but these alterations are not sufficient to be distinguishable from the uninfamed or normal conditions as they are the initial changes occurring in the system that ultimately leads to GVHD.

## Chapter 7. Concluding Remarks and Future Work

“The more I read, the more I acquire, the more certain I am that I know nothing.”

**-Voltaire**

## 7.1 Introduction

Since 1968, when the first successful allo-HSCT procedure was performed, globally thousands of patients have been cured of malignant haematological diseases. Currently, more than 70 disease types are treated with HSCTs that can be autologous or allogeneic. Last year, 2013 marked the one million HSCTs performed worldwide since 1957, when E. Donnall Thomas, treated the first patient with HSCTs. However, GVHD is still the primary complication of allo-HSCT. Similar to the global 'antibiotic discovery crisis', new GVHD treatment options are limited and fewer discoveries are made. Likewise, GVHD diagnosis still relies on manifestation of symptoms at the time of clinical evaluation. Over the last couple of decades, numerous potential biomarkers have been reported yet there is an absence of a fully validated biomarker that can be used in the transplantation clinic. This is mainly due to several reasons; (1) GVHD complexity, (2) lack of worldwide united multicenter collaborations with transparent regular reporting of results, (3) lack of standardized conditioning and prophylactic regimens and (4) inaccurate record keeping. As mentioned earlier (Chapter 1), the biomarker discoveries have looked at genes, proteins and SNPS. Therefore, this investigation aimed to study miRNAs that are the regulatory molecules that exist between mRNA transcripts and proteins. Investigating the regulatory mechanisms was proposed as being necessary for bridging the existing genomic and proteomic knowledge. Thus, this research sought to answer the following questions by incorporating both a screening based approach and the more traditional literature or evidence-based hypothesis-driven method of research. To my knowledge, the findings of this research have all been novel and no reports have been presented where the same methodology or experiments have been performed in the context of aGVHD and allo-HSCT.

- (4) Does aGVHD lead to the deregulation of miRNAs in the primary damaged target organ, skin?
  - a. Could the deregulated miRNAs be identified and used as diagnostic aGVHD biomarkers?
  - i. Could the deregulated miRNAs be predictive of OS and disease relapse?

- ii. What were the downstream effects of the deregulated miRNAs?
- (5) Do the immune-specific miRNAs (miR-146a and miR-155) in whole blood function in aGVHD?
- a. Could these miRNAs be used as predictive biomarkers of aGVHD incidence and severity?
  - b. Would there be any relationship between the miRNAs and their established targets?

In addition, using pathway mining techniques it was interesting to assess whether there was any overlap between the miRNAs identified via the screening experiment and those found to target the 18 genes. Since molecular interaction is a natural biological phenomenon, this study also looked for interactions between miRNAs as well as their targets.

### ***7.1.1 Eighteen genes were associated with immune-related, inflammatory, hematological and cutaneous conditions***

Pathway mining analyses performed in Chapter 3 showed that the 18 genes were involved in NF $\kappa$ B and p53 pathway as well as associated with TCR signaling. It was also shown that some of the genes were influenced by IFN- $\gamma$ . The list of miRNAs identified to target the 18 genes directed the miRNA signature list selection. This was an additional consideration to the significant differential expression observed between allo-HSCT skin biopsies and that of normal controls in the discovery cohort. The main limitation of the study in this Chapter was the lack of samples that overlapped with the miRNA skin investigation in Chapter 4. It would be interesting if matched samples were studied at the miRNA and mRNA expression levels to elucidate the regulatory mechanism involved with regards to the common pathways.

### ***7.1.2 Screening experiment in skin biopsies: MiR-503-5p, miR-34a and let-7c-5p were associated with allo-HSCT outcomes***

The screening experiments performed on a discovery cohort and then a validation cohort showed that miR-503-5p, miR-34a-5p/-3p and let-7c-5p were associated with aGVHD severity, OS and relapse. Therefore, miRNA expression was confirmed to be deregulated upon allo-HSCT and aGVHD in the target tissue, skin. The deregulation quantified also showed promising biomarker potential that would need to be further confirmed in a larger cohort potentially with skin biopsies collected from different transplantation centres. An attribute of a robust aGVHD biomarker would be its precision and accuracy in distinguishing the disease from that of controls independent of the conditioning regimens. Otherwise, the biomarker will only have a limited single centre application. Moreover, the miRNA targets are also required to be tested to understand the impact of their differential expression levels downstream and their link to the pathways already highlighted in Chapter 3. It would also be interesting to assess the miRNA expression levels and their 18 gene targets in the same skin biopsies both at the mRNA and protein level. The major limitation of this investigation has been the availability of cutaneous GVHD biopsies required to perform multiple studies. However, this limitation could be circumvented if biopsies of at least 2-4 mm were collected from five patients with skin histopathological aGVHD grades II-IV and five without aGVHD and run on a miRNA-mRNA Nanostring chip. This proposed study would both reduce the amount of starting total RNA material required to perform this research and also permit multiple matched comparisons to be performed looking at the main effects and interactions. The protein targets could always be detected by immunohistochemistry methods using FFPE blocks. The limiting factor in protein investigations is the availability of sensitive and specific antibodies.

### ***7.1.3 miR-34a-5p positively correlated with p53-positive cells in the epidermis***

The findings of Chapter 5 showed that there was a positive relationship between miR-34a-5p expression and p53-positive cells. It would be interesting to extend this section by looking at Sirt1 expression levels using immunohistochemical methods and then

assessing its relationship with both miR-34a-5p and p53. The finding would elucidate whether the direct control mechanism of p53 by miR-34a-4p through Sirt1 that is described in the literature is true under allo-HSCT conditions. The preliminary functional work optimisations showed the potential in inhibiting miR-34a-5p and observing lower T cell proliferation. Further knockdown optimisations in particular for miR-34a-3p and additional T cell proliferation experiments are required to assess the impact of miR-34a inhibition on T cells. A limitation of the RT-qPCR detection of the inhibited miRNA is that the miRNAs are not degraded by the inhibitors but inhibited or inactivated by a duplex formation of inhibitor-miRNA as they compete with the endogenous levels of miRNAs for binding to the RISC complex. Thus, when RT- qPCR is performed the duplex will dissociate and what is measured could be the miRNA that was released from the already formed duplex as if it was actively present in the sample. This increases the bias in RT-qPCR knockdown measurements. To eliminate this bias, detection of the downstream miRNA targets and/or luciferase-reporter assays are essential. In addition, co-transfection of the miR-34a strands would provide a more complete picture of the downstream impacts of miR-34a.

#### ***7.1.4 Whole blood investigation of immune-specific miRNAs: miR-146a-5p and miR-155-5p were associated in the prediction of aGVHD incidence***

The findings of Chapter 6 were independent of the first three results Chapters as they were based on evidence present in the literature with regards to both miR-146a-5p and miR-155-5p. However, the results are novel and interesting as it is the first reported study in which peripheral blood of allo-HSCT patients has been used to predict disease incidence and severity. The results are also in support of the recently published murine study where lower levels of miR-146a-5p were present in mice with severe aGVHD manifestation (Stickel *et al.*, 2014).

Unlike, miR-155-5p that was significantly differentially expressed in the skin at the time of aGVHD diagnosis, miR-146a-5p expression was not deregulated. This may have been due to the hierarchical pattern of expression mentioned in Chapter 6. The skin biopsies were collected at the time of aGVHD diagnosis which was indicative of the presence of damage to the host tissue and therefore severe levels of inflammation. This level might have breached miR-146a-5p level of control and therefore, miR-155-5p was

deregulated at this stage. Thus, to test this hypothesis it would be interesting to measure miR-146a-5p and miR-155-5p expression levels in skin biopsies prior to aGVHD onset. Another proposed reason might be that miR-146a-5p expression is mainly present in whole blood rather than skin tissues. This would qualify for the cell and tissue specificity of miRNAs. Therefore, it would be interesting to sort the different subsets of cells present in whole blood and quantify miRNA expression levels, likewise sort the different cells present in the skin and then detect miRNA expression levels. In all, the main limitation of this whole blood investigation was the lack of severe aGVHD patients. However, this has been a general limitation of this research which reiterates the need for multicenter-based investigations.

Overall, the research presented in this thesis was performed by looking at miRNAs at the tissue level. Therefore, to better understand the role of the miRNAs in allo-HSCT and in GVHD it would be ideal to step closer to the cellular level and investigate the expression levels in specific cell subsets (sorting by flow cytometry for whole blood and skin as well as electro-microdissection for skin tissues). At present all the conclusions have been made on a general basis rather than as per cell type. Allogeneic HSCT patients receive HSCT grafts and thus it would be reasonable to propose that to be able to segment these patients for specific therapies and discover new therapeutics it is essential to localize the miRNA expression levels at the cellular level. Likewise, to be able to take the miRNAs identified from this research into functional investigation it would be necessary to optimize the human *in vitro* skin explant model to reflect the changes in the clinical treatment regimens. The assay is a valuable tool for human based experiments, and it would, therefore, provide more informative results than animal-based model if they were to be used for extensions of the miRNA functional studies.

Taken together, the findings of this research has highlighted the complexity involved in GVHD and has shown that there is a combination of miRNAs involved that are controlling inflammation via interactions. In my opinion, it may not be feasible to have a systemic miRNA-based treatment available in the future to treat GVHD but there maybe be better topical options available that could deliver miRNAs such as via fabricated hydrogel dressings. These could then be used in steroid-resistant patients or

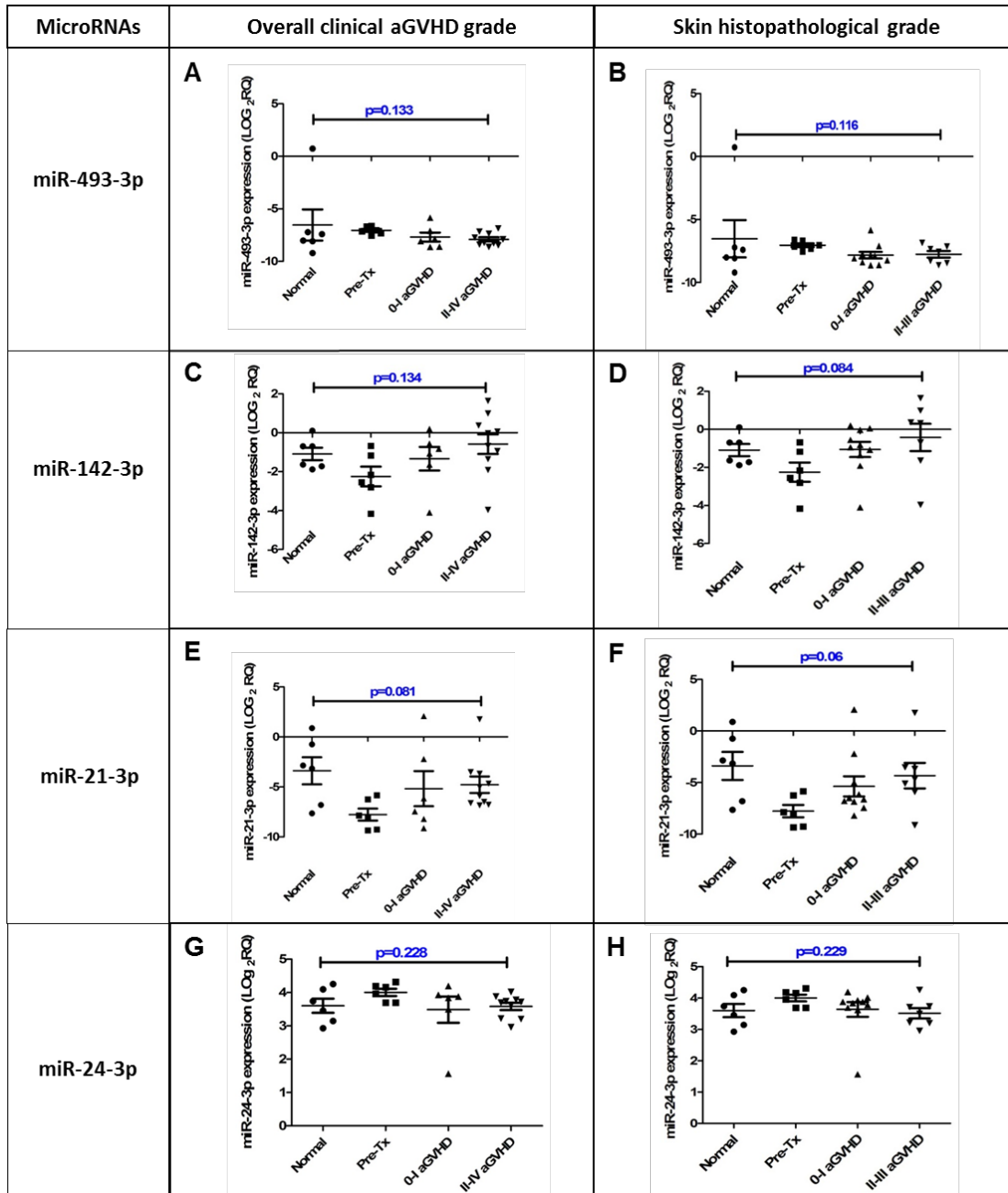
those suffering from severe skin GVHD. It would be interesting to investigate the impact of miRNAs on the GVL effect which was not investigated during this study.

In summary, this research has been novel in firstly, investigating miRNAs in one of the target organs of GVHD, the skin and also using peripheral blood to predict GVHD incidence prior to disease occurrence. The statistical approach has also been novel in the context of GVHD especially with regards to using miRNAs and their interactions to diagnose as well as predict disease incidence and relapse.

## Appendix I

Cohort Characteristics		aGVHD overall clinical grades				Difference (p-value)
		0-I		II-III		
		No.	%	No.	%	
Patient age (median years)		50.5 (19-65)				1.000
Patient gender	Female	1	33.3%	2	66.7%	1.000
	Male	5	38.5%	8	61.5%	
Donor gender	Female	1	20.0%	4	80.0%	0.580
	Male	5	50.0%	5	50.0%	
Graft source	BM	1	100.0%	0	0.0%	0.375
	PBSC	5	33.3%	10	66.7%	
Underlying Disease	ALL	1	50.0%	1	50.0%	0.293
	AML	0	0.0%	3	100.0%	
	MDS	3	75.0%	1	25.0%	
	MF	0	0.0%	1	100.0%	
	NHL	0	0.0%	1	100.0%	
	CLL	1	100.0%	0	0.0%	
	MM	1	25.0%	3	75.0%	
Regimen	Myeloablative	1	33.3%	2	66.7%	1.000
	RIC	5	38.5%	8	61.5%	
Protocol	Cy TBI Alem	1	33.3%	2	66.7%	1.000
	Flu Bus Alem	1	33.3%	2	66.7%	
	Flu Mel Alem	4	40.0%	6	60.0%	
Campath	30 mg	3	75.0%	1	25.0%	0.264
	60 mg	3	30.0%	7	70.0%	
	90 mg	0	0.0%	2	100.0%	
Relationship	SIB	2	66.7%	1	33.3%	0.518
	MUD	4	30.8%	9	69.2%	
Patient CMV status	Negative	1	20.0%	4	80.0%	0.600
	Positive	4	40.0%	6	60.0%	
Donor CMV status	Negative	4	44.4%	5	55.6%	1.000
	Positive	2	33.3%	4	66.7%	
HLA class I compatibility	None	5	45.5%	6	54.5%	0.588
	One	1	20.0%	4	80.0%	
HLA class II compatibility	None	3	60.0%	2	40.0%	0.537
	One	2	28.6%	5	71.4%	
	Two	1	25.0%	3	75.0%	
Survival status	Alive	4	44.4%	5	55.6%	0.633
	Dead	2	28.6%	5	71.4%	
Relapse status	No	3	27.3%	8	72.7%	0.299
	Yes	3	60.0%	2	40.0%	
Disease status at Transplant	CR	1	100.0%	0	0.0%	0.126
	CR1	0	0.0%	6	100.0%	
	CR2	2	40.0%	3	60.0%	
	PR	1	50.0%	1	50.0%	
Skin histopathological grade	0-I	6	60.0%	4	40.0%	0.034
	II-III	0	0.0%	6	100.0%	

**Table 1 Patient characteristic for the validation of the miRNA signature list (n=16) using the overall clinical aGVHD grades.** Fisher exact test was used to estimate the difference in frequencies between the aGVHD groups. Abbreviations:- BM: Bone marrow, PBSC: Peripheral blood stem cells, ALL: Acute lymphocytic leukaemia, AML: Acute myeloid leukaemia, CLL: Chronic lymphocytic leukaemia, MDS: Myelodysplastic syndrome, MM: Multiple myeloma, MPS: Multiple proliferative syndrome, NHL: Non-Hodgkin's lymphoma, RIC: Reduced intensity conditioning, Flu: Fludarabine, Mel: Melphalan, Bus: Busulfan, Cy: Cytrabine, TBI: Total body irradiation, Alem: Alemtuzumab, CsA: Cyclosporine, CMV: Cytomegalovirus, CR (1-3) Complete remission, PR: Progression, SIB: Sibling, MUD: Matched unrelated donor.



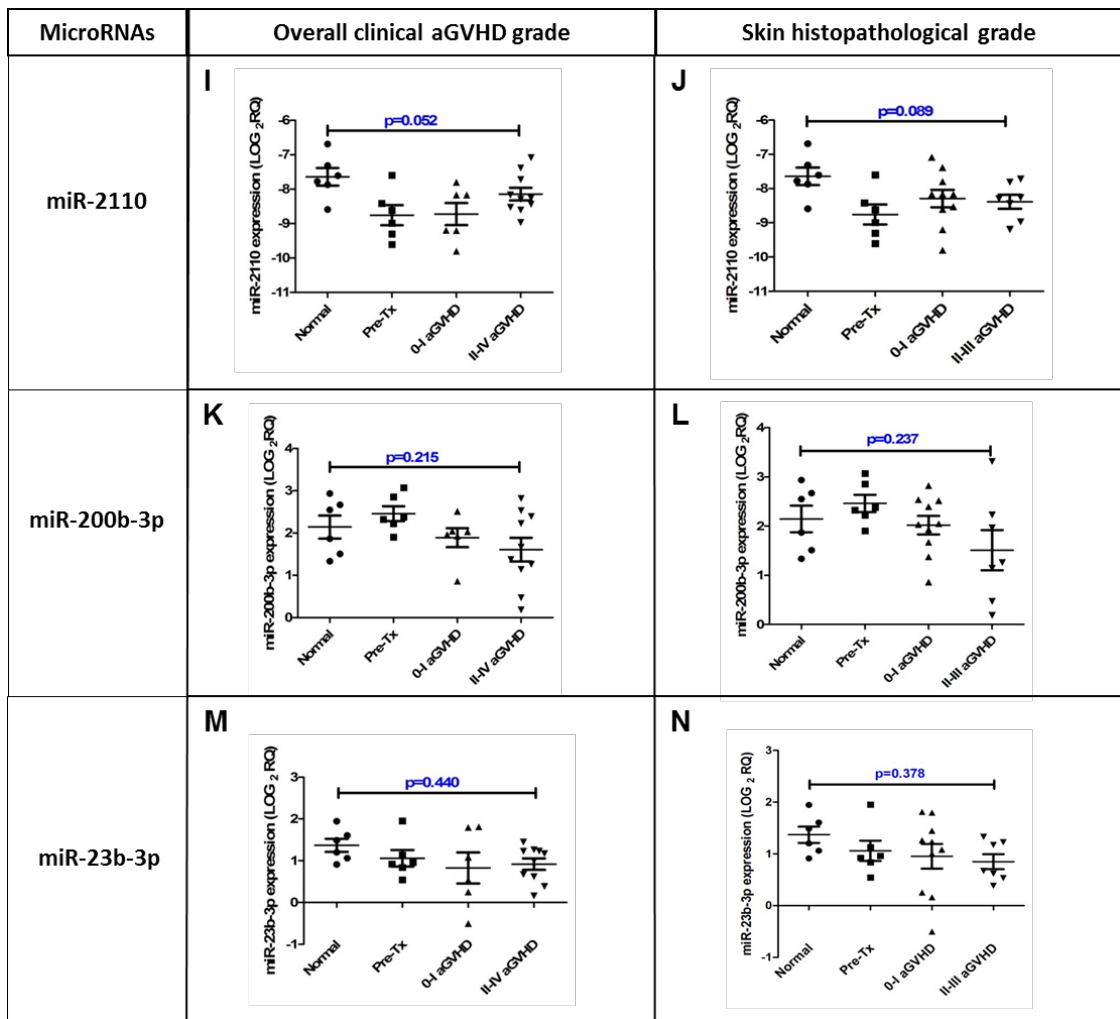


**Figure 1 Validation of miRNAs in clinical skin biopsies using histopathological grades.** Scatter plots show (A) miR-493-3p, (B) miR-142-3p, (C) miR-21-3p, (D) miR-24-3p, (E) miR-2110, (F) miR-200b-3p, (G) miR-23b-3p expression with error bars for SEM. RT-QPCR studied expression of miRNAs. Kruskal-Wallis analysis of variance was used to determine the significance set at  $p < 0.05$ . Normal: normal controls, Pre-Tx: Pre-transplant

## Appendix II

IRAK1 (NM\_001569, NM\_001025242, NM\_001025243)

**hsa-miR-146a/IRAK1 Alignment**

```

3' uuggguaCCUUAAAG--UCAAGAGu 5' hsa-miR-146a
      ||| | | | | | | | |
24:5' caaauccGGAAGUCAAAAGUUCUCa 3' IRAK1
  
```

**hsa-miR-146a/IRAK1 Alignment**

```

3' uuGGGUACCUUAAGUCAAGAGu 5' hsa-miR-146a
      |:| | | | | | | | |
42:5' uuCUCAUGGUCAGAAGUUCUCa 3' IRAK1
  
```

TRAF6 (NM\_004620, NM\_145803)

**hsa-miR-146a/TRAF6 Alignment**

```

3' uuGGGUACCUUAAGUCAAGAGu 5' hsa-miR-146a
      |:| | | | | | | | |
459:5' gcUCUAGAAAGUUGAGUUCUCa 3' TRAF6
  
```

STAT1-alpha (NM\_007315)

**hsa-miR-146a/STAT1 Alignment**

```

3' uuggguaccuuAAGUCAAGAGu 5' hsa-miR-146a
      | | | | | | | | |
774:5' acauuuuuuUACAGUUCUCc 3' STAT1
  
```

**hsa-miR-155/STAT1 Alignment**

```

3' uggggAUAGUGCUAUCGUAUu 5' hsa-miR-155
      ||| |:| | | | | | |
1375:5' uaaagUAUC-UGUAUUGCAUUAa 3' STAT1
  
```

IRF5 (NM\_002200, NM\_001098627, NM\_001098628, NM\_001098631, AY693668)

**hsa-miR-146a/IRF5 Alignment**

```

3' uuggGUACCUUAAGUCAAGAGu 5' hsa-miR-146a
      || | |:| | | | | | |
997:5' gggaCA-GUGAGUGAGUUCUCu 3' IRF5
  
```

SPI1 (NM\_003120, NM\_001080547)

**hsa-miR-155/SPI1 Alignment**

```

3' ugGGGAUAGUGCUAUCGUAUu 5' hsa-miR-155
      ||| | |:| | | | | | |
32:5' ucCCCGCUGGCCA-UAGCAUUAa 3' SPI1
  
```

**Figure 1** MiRNA targets for miR-146a and miR-155. The targets were predicted using the online database microrna.org. IRAK1, TRAF6, STAT1- $\alpha$ , IRF5 and SPI1 were all predicted to be targets of miR-146. STAT1- $\alpha$  and SPI1 were predicted as targets of miR-155. The figures show the alignment and partial complementarity between the seed sequences of the miRNAs and their predicted mRNA targets. The vertical lines show the binding.

Spearman Correlation		<i>TRAF6</i>	<i>IRAK1</i>	<i>STAT1A</i>	<i>IRF5</i>	<i>SPI1</i>	miR-146a -5p	miR-155 -5p	aGVHD incidence
<i>TRAF6</i>	$r_s$		0.80	0.77	0.68	0.48	-0.16	-0.17	0.20
	p-value		<b>0.000</b>	<b>0.000</b>	<b>0.000</b>	<b>0.000</b>	0.264	0.229	0.140
<i>IRAK1</i>	$r_s$	0.80		0.58	0.70	0.32	-0.12	-0.11	0.22
	p-value	<b>0.000</b>		<b>0.000</b>	<b>0.000</b>	<b>0.024</b>	0.392	0.438	0.118
<i>STAT1-<math>\alpha</math></i>	$r_s$	0.77	0.58		0.65	0.54	0.00	-0.12	0.23
	p-value	<b>0.000</b>	<b>0.000</b>		<b>0.000</b>	<b>0.000</b>	0.981	0.394	0.109
<i>IRF5</i>	$r_s$	0.68	0.70	0.65		0.39	-0.09	-0.10	0.13
	p-value	0.000	0.000	0.000		0.005	0.542	0.504	0.360
<i>SPI1</i>	$r_s$	0.48	0.32	0.54	0.39		-0.28	-0.35	0.17
	p-value	<b>0.000</b>	<b>0.024</b>	<b>0.000</b>	<b>0.005</b>		<b>0.040</b>	<b>0.010</b>	0.226
miR-146a -5p	$r_s$	-0.16	-0.12	0.00	-0.09	-0.28		0.22	0.07
	p-value	0.264	0.392	0.981	0.542	<b>0.040</b>		<b>0.114</b>	0.632
miR-155-5p	$r_s$	-0.17	-0.11	-0.12	-0.10	-0.35	0.22		-0.21
	p-value	0.229	0.438	0.394	0.504	<b>0.010</b>	0.114		0.120
aGVHD incidence	$r_s$	0.20	0.22	0.23	0.13	0.17	0.07	-0.21	
	p-value	0.140	0.118	0.109	0.360	0.226	0.632	0.120	

**Table 1** Spearman correlation showed significant positive correlation between all the mRNA targets in whole blood collected from allo-HSCT patients (n=51- 54) on Day+28. Significant negative correlation was present for both miR-146a-5p and miR-155-5p with *SPI1*.

Spearman Correlation			miR-146a-5p	<i>TRAF6</i>	<i>IRAK1</i>	<i>STAT1-<math>\alpha</math></i>	<i>IRF5</i>
Pre-transplant	miR-146a-5p	$r_s$	1.00	0.16	-0.24	-0.19	-0.24
		p-value		0.573	0.437	0.574	0.511
	<i>TRAF6</i>	$r_s$	0.16	1.00	0.79	0.59	-0.13
		p-value	0.573		<b>0.001</b>	<b>0.027</b>	0.697
	<i>IRAK1</i>	$r_s$	-0.24	0.79	1.00	0.52	0.48
		p-value	0.437	<b>0.001</b>		0.102	0.162
	<i>STAT1-<math>\alpha</math></i>	$r_s$	-0.19	0.59	0.52	1.00	0.24
		p-value	0.574	<b>0.027</b>	0.102		0.426
	<i>IRF5</i>	$r_s$	-0.24	-0.13	0.48	0.24	1.00
		p-value	0.511	0.697	0.162	0.426	

**Table 2** Spearman Correlation statistics between miR-146a-5p expression and its validated targets at pre-transplant.

Grade 0								
Spearman Correlation			miR-146a-5p	TRAF6	IRAK1	STAT1- $\alpha$	IRF5	
Day+28	miR-146a-5p	$r_s$	1.00	-0.37	-0.22	-0.26	-0.24	
		p-value		0.061	0.294	0.214	0.250	
	TRAF6	$r_s$	-0.37	1.00	0.81	0.77	0.85	
		p-value	0.061		<b>0.000</b>	<b>0.000</b>	<b>0.000</b>	
	IRAK1	$r_s$	-0.22	0.81	1.00	0.60	0.89	
		p-value	0.294	<b>0.000</b>		<b>0.002</b>	<b>0.000</b>	
	STAT1- $\alpha$	$r_s$	-0.26	0.77	0.60	1.00	0.64	
		p-value	0.214	<b>0.000</b>	<b>0.002</b>		<b>0.001</b>	
	IRF5	$r_s$	-0.24	0.85	0.89	0.64	1.00	
		p-value	0.250	<b>0.000</b>	<b>0.000</b>	<b>0.001</b>		
	3 months	miR-146a-5p	$r_s$	1.00	-0.60	-0.10	-0.20	-0.20
			p-value		0.400	0.873	0.704	0.704
TRAF6		$r_s$	-0.60	1.00	0.50	-0.40	0.80	
		p-value	0.400		0.667	0.600	0.200	
IRAK1		$r_s$	-0.10	0.50	1.00	0.30	0.80	
		p-value	0.873	0.667		0.624	0.104	
STAT1- $\alpha$		$r_s$	-0.20	-0.40	0.30	1.00	-0.03	
		p-value	0.704	0.600	0.624		0.957	
IRF5		$r_s$	-0.20	0.80	0.80	-0.03	1.00	
		p-value	0.704	0.200	0.104	0.957		

**Table 3** Spearman Correlation statistics between miR-146a-5p expression and its validated targets at Day+28 and three months in the no aGVHD cohort (Grade 0).

Grades I-III								
Spearman Correlation			miR-146a-5p	<i>TRAF6</i>	<i>IRAK1</i>	<i>STAT1-<math>\alpha</math></i>	<i>IRF5</i>	
Day+28	miR-146a-5p	$r_s$	1.00	0.06	-0.02	0.25	0.10	
		p-value		0.765	0.928	0.201	0.634	
	<i>TRAF6</i>	$r_s$	0.06	1.00	0.75	0.64	0.52	
		p-value	0.765		<b>0.000</b>	<b>0.000</b>	<b>0.006</b>	
	<i>IRAK1</i>	$r_s$	-0.02	0.75	1.00	0.47	0.45	
		p-value	0.928	<b>0.000</b>		<b>0.013</b>	<b>0.019</b>	
	<i>STAT1-<math>\alpha</math></i>	$r_s$	0.25	0.64	0.47	1.00	0.62	
		p-value	0.201	<b>0.000</b>	<b>0.013</b>		<b>0.001</b>	
	<i>IRF5</i>	$r_s$	0.10	0.52	0.45	0.62	1.00	
		p-value	0.634	<b>0.006</b>	<b>0.019</b>	<b>0.001</b>		
	3 months	miR-146a-5p	$r_s$	1.00	-0.42	-0.35	-0.39	-0.69
			p-value		0.229	0.298	0.235	<b>0.019</b>
<i>TRAF6</i>		$r_s$	-0.42	1.00	0.86	0.45	0.62	
		p-value	0.229		<b>0.001</b>	0.224	0.077	
<i>IRAK1</i>		$r_s$	-0.35	0.86	1.00	0.28	0.41	
		p-value	0.298	<b>0.001</b>		0.425	0.244	
<i>STAT1-<math>\alpha</math></i>		$r_s$	-0.39	0.45	0.28	1.00	0.51	
		p-value	0.235	0.224	0.425		0.110	
<i>IRF5</i>		$r_s$	-0.69	0.62	0.41	0.51	1.00	
		p-value	<b>0.019</b>	0.077	0.244	0.110		

**Table 4 Spearman Correlation statistics between miR-146a-5p expression and its validated targets at Day+28 and three months in the aGVHD cohort (Grades I-III).**

Spearman Correlation			miR-146a-5p	STAT1- $\alpha$	STAT1- $\alpha$ protein	IRF5	IRF5 protein
Pre-transplant	miR-146a-5p	$r_s$	1.00	-0.19	-0.05	-0.24	0.53
		p-value		0.574	0.873	0.511	0.096
	STAT1- $\alpha$	$r_s$	-0.19	1.00	0.30	0.24	0.41
		p-value	0.574		0.403	0.426	0.244
	STAT1- $\alpha$ protein	$r_s$	-0.05	0.30	1.00	0.40	-0.01
		p-value	0.873	0.403		0.250	0.980
	IRF5	$r_s$	-0.24	0.24	0.40	1.00	-0.20
		p-value	0.511	0.426	0.250		0.580
	IRF5 protein	$r_s$	0.53	0.41	-0.01	-0.20	1.00
		p-value	0.096	0.244	0.980	0.580	

**Table 5 Spearman Correlation statistics between miR-146a-5p expression and STAT1- $\alpha$  and IRF5 protein targets at pre-transplantation.**

Grade 0								
Spearman Correlation			miR-146a-5p	STAT1- $\alpha$	STAT1- $\alpha$ protein	IRF5	IRF5 protein	
Day+28	miR-146a-5p	$r_s$	1.00	-0.26	0.60	-0.24	0.30	
		p-value		0.214	0.285	0.250	0.624	
	STAT1- $\alpha$	$r_s$	-0.26	1.00	-0.10	0.64	0.20	
		p-value	0.214		0.873	0.001	0.747	
	STAT1- $\alpha$ protein	$r_s$	0.60	-0.10	1.00	-0.80	0.90	
		p-value	0.285	0.873		0.104	<b>0.037</b>	
	IRF5	$r_s$	-0.24	0.64	-0.80	1.00	-0.60	
		p-value	0.250	0.001	0.104		0.285	
	IRF5 protein	$r_s$	0.30	0.20	0.90	-0.60	1.00	
		p-value	0.624	0.747	<b>0.037</b>	0.285		
	3 months	miR-146a-5p	$r_s$	1.00	-0.20	0.10	-0.20	-0.10
			p-value		0.704	0.873	0.704	0.873
STAT1- $\alpha$		$r_s$	-0.20	1.00	0.60	-0.03	1.00	
		p-value	0.704		0.400	0.957		
STAT1- $\alpha$ protein		$r_s$	0.10	0.60	1.00	-0.40	0.50	
		p-value	0.873	0.400		0.600	0.391	
IRF5		$r_s$	-0.20	-0.03	-0.40	1.00	-0.40	
		p-value	0.704	0.957	0.600		0.600	
IRF5 protein		$r_s$	-0.10		0.50	-0.40	1.00	
		p-value	0.873		0.391	0.600		

**Table 6 Spearman Correlation statistics between miR-146a-5p expression and STAT1- $\alpha$  and IRF5 protein targets at Day+28 and three months in the no aGVHD cohort (Grade 0).**

Grades I-III								
Spearman Correlation			miR-146a-5p	STAT1- <i>a</i>	STAT1- $\alpha$ protein	IRF5	IRF5 protein	
Day+28	miR-146a-5p	$r_s$	1.00	0.25	0.53	0.10	-0.03	
		p-value		0.201	<b>0.092</b>	0.634	0.914	
	STAT1- <i>a</i>	$r_s$	0.25	1.00	0.57	0.62	0.34	
		p-value	0.201		<b>0.068</b>	<b>0.001</b>	0.286	
	STAT1- $\alpha$ protein	$r_s$	0.53	0.57	1.00	0.35	0.35	
		p-value	0.092	<b>0.068</b>		0.293	0.293	
	IRF5	$r_s$	0.10	0.62	0.35	1.00	0.71	
		p-value	0.634	<b>0.001</b>	0.293		<b>0.009</b>	
	IRF5 protein	$r_s$	-0.03	0.34	0.35	0.71	1.00	
		p-value	0.914	0.286	0.293	<b>0.009</b>		
	3 months	miR-146a-5p	$r_s$	1.00	-0.39	0.35	-0.69	0.45
			p-value		0.235	0.356	<b>0.019</b>	0.224
STAT1- <i>a</i>		$r_s$	-0.39	1.00	0.00	0.51	-0.18	
		p-value	0.235		1.000	0.110	0.702	
STAT1- $\alpha$ protein		$r_s$	0.35	0.00	1.00	-0.57	0.08	
		p-value	0.356	1.000		0.180	0.829	
IRF5		$r_s$	-0.69	0.51	-0.57	1.00	-0.32	
		p-value	<b>0.019</b>	0.110	0.180		0.482	
IRF5 protein		$r_s$	0.45	-0.18	0.08	-0.32	1.00	
		p-value	0.224	0.702	0.829	0.482		

**Table 7 Spearman Correlation statistics between miR-146a-5p expression and STAT1- $\alpha$  and IRF5 protein targets in the aGVHD cohort (Grades I-III).**

# Ethics Approval for Whole Blood Study



## National Research Ethics Service

### Newcastle & North Tyneside 1 Research Ethics Committee

Room G14  
Dental School  
Framlington Place  
Newcastle  
NE2 4BW

Telephone: (0191) 222 3581  
Facsimile: (0191) 222 3582  
E-mail: leonard.key@nhs.net

07 November 2007

Professor Anne Dickinson  
Professor of Marrow Transplant Biology  
Newcastle University  
Clinical & Laboratory Sciences  
Medical School  
Newcastle upon Tyne  
NE2 4HH

Dear Professor Dickinson

**Full title of study:** The development of new diagnostic tests, new tools and non-invasive methods for the prevention, early diagnosis and monitoring for haematopoietic stem cell transplantation (HSCT)

**REC reference number:** 07/H0906/131

Thank you for your letter of 16 October 2007, responding to the Committee's request for further information on the above research and submitting revised documentation.

The further information has been considered on behalf of the Committee by the Chair.

#### Confirmation of ethical opinion

On behalf of the Committee, I am pleased to confirm a favourable ethical opinion for the above research on the basis described in the application form, protocol and supporting documentation as revised.

#### Ethical review of research sites

The Committee has designated this study as exempt from site-specific assessment (SSA). There is no requirement for [other] Local Research Ethics Committees to be informed or for site-specific assessment to be carried out at each site.

#### Conditions of approval

The favourable opinion is given provided that you comply with the conditions set out in the attached document. You are advised to study the conditions carefully.

#### Approved documents

The final list of documents reviewed and approved by the Committee is as follows:

Document	Version	Date
Application	A+B+SSIF	28 August 2007

This Research Ethics Committee is an advisory committee to North East Strategic Health Authority  
07-H0906-131 071107  
The National Research Ethics Service (NRES) represents the NRES Directorate within  
the National Patient Safety Agency and Research Ethics Committees in England

Investigator CV	A M Dickinson	28 August 2007
Protocol	Version 1	28 August 2007
Covering Letter	A M Dickinson	28 August 2007
Peer Review	037703	
Participant Information Sheet: BMT Donor	Version 2.3	16 October 2007
Participant Information Sheet: Healthy volunteers	Version 2	16 October 2007
Participant Information Sheet: BMT patient	Version 2	16 October 2007
Participant Information Sheet: Autologous transplant	Version 2	16 October 2007
Participant Consent Form: Healthy volunteers	Version 2	16 October 2007
Participant Consent Form: Autologous transplant	Version 1	13 August 2007
Participant Consent Form: BMT Donor	Version 1	13 August 2007
Participant Consent Form: BMT Patient	Version 1	13 August 2007
Response to Request for Further Information	A M Dickinson	16 October 2007
Letter from funder	037703	09 October 2006

### R&D approval

All researchers and research collaborators who will be participating in the research at NHS sites should apply for R&D approval from the relevant care organisation, if they have not yet done so. R&D approval is required, whether or not the study is exempt from SSA. You should advise researchers and local collaborators accordingly.

Guidance on applying for R&D approval is available from <http://www.rdforum.nhs.uk/rdform.htm>.

### Statement of compliance

The Committee is constituted in accordance with the Governance Arrangements for Research Ethics Committees (July 2001) and complies fully with the Standard Operating Procedures for Research Ethics Committees in the UK.

### After ethical review

Now that you have completed the application process please visit the National Research Ethics Website > After Review

Here you will find links to the following

- a) Providing feedback. You are invited to give your view of the service that you have received from the National Research Ethics Service on the application procedure. If you wish to make your views known please use the feedback form available on the website.
- b) Progress Reports. Please refer to the attached Standard conditions of approval by Research Ethics Committees.
- c) Safety Reports. Please refer to the attached Standard conditions of approval by Research Ethics Committees.
- d) Amendments. Please refer to the attached Standard conditions of approval by Research Ethics Committees.
- e) End of Study/Project. Please refer to the attached Standard conditions of approval by Research Ethics Committees.

We would also like to inform you that we consult regularly with stakeholders to improve our service. If you would like to join our Reference Group please email [referencegroup@nationalres.org.uk](mailto:referencegroup@nationalres.org.uk).

This Research Ethics Committee is an advisory committee to North East Strategic Health Authority  
The National Research Ethics Service (NRES) represents the NRES Directorate within  
the National Patient Safety Agency and Research Ethics Committees in England

07/H0906/131

Please quote this number on all correspondence

With the Committee's best wishes for the success of this project

Yours sincerely

P.P.

**Professor Peter A Heasman**  
**Chair**

Enclosures:

*Standard approval conditions*

Copy to:

Newcastle upon Tyne Hospitals NHS Foundation Trust  
Research & Development  
Clinical Research Facility  
4th Floor - Leazes Wing  
Royal Victoria Infirmary  
Queen Victoria Road  
Newcastle upon Tyne  
NE1 4LP

This Research Ethics Committee is an advisory committee to North East Strategic Health Authority  
The National Research Ethics Service (NRES) represents the NRES Directorate within  
the National Patient Safety Agency and Research Ethics Committees in England

# Ethics Approval for the Skin Study: Pre- and Post Allo-HSCT Biopsies



## National Research Ethics Service Newcastle & North Tyneside 1 Research Ethics Committee

TEDCO Business Centre  
Room 002  
Rolling Mill Road  
Jarrow  
NE32 3DT

Tel: 0191 428 3564  
Fax: 0191 428 3432

09 March 2011

Professor Matthew Collin  
Haematological Sciences  
Newcastle University  
Framlington Place  
Newcastle upon Tyne  
NE2 4HH

Dear Professor Collin

**Study title:** Reconstitution of the cutaneous immune system after haematopoietic stem cell transplantation  
**REC reference:** 05/Q0905/200  
**Amendment number:** Amendment 1 20.02.2011  
**Amendment date:** 25 February 2011

The above amendment was reviewed at the meeting of the Sub-Committee held on 08 March 2011.

### Ethical opinion

The members of the Committee taking part in the review gave a favourable ethical opinion of the amendment on the basis described in the notice of amendment form and supporting documentation.

### Approved documents

The documents reviewed and approved at the meeting were:

Document	Version	Date
Notice of Substantial Amendment (non-CTIMPs)	Amendment 1 20.02.2011	25 February 2011
Investigator CV	Dr Stephen Todryk	22 February 2011
Investigator CV	Tracey Brown	22 February 2011
Investigator CV	Naomi McGovern	22 January 2011
Investigator CV	Rachel Emma Dickinson	22 February 2011

### Membership of the Committee

The members of the Committee who took part in the review are listed on the attached sheet.

### R&D approval

This Research Ethics Committee is an advisory committee to the North East Strategic Health Authority  
The National Research Ethics Service (NRES) represents the NRES Directorate within  
the National Patient Safety Agency and Research Ethics Committees in England

All investigators and research collaborators in the NHS should notify the R&D office for the relevant NHS care organisation of this amendment and check whether it affects R&D approval of the research.

**Statement of compliance**

The Committee is constituted in accordance with the Governance Arrangements for Research Ethics Committees (July 2001) and complies fully with the Standard Operating Procedures for Research Ethics Committees in the UK.

05/Q0905/200:

Please quote this number on all correspondence

Yours sincerely



**Miss Laura Kirkbride**  
**Committee Co-ordinator**

E-mail: [laura.kirkbride@sotw.nhs.uk](mailto:laura.kirkbride@sotw.nhs.uk)

*Enclosures: List of names and professions of members who took part in the review*

*Copy to: Newcastle upon Tyne Hospitals NHS Foundation Trust*

**Subject: Notification of Newcastle upon Tyne Hospitals NHS Foundation Trust Acceptance of Amendment**  
**Date:** Wednesday, 23 March 2011 15:23  
**From:** Walker, Jennifer <Jennifer.Walker@nuth.nhs.uk>  
**To:** Matthew Collin <matthew.collin@newcastle.ac.uk>

Dear Professor Collin

**Study Title: Reconstitution of the cutaneous immune system after haematopoietic stem cell transplantation**  
**Trust ref: 3599**  
**REC Reference: 05/Q0905/200**

**Date of submission to REC: 25th February 2011**  
**REC favourable opinion letter: 9th March 2011**

**Sponsor's Unique Amendment Number: Amendment 1 20.02.2011**

Following review of the above amendment, Newcastle upon Tyne Hospitals NHS Foundation Trust can confirm that we can accommodate this amendment.

The amendment may therefore be immediately implemented at this site under the existing NHS Permission. Please note that you may only implement changes that were described in the amendment notice or letter.

I am pleased to confirm that the extension to the study duration is approved. This does not affect Trust approval, which will remain in place until **31st December 2014**.

Kind regards,

**Jenn Walker**

Research and Development Facilitator  
Newcastle Upon Tyne Hospitals NHS Foundation Trust

*Joint Research Office  
Level 6, Leazes Wing  
Royal Victoria Infirmary  
Queen Victoria Rd  
Newcastle upon Tyne  
NE1 4LP*

(: 0191 28 24520 **Fax:** 0191 28 24524

For more information please visit: [http://www.newcastle-hospitals.org.uk/about-us/staff-information\\_research-development.aspx](http://www.newcastle-hospitals.org.uk/about-us/staff-information_research-development.aspx) <[http://www.newcastle-hospitals.org.uk/about-us/staff-information\\_research-development.aspx](http://www.newcastle-hospitals.org.uk/about-us/staff-information_research-development.aspx)>

# Ethics Approval for the Skin Study: Healthy Volunteers Skin Biopsies

SL27 Valid notice of substantial amendment  
Version 3, June 2005



**National Research Ethics Service**  
Newcastle and North Tyneside 1 Research Ethics Committee  
Room G14  
The Dental School  
Framlington Place  
Newcastle upon Tyne  
NE2 4BW

Tel: 0191 222 3581  
Fax: 0191 222 3582  
Email: [leonard.key@nhs.net](mailto:leonard.key@nhs.net)

09 October 2007

Dr M Collin  
Haematological Sciences  
School of Clinical and Laboratory Sciences  
University of Newcastle

Dear Dr Collin

**Study title:** Investigation Of Graft-Versus-Host Disease Using Normal Skin  
Routinely Excised From Patients Undergoing Plastic Surgery  
**REC reference:** 2002/204  
**Protocol number:** [where applicable]  
**EudraCT number:** [CTIMPs only]

**Amendment number:** 03  
**Amendment date:** 10 September 2007

Thank you for submitting the above amendment, which was received on 28 September 2007. I can confirm that this is a valid notice of a substantial amendment and will be reviewed by the Sub-Committee at its next meeting.

## Documents received

The documents to be reviewed are as follows:

<u>document</u>	<u>reference</u>	<u>date</u>
Covering letter	MC	10 September 2007
Notice of substantial amendment	03	10 September 2007
Protocol	Version 2	01 September 2007
Participant Information Document	Version 4	01 September 2007
Consent Form		

## Notification of the Committee's decision

The Committee will issue an ethical opinion on the amendment within a maximum of 35 days from the date of receipt.

## Research governance approval

All investigators and research collaborators in the NHS should notify the R&D Department for the relevant NHS care organisation of this amendment and check whether it affects research governance approval for the research.

This Research Ethics Committee is an advisory committee to North East Strategic Health Authority  
2002-204 071009  
The National Research Ethics Service (NRES) represents the NRES Directorate within  
the National Patient Safety Agency and Research Ethics Committees in England

2002/204: **Please quote this number on all correspondence**

Yours sincerely



**Mr Leonard Key**  
**Committee Co-ordinator**

Copy to:

Newcastle upon Tyne Hospitals NHS Foundation Trust  
Research & Development  
Clinical Research Facility  
4th Floor - Leazes Wing  
Royal Victoria Infirmary  
Queen Victoria Road  
Newcastle upon Tyne  
NE1 4LP

## Bibliography

- Akira, S., Hirano, T., Taga, T. and Kishimoto, T. (1990) 'Biology of multifunctional cytokines: IL 6 and related molecules (IL 1 and TNF)', *FASEB J*, 4(11), pp. 2860-7.
- Alevizos, I. and Illei, G.G. (2010) 'MicroRNAs as biomarkers in rheumatic diseases', *Nat Rev Rheumatol*, 6(7), pp. 391-398.
- Alexiou, P., Maragkakis, M., Papadopoulos, G.L., Simmosis, V.A., Zhang, L. and Hatzigeorgiou, A.G. (2010) 'The DIANA-mirExTra web server: from gene expression data to microRNA function', *PLoS One*, 5(2), p. e9171.
- Allantaz, F., Cheng, D.T., Bergauer, T., Ravindran, P., Rossier, M.F., Ebeling, M., Badi, L., Reis, B., Bitter, H., D'Asaro, M., Chiappe, A., Sridhar, S., Pacheco, G.D., Burczynski, M.E., Hochstrasser, D., Vonderscher, J. and Matthes, T. (2012) 'Expression Profiling of Human Immune Cell Subsets Identifies miRNA-mRNA Regulatory Relationships Correlated with Cell Type Specific Expression', *PLoS ONE*, 7(1), p. e29979.
- Ambros, V., Bartel, B., Bartel, D.P., Burge, C.B., Carrington, J.C., Chen, X., Dreyfuss, G., Eddy, S.R., Griffiths-Jones, S.A.M., Marshall, M., Matzke, M., Ruvkun, G. and Tuschl, T. (2003) 'A uniform system for microRNA annotation', *RNA*, 9(3), pp. 277-279.
- Amelio, I., Lena, A.M., Bonanno, E., Melino, G. and Candi, E. (2013) 'miR-24 affects hair follicle morphogenesis targeting Tcf-3', *Cell Death Dis*, 4, p. e922.
- Antin, J. and Ferrara, J. (1992) 'Cytokine dysregulation and acute graft-versus-host disease', *Blood*, 80, pp. 2964-2968.
- Antonini, D., Russo, M.T., De Rosa, L., Gorrese, M., Del Vecchio, L. and Missero, C. (2010) 'Transcriptional Repression of miR-34 Family Contributes to p63-Mediated Cell Cycle Progression in Epidermal Cells', *J Invest Dermatol*, 130(5), pp. 1249-1257.
- Antonson, P. and Xanthopoulos, K.G. (1995) 'Molecular Cloning, Sequence, and Expression Patterns of the Human Gene Encoding CCAAT/Enhancer Binding Protein  $\alpha$  (C/EBP $\alpha$ )', *Biochemical and Biophysical Research Communications*, 215(1), pp. 106-113.
- Appelbaum, F.R. (2007) 'Hematopoietic-Cell Transplantation at 50', *The New England Journal of Medicine*, 357, pp. 1472-1475.
- Apperley, J. and Masszi, T. (2012) 'Graft-versus-host disease', in Apperley, J., Carreras, E., Gluckman, E. and Masszi, T. (eds.) *EBMT-ESH Handbook on Haemopoietic Stem Cell Transplantation*. 6 edn. Italy: forum service editore, pp. 216-233.

Arasappan, D., Tong, W., Mummaneni, P., Fang, H. and Amur, S. (2011) 'Meta-analysis of microarray data using a pathway-based approach identifies a 37-gene expression signature for systemic lupus erythematosus in human peripheral blood mononuclear cells', *BMC Med*, 9, p. 65.

Armitage, J.O. (1994) 'Bone marrow transplantation', *N Engl J Med*, 330, pp. 827-838.

Asai, O., Longo, D.L., Tian, Z.G., Hornung, R.L., Taub, D.D., Ruscetti, F.W. and Murphy, W.J. (1998) 'Suppression of graft-versus-host disease and amplification of graft-versus-tumor effects by activated natural killer cells after allogeneic bone marrow transplantation', *The Journal of Clinical Investigation*, 101(9), pp. 1835-42.

Atkinson, K., Matias, C., Guiffre, A., Seymour, R., Cooley, M., Biggs, J., Munro, V. and Gillis, S. (1991) 'In vivo administration of granulocyte colony-stimulating factor (G-CSF), granulocyte-macrophage CSF, interleukin-1 (IL-1), and IL-4, alone and in combination, after allogeneic murine hematopoietic stem cell transplantation', *Blood*, 77(6), pp. 1376-1382.

Attiyeh, E.F., London, W.B., Mossé, Y.P., Wang, Q., Winter, C., Khazi, D., McGrady, P.W., Seeger, R.C., Look, A.T., Shimada, H., Brodeur, G.M., Cohn, S.L., Matthay, K.K. and Maris, J.M. (2005) 'Chromosome 1p and 11q Deletions and Outcome in Neuroblastoma', *New England Journal of Medicine*, 353(21), pp. 2243-2253.

Ayala, G., a, M.A., Gonz, lez Yebra, B., pez Flores, A.L., Guan and Guerra, E. (2012) 'The Major Histocompatibility Complex in Transplantation', *Journal of Transplantation*, 2012, p. 7.

Babiarz, J., Ruby, J., Wang, Y., Bartel, D. and Blelloch, R. (2008) 'Mouse ES cells express endogenous shRNAs, siRNAs, and other Microprocessor-independent, Dicer-dependent small RNAs', *Genes and Development*, 20, pp. 2773-2785.

Bader, A.G., Brown, D. and Winkler, M. (2010) 'The Promise of MicroRNA Replacement Therapy', *Cancer Research*, 70(18), pp. 7027-7030.

Bandres, E., Cubedo, E., Agirre, X., Malumbres, R., Zarate, R., Ramirez, N., Abajo, A., Navarro, A., Moreno, I., Monzo, M. and Garcia-Foncillas, J. (2006) 'Identification by Real-time PCR of 13 mature microRNAs differentially expressed in colorectal cancer and non-tumoral tissues', *Mol Cancer*, 5, p. 29.

Banerjee, A., Schambach, F., DeJong, C.S., Hammond, S.M. and Reiner, S.L. (2010) 'Micro-RNA-155 inhibits IFN-gamma signaling in CD4+ T cells', *Eur J Immunol*, 40(1), pp. 225-31.

Banerjee, J., Chan, Y.C. and Sen, C.K. (2011) 'MicroRNAs in skin and wound healing', *Physiol Genomics*, 43(10), pp. 543-56.

Baran, W., Szepietowski, J.C. and Szybejko-Machaj, G. (2005) 'Expression of p53 protein in psoriasis', *Acta Dermatovenerol Alp Pannonica Adriat*, 14(3), pp. 79-83.

Barao, I. and Murphy, W.J. (2003) 'The immunobiology of natural killer cells and bone marrow allograft rejection', *Biol Blood Marrow Transplant*, 9(12), pp. 727-41.

Barker, J.N. and Wagner, J.E. (2003) 'Umbilical-cord blood transplantation for the treatment of cancer', *Nat Rev Cancer*, 3(7), pp. 526-32.

Baron, C., Somogyi, R., Greller, L.D., Rineau, V., Wilkinson, P., Cho, C.R., Cameron, M.J., Kelvin, D.J., Chagnon, P., Roy, D.-C., Busque, L., SÃ©kaly, R.-P. and Perreault, C. (2007) 'Prediction of Graft-Versus-Host Disease in Humans by Donor Gene-Expression Profiling', *PLoS Med*, 4(1), p. e23.

Bartel, D.P. (2004) 'MicroRNAs: Genomics, Biogenesis, Mechanism, and Function', *Cell*, 116(2), pp. 281-297.

Bartel, D.P. (2009) 'MicroRNAs: target recognition and regulatory functions', *Cell*, 136(2), pp. 215-33.

Basyuk, E., Suavet, F., Doglio, A., Bordonne, R. and Bertrand, E. (2003) 'Human let-7 stem-loop precursors harbor features of RNase III cleavage products', *Nucleic Acids Research*, 31(22), pp. 6593-6597.

Baum, W., Kirkin, V., Fernandez, S.B., Pick, R., Lettau, M., Janssen, O. and Zornig, M. (2005) 'Binding of the Intracellular Fas Ligand (FasL) Domain to the Adaptor Protein PSTPIP Results in a Cytoplasmic Localization of FasL', *J Biol Chem*, 280(48), pp. 40012-24.

Baxter, A.G. and Hodgkin, P.D. (2002) 'Activation rules: The two-signal theories of immune activation', *Nature Reviews Immunology*, 2(6), pp. 439-446.

Beck, S. and Trowsdale, J. (2000) 'The human major histocompatibility complex: lessons from the DNA sequence', *Annu Rev Genomics Hum Genet*, 1, pp. 117-37.

Bentwich, I. (2005) 'Prediction and validation of microRNAs and their targets', *FEBS Lett*, 579(26), pp. 5904-10.

Bernstein, E., Caudy, A.A., Hammond, S.M. and Hannon, G.J. (2001) 'Role for a bidentate ribonuclease in the initiation step of RNA interference', *Nature*, 409(6818), pp. 363-366.

Betel, D., Wilson, M., Gabow, A., Marks, D.S. and Sander, C. (2008) 'The microRNA.org resource: targets and expression', *Nucleic Acids Research*, 36(suppl 1), pp. D149-D153.

Bhaumik D, P.C., Campisi J. (2009) 'MicroRNAs: an important player in maintaining a balance between inflammation and tumor suppression', *Cell Cycle*, 8, p. 1822.

Bhaumik, D., Scott, G.K., Schokrpur, S., Patil, C.K., Campisi, J. and Benz, C.C. (2008) 'Expression of microRNA-146 suppresses NF-kappa B activity with reduction of metastatic potential in breast cancer cells', *Oncogene*, 27(42), pp. 5643-5647.

Bland, J.M. and Altman, D.G. (2012) 'Agreed statistics: measurement method comparison', *Anesthesiology*, 116(1), pp. 182-5.

Blazar, B.R., Murphy, W.J. and Abedi, M. (2012) 'Advances in graft-versus-host disease biology and therapy', *Nat Rev Immunol*, 12(6), pp. 443-58.

Blazar, B.R., Taylor, P.A., Noelle, R.J. and Vallera, D.A. (1998) 'CD4(+) T cells tolerized ex vivo to host alloantigen by anti-CD40 ligand (CD40L:CD154) antibody lose their graft-versus-host disease lethality capacity but retain nominal antigen responses', *The Journal of Clinical Investigation*, 102(3), pp. 473-482.

Bleakley, M. and Riddell, S.R. (2004) 'Molecules and mechanisms of the graft-versus-leukaemia effect', *Nat Rev Cancer*, 4(5), pp. 371-380.

Boldin, M.P., Taganov, K.D., Rao, D.S., Yang, L., Zhao, J.L., Kalwani, M., Garcia-Flores, Y., Luong, M., Devrekanli, A., Xu, J., Sun, G., Tay, J., Linsley, P.S. and Baltimore, D. (2011) 'miR-146a is a significant brake on autoimmunity, myeloproliferation, and cancer in mice', *The Journal of Experimental Medicine*.

Boss, J.M. (1997) 'Regulation of transcription of MHC class-II genes', *Current Opinions in Immunology*, 9, pp. 107-113.

Brennecke, J., Hipfner, D.R., Stark, A., Russell, R.B. and Cohen, S.M. (2003) 'bantam Encodes a Developmentally Regulated microRNA that Controls Cell Proliferation and Regulates the Proapoptotic Gene hid in Drosophila', *Cell*, 113(1), pp. 25-36.

Briones, J., Novelli, S. and Sierra, J. (2011) 'T-Cell Costimulatory Molecules in Acute-Graft-Versus Host Disease: Therapeutic Implications', *Bone Marrow Research*, 2011.

Brown, H. and Prescott, R. (1999) in *Applied mixed models in medicine*. Second edn. J. Wiley & Sons, pp. 107-181.

Brunati, A.M., Deana, R., Folda, A., Massimino, M.L., Marin, O., Ledro, S., Pinna, L.A. and Donella-Deana, A. (2005) 'Thrombin-induced Tyrosine Phosphorylation of HS1 in Human Platelets Is Sequentially Catalyzed by Syk and Lyn Tyrosine Kinases and

Associated with the Cellular Migration of the Protein', *J Biol Chem*, 280(22), pp. 21029-35.

Buzzeo, M.P., Yang, J., Casella, G. and Reddy, V. (2008) 'A preliminary gene expression profile of acute graft-versus-host disease', *Cell Transplant*, 17(5), pp. 489-94.

Cahn, J.-Y., Klein, J.P., Lee, S.J., Milpied, N., Blaise, D., Antin, J.H., Leblond, V., Ifrah, N., Jouet, J.-P., Loberiza, F., Ringden, O., Barrett, A.J., Horowitz, M.M. and Socie, G. (2005) 'Prospective evaluation of 2 acute graft-versus-host (GVHD) grading systems: a joint Societe Francaise de Greffe de Moelle et Therapie Cellulaire (SFGM-TC), Dana Farber Cancer Institute (DFCI), and International Bone Marrow Transplant Registry (IBMTR) prospective study', *Blood*, 106(4), pp. 1495-1500.

Carlens, S., Ringdén, O., Remberger, M., Lönnqvist, B., Hägglund, H., Klaesson, S., Mattsson, J., Svahn, B., Winiarski, J., Ljungman, P. and Aschan, J. (1998) 'Risk factors for chronic graft-versus-host disease after bone marrow transplantation: a retrospective single centre analysis.', *bone Marrow Transplantation*, 22, pp. 755-761.

Chang, T.C., Zeitels, L.R., Hwang, H.W., Chivukula, R.R., Wentzel, E.A., Dews, M., Jung, J., Gao, P., Dang, C.V., Beer, M.A., Thomas-Tikhonenko, A. and Mendell, J.T. (2009) 'Lin-28B transactivation is necessary for Myc-mediated let-7 repression and proliferation', *Proc Natl Acad Sci U S A*, 106(9), pp. 3384-9.

Chen, C.-Z., Li, L., Lodish, H.F. and Bartel, D.P. (2004) 'MicroRNAs Modulate Hematopoietic Lineage Differentiation', *Science*, 303(5654), pp. 83-86.

Cheng, G., Sun, S., Wang, Z. and Jin, S. (2012) 'Investigation of the interaction between the MIR-503 and CD40 genes in irradiated U937 cells', *Radiation Oncology*, 7(1), p. 38.

Choi, H., Shen, R., Chinnaiyan, A.M. and Ghosh, D. (2007) 'A latent variable approach for meta-analysis of gene expression data from multiple microarray experiments', *BMC Bioinformatics*, 8, p. 364.

Choi, Y. (2005) 'Role of TRAF6 in the immune system', *Adv Exp Med Biol*, 560, pp. 77-82.

Chowdhury, F.Z., Ramos, H.J., Davis, L.S., Forman, J. and Farrar, J.D. 'IL-12 selectively programs effector pathways that are stably expressed in human CD8+ effector memory T cells in vivo', *Blood*, 118(14), pp. 3890-900.

Clark, R.A., Chong, B., Mirchandani, N., Brinster, N.K., Yamanaka, K., Dowgiert, R.K. and Kupper, T.S. (2006) 'The vast majority of CLA+ T cells are resident in normal skin', *J Immunol*, 176(7), pp. 4431-9.

Cooke, K.R., Hill, G.R., Crawford, J.M., Bungard, D., Brinson, Y.S., Delmonte, J., Jr. and Ferrara, J.L. (1998) 'Tumor necrosis factor- alpha production to lipopolysaccharide stimulation by donor cells predicts the severity of experimental acute graft-versus-host disease', *J Clin Invest*, 102(10), pp. 1882-91.

Couriel, D., Saliba, R., Hicks, K., Ippoliti, C., de Lima, M., Hosing, C., Khouri, I., Andersson, B., Gajewski, J., Donato, M., Anderlini, P., Kontoyiannis, D.P., Cohen, A., Martin, T., Giralt, S. and Champlin, R. (2004) 'Tumor necrosis factor-alpha blockade for the treatment of acute GVHD', *Blood*, 104(3), pp. 649-54.

Culpin, R.E., Sieniawski, M., Proctor, S.J., Menon, G. and Mainou-Fowler, T. (2013) 'MicroRNAs are suitable for assessment as biomarkers from formalin-fixed paraffin-embedded tissue, and miR-24 represents an appropriate reference microRNA for diffuse large B-cell lymphoma studies', *J Clin Pathol*, 66(3), pp. 249-52.

Curtale, G., Citarella, F., Carissimi, C., Goldoni, M., Carucci, N., Fulci, V., Franceschini, D., Meloni, F., Barnaba, V. and Macino, G. (2010) 'An emerging player in the adaptive immune response: microRNA-146a is a modulator of IL-2 expression and activation-induced cell death in T lymphocytes', *Blood*, 115(2), pp. 265-273.

Cutler, C., Miklos, D., Kim, H.T., Treister, N., Woo, S.-B., Bienfang, D., Klickstein, L.B., Levin, J., Miller, K., Reynolds, C., Macdonell, R., Pasek, M., Lee, S.J., Ho, V., Soiffer, R., Antin, J.H., Ritz, J. and Alyea, E. (2006) 'Rituximab for steroid-refractory chronic graft-versus-host disease', *Blood*, 108(2), pp. 756-762.

Daoud, S.S., Munson, P.J., Reinhold, W., Young, L., Prabhu, V.V., Yu, Q., LaRose, J., Kohn, K.W., Weinstein, J.N. and Pommier, Y. (2003) 'Impact of p53 knockout and topotecan treatment on gene expression profiles in human colon carcinoma cells: a pharmacogenomic study', *Cancer Res*, 63(11), pp. 2782-93.

Deeg, H.J. and Storb, R. (1986) 'Acute and chronic graft-versus-host disease: clinical manifestations, prophylaxis, and treatment', *J Natl Cancer Inst*, 76(6), pp. 1325-8.

Denfeld, R.W., Hollenbaugh, D., Fehrenbach, A., Weiss, J.M., von Leoprechting, A., Mai, B., Voith, U., Schöpf, E., Aruffo, A. and Simon, J.C. (1996) 'CD40 is functionally expressed on human keratinocytes', *European Journal of Immunology*, 26(10), pp. 2329-2334.

Deng, C., Radu, C., Diab, A., Tsen, M.F., Hussain, R., Cowdery, J.S., Racke, M.K. and Thomas, J.A. (2003) 'IL-1 receptor-associated kinase 1 regulates susceptibility to organ-specific autoimmunity', *J Immunol*, 170(6), pp. 2833-42.

Detre, S., Saclani Jotti, G. and Dowsett, M. (1995) 'A "quickscore" method for immunohistochemical semiquantitation: validation for oestrogen receptor in breast carcinomas', *Journal of Clinical Pathology*, 48(9), pp. 876-878.

Devergie, A. (2008) 'Graft versus host disease', in J.Apperley, E.C., E. Gluckman, A. Gratwohl, T.Masszi (ed.) *Haematopoietic Stem Cell Transplantation*. 5 edn., pp. 219-235.

Di Ianni, M., Falzetti, F., Carotti, A., Terenzi, A., Castellino, F., Bonifacio, E., Del Papa, B., Zei, T., Iacucci Ostini, R., Cecchini, D., Aloisi, T., Perruccio, K., Ruggeri, L., Balucani, C., Pierini, A., Sportoletti, P., Aristei, C., Falini, B., Reisner, Y., Velardi, A., Aversa, F. and Martelli, M.F. (2011) 'Tregs prevent GvHD and promote immune reconstitution in HLA-haploidentical transplantation', *Blood*, 2011, p. 3.

Dickinson, A., Dressel, R., Rolstadt, B. and Walter, L. (2012) 'MHC genes and risk of graft versus host disease'. Google Patents. Available at: <http://www.google.com/patents/WO2012080359A3?cl=en>.

Dickinson, A.M. and Holler, E. (2008) 'Polymorphisms of cytokine and innate immunity genes and GVHD', *Best Practice & Research Clinical Haematology*, 21(2), pp. 149-164.

Dickinson, A.M., Pearce, K.F., Norden, J., O'Brien, S.G., Holler, E., Bickeböllner, H., Balavarca, Y., Rocha, V., Kolb, H.-J., Hromadnikova, I., Sedlacek, P., Niederwieser, D., Brand, R., Ruutu, T., Apperley, J., Szydlo, R., Goulmy, E., Siegert, W., de Witte, T. and Gratwohl, A. (2010) *Impact of genomic risk factors on outcome after hematopoietic stem cell transplantation for patients with chronic myeloid leukemia*.

Dickinson AM, S.L., Dunn J, Carey P, Proctor SJ. (1991) 'Demonstration of direct involvement of cytokines in graft-versus-host reactions using an in vitro human skin explant model.', *Bone Marrow Transplant*, 7, pp. 209-216.

Dickinson, A.M., Sviland, L., Wang, X.N., Jackson, G., Taylor, P.R., Dunn, A. and Proctor, S.J. (1998) 'Predicting graft-versus-host disease in HLA-identical bone marrow transplant: a comparison of T-cell frequency analysis and a human skin explant model', *Transplantation*, 66(7), pp. 857-63.

Dieguez-Gonzalez, R., Calaza, M., Perez-Pampin, E., de la Serna, A.R., Fernandez-Gutierrez, B., Castaneda, S., Largo, R., Joven, B., Narvaez, J., Navarro, F., Marengo, J.L., Vicario, J.L., Blanco, F.J., Fernandez-Lopez, J.C., Caliz, R., Collado-Escobar, M.D., Carreno, L., Lopez-Longo, J., Canete, J.D., Gomez-Reino, J.J. and Gonzalez, A. (2008)

'Association of interferon regulatory factor 5 haplotypes, similar to that found in systemic lupus erythematosus, in a large subgroup of patients with rheumatoid arthritis', *Arthritis Rheum*, 58(5), pp. 1264-74.

Ding, A.H., Nathan, C.F. and Stuehr, D.J. (1988) 'Release of reactive nitrogen intermediates and reactive oxygen intermediates from mouse peritoneal macrophages. Comparison of activating cytokines and evidence for independent production', *The Journal of Immunology*, 141(7), pp. 2407-2412.

Donnini, S., Finetti, F., Solito, R., Terzuoli, E., Sacchetti, A., Morbidelli, L., Patrignani, P. and Ziche, M. (2007) 'EP2 prostanoid receptor promotes squamous cell carcinoma growth through epidermal growth factor receptor transactivation and iNOS and ERK1/2 pathways', *FASEB J*, 21(10), pp. 2418-30.

Dostalova Merkerova, M., Krejcek, Z., Votavova, H., Belickova, M., Vasikova, A. and Cermak, J. (2011) 'Distinctive microRNA expression profiles in CD34+ bone marrow cells from patients with myelodysplastic syndrome', *Eur J Hum Genet*, 19(3), pp. 313-9.

Dueck, A. and Meister, G. (2010) 'MicroRNA processing without Dicer', *Genome Biology*, 11(6), p. 123.

Durie, F.H., Aruffo, A., Ledbetter, J., Crassi, K.M., Green, W.R., Fast, L.D. and Noelle, R.J. (1994) 'Antibody to the ligand of CD40, gp39, blocks the occurrence of the acute and chronic forms of graft-vs-host disease', *J Clin Invest*, 94(3), pp. 1333-8.

Dweep, H., Sticht, C., Pandey, P. and Gretz, N. (2011) 'miRWalk--database: prediction of possible miRNA binding sites by "walking" the genes of three genomes', *J Biomed Inform*, 44(5), pp. 839-47.

Dzierzak-Mietla, M., Markiewicz, M., Siekiera, U., Mizia, S., Koclega, A., Zielinska, P., Sobczyk-Kruszelnicka, M. and Kyrzcz-Krzemien, S. (2012) 'Occurrence and Impact of Minor Histocompatibility Antigens' Disparities on Outcomes of Hematopoietic Stem Cell Transplantation from HLA-Matched Sibling Donors', *Bone Marrow Research*, 2012, p. 12.

Eapen, M., Logan, B.R., Confer, D.L., Haagenson, M., Wagner, J.E., Weisdorf, D.J., Wingard, J.R., Rowley, S.D., Stroncek, D., Gee, A.P., Horowitz, M.M. and Anasetti, C. (2007) 'Peripheral blood grafts from unrelated donors are associated with increased acute and chronic graft-versus-host disease without improved survival', *Biology of Blood and Marrow Transplantation*, 13(12), pp. 1461-1468.

Ebner, O.A. and Selbach, M. (2014) 'Quantitative Proteomic Analysis of Gene Regulation by miR-34a and miR-34c', *PLoS One*, 9(3), p. e92166.

Elbashir, S.M., Lendeckel, W. and Tuschl, T. (2001) 'RNA interference is mediated by 21- and 22-nucleotide RNAs', *Genes and Development*, 15(2), pp. 188-200.

Esquela-Kerscher, A. and Slack, F.J. (2006) 'Oncomirs - microRNAs with a role in cancer', *Nat Rev Cancer*, 6(4), pp. 259-69.

Fan, M.Q., Huang, C.B., Gu, Y., Xiao, Y., Sheng, J.X. and Zhong, L. (2013) 'Decrease expression of microRNA-20a promotes cancer cell proliferation and predicts poor survival of hepatocellular carcinoma', *J Exp Clin Cancer Res*, 32(1), p. 21.

Ferrara, J.L.M. (1993) 'Cytokine dysregulation as a mechanism of graft versus host disease', *Current Opinion in Immunology*, 5(5), pp. 794-799.

Ferrara, J.L.M., Guillen, F.J., van Duken, P.J., Marion, A., Murphy, G.F. and Burakoff, S.J. (1989) 'Evidence That Large Granular Lymphocytes of Donor Origin Mediate Acute Graft-Versus-Host Disease', *Transplantation*, 47(1), pp. 50-54.

Ferrara, J.L.M., Levine, J., Reddy, P. and Holler, E. (2009) 'Graft-versus-host disease', *Lancet*, 373, pp. 1550-1561.

Ferrara, J.L.M., Levy, R. and Chao, N.J. (1999) 'Pathophysiologic mechanisms of acute graft-vs.-host disease', *Biol Blood Marrow Transplant*, 5(6), pp. 347-56.

Ferrara, J.L.M., Marion, A., McIntyre, J.F., Murphy, G.F. and Burakoff, S.J. (1986) 'Amelioration of acute graft vs host disease due to minor histocompatibility antigens by in vivo administration of anti- interleukin 2 receptor antibody', *The Journal of Immunology*, 137(6), pp. 1874-1877.

Filep, J.G., Baron, C., Lachance, S., Perreault, C. and Chan, J.S. (1996) 'Involvement of nitric oxide in target-cell lysis and DNA fragmentation induced by murine natural killer cells', *Blood*, 87(12), pp. 5136-5143.

Filipovich, A.H., Weisdorf, D., Pavletic, S., Socie, G., Wingard, J.R., Lee, S.J., Martin, P., Chien, J., Przepiorka, D., Couriel, D., Cowen, E.W., Dinndorf, P., Farrell, A., Hartzman, R., Henslee-Downey, J., Jacobsohn, D., McDonald, G., Mittleman, B., Rizzo, J.D., Robinson, M., Schubert, M., Schultz, K., Shulman, H., Turner, M., Vogelsang, G. and Flowers, M.E.D. (2005) 'National Institutes of Health Consensus Development Project on Criteria for Clinical Trials in Chronic Graft-versus-Host Disease: I. Diagnosis and Staging Working Group Report', *Biology of Blood and Marrow Transplantation*, 11(12), pp. 945-956.

Filipowicz, W., Bhattacharyya, S.N. and Sonenberg, N. (2008) 'Mechanisms of post-transcriptional regulation by microRNAs: are the answers in sight?', *Nat Rev Genet*, 9(2), pp. 102-114.

Fiorentino, D.F., Zlotnik, A., Mosmann, T.R., Howard, M. and O'Garra, A. (1991) 'IL-10 inhibits cytokine production by activated macrophages', *J Immunol*, 147(11), pp. 3815-22.

Forrest, A.R., Kanamori-Katayama, M., Tomaru, Y., Lassmann, T., Ninomiya, N., Takahashi, Y., de Hoon, M.J., Kubosaki, A., Kaiho, A., Suzuki, M., Yasuda, J., Kawai, J., Hayashizaki, Y., Hume, D.A. and Suzuki, H. (2010) 'Induction of microRNAs, mir-155, mir-222, mir-424 and mir-503, promotes monocytic differentiation through combinatorial regulation', *Leukemia*, 24(2), pp. 460-6.

Frank, D.A., Mahajan, S. and Ritz, J. (1999) 'Fludarabine-induced immunosuppression is associated with inhibition of STAT1 signaling', *Nat Med*, 5(4), pp. 444-447.

Fraser, C. and Scott Baker, K. (2007) 'The management and outcome of chronic graft-versus-host disease.', *British Journal of Haematology*, 138, pp. 131-145.

Fredhutch.org (2014) *History of Transplantation*. Available at: <http://www.fredhutch.org/en/treatment/long-term-follow-up/FAQs/transplantation.html>.

Fridman, J.S. and Lowe, S.W. (2003) 'Control of apoptosis by p53', *Oncogene*, 22(56), pp. 9030-9040.

Gangaraju, V.K. and Lin, H. (2009) 'MicroRNAs: key regulators of stem cells', *Nat Rev Mol Cell Biol*, 10(2), pp. 116-125.

Gennarino, V.A., Sardiello, M., Avellino, R., Meola, N., Maselli, V., Anand, S., Cutillo, L., Ballabio, A. and Banfi, S. (2008) 'MicroRNA target prediction by expression analysis of host genes', *Genome Res*. 2009 Mar;19(3):481-90. Epub 2008 Dec 16.

Ghani, S., Riemke, P., Schönheit, J., Lenze, D., Stumm, J., Hoogenkamp, M., Lagendijk, A., Heinz, S., Bonifer, C., Bakkers, J., Abdelilah-Seyfried, S., Hummel, M. and Rosenbauer, F. (2011) *Macrophage development from HSCs requires PU.1-coordinated microRNA expression*.

Gifford GE, L.-M.M. (1987) 'Gamma interferon priming of mouse and human macrophages for induction of tumor necrosis factor production by bacterial lipopolysaccharide.', *Journal of the National Cancer Institute*, 78, pp. 121-124.

Ginhoux, F. and Jung, S. (2014) 'Monocytes and macrophages: developmental pathways and tissue homeostasis', *Nat Rev Immunol*, 14(6), pp. 392-404.

Glucksberg H, S.R., Fefer A, Buckner CD, Neiman PE, Clift RA, Lerner KG, Thomas ED. (1974) 'Clinical manifestations of graft-versus-host disease in human recipients of marrow from HL-A-matched sibling donors.', *Transplantation*, 18, pp. 295-304.

Goker H, H.I., Chao NJ (2001) 'Acute graft-vs-host disease: pathobiology and management', *Experimental Haematology*, 29, pp. 259-277.

Goulmy, E., Termijtelen, A., Bradley, B.A. and van Rood, J.J. (1976) 'Alloimmunity to human H-Y', *Lancet*, 2, p. 1206.

Gracias, D.T., Stelekati, E., Hope, J.L., Boesteanu, A.C., Doering, T.A., Norton, J., Mueller, Y.M., Fraietta, J.A., Wherry, E.J., Turner, M. and Katsikis, P.D. (2013) 'The microRNA miR-155 controls CD8+ T cell responses by regulating interferon signaling', *Nat Immunol*, 14(6), pp. 593-602.

Graham, R.R., Kozyrev, S.V., Baechler, E.C., Reddy, M.V., Plenge, R.M., Bauer, J.W., Ortmann, W.A., Koeth, T., Gonzalez Escribano, M.F., Pons-Estel, B., Petri, M., Daly, M., Gregersen, P.K., Martin, J., Altshuler, D., Behrens, T.W. and Alarcon-Riquelme, M.E. (2006) 'A common haplotype of interferon regulatory factor 5 (IRF5) regulates splicing and expression and is associated with increased risk of systemic lupus erythematosus', *Nat Genet*, 38(5), pp. 550-5.

Gratwohl, A. (2012) 'The EBMT risk score', *Bone Marrow Transplant*, 47(6), pp. 749-756.

Gratwohl, A., Brand, R., Niederwieser, D., Baldomero, H., Chabannon, C. and Cornelissen, J. (2010) 'Introduction of a quality management system and outcome after hematopoietic stem cell transplantation'.

Gratwohl, A., Hermans, J., Goldman, J.M., Arcese, W., Carreras, E. and Devergie, A. (1998) 'Risk assessment for patients with chronic myeloid leukaemia before allogeneic blood or marrow transplantation. Chronic Leukemia Working Party of the European Group for Blood and Marrow Transplantation', *Lancet*, 352, pp. 1087-1092.

Gratwohl, A., Stern, M., Brand, R., Apperley, J., Baldomero, H. and de Witte, T. (2009) 'Risk score for outcome after allogeneic hematopoietic stem cell transplantation: a retrospective analysis', *Cancer*, 115, pp. 4715-4726.

Gray, R.J. (1988) 'A Class of K-Sample Tests for Comparing the Cumulative Incidence of a Competing Risk', pp. 1141-1154.

- Graze, P.R. and Gale, R.P. (1979) 'Chronic graft versus host disease: a syndrome of disordered immunity', *Am J Med*, 66(4), pp. 611-20.
- Griffiths-Jones, S., Grocock, R.J., van Dongen, S., Bateman, A. and Enright, A.J. (2006) 'miRBase: microRNA sequences, targets and gene nomenclature', *Nucleic Acids Res*, 34, pp. D140 - D144.
- Gupta, V., Eapen, M., Brazauskas, R., Carreras, J., Aljurf, M. and Gale, R.P. (2010) 'Impact of age on outcomes after bone marrow transplantation for acquired aplastic anemia using HLA-matched sibling donors', *Haematologica*, 95, pp. 2119-2125.
- Hahn, S., Jackstadt, R., Siemens, H., Hunten, S. and Hermeking, H. (2013) 'SNAIL and miR-34a feed-forward regulation of ZNF281/ZBP99 promotes epithelial-mesenchymal transition', *Embo j*, 32(23), pp. 3079-95.
- Hainaut, P. and Hollstein, M. (2000) 'p53 and human cancer: the first ten thousand mutations', *Adv Cancer Res*, 77, pp. 81-137.
- Han, Z.B., Chen, H.Y., Fan, J.W., Wu, J.Y., Peng, Z.H. and Wang, Z.W. (2013) '[Expression and survival prediction of microRNA-155 in hepatocellular carcinoma after liver transplantation]', *Zhonghua Yi Xue Za Zhi*, 93(12), pp. 884-7.
- Harrell, F.E., Jr., Lee, K.L., Califf, R.M., Pryor, D.B. and Rosati, R.A. (1984) 'Regression modelling strategies for improved prognostic prediction', *Stat Med*, 3(2), pp. 143-52.
- He, L., He, X., Lim, L.P., de Stanchina, E., Xuan, Z., Liang, Y., Xue, W., Zender, L., Magnus, J., Ridzon, D., Jackson, A.L., Linsley, P.S., Chen, C., Lowe, S.W., Cleary, M.A. and Hannon, G.J. (2007) 'A microRNA component of the p53 tumour suppressor network', *Nature*, 447(7148), pp. 1130-4.
- He, M., Gao, L., Zhang, S., Tao, L., Wang, J., Yang, J. and Zhu, M. (2013) 'Prognostic significance of miR-34a and its target proteins of FOXP1, p53, and BCL2 in gastric MALT lymphoma and DLBCL', *Gastric Cancer*.
- Hendricks, K.B., Shanahan, F. and Lees, E. (2004) 'Role for BRG1 in cell cycle control and tumor suppression', *Mol Cell Biol*, 24(1), pp. 362-76.
- Heremans H, D.R., Sobis H, Vandekerckhove F, Billiau A. (1987) 'Regulation by interferons of the local inflammatory response to bacterial lipopolysaccharide.', *Journal of Immunology*, 138, pp. 4175-4179.
- Hildebrand, J., Rutze, M., Walz, N., Gallinat, S., Wenck, H., Deppert, W., Grundhoff, A. and Knott, A. (2011) 'A Comprehensive Analysis of MicroRNA Expression During Human Keratinocyte Differentiation In Vitro and In Vivo', *J Invest Dermatol*, 131(1), pp. 20-29.

Hill, G.R., Crawford, J.M., Cooke, K.R., Brinson, Y.S., Pan, L. and Ferrara, J.L.M. (1997) 'Total Body Irradiation and Acute Graft-Versus-Host Disease: The Role of Gastrointestinal Damage and Inflammatory Cytokines', *Blood*, 90(8), pp. 3204-3213.

Hill, G.R. and Ferrara, J.L. (2000) 'The primacy of the gastrointestinal tract as a target organ of acute graft-versus-host disease: rationale for the use of cytokine shields in allogeneic bone marrow transplantation', *Blood*, 95(9), pp. 2754-9.

Hinton, P.R. (2014) 'Interaction of factors in the analysis of variance', in *Statistics Explained*. 3rd edn. Routledge, pp. 157-165.

Hirotsu, T., Yamamoto, M., Kumagai, Y., Uematsu, S., Kawase, I., Takeuchi, O. and Akira, S. (2005) 'Regulation of lipopolysaccharide-inducible genes by MyD88 and Toll/IL-1 domain containing adaptor inducing IFN- $\beta$ ', *Biochemical and Biophysical Research Communications*, 328(2), pp. 383-392.

Hofmeister, C.C., Quinn, A., Cooke, K.R., Stiff, P., Nickoloff, B. and Ferrara, J.L. (2004) 'Graft-versus-host disease of the skin: life and death on the epidermal edge', *Biol Blood Marrow Transplant*, 10(6), pp. 366-72.

Holler, E., Kolb, H.J., Moller, A., Kempeni, J., Liesenfeld, S., Pechumer, H., Lehmacher, W., Ruckdeschel, G., Gleixner, B. and Riedner, C. (1990) 'Increased serum levels of tumor necrosis factor alpha precede major complications of bone marrow transplantation [see comments]', *Blood*, 75(4), pp. 1011-1016.

Horwitz, M. and Sullivan, K. (2006) 'Chronic graft-versus-host disease', *Blood Reviews*, 20, pp. 15-27.

Huang da, W., Sherman, B.T. and Lempicki, R.A. (2009) 'Systematic and integrative analysis of large gene lists using DAVID bioinformatics resources', *Nat Protoc*, 4(1), pp. 44-57.

Huang da, W., Sherman, B.T., Tan, Q., Kir, J., Liu, D., Bryant, D., Guo, Y., Stephens, R., Baseler, M.W., Lane, H.C. and Lempicki, R.A. (2007) 'DAVID Bioinformatics Resources: expanded annotation database and novel algorithms to better extract biology from large gene lists', *Nucleic Acids Res*, 35(Web Server issue), pp. W169-75.

Hurgin, V., Novick, D., Werman, A., Dinarello, C.A. and Rubinstein, M. (2007) 'Antiviral and immunoregulatory activities of IFN- $\gamma$  depend on constitutively expressed IL-1 $\alpha$ ', *Proc Natl Acad Sci U S A*, 104(12), pp. 5044-9.

- Iacobelli, S. (2013) 'Suggestions on the use of statistical methodologies in studies of the European Group for Blood and Marrow Transplantation', *Bone Marrow Transplant*, 48(S1), pp. S1-S37.
- Ishiguro, K., Green, T., Rapley, J., Wachtel, H., Giallourakis, C., Landry, A., Cao, Z., Lu, N., Takafumi, A., Goto, H., Daly, M.J. and Xavier, R.J. (2006) 'Ca<sup>2+</sup>/calmodulin-dependent protein kinase II is a modulator of CARMA1-mediated NF-kappaB activation', *Mol Cell Biol*, 26(14), pp. 5497-508.
- Iwai, N. and Naraba, H. (2005) 'Polymorphisms in human pre-miRNAs', *Biochemical and Biophysical Research Communications*, 331(4), pp. 1439-1444.
- Jackstadt, R. and Hermeking, H. (2014) 'MicroRNAs as regulators and mediators of c-MYC function', *Biochim Biophys Acta*.
- Jagasia, M.H., Abonour, R., Long, G.D., Bolwell, B.J., Laport, G.G., Shore, T.B., Durrant, S., Szer, J., Chen, M.G., Lizambri, R. and Waller, E.K. (2012) 'Palifermin for the reduction of acute GVHD: a randomized, double-blind, placebo-controlled trial', *Bone Marrow Transplant*, 47(10), pp. 1350-5.
- Jaksch, M. and Mattsson, J. (2005) 'The Pathophysiology of Acute Graft-Versus-Host Disease', *Scandinavian Journal of Immunology*, 61(5), pp. 398-409.
- Jaksch, M., Remberger, M. and Mattsson, J. (2005) 'Increased gene expression of chemokine receptors is correlated with acute graft-versus-host disease after allogeneic stem cell transplantation', *Biology of Blood and Marrow Transplantation*, 11(4), pp. 280-287.
- Joyce, C.E. and Novina, C.D. (2013) 'miR-155 in Acute Myeloid Leukemia: Not Merely a Prognostic Marker?', *Journal of Clinical Oncology*, 31(17), pp. 2219-2221.
- Kalman, V.K. and Klimpel, G.R. (1983) 'Cyclosporin A inhibits the production of gamma interferon (IFN gamma), but does not inhibit production of virus-induced IFN alpha/beta', *Cell Immunol*, 78(1), pp. 122-9.
- Khvorova, A., Reynolds, A. and Jayasena, S.D. (2003) 'Functional siRNAs and miRNAs Exhibit Strand Bias', *Cell*, 115(2), pp. 209-216.
- Kim, V.N. (2005) 'MicroRNA biogenesis: coordinated cropping and dicing', *Nat Rev Mol Cell Biol*, 6(5), pp. 376-85.
- Klimpel, G.R., Annable, C.R., Cleveland, M.G., Jerrells, T.R. and Patterson, J.C. (1990) 'Immunosuppression and lymphoid hypoplasia associated with chronic graft versus

host disease is dependent upon IFN-gamma production', *The Journal of Immunology*, 144(1), pp. 84-93.

Koch, A.E., Kronfeld-Harrington, L.B., Szekanecz, Z., Cho, M.M., Haines, G.K., Harlow, L.A., Strieter, R.M., Kunkel, S.L., Massa, M.C., Barr, W.G. and et al. (1993) 'In situ expression of cytokines and cellular adhesion molecules in the skin of patients with systemic sclerosis. Their role in early and late disease', *Pathobiology*, 61(5-6), pp. 239-46.

Kolb, H.-J. (2008) 'Graft-versus-leukemia effects of transplantation and donor lymphocytes', *Blood*, 112(12), pp. 4371-4383.

Kolb, H.J., Schattenberg, A., Goldman, J.M., Hertenstein, B., Jacobsen, N., Arcese, W., Ljungman, P., Ferrant, A., Verdonck, L., Niederwieser, D., van Rhee, F., Mittermueller, J., de Witte, T., Holler, E. and Ansari, H. (1995) 'Graft-versus-leukemia effect of donor lymphocyte transfusions in marrow grafted patients', *Blood*, 86(5), pp. 2041-50.

Koyama, M., Kuns, R.D., Olver, S.D., Raffelt, N.C., Wilson, Y.A., Don, A.L., Lineburg, K.E., Cheong, M., Robb, R.J., Markey, K.A., Varelias, A., Malissen, B., Hammerling, G.J., Clouston, A.D., Engwerda, C.R., Bhat, P., MacDonald, K.P. and Hill, G.R. (2012) 'Recipient nonhematopoietic antigen-presenting cells are sufficient to induce lethal acute graft-versus-host disease', *Nat Med*, 18(1), pp. 135-42.

Kozomara, A. and Griffiths-Jones, S. (2011) 'miRBase: integrating microRNA annotation and deep-sequencing data', *Nucleic Acids Res*, 39(Database issue), pp. D152-7.

Kozomara, A. and Griffiths-Jones, S. (2014) 'miRBase: annotating high confidence microRNAs using deep sequencing data', *Nucleic Acids Research*, 42(D1), pp. D68-D73.

Krausgruber, T., Blazek, K., Smallie, T., Alzabin, S., Lockstone, H., Sahgal, N., Hussell, T., Feldmann, M. and Udalova, I.A. (2010) 'IRF5 promotes inflammatory macrophage polarization and TH1-TH17 responses', *Nat Immunol*, 12(3), pp. 231-238.

Krenger, W., Hill, G.R. and Ferrara, J.L.M. (1997) 'Cytokine Cascades in Acute Graft-Versus-Host Disease 1', *Transplantation*, 64(4), pp. 553-558.

Kroger, N., Brand, R., van Biezen, A., Zander, A., Dierlamm, J. and Niederwieser, D. (2009) 'Risk factors for therapy-related myelodysplastic syndrome and acute myeloid leukemia treated with allogeneic stem cell transplantation', *Haematologica*, 94, pp. 542-549.

Kumaki S, M.M., Fujie H, Sasahara Y, Ohashi Y, Tsuchiya S, Konno T. (1998) 'Prolonged secretion of IL-15 in patients with severe forms of acute graft-versus-host disease after

allogeneic bone marrow transplantation in children.', *International Journal of Haematology*, 67, pp. 307-312.

Labbaye, C., Spinello, I., Quaranta, M.T., Pelosi, E., Pasquini, L., Petrucci, E., Biffoni, M., Nuzzolo, E.R., Billi, M., Foa, R., Brunetti, E., Grignani, F., Testa, U. and Peschle, C. (2008) 'A three-step pathway comprising PLZF/miR-146a/CXCR4 controls megakaryopoiesis', *Nat Cell Biol*, 10(7), pp. 788-801.

Labbaye, C. and Testa, U. (2012) 'The emerging role of MIR-146A in the control of hematopoiesis, immune function and cancer', *Journal of Hematology & Oncology*, 5(1), p. 13.

Lagana, A., Forte, S., Giudice, A., Arena, M.R., Puglisi, P.L., Giugno, R., Pulvirenti, A., Shasha, D. and Ferro, A. (2009) 'miRo: a miRNA knowledge base', *Database*, 2009.

Lagos-Quintana, M., Rauhut, R., Lendeckel, W. and Tuschl, T. (2001) 'Identification of novel genes coding for small expressed RNAs', *Science*, 294(5543), pp. 853-858.

Lagos-Quintana, M., Rauhut, R., Meyer, J., Borkhardt, A. and Tuschl, T. (2003) 'New microRNAs from mouse and human', *RNA*, 9(2), pp. 175-179.

Lagos-Quintana, M., Rauhut, R., Yalcin, A., Meyer, J., Lendeckel, W. and Tuschl, T. (2002) 'Identification of tissue-specific MicroRNAs from mouse', *Current Biology*, 12(9), pp. 735-739.

Lall, S., Grün, D., Krek, A., Chen, K., Wang, Y.-L., Dewey, C.N., Sood, P., Colombo, T., Bray, N., MacMenamin, P., Kao, H.-L., Gunsalus, K.C., Pachter, L., Piano, F. and Rajewsky, N. (2006) 'A Genome-Wide Map of Conserved MicroRNA Targets in *C. elegans*', *Current Biology*, 16(5), pp. 460-471.

Lau, N.C., Lim, L.P., Weinstein, E.G. and Bartel, D.P. (2001) 'An abundant class of tiny RNAs with probable regulatory roles in *Caenorhabditis elegans*', *Science*, 294(5543), pp. 858-62.

Lawrie, C.H., Soneji, S., Marafioti, T., Cooper, C.D., Palazzo, S., Paterson, J.C., Cattan, H., Enver, T., Mager, R., Boulwood, J., Wainscoat, J.S. and Hatton, C.S. (2007) 'MicroRNA expression distinguishes between germinal center B cell-like and activated B cell-like subtypes of diffuse large B cell lymphoma', *Int J Cancer*, 121(5), pp. 1156-61.

Leah, E. (2011) 'Rheumatoid arthritis: miR-155 mediates inflammation', *Nat Rev Rheumatol*, 7(8), p. 437.

Lee, R.C. and Ambros, V. (2001) 'An extensive class of small RNAs in *Caenorhabditis elegans*', *Science*, 294(5543), pp. 862-4.

Lee, R.C., Feinbaum, R.L. and Ambros, V. (1993) 'The *C. elegans* heterochronic gene *lin-4* encodes small RNAs with antisense complementarity to *lin-14*', *Cell*, 75(5), pp. 843-854.

Lee, S., Klein, J., Haagensohn, M., Baxter-Lowe, L., Confer, D., Eapen, M., Fernandez-Vina, M., Flomenberg, N., Horowitz, M., Hurley, C., Noreen, H., Oudshoorn, M., Petersdorf, E., Setterholm, M., Spellman, S., Weisdorf, D., Williams, T. and Anasetti, C. (2007) 'High-resolution donor-recipient HLA matching contributes to the success of unrelated donor marrow transplantation', *Blood*, 110, pp. 4576-4583.

Lee, Y., Ahn, C., Han, J., Choi, H., Kim, J., Yim, J., Lee, J., Provost, P., Radmark, O., Kim, S. and Kim, V.N. (2003) 'The nuclear RNase III Drosha initiates microRNA processing', *Nature*, 425(6956), pp. 415-419.

Lee, Y., Jeon, K., Lee, J.T., Kim, S. and Kim, V.N. (2002) 'MicroRNA maturation: Stepwise processing and subcellular localization', *EMBO Journal*, 21(17), pp. 4663-4670.

Lee, Y.J. and Benveniste, E.N. (1996) 'Stat1 alpha expression is involved in IFN-gamma induction of the class II transactivator and class II MHC genes', *The Journal of Immunology*, 157(4), pp. 1559-68.

Lena, A.M., Shalom-Feuerstein, R., Rivetti di Val Cervo, P., Aberdam, D., Knight, R.A., Melino, G. and Candi, E. (2008) 'miR-203 represses 'stemness' by repressing DeltaNp63', *Cell Death Differ*, 15(7), pp. 1187-95.

Leonhardt, F., Grundmann, S., Behe, M., Bluhm, F., Dumont, R.A., Braun, F., Fani, M., Riesner, K., Prinz, G., Hechinger, A.K., Gerlach, U.V., Dierbach, H., Penack, O., Schmitt-Graff, A., Finke, J., Weber, W.A. and Zeiser, R. (2013) 'Inflammatory neovascularization during graft-versus-host disease is regulated by alphaV integrin and miR-100', *Blood*, pp. 3307-3318.

Lerner, K.G., Kao, G.F., Storb, R., Buckner, C.D., Clift, R.A. and Thomas, E.D. (1974) 'Histopathology of graft-vs.-host reaction (GvHR) in human recipients of marrow from HL-A-matched sibling donors', *Transplant Proc*, 6(4), pp. 367-71.

Levine, A.J. (1997) 'p53, the cellular gatekeeper for growth and division', *Cell*, 88(3), pp. 323-31.

Lewis, B.P., Burge, C.B. and Bartel, D.P. (2005) 'Conserved seed pairing, often flanked by adenosines, indicates that thousands of human genes are microRNA targets', *Cell*, 120, pp. 15 - 20.

- Lewis, B.P., Shih, I.h., Jones-Rhoades, M.W., Bartel, D.P. and Burge, C.B. (2003) 'Prediction of Mammalian MicroRNA Targets', *Cell*, 115(7), pp. 787-798.
- Li, P., He, Q.-Y. and Luo, C.-Q. (2014a) 'Overexpression of miR-200b inhibits the cell proliferation and promotes apoptosis of human hypertrophic scar fibroblasts in vitro', *The Journal of Dermatology*, 41(10), pp. 903-911.
- Li, X.J., Ren, Z.J. and Tang, J.H. (2014b) 'MicroRNA-34a: a potential therapeutic target in human cancer', *Cell Death Dis*, 5, p. e1327.
- Lim, L.P., Lau, N.C., Weinstein, E.G., Abdelhakim, A., Yekta, S., Rhoades, M.W., Burge, C.B. and Bartel, D.P. (2003) 'The microRNAs of *Caenorhabditis elegans*', *Genes and Development*, 17(8), pp. 991-1008.
- Lin, M.-T., Storer, B., Martin, P.J., Tseng, L.-H., Grogan, B., Chen, P.-J., Zhao, L.P. and Hansen, J.A. (2005) 'Genetic variation in the IL-10 pathway modulates severity of acute graft-versus-host disease following hematopoietic cell transplantation: synergism between IL-10 genotype of patient and IL-10 receptor  $\beta$  genotype of donor', *Blood*, 106(12), pp. 3995-4001.
- Lindsay, M.A. (2008) 'microRNAs and the immune response', *Trends Immunol*, 29(7), pp. 343-51.
- Liu, J., Carmell, M.A., Rivas, F.V., Marsden, C.G., Thomson, J.M., Song, J.-J., Hammond, S.M., Joshua-Tor, L. and Hannon, G.J. (2004) 'Argonaute2 Is the Catalytic Engine of Mammalian RNAi', *Science*, 305(5689), pp. 1437-1441.
- Liu, R., Liao, J., Yang, M., Shi, Y., Peng, Y., Wang, Y., Pan, E., Guo, W., Pu, Y. and Yin, L. (2012) 'Circulating miR-155 expression in plasma: a potential biomarker for early diagnosis of esophageal cancer in humans', *J Toxicol Environ Health A*, 75(18), pp. 1154-62.
- Ljungman, P., Hakki, M. and Boeckh, M. (2010) 'Cytomegalovirus in hematopoietic stem cell transplant recipients', *Infect Dis Clin North Am*, 24, pp. 319-337.
- Lodygin, D., Tarasov, V., Epanchintsev, A., Berking, C., Knyazeva, T., Korner, H., Knyazev, P., Diebold, J. and Hermeking, H. (2008) 'Inactivation of miR-34a by aberrant CpG methylation in multiple types of cancer', *Cell Cycle*, 7(16), pp. 2591-600.
- Lorenz, E., Congdon, C. and Uphoff, D. (1952) 'Modification of Acute Irradiation Injury in Mice and Guinea-Pigs by Bone Marrow Injections', *Radiology*, 58(6), pp. 863-877.

LoVecchio, F., Welch, S., Klemens, J., Curry, S.C. and Thomas, R. (1999) 'Incidence of immediate and delayed hypersensitivity to *Centruroides antivenom*', *Ann Emerg Med*, 34(5), pp. 615-9.

Lowe, S.W. and Lin, A.W. (2000) 'Apoptosis in cancer', *Carcinogenesis*, 21(3), pp. 485-95.

Lowenberg, B., Downing, J.R. and Burnett, A. (1999) 'Acute myeloid leukemia', *N Engl J Med*, 341, pp. 1051-1062.

Lu, J., Getz, G., Miska, E.A., Alvarez-Saavedra, E., Lamb, J., Peck, D., Sweet-Cordero, A., Ebert, B.L., Mak, R.H. and Ferrando, A.A. (2005) 'MicroRNA expression profiles classify human cancers', *Nature*, 435(7043), pp. 834 - 838.

Lu, L.-F., Boldin, M.P., Chaudhry, A., Lin, L.-L., Taganov, K.D., Hanada, T., Yoshimura, A., Baltimore, D. and Rudensky, A.Y. (2010) 'Function of miR-146a in Controlling Treg Cell-Mediated Regulation of Th1 Responses', *Cell*, 142(6), pp. 914-929.

Lu, N.Z., Collins, J.B., Grissom, S.F. and Cidlowski, J.A. (2007) 'Selective regulation of bone cell apoptosis by translational isoforms of the glucocorticoid receptor', *Mol Cell Biol*, 27(20), pp. 7143-60.

Lu, Y. and Waller, E.K. (2009) 'Dichotomous role of interferon-gamma in allogeneic bone marrow transplant', *Biol Blood Marrow Transplant*, 15(11), pp. 1347-53.

Lund, E., Guttinger, S., Calado, A., Dahlberg, J.E. and Kutay, U. (2004) 'Nuclear export of microRNA precursors', *Science*, 303(5654), pp. 95-8.

Luo, X., Tsai, L.M., Shen, N. and Yu, D. (2010) 'Evidence for microRNA-mediated regulation in rheumatic diseases', *Annals of the Rheumatic Diseases*, 69(Suppl 1), pp. i30-i36.

Ma, H.-H., Ziegler, J., Li, C., Sepulveda, A., Bedeir, A., Grandis, J., Lentzsch, S. and Mapara, M.Y. (2011) 'Sequential activation of inflammatory signaling pathways during graft-versus-host disease (GVHD): Early role for STAT1 and STAT3', *Cellular Immunology*, 268(1), pp. 37-46.

MacMillan, M.L., Weisdorf, D.J., Wagner, J.E., DeFor, T.E., Burns, L.J., Ramsay, N.K.C., Davies, S.M. and Blazar, B.R. (2002) 'Response of 443 patients to steroids as primary therapy for acute graft-versus-host disease: Comparison of grading systems', *Biology of Blood and Marrow Transplantation*, 8(7), pp. 387-394.

Mancini, M., Lena, A.M., Saintigny, G., Mahe, C., Di Daniele, N., Melino, G. and Candi, E. (2014) 'MicroRNAs in human skin ageing', *Ageing Res Rev*, 17, pp. 9-15.

Markey, K.A., MacDonald, K.P. and Hill, G.R. (2014) 'The biology of graft-versus-host disease: experimental systems instructing clinical practice', *Blood*, 124(3), pp. 354-62.

Martin, D., Brun, C., Remy, E., Mouren, P., Thieffry, D. and Jacq, B. (2004) 'GOToolBox: functional analysis of gene datasets based on Gene Ontology', *Genome Biol*, 5(12), p. R101.

Martinez, J. and Tuschl, T. (2004) 'RISC is a 5' phosphomonoester-producing RNA endonuclease', *Genes and Development*, 18, pp. 975-980.

Matzinger, P. (2002) 'The Danger Model: A Renewed Sense of Self', *Science*, 296(5566), pp. 301-305.

Mauri, C. and Ehrenstein, M.R. (2008) 'The 'short' history of regulatory B cells', *Trends in Immunology*, 29(1), pp. 34-40.

McDonald, J.H. (2009) *Handbook of Biological Statistics*. 2 edn. Baltimore, Maryland: Sparky House Publishing.

McNeil, B.J., Keeler, E. and Adelstein, S.J. (1975) 'Primer on Certain Elements of Medical Decision Making', *New England Journal of Medicine*, 293(5), pp. 211-215.

Mendell, J.T. (2008) 'miRiad Roles for the miR-17-92 Cluster in Development and Disease', *Cell*, 133(2), pp. 217-222.

Merad, M., Hoffmann, P., Ranheim, E., Slaymaker, S., Manz, M.G., Lira, S.A., Charo, I., Cook, D.N., Weissman, I.L., Strober, S. and Engleman, E.G. (2004) 'Depletion of host Langerhans cells before transplantation of donor alloreactive T cells prevents skin graft-versus-host disease', *Nat Med*, 10(5), pp. 510-7.

Min, C.-K., Maeda, Y., Lowler, K., Liu, C., Clouthier, S., Lofthus, D., Weisiger, E., Ferrara, J.L.M. and Reddy, P. (2004) 'Paradoxical effects of interleukin-18 on the severity of acute graft-versus-host disease mediated by CD4+ and CD8+ T-cell subsets after experimental allogeneic bone marrow transplantation', *Blood*, 104(10), pp. 3393-3399.

Mingari, M.C., Moretta, A. and Moretta, L. (1998) 'Regulation of KIR expression in human T cells: a safety mechanism that may impair protective T-cell responses', *Immunology Today*, 19(4), pp. 153-157.

Mingari, M.C., Schiavetti, F., Ponte, M., Vitale, C., Maggi, E., Romagnani, S., Demarest, J., Pantaleo, G., Fauci, A.S. and Moretta, L. (1996) 'Human CD8<sup>+</sup> T lymphocyte subsets that express HLA class I-specific inhibitory receptors represent oligoclonally or monoclonally expanded cell populations', *Proceedings of the National Academy of Sciences of the United States of America*, 93(22), pp. 12433-12438.

Mitchell, P.S., Parkin, R.K., Kroh, E.M., Fritz, B.R., Wyman, S.K., Pogosova-Agadjanyan, E.L., Peterson, A., Noteboom, J., O'Briant, K.C., Allen, A., Lin, D.W., Urban, N., Drescher, C.W., Knudsen, B.S., Stirewalt, D.L., Gentleman, R., Vessella, R.L., Nelson, P.S., Martin, D.B. and Tewari, M. (2008) 'Circulating microRNAs as stable blood-based markers for cancer detection', *Proc Natl Acad Sci U S A*, 105(30), pp. 10513-8.

Mohty, M., Blaise, D., Faucher, C., Vey, N., Bouabdallah, R., Stoppa, A.M., Viret, F., Gravis, G., Olive, D. and Gaugler, B. (2005) 'Inflammatory cytokines and acute graft-versus-host disease after reduced-intensity conditioning allogeneic stem cell transplantation', *Blood*, 106(13), pp. 4407-11.

Mohty, M., Kuentz, M., Michallet, M., Bourhis, J.-H., Milpied, N., Sutton, L., Jouet, J.-P., Attal, M., Bordigoni, P., Cahn, J.-Y., Boiron, J.-M. and Blaise, D. (2002) 'Chronic graft-versus-host disease after allogeneic blood stem cell transplantation: long-term results of a randomized study', *Blood*, 100(9), pp. 3128-3134.

Mudhasani, R., Zhu, Z., Hutvagner, G., Eischen, C.M., Lyle, S., Hall, L.L., Lawrence, J.B., Imbalzano, A.N. and Jones, S.N. (2008) 'Loss of miRNA biogenesis induces p19Arf-p53 signaling and senescence in primary cells', *J Cell Biol*, 181(7), pp. 1055-63.

Nahid, M.A., Pauley, K.M., Satoh, M. and Chan, E.K.L. (2009) 'miR-146a Is Critical for Endotoxin-induced Tolerance', *Journal of Biological Chemistry*, 284(50), pp. 34590-34599.

Nakielnny, S. and Dreyfuss, G. (1999) 'Transport of proteins and RNAs in and out of the nucleus', *Cell*, 99(7), pp. 677-90.

Nestel FP, P.K., Seemayer TA, Lapp WS. (1992) 'Macrophage priming and lipopolysaccharide-triggered release of tumor necrosis factor alpha during graft-versus-host disease.', *The Journal of Experimental Medicine*, 175, pp. 405-413.

Nguyen, V.T., Arredondo, J., Chernyavsky, A.I., Kitajima, Y., Pittelkow, M. and Grando, S.A. (2004) 'Pemphigus vulgaris IgG and methylprednisolone exhibit reciprocal effects on keratinocytes', *J Biol Chem*, 279(3), pp. 2135-46.

Noren Hooten, N., Fitzpatrick, M., Wood, W.H., 3rd, De, S., Ejiogu, N., Zhang, Y., Mattison, J.A., Becker, K.G., Zonderman, A.B. and Evans, M.K. (2013) 'Age-related changes in microRNA levels in serum', *Aging (Albany NY)*, 5(10), pp. 725-40.

Novota, P., Zinöcker, S., Norden, J., Wang, X.N., Sviland, L., Opitz, L., Salinas-Riester, G., Rolstad, B., Dickinson, A.M., Walter, L. and Dressel, R. (2011) 'Expression Profiling of

Major Histocompatibility and Natural Killer Complex Genes Reveals Candidates for Controlling Risk of Graft versus Host Disease', *PLoS ONE*, 6(1), p. e16582.

O'Connell, R.M., Rao, D.S., Chaudhuri, A.A. and Baltimore, D. (2010) 'Physiological and pathological roles for microRNAs in the immune system', *Nat Rev Immunol*, 10(2), pp. 111-122.

O'Connell, R.M., Taganov, K.D., Boldin, M.P., Cheng, G. and Baltimore, D. (2007) 'MicroRNA-155 is induced during the macrophage inflammatory response', *Proc Natl Acad Sci U S A*, 104, pp. 1604 - 1609.

Okamoto, Y., Folco, E.J., Minami, M., Wara, A.K., Feinberg, M.W., Sukhova, G.K., Colvin, R.A., Kihara, S., Funahashi, T., Luster, A.D. and Libby, P. (2008) 'Adiponectin inhibits the production of CXC receptor 3 chemokine ligands in macrophages and reduces T-lymphocyte recruitment in atherogenesis', *Circ Res*, 102(2), pp. 218-25.

Okamura, K., Hagen, J., Duan, H., Tyler, D. and Lai, E. (2007) 'The Mitron Pathway Generates microRNA-Class Regulatory RNAs in *Drosophila*', *Cell*, 130(1), pp. 89-100.

Okamura, K., Phillips, M.D., Tyler, D.M., Duan, H., Chou, Y.-t. and Lai, E.C. (2008) 'The regulatory activity of microRNA\* species has substantial influence on microRNA and 3[prime] UTR evolution', *Nat Struct Mol Biol*, 15(4), pp. 354-363.

Olsen, P.H. and Ambros, V. (1999) 'The lin-4 Regulatory RNA Controls Developmental Timing in *Caenorhabditis elegans* by Blocking LIN-14 Protein Synthesis after the Initiation of Translation', *Developmental Biology*, 216(2), pp. 671-680.

Ouchi, N., Kihara, S., Arita, Y., Nishida, M., Matsuyama, A., Okamoto, Y., Ishigami, M., Kuriyama, H., Kishida, K., Nishizawa, H., Hotta, K., Muraguchi, M., Ohmoto, Y., Yamashita, S., Funahashi, T. and Matsuzawa, Y. (2001) 'Adipocyte-derived plasma protein, adiponectin, suppresses lipid accumulation and class A scavenger receptor expression in human monocyte-derived macrophages', *Circulation*, 103(8), pp. 1057-63.

Paczesny, S. (2012) 'Biomarkers for the detection of graft-versus-host disease in cancer patients after bone marrow transplantation', *Current Biomarker Findings*, 2, pp. 29-42.

Pålsson-McDermott, E.M. and O'Neill, L.A.J. (2004) 'Signal transduction by the lipopolysaccharide receptor, Toll-like receptor-4', *Immunology*, 113(2), pp. 153-162.

Pan, L., Delmonte, J., Jr., Jalonen, C.K. and Ferrara, J.L. (1995) 'Pretreatment of donor mice with granulocyte colony-stimulating factor polarizes donor T lymphocytes toward

type-2 cytokine production and reduces severity of experimental graft-versus-host disease', *Blood*, 86(12), pp. 4422-4429.

Pan, L., Teshima, T., Hill, G.R., Bungard, D., Brinson, Y.S., Reddy, V.S., Cooke, K.R. and Ferrara, J.L.M. (1999) 'Granulocyte Colony-Stimulating Factor-Mobilized Allogeneic Stem Cell Transplantation Maintains Graft-Versus-Leukemia Effects Through a Perforin-Dependent Pathway While Preventing Graft-Versus-Host Disease', *Blood*, 93(12), pp. 4071-4078.

Park, N.J., Zhou, H., Elashoff, D., Henson, B.S., Kastratovic, D.A., Abemayor, E. and Wong, D.T. (2009) 'Salivary microRNA: discovery, characterization, and clinical utility for oral cancer detection', *Clin Cancer Res*, 15(17), pp. 5473-7.

Pasparakis, M., Haase, I. and Nestle, F.O. (2014) 'Mechanisms regulating skin immunity and inflammation', *Nat Rev Immunol*.

Pasquini, M.C. (2008) 'Impact of graft-versus-host disease on survival', *Best Pract Res Clin Haematol*, 21(2), pp. 193-204.

Pasquini MC, W.Z. (2011) *Current use and outcome of hematopoietic stem cell transplantation: CIBMTR Summary Slides*. Available at: <http://www.cibmtr.org>.

Passweg, J.R., Walker, I., Sobocinski, K.A., Klein, J.P., Horowitz, M.M. and Giralt, S.A. (2004) 'Validation and extension of the EBMT Risk Score for patients with chronic myeloid leukaemia (CML) receiving allogeneic haematopoietic stem cell transplants', *Br J Haematol*, 125, pp. 613-620.

Pauley, K.M., Satoh, M., Chan, A.L., Bubb, M.R., Reeves, W.H. and Chan, E.K. (2008) 'Upregulated miR-146a expression in peripheral blood mononuclear cells from rheumatoid arthritis patients', *Arthritis Res Ther*, 10(4), p. R101.

Pavan, R. and Reddy, P. (2013) *Pathobiology of graft-versus-host disease. The BMT Data Book*. Cambridge University Press.

Pavletic, S.Z. and Fowler, D.H. (2012) 'Are we making progress in GVHD prophylaxis and treatment?', *ASH Education Program Book*, 2012(1), pp. 251-264.

Pavord, S., Sivakumaran, M., Durrant, S. and Chapman, C. (1992) 'The role of alpha interferon in the pathogenesis of GVHD', *Bone Marrow Transplant*, 10(5), p. 477.

Pelengaris, S., Khan, M. and Evan, G.I. (2002) 'Suppression of Myc-Induced Apoptosis in  $\beta$  Cells Exposes Multiple Oncogenic Properties of Myc and Triggers Carcinogenic Progression', *Cell*, 109(3), pp. 321-334.

Perry, M.M., Moschos, S.A., Williams, A.E., Shepherd, N.J., Larner-Svensson, H.M. and Lindsay, M.A. (2008) 'Rapid Changes in MicroRNA-146a Expression Negatively Regulate the IL-1 $\beta$ -Induced Inflammatory Response in Human Lung Alveolar Epithelial Cells', *The Journal of Immunology*, 180(8), pp. 5689-5698.

Petropoulos, A. and University of Newcastle upon Tyne. Institute of Cellular, M. (2010) *Assessment of Pharmacogenetic Polymorphisms in Haematopoietic Stem Cell Transplantation*. University of Newcastle upon Tyne.

Przepiorka, D., Weisdorf, D., Martin, P., Klingemann, H.G., Beatty, P., Hows, J. and Thomas, E.D. (1995) '1994 Consensus Conference on Acute GVHD Grading', *Bone Marrow Transplant*, 15(6), pp. 825-8.

Rai, D., Karanti, S., Jung, I., Dahia, P.L. and Aguiar, R.C. (2008) 'Coordinated expression of microRNA-155 and predicted target genes in diffuse large B-cell lymphoma', *Cancer Genet Cytogenet*, 181(1), pp. 8-15.

Ranganathan, P., Heaphy, C.E., Costinean, S., Stauffer, N., Na, C., Hamadani, M., Santhanam, R., Mao, C., Taylor, P.A., Sandhu, S., He, G., Shana'ah, A., Nuovo, G.J., Lagana, A., Cascione, L., Obad, S., Broom, O., Kauppinen, S., Byrd, J.C., Caligiuri, M., Perrotti, D., Hadley, G.A., Marcucci, G., Devine, S.M., Blazar, B.R., Croce, C.M. and Garzon, R. (2012) 'Regulation of acute graft-versus-host disease by microRNA-155', *Blood*, 119(20), pp. 4786-97.

Raver-Shapira, N., Marciano, E., Meiri, E., Spector, Y., Rosenfeld, N., Moskovits, N., Bentwich, Z. and Oren, M. (2007) 'Transcriptional activation of miR-34a contributes to p53-mediated apoptosis', *Mol Cell*, 26(5), pp. 731-43.

Ray, A. and Prefontaine, K.E. (1994) 'Physical association and functional antagonism between the p65 subunit of transcription factor NF-kappa B and the glucocorticoid receptor', *Proc Natl Acad Sci U S A*, 91(2), pp. 752-6.

Reddy, P. and Ferrara, J.L.M. (2003) 'Immunobiology of acute graft-versus-host disease', *Blood Reviews*, 17, pp. 187-194.

Reshchikov, V.P., Khoklova, M.P. and Fertukhova, H.M. (1961) 'The effect of homologous bone marrow transplantation on the course of the leukaemic process in mice with transplanted leukaemia', *Probl Gematol Pereliv Krovi*, 6, pp. 593-9.

Reyes, V.E. and Klimpel, G.R. (1987) 'Interferon [alpha]/[beta] synthesis during acute graft-versus-host disease', *Transplantation*, 43(3), pp. 412-416.

Rhodes, D.R., Yu, J., Shanker, K., Deshpande, N., Varambally, R., Ghosh, D., Barrette, T., Pandey, A. and Chinnaiyan, A.M. (2004) 'Large-scale meta-analysis of cancer microarray data identifies common transcriptional profiles of neoplastic transformation and progression', *Proc Natl Acad Sci U S A*, 101(25), pp. 9309-14.

Rieu, I. and Powers, S.J. (2009) 'Real-Time Quantitative RT-PCR: Design, Calculations, and Statistics', *The Plant Cell Online*, 21(4), pp. 1031-1033.

Ringdén O, L.M., Gorin NC, Le Blanc K, Rocha V, Gluckman E, Reiffers J, Arcese W, Vossen JM, Jouet JP, Cordonnier C, Frassoni F. (2004) 'Treatment with granulocyte colony-stimulating factor after allogeneic bone marrow transplantation for acute leukemia increases the risk of graft-versus-host disease and death: a study from the Acute Leukemia Working Party of the European Group for Blood and Marrow Transplantation.', *Journal of Clinical Oncology*, 98, pp. 3186-3191.

Ritchie, W., Flamant, S. and Rasko, J.E. (2009) 'mimiRNA: a microRNA expression profiler and classification resource designed to identify functional correlations between microRNAs and their targets', *Bioinformatics*, 26(2), pp. 223-7.

Ro, S., Park, C., Young, D., Sanders, K.M. and Yan, W. (2007) 'Tissue-dependent paired expression of miRNAs', *Nucleic Acids Res*, 35(17), pp. 5944-53.

Rokavec, M., Li, H., Jiang, L. and Hermeking, H. (2014) 'The p53/microRNA connection in gastrointestinal cancer', *Clin Exp Gastroenterol*, 7, pp. 395-413.

Rosenbauer, F., Owens, B.M., Yu, L., Tumang, J.R., Steidl, U., Kutok, J.L., Clayton, L.K., Wagner, K., Scheller, M., Iwasaki, H., Liu, C., Hackanson, B., Akashi, K., Leutz, A., Rothstein, T.L., Plass, C. and Tenen, D.G. (2006) 'Lymphoid cell growth and transformation are suppressed by a key regulatory element of the gene encoding PU.1', *Nat Genet*, 38(1), pp. 27-37.

Roy, S., Levi, E., Majumdar, A.P. and Sarkar, F.H. (2012) 'Expression of miR-34 is lost in colon cancer which can be re-expressed by a novel agent CDF', *J Hematol Oncol*, 5, p. 58.

Ruggeri, L., Capanni, M., Martelli, M.F. and Velardi, A. (2001) 'Cellular therapy: exploiting NK cell alloreactivity in transplantation', *Current Opinion in Hematology*, 8(6), pp. 355-359.

Ruggeri, L., Capanni, M., Urbani, E., Perruccio, K., Shlomchik, W.D., Tosti, A., Posati, S., Rogaia, D., Frassoni, F., Aversa, F., Martelli, M.F. and Velardi, A. (2002) 'Effectiveness of

Donor Natural Killer Cell Alloreactivity in Mismatched Hematopoietic Transplants', *Science*, 295(5562), pp. 2097-2100.

Rusca, N. and Monticelli, S. (2011) 'MiR-146a in Immunity and Disease', *Molecular Biology International*, 2011, pp. 1-7.

Sarantopoulos, S., Stevenson, K.E., Kim, H.T., Cutler, C.S., Bhuiya, N.S., Schowalter, M., Ho, V.T., Alyea, E.P., Koreth, J., Blazar, B.R., Soiffer, R.J., Antin, J.H. and Ritz, J. (2009) 'Altered B-cell homeostasis and excess BAFF in human chronic graft-versus-host disease', *Blood*, 113(16), pp. 3865-74.

Schindler, C. and Plumlee, C. (2008) 'Interferons pen the JAK-STAT pathway', *Semin Cell Dev Biol*, 19(4), pp. 311-8.

Schlenk, R.F., Dohner, K., Mack, S., Stoppel, M., Kiraly, F. and Gotze, K. (2010) 'Prospective evaluation of allogeneic hematopoietic stem-cell transplantation from matched related and matched unrelated donors in younger adults with high-risk acute myeloid leukemia: German-Austrian trial AMLHD98A', *J Clin Oncol*, 28, pp. 4642-4648.

Schmitz, N., Dreger, P., Suttorp, M., Rohwedder, E.B., Haferlach, T., Loffler, H., Hunter, A. and Russell, N.H. (1995) 'Primary transplantation of allogeneic peripheral blood progenitor cells mobilized by filgrastim (granulocyte colony-stimulating factor) [see comments]', *Blood*, 85(6), pp. 1666-1672.

Schramedei, K., Morbt, N., Pfeifer, G., Lauter, J., Rosolowski, M., Tomm, J.M., von Bergen, M., Horn, F. and Brocke-Heidrich, K. (2011) 'MicroRNA-21 targets tumor suppressor genes ANP32A and SMARCA4', *Oncogene*, 30(26), pp. 2975-2985.

Schuhmacher, M., Staeger, M.S., Pajic, A., Polack, A., Weidle, U.H., Bornkamm, G.W., Eick, D. and Kohlhuber, F. (1999) 'Control of cell growth by c-Myc in the absence of cell division', *Current Biology*, 9(21), pp. 1255-1258.

Schulte, L.N., Westermann, A.J. and Vogel, J. (2012) 'Differential activation and functional specialization of miR-146 and miR-155 in innate immune sensing', *Nucleic Acids Research*.

Schwarz, D.S., Hutvagner, G., Du, T., Xu, Z., Aronin, N. and Zamore, P.D. (2003) 'Asymmetry in the Assembly of the RNAi Enzyme Complex', *Cell*, 115(2), pp. 199-208.

Scotton, C.J., Martinez, F.O., Smelt, M.J., Sironi, M., Locati, M., Mantovani, A. and Sozzani, S. (2005) 'Transcriptional profiling reveals complex regulation of the monocyte IL-1beta system by IL-13', *J Immunol*, 174(2), pp. 834-45.

Segalen, I., Fali, T., Pers, J.O., Le Meur, Y., Youinou, P. and Loisel, S. (2010) 'A case for the graft-versus-host disease as a model for B cell-mediated autoimmunity', *Autoimmun Rev*, 2010, p. 16.

Senoo, M., Pinto, F., Crum, C.P. and McKeon, F. (2007) 'p63 Is essential for the proliferative potential of stem cells in stratified epithelia', *Cell*, 129(3), pp. 523-36.

Shen, N., Liang, D., Tang, Y., de Vries, N. and Tak, P.-P. (2012) 'MicroRNAs[mdash]novel regulators of systemic lupus erythematosus pathogenesis', *Nat Rev Rheumatol*, advance online publication.

Shen, R., Ghosh, D. and Chinnaiyan, A.M. (2004) 'Prognostic meta-signature of breast cancer developed by two-stage mixture modeling of microarray data', *BMC Genomics*, 5(1), p. 94.

Shimabukuro-Vornhagen, A., Hallek, M.J., Storb, R.F. and von Bergwelt-Baildon, M.S. (2009) 'The role of B cells in the pathogenesis of graft-versus-host disease', *Blood*, 114(24), pp. 4919-4927.

Shin, J., Xie, D. and Zhong, X.-P. (2013) 'MicroRNA-34a Enhances T Cell Activation by Targeting Diacylglycerol Kinase  $\zeta$ ', *PLoS ONE*, 8(10), p. e77983.

Shlomchik, W.D. (2007) 'Graft-versus-host disease', *Nat Rev Immunol*, 7(5), pp. 340-52.

Shulman, H.M., Sullivan, K.M., Weiden, P.L., McDonald, G.B., Striker, G.E., Sale, G.E., Hackman, R., Tsoi, M.S., Storb, R. and Thomas, E.D. (1980) 'Chronic graft-versus-host syndrome in man. A long-term clinicopathologic study of 20 Seattle patients', *Am J Med*, 69(2), pp. 204-17.

Sica, A., Dorman, L., Viggiano, V., Cippitelli, M., Ghosh, P., Rice, N. and Young, H.A. (1997) 'Interaction of NF-kappaB and NFAT with the interferon-gamma promoter', *J Biol Chem*, 272(48), pp. 30412-20.

Sierra, J., Storer, B., Hansen, J.A., Bjerke, J.W., Martin, P.J. and Petersdorf, E.W. (1997) 'Transplantation of marrow cells from unrelated donors for treatment of high-risk acute leukemia: the effect of leukemic burden, donor HLA-matching, and marrow cell dose', *Blood*, 89, pp. 4226-4235.

Simpson, E., Scott, D. and Chandler, P. (1997) 'The male-specific histocompatibility antigen, H-Y: a history of transplantation, immune response genes, sex determination and expression cloning', *Annu Rev Immunol*, 15, pp. 39-61.

Smith, M.L., Cavenagh, J.D., Lister, T.A. and Fitzgibbon, J. (2004) 'Mutation of CEBPA in familial acute myeloid leukemia', *N Engl J Med*, 351(23), pp. 2403-7.

Snanoudj, R., Frangie, C., Derouere, B., Francois, H., Creput, C., Beaudreuil, S., Durrbach, A. and Charpentier, B. (2007) 'The blockade of T-cell co-stimulation as a therapeutic stratagem for immunosuppression: Focus on belatacept', *Biologics*, 1(3), pp. 203-13.

Socie, G. (2009) 'The NIH consensus criteria for chronic graft-versus-host disease: far more than just another classification', *Leukemia*, 23(1), pp. 1-2.

Socie, G. and Ritz, J. (2014) 'Current issues in chronic graft-versus-host disease', *Blood*, 124(3), pp. 374-84.

Sonkoly, E. and Pivarcsi, A. (2009) 'Advances in microRNAs: implications for immunity and inflammatory diseases', *Journal of Cellular and Molecular Medicine*, 13(1), pp. 24-38.

Sonkoly, E., Stahle, M. and Pivarcsi, A. (2008) 'MicroRNAs: novel regulators in skin inflammation', *Clin Exp Dermatol*, 33(3), pp. 312-5.

Sonkoly, E., Wei, T., Janson, P.C., Saaf, A., Lundeberg, L., Tengvall-Linder, M., Norstedt, G., Alenius, H., Homey, B., Scheynius, A., Stahle, M. and Pivarcsi, A. (2007) 'MicroRNAs: novel regulators involved in the pathogenesis of psoriasis?', *PLoS One*, 2(7), p. e610.

Sprent, J., Schaefer, M., Gao, E.K. and Korngold, R. (1988) 'Role of T cell subsets in lethal graft-versus-host disease (GVHD) directed to class I versus class II H-2 differences. I. L3T4+ cells can either augment or retard GVHD elicited by Lyt-2+ cells in class I different hosts', *The Journal of Experimental Medicine*, 167(2), pp. 556-569.

Starczynowski, D.T., Kuchenbauer, F., Argiropoulos, B., Sung, S., Morin, R., Muranyi, A., Hirst, M., Hogge, D., Marra, M., Wells, R.A., Buckstein, R., Lam, W., Humphries, R.K. and Karsan, A. (2009) 'Identification of miR-145 and miR-146a as mediators of the 5q-syndrome phenotype', *Nat Med*, 16(1), pp. 49-58.

Stark, A., Brennecke, J., Russell, R.B. and Cohen, S.M. (2003) 'Identification of Drosophila MicroRNA targets', *PLoS biology*, 1(3), p. E60.

Stauffer, N., Hamadani, S.M., Heaphy, C., Santhanam, R., Sandhu, S., Costinean, S., Nuovo, J., Perrotti, D., Croce, C.M., Hadley, G., Marcucci, G., Devine, S.M. and Garzon, R. (2010) *Experimental Transplantation - GVHD and GVL: Modulation of GVHD by Innate Immune Pathways* United States of America.

Stickel, N., Prinz, G., Pfeifer, D., Hasselblatt, P., Schmitt-Graeff, A., Follo, M., Thimme, R., Finke, J., Duyster, J., Salzer, U. and Zeiser, R. (2014) *MiR-146a regulates the TRAF6/TNF-axis in donor T cells during GvHD.*

Su, X., Chakravarti, D., Cho, M.S., Liu, L., Gi, Y.J., Lin, Y.L., Leung, M.L., El-Naggar, A., Creighton, C.J., Suraokar, M.B., Wistuba, I. and Flores, E.R. (2010) 'TAp63 suppresses metastasis through coordinate regulation of Dicer and miRNAs', *Nature*, 467(7318), pp. 986-90.

Sugerman, P.B., Faber, S.B., Willis, L.M., Petrovic, A., Murphy, G.F., Pappo, J., Silberstein, D. and van den Brink, M.R. (2004) 'Kinetics of gene expression in murine cutaneous graft-versus-host disease', *Am J Pathol*, 164(6), pp. 2189-202.

Sullivan, K.M., Witherspoon, R.P., Storb, R., Deeg, H.J., Dahlberg, S., Sanders, J.E., Appelbaum, F.R., Doney, K.C., Weiden, P. and Anasetti, C. (1988) 'Alternating-day cyclosporine and prednisone for treatment of high-risk chronic graft-v-host disease', *Blood*, 72(2), pp. 555-561.

Sun, G., Yan, J., Noltner, K., Feng, J., Li, H., Sarkis, D.A., Sommer, S.S. and Rossi, J.J. (2009) 'SNPs in human miRNA genes affect biogenesis and function'. Cold Spring Harbor Laboratory Press.

Suzuki, H.I., Yamagata, K., Sugimoto, K., Iwamoto, T., Kato, S. and Miyazono, K. (2009) 'Modulation of microRNA processing by p53', *Nature*, 460(7254), pp. 529-533.

Swaminathan, S., Suzuki, K., Seddiki, N., Kaplan, W., Cowley, M.J., Hood, C.L., Clancy, J.L., Murray, D.D., MÃ©ndez, C., Gelgor, L., Anderson, B., Roth, N., Cooper, D.A. and Kelleher, A.D. (2011) 'Differential Regulation of the Let-7 Family of MicroRNAs in CD4+ T Cells Alters IL-10 Expression', *The Journal of Immunology*, 188(12), pp. 6238-6246.

Symington, F.W., Symington, B.E., Liu, P.Y., Viguier, H., Santhanam, U. and Sehgal, P.B. (1992) 'The relationship of serum IL-6 levels to acute graft-versus-host disease and hepatorenal disease after human bone marrow transplantation', *Transplantation*, 54(3), pp. 457-62.

Systems, I. (2012) 'Ingenuity Pathways Analysis software web link'. Available at: <http://www.ingenuity.com/>.

Takeda, K. and Akira, S. (2005) 'Toll-like receptors in innate immunity', *International Immunology*, 17(1), pp. 1-14.

Taganov, K.D., Boldin, M.P. and Baltimore, D. (2007) 'MicroRNAs and Immunity: Tiny Players in a Big Field', *Immunity*, 26(2), pp. 133-137.

Taganov, K.D., Boldin, M.P., Chang, K.J. and Baltimore, D. (2006) 'NF-kappaB-dependent induction of microRNA miR-146, an inhibitor targeted to signaling proteins of innate immune responses', *Proc Natl Acad Sci U S A*, 103, pp. 12481 - 12486.

Takahashi, N., Nakaoka, T. and Yamashita, N. (2012) 'Profiling of immune-related microRNA expression in human cord blood and adult peripheral blood cells upon proinflammatory stimulation', *European Journal of Haematology*, 88(1), pp. 31-38.

Tanabe, Y., Nishibori, T., Su, L., Arduini, R.M., Baker, D.P. and David, M. (2005) 'Cutting Edge: Role of STAT1, STAT3, and STAT5 in IFN- $\alpha\beta$  Responses in T Lymphocytes', *The Journal of Immunology*, 174(2), pp. 609-613.

Tang, F., Hajkova, P., O'Carroll, D., Lee, C., Tarakhovsky, A., Lao, K. and Surani, M.A. (2008) 'MicroRNAs are tightly associated with RNA-induced gene silencing complexes in vivo', *Biochemical and Biophysical Research Communications*, 372(1), pp. 24-29.

Tang, Y., Luo, X., Cui, H., Ni, X., Yuan, M., Guo, Y., Huang, X., Zhou, H., de Vries, N., Tak, P.P., Chen, S. and Shen, N. (2009) 'MicroRNA-146a contributes to abnormal activation of the type I interferon pathway in human lupus by targeting the key signaling proteins', *Arthritis & Rheumatism*, 60(4), pp. 1065-1075.

Tavor, S., Park, D.J., Gery, S., Vuong, P.T., Gombart, A.F. and Koeffler, H.P. (2003) 'Restoration of C/EBPalpha expression in a BCR-ABL+ cell line induces terminal granulocytic differentiation', *J Biol Chem*, 278(52), pp. 52651-9.

Teshima, T. and Ferrara, J.L.M. (2002) 'Understanding the alloresponse: New approaches to graft-versus-host disease prevention', *Seminars in Hematology*, 39(1), pp. 15-22.

Thomas, E.D., Lochte, H.L., Jr., Lu, W.C. and Ferrebee, J.W. (1957) 'Intravenous infusion of bone marrow in patients receiving radiation and chemotherapy', *N Engl J Med*, 257(11), pp. 491-6.

Thomas, E.D., Storb, R., Clift, R.A., Fefer, A., Johnson, L. and Neiman, P.E. (1975) 'Bone-marrow transplantation', *N Engl J Med*, 292, pp. 895-902.

Thompson, R.C., Herscovitch, M., Zhao, I., Ford, T.J. and Gilmore, T.D. (2011) 'NF-kappaB down-regulates expression of the B-lymphoma marker CD10 through a miR-155/PU.1 pathway', *J Biol Chem*, 286(3), pp. 1675-82.

Tili, E., Croce, C.M. and Michaille, J.-J. (2009) 'miR-155: On the Crosstalk Between Inflammation and Cancer', *International Reviews of Immunology*, 28(5), pp. 264-284.

Van Camp, K., Cools, N., Stein, B., Van de Velde, A., Goossens, H., Berneman, Z.N. and Van Tendeloo, V. (2010) 'Efficient mRNA electroporation of peripheral blood mononuclear cells to detect memory T cell responses for immunomonitoring purposes', *J Immunol Methods*, 354(1-2), pp. 1-10.

Van Rossum, A.G., Schuurin-Scholtes, E., van Buuren-van Seggelen, V., Kluin, P.M. and Schuurin, E. (2005) 'Comparative genome analysis of cortactin and HS1: the significance of the F-actin binding repeat domain', *BMC Genomics*, 6, p. 15.

Vangala, R.K., Heiss-Neumann, M.S., Rangatia, J.S., Singh, S.M., Schoch, C., Tenen, D.G., Hiddemann, W. and Behre, G. (2003) *The myeloid master regulator transcription factor PU.1 is inactivated by AML1-ETO in t(8;21) myeloid leukemia.*

Viprey, V.F., Corrias, M.V. and Burchill, S.A. (2012) 'Identification of reference microRNAs and suitability of archived hemopoietic samples for robust microRNA expression profiling', *Analytical Biochemistry*, 421(2), pp. 566-572.

Vogelstein, B., Lane, D. and Levine, A.J. (2000) 'Surfing the p53 network', *Nature*, 408(6810), pp. 307-310.

Wagner, J.E., Kernan, N.A., Steinbuch, M., Broxmeyer, H.E. and Gluckman, E. (1995) 'Allogeneic sibling umbilical-cord-blood transplantation in children with malignant and non-malignant disease', *Lancet*, 346(8969), pp. 214-9.

Wall DA, S.K. (1994) 'The role of tumor necrosis factor and interferon gamma in graft-versus-host disease and related immunodeficiency', *Transplantation*, 57, pp. 273-279.

Wang, G., Tam, L.S., Kwan, B.C., Li, E.K., Chow, K.M., Luk, C.C., Li, P.K. and Szeto, C.C. (2012) 'Expression of miR-146a and miR-155 in the urinary sediment of systemic lupus erythematosus', *Clin Rheumatol*, 31(3), pp. 435-40.

Wang, G., Tam, L.S., Li, E.K., Kwan, B.C., Chow, K.M., Luk, C.C., Li, P.K. and Szeto, C.C. (2010) 'Serum and urinary cell-free MiR-146a and MiR-155 in patients with systemic lupus erythematosus', *J Rheumatol*, 37(12), pp. 2516-22.

Wang, J., Coombes, K.R., Highsmith, W.E., Keating, M.J. and Abruzzo, L.V. (2004) 'Differences in gene expression between B-cell chronic lymphocytic leukemia and normal B cells: a meta-analysis of three microarray studies', *Bioinformatics*, 20(17), pp. 3166-3178.

Wang, L., Romero, M., Ratajczak, P., Leboeuf, C., Belhadj, S., Peffault de Latour, R., Zhao, W.L., Socie, G. and Janin, A. (2013) 'Increased apoptosis is linked to severe acute GVHD in patients with Fanconi anemia', *Bone Marrow Transplant*, 48(6), pp. 849-53.

Wang, X.-N., Collin, M., Sviland, L., Marshall, S., Jackson, G., Schulz, U., Holler, E., Karrer, S., Greinix, H., Elahi, F., Hromadnikova, I. and Dickinson, A.M. (2006) 'Skin Explant Model of Human Graft-versus-Host Disease: Prediction of Clinical Outcome and Correlation with Biological Risk Factors', *Biology of Blood and Marrow Transplantation*, 12(2), pp. 152-159.

Wang, X., Zhao, X., Gao, P. and Wu, M. (2013b) 'c-Myc modulates microRNA processing via the transcriptional regulation of Drosha', *Sci Rep*, 3, p. 1942.

Weiden, P.L., Flournoy, N., Thomas, E.D., Prentice, R., Fefer, A., Buckner, C.D. and Storb, R. (1979) 'Antileukemic Effect of Graft-versus-Host Disease in Human Recipients of Allogeneic-Marrow Grafts', *New England Journal of Medicine*, 300(19), pp. 1068-1073.

Weitzel, R.P., Lesniewski, M.L., Haviernik, P., Kadereit, S., Leahy, P., Greco, N.J. and Laughlin, M.J. (2009) 'microRNA 184 regulates expression of NFAT1 in umbilical cord blood CD4+ T cells', *Blood*, 113(26), pp. 6648-6657.

Welniak, L.A., Blazar, B.R., Anver, M.R., Wiltrott, R.H. and Murphy, W.J. (2000) 'Opposing roles of interferon-gamma on CD4+ T cell-mediated graft-versus-host disease: effects of conditioning', *Biol Blood Marrow Transplant*, 6(6), pp. 604-12.

Welniak, L.A., Blazar, B.R. and Murphy, W.J. (2007) 'Immunobiology of allogeneic hematopoietic stem cell transplantation', *Annu Rev Immunol*, 25, pp. 139-70.

Wiggins, J.F., Ruffino, L., Kelnar, K., Omotola, M., Patrawala, L., Brown, D. and Bader, A.G. (2010) 'Development of a Lung Cancer Therapeutic Based on the Tumor Suppressor MicroRNA-34', *Cancer Research*, 70(14), pp. 5923-5930.

Wightman, B., Ha, I. and Ruvkun, G. (1993) 'Posttranscriptional regulation of the heterochronic gene lin-14 by lin-4 mediates temporal pattern formation in *C. elegans*', *Cell*, 75(5), pp. 855-862.

Williams, A. (2008) 'Functional aspects of animal microRNAs', *Cellular and Molecular Life Sciences*, 65(4), pp. 545-562.

Wilson, A., Murphy, M.J., Oskarsson, T., Kaloulis, K., Bettess, M.D., Oser, G.M., Pasche, A.-C., Knabenhans, C., MacDonald, H.R. and Trumpp, A. (2004) 'c-Myc controls the balance between hematopoietic stem cell self-renewal and differentiation', *Genes & Development*, 18(22), pp. 2747-2763.

Wu, T., Xie, M., Wang, X., Jiang, X., Li, J. and Huang, H. (2012) 'miR-155 modulates TNF- $\alpha$ -inhibited osteogenic differentiation by targeting SOCS1 expression', *Bone*, 51(3), pp. 498-505.

Xian Chang Li, G.D., Sylvie Ferrari-Lacraz, Chris Groves, Anthony Coyle, Thomas . Malek & Terry B. Strom (2001) 'IL-15 and IL-2: a matter of life and death for T cells in vivo', *Nature*, 7, pp. 114-118.

Xiao, B., Wang, Y., Li, W., Baker, M., Guo, J., Corbet, K., Tsalik, E.L., Li, Q.-J., Palmer, S.M., Woods, C.W., Li, Z., Chao, N.J. and He, Y.-W. (2013) 'Plasma microRNA signature as a noninvasive biomarker for acute graft-versus-host disease', *Blood*, 122(19), pp. 3365-3375.

Xie, L.N., Zhou, F., Liu, X.M., Fang, Y., Yu, Z., Song, N.X. and Kong, F.S. (2014) 'Serum microRNA155 is increased in patients with acute graft-versus-host disease', *Clin Transplant*, 28(3), pp. 314-23.

Xu, P., Vernooy, S.Y., Guo, M. and Hay, B.A. (2003) 'The Drosophila MicroRNA Mir-14 Suppresses Cell Death and Is Required for Normal Fat Metabolism', *Current Biology*, 13(9), pp. 790-795.

Xu, Z., Xiao, S.-B., Xu, P., Xie, Q., Cao, L., Wang, D., Luo, R., Zhong, Y., Chen, H.-C. and Fang, L.-R. (2011) 'miR-365, a Novel Negative Regulator of Interleukin-6 Gene Expression, Is Cooperatively Regulated by Sp1 and NF- $\kappa$ B', *Journal of Biological Chemistry*, 286(24), pp. 21401-21412.

Xun, C., Thompson, J., Jennings, C., Brown, S. and Widmer, M. (1994) 'Effect of total body irradiation, busulfan-cyclophosphamide, or cyclophosphamide conditioning on inflammatory cytokine release and development of acute and chronic graft-versus-host disease in H-2-incompatible transplanted SCID mice.', *Blood*, 83, pp. 2360-2367.

Yada, S., Takamura, N., Inagaki-Ohara, K., O'Leary M, K., Wasem, C., Brunner, T., Green, D.R., Lin, T. and Pinkoski, M.J. (2005) 'The role of p53 and Fas in a model of acute murine graft-versus-host disease', *J Immunol*, 174(3), pp. 1291-7.

Yamakuchi, M. and Lowenstein, C.J. (2009) 'MiR-34, SIRT1 and p53: the feedback loop', *Cell Cycle*, 8(5), pp. 712-5.

Yang, J.-S., Maurin, T. and Lai, E.C. (2012) 'Functional parameters of Dicer-independent microRNA biogenesis', *RNA*.

- Yang, J.-S., Phillips, M.D., Betel, D., Mu, P., Ventura, A., Siepel, A.C., Chen, K.C. and Lai, E.C. (2011) 'Widespread regulatory activity of vertebrate microRNA\* species', *RNA*, 17(2), pp. 312-326.
- Yang YG, D.B., Sergio JJ, Pearson DA, Sykes M. (1998) 'Donor-derived interferon gamma is required for inhibition of acute graft-versus-host disease by interleukin 12.', *The Journal of Clinical Investigation*, 102, pp. 2126-2135.
- Yi, R., Qin, Y., Macara, I.G. and Cullen, B.R. (2003) 'Exportin-5 mediates the nuclear export of pre-microRNAs and short hairpin RNAs', *Genes and Development*, 17(24), pp. 3011-3016.
- Yonish-Rouach, E., Resnitzky, D., Lotem, J., Sachs, L., Kimchi, A. and Oren, M. (1991) 'Wild-type p53 induces apoptosis of myeloid leukaemic cells that is inhibited by interleukin-6', *Nature*, 352(6333), pp. 345-7.
- York IA, R.K. (1996) 'Antigen processing and presentation by the class I major histocompatibility complex', *Annual Review of Immunology*, 14, pp. 369-396.
- Yu, X.-Z., Martin, P.J. and Anasetti, C. (1998) 'Role of CD28 in Acute Graft-Versus-Host Disease', *Blood*, 92(8), pp. 2963-2970.
- Zamore, P.D., Tuschl, T., Sharp, P.A. and Bartel, D.P. (2000) 'RNAi: double-stranded RNA directs the ATP-dependent cleavage of mRNA at 21 to 23 nucleotide intervals', *Cell*, 101(1), pp. 25-33.
- Zampetaki, A., Kiechl, S., Drozdov, I., Willeit, P., Mayr, U., Prokopi, M., Mayr, A., Weger, S., Oberhollenzer, F., Bonora, E., Shah, A., Willeit, J. and Mayr, M. (2010) 'Plasma MicroRNA Profiling Reveals Loss of Endothelial MiR-126 and Other MicroRNAs in Type 2 Diabetes', *Circ Res*, 107(6), pp. 810-817.
- Zeeberg, B.R., Qin, H., Narasimhan, S., Sunshine, M., Cao, H., Kane, D.W., Reimers, M., Stephens, R.M., Bryant, D., Burt, S.K., Elnekave, E., Hari, D.M., Wynn, T.A., Cunningham-Rundles, C., Stewart, D.M., Nelson, D. and Weinstein, J.N. (2005) 'High-Throughput GoMiner, an 'industrial-strength' integrative gene ontology tool for interpretation of multiple-microarray experiments, with application to studies of Common Variable Immune Deficiency (CVID)', *BMC Bioinformatics*, 6, p. 168.
- Zeng, Y., Yi, R. and Cullen, B.R. (2003) 'MicroRNAs and small interfering RNAs can inhibit mRNA expression by similar mechanisms', *Proceedings of the National Academy of Sciences of the United States of America*, 100(17), pp. 9779-9784.

- Zhang, H., Kolb, F.A., Brondani, V., Billy, E. and Filipowicz, W. (2002) 'Human Dicer preferentially cleaves dsRNAs at their termini without a requirement for ATP', *EMBO Journal*, 21(21), pp. 5875-5885.
- Zhang, J., Cheng, C., Yuan, X., He, J.T., Pan, Q.H. and Sun, F.Y. (2014) 'microRNA-155 acts as an oncogene by targeting the tumor protein 53-induced nuclear protein 1 in esophageal squamous cell carcinoma', *Int J Clin Exp Pathol*, 7(2), pp. 602-10.
- Zhao, H., Wang, D., Du, W., Gu, D. and Yang, R. (2010) 'MicroRNA and leukemia: Tiny molecule, great function', *Critical Reviews in Oncology/Hematology*, 74(3), pp. 149-155.
- Zhou, Y., Barnett, M.J. and Rivers, J.K. (2000) 'Clinical significance of skin biopsies in the diagnosis and management of graft-vs-host disease in early postallogeic bone marrow transplantation', *Arch Dermatol*, 136(6), pp. 717-21.
- Zhu, W. and Xu, B. (2014) 'MicroRNA-21 Identified as Predictor of Cancer Outcome: A Meta-Analysis', *PLoS One*, 9(8), p. e103373.
- Ziemer, M. (2013) 'Graft-versus-host disease of the skin and adjacent mucous membranes', *J Dtsch Dermatol Ges*, 11(6), pp. 477-95.
- Zorn, E., Kim, H.T., Lee, S.J., Floyd, B.H., Litsa, D., Arumugarajah, S., Bellucci, R., Alyea, E.P., Antin, J.H., Soiffer, R.J. and Ritz, J. (2005) 'Reduced frequency of FOXP3+ CD4+CD25+ regulatory T cells in patients with chronic graft-versus-host disease', *Blood*, 106(8), pp. 2903-11.

“I am Winter, that do keep  
Longing safe amidst of sleep:  
Who shall say if I were dead  
What should be remembered?”  
-**William Morris** (Verses for Pictures)

